HOST RANGE FUNCTIONS OF POXVIRUS PROTEINS ARE MEDIATED BY SPECIES-SPECIFIC INHIBITION OF THE ANTIVIRAL PROTEIN KINASE PKR

by

SHERRY LARAE HALLER

B.S., University of Minnesota, 2010

AN ABSTRACT OF A DISSERTATION

submitted in partial fulfillment of the requirements for the degree

DOCTOR OF PHILOSOPHY

Division of Biology
College of Arts and Sciences

KANSAS STATE UNIVERSITY
Manhattan, Kansas

2016

Abstract

Vaccinia virus is the prototypic poxvirus that has been widely used as a model for investigating poxvirus biology and genetics. Like several members of the *Poxviridae* family, vaccinia virus can infect several different species including mice, cows and humans. Because the entry of poxviruses into a host cell relies on ubiquitously expressed surface molecules, which are found in many species, the ability of poxviruses to infect and replicate in different host cells primarily depends on their ability to subvert the host's innate immune response. One critical barrier to infection is overcoming the general shutdown of protein translation initiated by the cellular protein kinase PKR. PKR detects cytoplasmic double-stranded (ds) RNA generated during infection by the replicating virus, which activates it to phosphorylate the alpha-subunit of the eukaryotic translation initiation factor 2 (eIF2) and suppress general translation. Poxviruses are large viruses with dsDNA genomes that encode around 200 genes. Several of these genes are known as host range genes and are important for replication in different host species and many interact with components of the host immune response to promote viral replication. Two genes in vaccinia virus, called E3L and K3L, are known inhibitors of PKR and have previously been shown to be important for virus replication in cells from different species. The molecular explanation behind their host range function, however, is unknown. The main goal of the research presented in this thesis is to determine the molecular mechanisms for the host range function of vaccinia virus E3L and K3L, particularly in different hamster host cells. Along with an analysis of vaccinia virus host range genes, we have used genome-wide comparisons between host-restricted poxviruses in the *Leporipoxvirus* genus to parse out the potential genomic determinants of host range restriction in this clade of poxviruses. The overarching aim of this thesis work is to better understand the molecular mechanisms for host range in poxviruses.

HOST RANGE FUNCTIONS OF POXVIRUS PROTEINS ARE MEDIATED BY SPECIES-SPECIFIC INHIBITION OF THE ANTIVIRAL PROTEIN KINASE PKR

by

SHERRY LARAE HALLER

B.S., University of Minnesota, 2010

A DISSERTATION

submitted in partial fulfillment of the requirements for the degree

DOCTOR OF PHILOSOPHY

Division of Biology
College of Arts and Sciences

KANSAS STATE UNIVERSITY
Manhattan, Kansas

2016

Approved by:

Major Professor
Stefan Rothenburg

Copyright

Abstract

Vaccinia virus is the prototypic poxvirus that has been widely used as a model for investigating poxvirus biology and genetics. Like several members of the *Poxviridae* family, vaccinia virus can infect several different species including mice, cows and humans. Because the entry of poxviruses into a host cell relies on ubiquitously expressed surface molecules, which are found in many species, the ability of poxviruses to infect and replicate in different host cells primarily depends on their ability to subvert the host's innate immune response. One critical barrier to infection is overcoming the general shutdown of protein translation initiated by the cellular protein kinase PKR. PKR detects cytoplasmic double-stranded (ds) RNA generated during infection by the replicating virus, which activates it to phosphorylate the alpha-subunit of the eukaryotic translation initiation factor 2 (eIF2) and suppress general translation. Poxviruses are large viruses with dsDNA genomes that encode around 200 genes. Several of these genes are known as host range genes and are important for replication in different host species and many interact with components of the host immune response to promote viral replication. Two genes in vaccinia virus, called E3L and K3L, are known inhibitors of PKR and have previously been shown to be important for virus replication in cells from different species. The molecular explanation behind their host range function, however, is unknown. The main goal of the research presented in this thesis is to determine the molecular mechanisms for the host range function of vaccinia virus E3L and K3L, particularly in different hamster host cells. Along with an analysis of vaccinia virus host range genes, we have used genome-wide comparisons between host-restricted poxviruses in the *Leporipoxvirus* genus to parse out the potential genomic determinants of host range restriction in this clade of poxviruses. The overarching aim of this thesis work is to better understand the molecular mechanisms for host range in poxviruses.

Table of Contents

List of Figures x
List of Tables xiv
Acknowledgements xv
Chapter 1 - Introduction 1
Poxviruses 1
Poxvirus genomes 2
Gene expression in poxviruses 4
Poxvirus phylogeny and host range 5
Avipoxviruses, molluscipoxviruses, and parapoxviruses 7
Orthopoxviruses 9
Variola virus, camelpox virus, and taterapox virus 9
Cowpox virus 10
Monkeypox virus 10
Vaccinia virus, horsepox virus and rabbitpox virus 11
North American orthopoxviruses 13
Clade II Poxviruses 14
Yatapoxviruses 14
Leporipoxviruses 14
Cervidpoxviruses, suipoxviruses and capripoxviruses 16
Poxvirus immune evasion by host range genes 17
Poxviral antagonism of the interferon response 18
Poxviral defenses against cellular inflammation and host complement 21
Induction and inhibition of apoptosis by poxviruses 24
Cellular sensors of double-stranded RNA and poxviral evasion strategies 25
RNA-dependent protein kinase, PKR 27
Chapter 2 - Host range functions of vaccinia virus E3L and K3L are mediated by species-specific PKR inhibition 56
Abstract 57

Significance 58
Introduction 59
Methods 61
Cell lines, viruses, yeast strains and plasmids 61
Virus infections and interferon and siRNA treatments 62
Luciferase assay for PKR inhibition 64
Yeast assay for PKR inhibition 64
Generation of hamster PKR-expressing HeLa cell lines 65
Generation of tetracycline-inducible Flp-In HeLa cells 65
Generation of tetracycline-inducible hamster PKR-expressing 293 cells 66
Quantitative PCR and RT-PCR analyses 66
Western blotting 67
Results 68
E3L and K3L are differentially required for VACV replication in cell culture 68
PKR inhibition by E3L and K3L is important for VACV replication 70
Syrian hamster PKR from BHK-21 cells is resistant to inhibition by VACV E3L 73
VACV E3L and K3L exhibit differential inhibition of PKR from hamster species 75
Requirement for E3L or K3L for VACV replication in hamster cells correlates with PKR inhibition and eIF2α phosphorylation 82
Induction or suppression of PKR expression affects VACV replication in hamster cells 86
Generation of hamster PKR expressing cell lines and an inducible-expression system 95
Discussion 104
Author contributions 108
Chapter 3 - Molecular mechanisms of species-specific PKR resistance to vaccinia virus E3L and K3L 112
Abstract 113
Significance 114
Introduction 115
Methods 117
Cell lines and plasmids 117
Luciferase assay for PKR inhibition 118

Phylogenetic and positive selection analysis 118
Results 119
Syrian hamster PKR is resistant to dsRNA-binding proteins from different viruses 119
Domain swapping of hamster PKRs reveals regions important for resistance to VACV E3L and K3L 123
Residues in the linker region are important for PKR sensitivity to VACV E3L 131
Positive selection in hamster PKR reveals the molecular basis for PKR resistance to VACV K3L but not VACV E3L 135
PKR dsRNA-binding and dimerization affect PKR sensitivity to VACV E3L 148
Discussion 156
Author contributions 164
Chapter 4 - The genome of the leporipoxvirus squirrel fibroma virus reveals recombination between distantly related poxviruses 170
Abstract 171
Significance 172
Introduction 173
Methods 175
Cell lines, plasmids, and viruses 175
Virus Infections 176
DNA sequencing and genome assembly and annotation 177
Promoter motif analysis 181
Generation of recombinant squirrel fibroma virus 182
Phylogenetic analyses 183
PKR inhibition luciferase assay 186
Results 186
Genome of the squirrel fibroma virus 186
General features of the genome 186
Phylogeny of squirrel fibroma virus 197
Transcriptional regulation 198
Genetic differences between squirrel fibroma virus and other leporipoxviruses 199
Identification of regions of dynamic gene loss/fragmentation in leporipoxviruses 199

Loss of other potential immunomodulatory genes in the squirrel fibroma virus 202
Potential horizontal gene transfer 204
Evidence for recombination with an orthopoxvirus 205
Analysis of a distinct squirrel fibroma virus isolate 208
Squirrel fibroma virus replication in cell culture 210
Squirrel fibroma virus PKR inhibitors 222
Discussion 227
Author contributions 234
Chapter 5 - Concluding remarks and future directions 254

List of Figures

Figure 1.1 Host range and phylogeny of sequenced poxviruses..... 6
Figure 1.2 Molecular interactions of host range factors in poxviruses..... 20
Figure 1.3 Hamster home territories. 30
Figure 2.1 VACV E3L and K3L are differentially required for replication in cell culture. 69
Figure 2.2 VACV E3L and K3L inhibition of PKR is required for VACV replication in RK13 cells. 70
Figure 2.3 PKR inhibition is a critical barrier to VACV replication in HeLa cells..... 71
Figure 2.4 PKR inhibition by VACV E3L and K3L. 73
Figure 2.5 Syrian hamster PKR is resistant to inhibition by VACV E3L. 74
Figure 2.6 Percent sequence identiies of the hamster PKRs and human PKR. 75
Figure 2.7 Protein sequence alignment of hamster PKRs with human PKR..... 76
Figure 2.8 Species-specific PKR inhibition by VACV E3L and K3L. 78
Figure 2.9 Co-transfection of PKR from different species with VACV E3L and K3L..... 79
Figure 2.10 Species-specific PKR inhibition by VACV E3L and K3L in yeast.....80
Figure 2.11 VACV K3L-H47R inhibits PKR similarly to VACV K3L..... 81
Figure 2.12 Ectopic expression of hamster PKR in VACV infected cells. 82
Figure 2.13 VACV replication in hamster cells..... 83
Figure 2.14 Phosphorylation of eIF2α in mutant VACV infected hamster cells. 84
Figure 2.15 VACV mutant replication in hamster cells. 86
Figure 2.16 Interferon induces PKR expression in Syrian hamster cells. 87
Figure 2.17 VACV replication in interferon treated Syrian hamster cells. 88
Figure 2.18 VACV replication in human interferon treated hamster cells. 89
Figure 2.19 Mutant VACV replication in mouse interferon treated BHK-21 cells..... 90
Figure 2.20 Mutant VACV replication in mouse interferon treated hamster cells..... 91
Figure 2.21 siRNA knock-down of PKR in hamster cells..... 93
Figure 2.22 siRNA knock-down of PKR in hamster cells rescues mutant VACV replication. ... 94
Figure 2.23 Screening of hamster PKR-expressing HeLa cells..... 97
Figure 2.24 Unstable expression from hamster PKR-reconstituted HeLa cells. 98
Figure 2.25 PKR-reconstituted HeLa cells suppress VC-R2 but do not express hamster PKR.. 99

Figure 2.26 Screening HeLa-PKRkd clones for Flp-In site integration. 101
Figure 2.27 Quantitative PCR test for single Flp-In site in 293-T-REx cells. 102
Figure 2.28 293-T-REx cells express hamster PKRs following induction with tetracycline or doxycycline. 103
Figure 2.29 siRNA treatment test to knock-down human PKR in 293-T-REx cells. 103
Figure 3.1 Syrian hamster PKR is resistant to other E3L orthologs from poxviruses. 120
Figure 3.2 Syrian hamster PKR is resistant to other viral dsRNA-binding proteins. 122
Figure 3.3 Domain map of PKR. 123
Figure 3.4 Resistance to VACV E3L and K3L lie in N- or C-terminal domains of PKR. 124
Figure 3.5 The N-terminus of Syrian hamster PKR mostly confers resistance to VACV-E3L. 125
Figure 3.6 Resistance to E3L may involve the kinase domain. 126
Figure 3.7 Domain exchanges of Syrian hamster and Armenian hamster PKR alter sensitivity of VACV E3L and K3L. 127
Figure 3.8 Resistance to E3L involves multiple domains..... 128
Figure 3.9 Syrian hamster linker region is important for resistance to E3L. 129
Figure 3.10 First dsRNA-binding domain of human PKR increases Syrian hamster PKR sensitivity to E3L. 130
Figure 3.11 Splice variant forms of hamster PKR do not exhibit altered sensitivity to VACV E3L. 132
Figure 3.12 Linker region deletion mutants of Syrian hamster PKR are sensitive to E3L..... 133
Figure 3.14 Protein sequence alignment of 12 rodent and rabbit PKRs. 137
Figure 3.15 Phylogenetic tree of 12 rodent and rabbit PKRs used for positive selection analysis. 137
Figure 3.16 Residues under positive selection in rodent/lagomorph PKRs..... 140
Figure 3.17 Residues under positive selection are clustered on the helix-αG of the PKR kinase domain. 143
Figure 3.18 Single amino acid exchanges in the helix-αG of the PKR kinase domain..... 144
Figure 3.19 Two amino acid exchanges in the helix-αG of the PKR kinase domain alter PKR sensitivity to K3L. 145
Figure 3.20 Helix-αG mutations do not affect PKR sensitivity to E3L. 146
Figure 3.21 Point mutations in hamster PKR do not alter sensitivity to E3L..... 147

Figure 3.22 Residues important for dsRNA-binding in the first dsRNA-binding domain are most important for PKR activity. 149
Figure 3.23 Mutations in residues important for dsRNA-binding prevent E3L inhibition. 150
Figure 3.24 Syrian hamster dsRNA-binding domains can inhibit Armenian hamster PKR like E3L. 151
Figure 3.25 Residues under positive selection are clustered on the dimerization region of the PKR kinase domain. 152
Figure 3.26 Hamster PKRs require residues forming salt-bridge during dimerization for PKR activity. 154
Figure 3.27 Reversion of salt-bridge residues in dimerization region of PKR does not completely restore PKR activity and makes Syrian hamster PKR sensitive to E3L. 155
Figure 3.28 Diagram of the stages of PKR activation. 160
Figure 3.29 Diagram of models of E3L inhibition of PKR. 163
Figure 4.1 Genome map of SQFV-Kilham. 188
Figure 4.2 SQFV is the most divergent leporipoxvirus. 197
Figure 4.3 SQFV early and late promoter motifs. 199
Figure 4.4 Genomic region of dynamic gene loss and fragmentation in leporipoxviruses. 200
Figure 4.5. Gene inactivation and gene loss in leporipoxvirus genomes. 202
Figure 4.6 Multiple sequence alignment of S150 and similar sequences in GenBank. 205
Figure 4.7 Protein sequence identities of SQFV ITR genes to poxvirus orthologs. 206
Figure 4.8 Phylogenetic analysis of SQFV ORF S004/S162 indicates recombination with an old-world OPV. 207
Figure 4.9 Fox squirrel lesions from presumable SQFV infection. 208
Figure 4.10 SQFV-CDC isolate DNA PCR. 209
Figure 4.11 Map of SQFV regions amplified by PCR and confirmed by Sanger sequencing. 210
Figure 4.12 Replication of SQFV-Kilham in RK13 cells. 212
Figure 4.13 Replication kinetics of SQFV-mCherry and other poxviruses in RK13 cells. 213
Figure 4.14 Replication kinetics of SQFV-mCherry and other poxviruses in BHK-21 cells. 214
Figure 4.15 SQFV-mCherry forms tight foci of infection on RK13 cells. 215
Figure 4.16 Replication of SQFV-mCherry, MYXV-GFP, and VACV-GFP in BHK-21 cells. 216

Figure 4.17 SQFV-mCherry replication in mammalian cell lines compared to other poxviruses. 217
Figure 4.18 SQFV-mCherry (mC) replication in NRK cells. 219
Figure 4.19 SQFV-mCherry (mC) replication in CHO cells. 219
Figure 4.20 SQFV-mCherry (mC) replication in Vero cells. 220
Figure 4.21 SQFV-mCherry (mC) replication in HeLa cells. 220
Figure 4.22 SQFV-mCherry (mC) replication in 293T cells. 221
Figure 4.23 SQFV-mCherry (mC) replication in NIH/3T3 cells. 221
Figure 4.24 SQFV-mCherry (mC) replication in BSC-1 cells. 222
Figure 4.25 Sequence alignment of K3 orthologs. 223
Figure 4.26 Species-specific inhibition of PKR by MYXV M156R and SQFV S152. 224
Figure 4.27 Alignment of SQFV S033 dsRNA-binding motif with other E3 orthologs. 225
Figure 4.28 SQFV S033 is a functional inhibitor of PKR. 226
Figure 4.29 Conserved synteny of SQFV and CPXV genes. 231

List of Tables

Table 2.1 Sequences of hamster PKR siRNA duplexes. 63
Table 3.1. Gene sequences used in the positive selection analysis. 119
Table 3.2 Screened residues under positive selection in PKR. 139
Table 3.3 Residues in PKR under positive selection. 141
Table 3.4. Dimerization and dsRNA-binding mutant PKRs tested in the luciferase assay. 153
Table 3.5. Hamster PKR mutant constructs tested in the luciferase assay. 158
Table 4.1 Primer pairs used in this study. 181
Table 4.2 Genes used in promoter analysis 182
Table 4.3 VACV-Cop genes used in the phylogenetic analysis 184
Table 4.4 Poxvirus genomes used in the phylogenetic analysis 186
Table 4.5 SQFV genome annotation table 196
Table 4.6 A comparison of leporipoxvirus gene differences. 201
Table 4.7 Recombined genes may compensate for missing leporipoxvirus genes. 229
Table 4.8 Novel genes in SQFV not found in other leporipoxviruses. 232

Acknowledgements

I would like to express my sincerest gratitude to all of the people who have helped me get to where I am today. First and foremost I have to thank my advisor Dr. Stefan Rothenburg for all of his guidance and support. I thank him for giving me the opportunity to work on so many interesting projects and for taking the time to teach me to think critically while allowing me to gain confidence in my abilities as a scientist. I will always be indebted to the time and energy that he has put into my scientific and professional development.

I would never have been able to accomplish anything without the encouragement and support from my fellow lab mates, Chen and Julhasur. I appreciate their patience with me over the years and greatly value their friendship. In particular I want to thank Chen, who was with me from the beginning, for showing me how to do everything and for being a great role model to look up to as a scientist and as a person.

I have had the pleasure of working with several great students and professors over my graduate career – too many to list here – who have provided great conversations in and out of the lab and a friendly learning environment that I hope was felt mutually. I would like to thank my committee members especially, Dr. Revathi Govind, Dr. Loubna Tazi and Dr. Roman Ganta, for their mentorship and guidance, as well as Dr. Rollie Clem who was always more than happy to help answer questions when I had them and offer support for my endeavors. I have learned a great deal from every one of them, and I appreciate the time each has taken to provide counsel for my work and for my career.

Finally, I would like to thank my husband for tolerating my ambitions and the stresses that come with graduate school and for always being there for me even when it wasn't easy. Your love has been a true strength and, at times, a great motivator for me. I must extend this gratitude to the rest of my family as well, because they have been exceedingly sympathetic and understanding of the time I have committed to my work and have always had great confidence in me to accomplish my goals.

Chapter 1 - Introduction

Viruses continue to be an economic and social concern globally as the diseases they cause threaten human and animal populations (1). The adaptation of viruses to new hosts or niches within their hosts is a consequence of their evolution and ecology and can lead to the emergence of zoonotic viral diseases that pose problems for humans and the animal populations they depend on (2). It is therefore critically important to understand the interactions between these viruses and their hosts that affect virus host range and virulence or host susceptibility. Poxviruses are a group of important human and animal pathogens that historically have had a great impact on these populations, and their continued emergence and discovery in surveillance efforts offer evidence that these viruses will continue to play an important role in the global ecosystem (3, 4). The sequencing of entire poxvirus genomes has begun to reveal the genetic and molecular determinants for poxvirus infection, replication, and virulence, yet our understanding of how species-specific differences in host-virus interactions affect the host range of poxviruses is limited and requires further study.

Poxviruses

Poxviruses are a family of large double-stranded (ds) DNA viruses that replicate exclusively in the cytoplasm of host cells. Poxviruses have complex, enveloped virions that are large enough to be visible by a light microscope (~250x350nm) and ultrastructural examination of samples by electron microscopy has long been the gold standard for diagnosing poxviral infections. The virions of poxviruses are shaped like rounded bricks, and a cross section of these viruses reveals a unique dumb-bell shaped interior that is caused by the presence of two lateral bodies that sit on either side of the viral core, which houses the structural proteins, some transcriptional enzymes, and the dsDNA genome (5, 6). The genomes of poxviruses range in size from 135-360 kilobase pairs (kb), and therefore poxviruses have some of the largest viral genomes ever studied and the largest genomes of any animal viral pathogen. Approximately 130-360 open reading frames (ORFs) are encoded in the genomes of poxviruses, which vary between genera and between different strains of each species (7).

Poxviruses as a family display very different host range sizes and infect a wide range of hosts from insects to mammals (Fig. 1.1). For example, variola virus (VARV) can only infect humans, while the closely related cowpox virus has one of the largest host range sizes of all poxviruses and has been documented to infect more than 200 mammalian species. However, poxvirus entry is not dependent on binding a specific cell receptor. Instead poxviruses enter host cells by membrane fusion or are internalized by macropinocytosis (8). Poxvirus attachment and membrane fusion is facilitated by a complex of proteins in the viral envelope, which bind to cell surface glycosaminoglycans like chondroitin sulfate or heparin sulfate that are ubiquitously expressed on many host cells (9-11). Therefore, the ability of individual poxviruses to replicate in different host cells depends on the successful manipulation of the host antiviral response. In experimental settings, several genes have been shown to influence the host tropism of different poxviruses and are therefore identified as host range genes (12, 13). These host range genes perform many functions during virus infection including suppressing the induction of pro-inflammatory and interferon-stimulated genes, inhibiting apoptosis and the virus-induced host shut-off of protein translation, as well as inducing the degradation of antiviral proteins (Fig. 1.2) (14). Additionally, these gene products are involved in the maturation of infectious particles or the stimulation of actin polymerization that is important for viral egress and cell-to-cell spread. The work done in this thesis focuses largely on the interactions between E3L and K3L from vaccinia virus (VACV) with the innate immune response protein kinase PKR and the role these interactions play in determining the host range of VACV and the role their orthologs play in influencing the evolution of host range in other poxviruses.

Poxvirus genomes

The central region of poxvirus genomes (~100kb) is highly conserved in gene order as well as in sequence, while the ends of the genomes are more variable in length and content (15). The conserved central region mostly encodes genes whose protein products are involved in critical functions such as transcription, DNA replication, and virion assembly. Genes encoding host response proteins and other non-essential genes tend to be distributed towards the ends of the genome (7, 16, 17). The most terminal regions of the genome are inverted and duplicated at either end and are therefore referred to as the inverted terminal repeat (ITR) region. The ITRs of poxvirus genomes range in size from 0.1-16kb in chordopoxviruses (14, 18) and can be up to

23kb in some entomopoxviruses (19, 20). In VACV, the ITR length ranges from 3.4-16.4kb between different strains (14). Although many of the VACV vaccine strains have shorter ITRs than the laboratory strains, there is no obvious correlation between ITR length and virulence. The ITR of VARV (Bangladesh strain) for example is only about 700bp in length and does not encode a single ORF (21). The variation in size of poxvirus ITRs is believed to be largely due to large genetic duplications that occur during virus replication or by the incorporation of new genetic material from within a co-infected cell as this region of the genome is highly prone to recombination due to the nature of poxvirus genome replication (22, 23). Duplication of large genomic segments in laboratory passaged cowpoxviruses (CPXVs) has even resulted in progeny virus strains with ITRs more than 50kb in length, and genetic recombination has been observed between closely related poxvirus species and between strains of the same species (24, 25). The recombinogenic nature of poxviruses paired with the flexibility to incorporate relatively large DNA sequences into their genome has expanded their use as vaccine vectors and as tools in molecular biology while at the same time making them excellent models for studying genome evolution and host-virus co-evolution (26, 27).

Poxvirus genomes are linear, however at each terminus, a hairpin loop is formed to covalently link the ends of the genome (28). DNA replication begins when this loop is nicked, which allows the viral DNA polymerase to attach and copy the hairpin. The copied sequence then folds back on itself and the two DNA strands separate to allow replication towards the other end of the genome. Following replication a long concatemer of genomes is formed that is resolved by viral nucleases and resolvases (29-31).

Many poxvirus genomes themselves are notably A/T-rich, although distinct ratios of A/T content has been observed in and associated with different poxvirus genera. The A/T-content of parapoxvirus genomes average ~35%, while the A/T-content of entomopoxvirus genomes is more than 80%, and most orthopoxviruses genomes are around 65% A/T-rich (18, 32, 33). The A/T-content within a single poxvirus genome can vary considerably as well. In the orf virus NZ2 strain, for example, the A/T-content ranges from 18-61% for different genes (18). The distinct A/T-content of different poxvirus genera may act as a way to identify potential genomic regions or genes that were recently acquired or horizontally transferred (34). Furthermore, because more closely related poxviruses tend to share similar A/T-contents, this characteristic can also aid in

determining the relationships of different poxvirus species, although the reason behind the differences in A/T-content is unknown.

Gene expression in poxviruses

The ORFs of poxvirus genomes are tightly packed and often overlap with adjacent ORFs. Poxvirus genes are transcribed by viral RNA polymerases in the cytoplasm of host cells and are therefore not spliced but are expressed from the uninterrupted coding sequence. Poxvirus ORFs are transcribed from either the top or bottom strands of DNA, designated as being read to the right or to the left, respectively. The naming of poxvirus genes, therefore, often reflects this transcriptional direction either with an "R" or an "L" after the gene designation. There does not appear to be a correlation between the direction in which a particular gene is transcribed and its transcriptional regulation, although most genes near the termini of poxvirus genomes are transcribed toward the ends and groups of genes are often arranged in transcriptional clusters of the same orientation, presumably to reduce interfering with transcription complexes during gene expression (18). Transcriptional read-through that occurs, particularly during late stages of replication, therefore, produces a large quantity of complementary RNA molecules that can form dsRNA and stimulate an immune response in the host (35).

Transcription of poxvirus genes is regulated temporally by short, conserved promoter motifs and occurs in three stages: early, intermediate and late (36). Poxvirus promoters have been best characterized in VACV and mostly consist of short poly-A/T stretches (37). These promoter motifs are not recognized by cellular RNA polymerases but are instead transcribed by a virally encoded multi-subunit DNA-dependent RNA polymerase along with stage-specific transcription factors (38). Early gene transcription factors are packaged within the infectious virions along with the RNA polymerase to allow gene transcription immediately following infection (39-41). Transcription of intermediate and late genes occurs following DNA replication of the genome (42-44), and several genes have both early and post-replicative promoters and are therefore expressed at both early and late times during infection (45, 46) A synthetic poxvirus promoter often used in the construction of recombinant viruses that is derived from sequences found in VACV is also an early/late promoter that is presumably recognized by all poxviruses to allow gene expression throughout virus replication (36).

Like all viruses, poxviruses use the host translational machinery to translate their mRNAs into proteins. Poxviruses therefore encode proteins that serve to prevent the host shutdown of protein translation that would otherwise occur following infection. A large percentage of genes that are expressed immediately following virion entry and uncoating encode for proteins that are involved in evading the immune response as well as proteins that are required for DNA replication and transcription of intermediate and late stage genes (47). A single round of virus replication from entry to the production of new virus takes approximately 8 hours for VACV, and genome replication usually takes place within the first 2 hours (38). There are four distinguishable virions produced by poxvirus infection (48). The intracellular mature virus (IMV) is a non-enveloped virus particle that is the most abundant form found in the infected cell. Some intracellular virus particles are wrapped by a double membrane derived from the host Golgi network, which forms the intracellular enveloped virus (IEV) (49). As the assembled IEVs begin to bud out of the cell, their membranes fuse with the plasma membrane to form the cell-associated enveloped viruses (CEV), and the virion is propelled outward by growing actin filaments. The released virion is known as the extracellular enveloped virus (EEV), and this form plays an important role in virus dissemination and virulence (50).

Poxvirus phylogeny and host range

There are several complete poxvirus genome sequences available, which has allowed the study of their phylogenetic relationships and gene conservation. A representative phylogenetic tree of 37 fully sequenced poxviruses is shown in Figure 1.1. The entomopoxviruses, which infect insect hosts, represent a sub-family within the *Poxviridae* family and form a separate clade from the chordopoxviruses, which infect vertebrate species. Currently, the chordopoxviruses are further sub-divided into 10 genera: *Avipoxviridae, Crocodilidpoxviridae, Molluscipoxviridae, Parapoxviridae, Orthopoxviridae, Yatapoxviridae, Leporipoxviridae, Cervidpoxviridae, Capripoxviridae,* and *Suipoxviridae*. The latter five genera form a sister clade to the orthopoxviruses and are known as Clade II viruses.

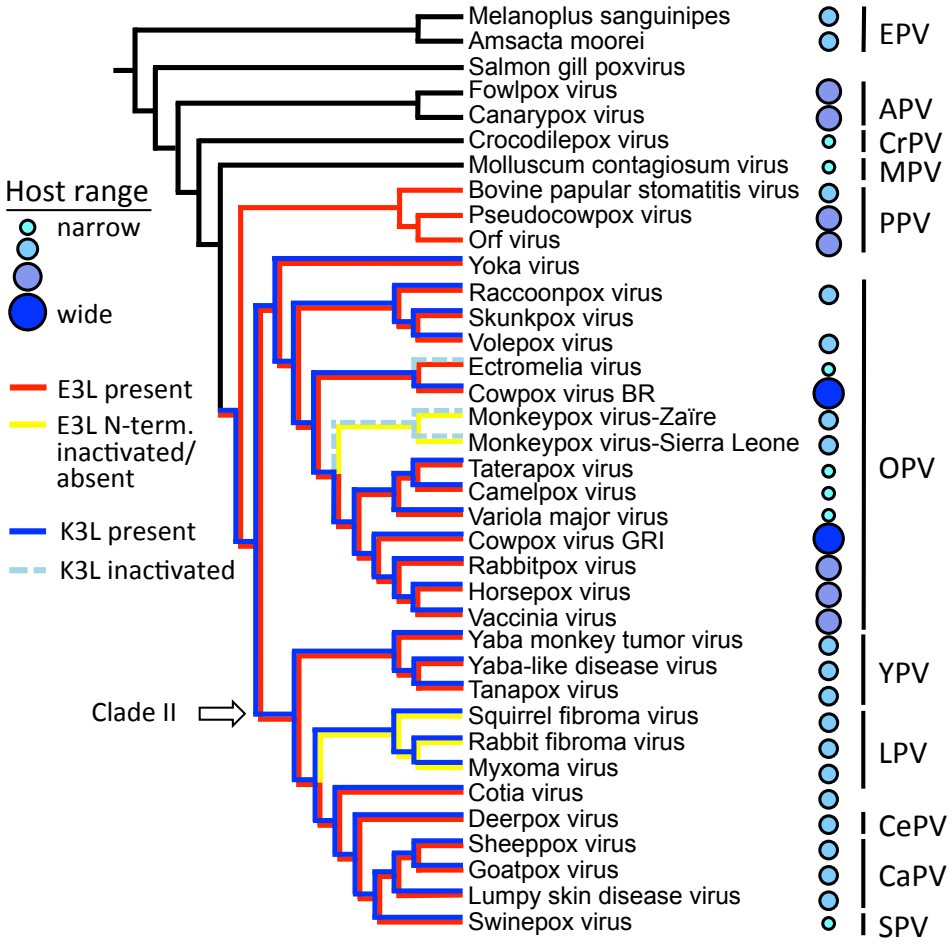

Figure 1.1 Host range and phylogeny of sequenced poxviruses

The poxvirus phylogeny shown is adapted from (14) *and* (57). *The phylogenetic positions of pseudocowpox virus (PCPV), Yoka virus (YKV), Cotia virus (COTV), raccoonpox virus (RCPV), skunkpox virus (SKPV), volepox virus (VPXV), and salmon gill poxvirus (SGPV) are incorporated as published* (53, 55, 56, 58, 59). *The position of squirrel fibroma virus (SQFV) is also included as it is described in Ch. 4. The approximate host range size is indicated by the circles: large dark blue circles represent larger host ranges and small light blue circles represent host ranges restricted to only one or a few species. No circle indicates insufficient data to project the host range. Branches highlighted in red correspond to poxvirus lineages that encode a full-length E3L ortholog and blue branches correspond to lineages encoding a functional K3L ortholog. Poxvirus lineages highlighted with yellow branches encode E3L orthologs that lack a functional N-terminal Zα domain. Lineages highlighted with teal dashes encode a non-functional K3L ortholog due to early stop codons and inactivating mutations. Abbreviations for poxvirus genera are: EPV = entomopoxvirus; APV = avipoxvirus: CrPV = crocodylidpoxvirus; MPV = molluscipoxvirus; PPV = parapoxvirus; OPV = orthopoxvirus; YPV = yatapoxvirus; LPV = leporipoxvirus; CePV = cervidpoxvirus; CaPV = capripoxvirus; SPV = suipoxvirus.*

The identification of new poxvirus species in nature, such as the crocodilepox virus (CRV), which was sequenced from lesions of infected Nile crocodiles on a farm in Zimbabwe, or the unclassified Cotia virus (COTV), which was detected in mice at the Cotia field station in São Paulo, Brazil in 1961, has prompted the need to name new poxvirus genera (51-53). Another example is the Yoka virus (YKV), which was originally discovered in a mosquito pool in the Central African Republic in 1972 (54). YKV groups closely with the *Orthopoxvirus* clade, however, it has been suggested that this virus actually represents a separate genus (55). The recent publication of the genome of salmon gill poxvirus (SGPV) likewise provided evidence that this poxvirus should be classified within its own genus (56). While SGPV encodes several genes found in chordopoxviruses, the authors observed substantial differences in gene order and sequence variation that suggested it is the most evolutionarily divergent member of the *Chordopoxvirus* sub-family. With increased surveillance for environmental poxviruses and the current advances in sequencing technology, it is probable that many more genera will be added to the *Poxviridae* family in the future and a continued analysis of their evolution and host range will be needed. The following is a brief overview of the genomics and host range of the established *Chordopoxvirus* genera.

Avipoxviruses, molluscipoxviruses, and parapoxviruses

The avipoxviruses represent an evolutionarily divergent group of poxviruses that have been found to cause disease in hundreds of bird species in 23 different orders (60). The genomes of four avipoxvirus species have been completely sequenced: fowlpox virus (FWPV), turkeypox virus (TKPV), pigeonpox virus (PGPV), and canarypox virus (CNPV), although 9 species are currently recognized (61-63). Phylogenetic analyses have indicated there are 3 major avipoxvirus clades (designated A, B, and C), and the high sequence divergence between these avipoxviruses and the variability in their genomic organization has led some to suggest the avipoxviruses may be a distinct sub-family within the chordopoxviruses (64). Avipoxvirus genomes are the biggest of all poxviruses and are characterized by multiple gene duplications, which is particularly profound in the ankyrin repeat family genes, N1R/p28 and B22R-related genes. All together, these gene families make up 36% of the CNPV genome (62). The host range of avipoxviruses appears to be broad, but detailed information is limited and determining the exact host range of each species is complicated by the existence of the many avipoxvirus species.

As it is observed for several other poxviruses, mechanical transmission by mosquitos and other biting insects is implicated in the transmission of avipoxviruses between avian hosts (63). Avipoxviruses cannot replicate in non-avian species, but they can initiate protein expression and induce an immune response. For this reason, these viruses have been successfully used for the construction of live recombinant vaccines against many infections including HIV and malaria (63).

Molluscum contagiousum virus (MOCV) is the only identified member of the genus *Molluscipoxviridae* and displays the narrowest host range and tissue tropism of all known poxviruses. MOCV exclusively replicates in human basal keratinocytes, but it's known for causing a skin disease mainly affecting children and immunocompromised people called molluscum contagiosum (65). MOCV as well as the avipoxviruses lack many host range genes that are found in other chordopoxviruses, including orthologs of VACV E3L and K3L (Fig. 1.1). MOCV, on the other hand, possesses many genes that are absent in most other poxviruses, many of which are homologous to cellular genes and may have important immunomodulatory functions for MOCV (66, 67). These viruses must have evolved unique strategies to counteract the host response in their hosts.

Parapoxviruses are widespread pathogens that infect a variety of different mammals including humans. Representatives of this genus include bovine papular stomatitis virus (BPSV), the pseudocowpox virus (PCPV) and orf virus (ORFV), which have been fully sequenced (58, 68). Parapoxvirus genomes are remarkably G/C-rich compared to other poxviruses (>60%), a feature which is also observed in MOCV and CRV (18). BPSV and PCPV cause skin diseases in cattle all over the world, and transmission from cattle to humans can occur (69, 70). Lesions in humans are generally localized and resolve after 4-6 weeks, but more serious complications can occur in immunocompromised people. Orf virus causes serious infections in sheep and goats and can be a significant economic burden in affected areas (69). Orf virus has a moderately large host range and can also infect camels, musk ox, cats, reindeer and humans. Although several genes with recognized host range function are missing from parapoxvirus genomes, parapoxviruses are the only non-orthopoxvirus/non-Clade II poxviruses that contain E3L orthologs, indicating that E3L evolved in a common ancestor (57).

Orthopoxviruses

The most well studied groups of poxviruses are the orthopoxviruses, whose member species share a higher degree of genetic similarity than is observed between members of any other clade of poxviruses (7). Orthopoxviruses exhibit some of the widest variation in host range, but all known orthopoxviruses have mammalian hosts and most infect rodents or small mammals naturally. Most fully sequenced poxviruses fall within this clade of viruses, which is not to say that most poxviruses are orthopoxviruses. Instead, this likely reflects the fact that most of these viruses are important human and animal pathogens, such as VARV and VACV, which both serve as models for poxvirus biology.

Variola virus, camelpox virus, and taterapox virus

VARV caused human smallpox and therefore had a huge impact on human history having killed more people than all other infectious diseases combined (12). Multiple VARV strains existed that exhibited major differences in disease severity. Depending on the case fatality rates (CFRs), VARV strains are classified as either VARV major (CFR 10-30%) or VARV minor (CFR <1%). Edward Jenner himself, who developed the first vaccine against smallpox, observed the natural occurrence of these strains in his original descriptions, and the fluctuation between major and minor strains was similarly observed globally (71). Phylogenetic analyses of VARV strains isolated during the 20th century also indicated that the emergence of VARV minor strains with reduced CFRs occurred independently at least twice during its evolution (72, 73).

VARV is a human specific pathogen and its closest relatives, taterapox virus (TATV) and camelpox virus (CMLV), are also host-specific (Fig. 1.1). CMLV is a widespread pathogen of camels that causes an infection resembling smallpox in humans, but despite the close relationship with VARV, human handlers of infected camels are rarely infected and infections are usually localized and self-limited (74-77). Both VARV and CMLV cause high case fatality rates in their hosts (78, 79). Meanwhile, TATV was isolated from an apparently healthy Kemp's gerbil (*Tatera kempii*) in Benin, but like VARV and CMLV, TATV is also thought to also have a narrow host range, as experimental infections of Mongolian gerbils (*Meriones unguiculatus*), European rabbits (*Oryctolagus cuniculus*) and a rhesus monkey (*Macaca mulatta*) were not productive (80). Although molecular dating of poxviruses is a subject of intense debate (the emergence of VARV is dated between 3,000 and 60,000 years ago depending on the analysis),

phylogenetic analyses of VARV, CMLV and TATV suggest that they diverged from a common ancestor at around the same time (59, 81-84).

Cowpox virus

There are ~90 genes conserved in all sequenced orthopoxviruses, which are thought to represent the minimal genome encoded by the ancestral poxvirus (16). It has been suggested that a cowpox (CPXV)-like virus was the progenitor virus for VARV and all orthopoxviruses because it has the biggest genome of all the orthopoxviruses including all genes said to represent the minimal orthopoxvirus genome, and it has the broadest host range (7). The evolution towards host restriction in VARV and other orthopoxviruses then is presumed to have occurred via successive series of gene deletions and inactivation events (18, 85, 86). CPXV is represented by at least two evolutionarily distinct species, which are represented by the Brighton Red and GRI-90 strains. Phylogenetic analyses indicate that the Brighton Red CPXV strain is most closely related to the murine-specific ectromelia virus (ECTV), while the GRI-90 strain is more closely related to VACV (87). Both CPXV species have an extensive host range, but despite their names, these viruses are most likely maintained naturally in rodent populations, and infections are most often reported in domestic cats (4, 88, 89). The natural hosts of the ancestral orthopoxvirus were presumably also of the order *Rodentia* as the majority of the extant orthopoxviruses have rodent hosts with the exception of VARV and CMLV (4).

Monkeypox virus

Similar to CPXV, there are two distinct monkeypox virus (MPXV) clades, which originate from western and central Africa, respectively (90). While the two MPXV clades are still more closely related to each other than to other orthopoxviruses, they differ greatly in virulence and transmissibility, and there are major genomic differences between them (4, 57, 91, 92). The natural hosts of MPXV are probably also rodents as indicated by a high seroprevalence in rodent species of western African countries where MPXV is endemic. Interest in MPXV has increased since its emergence as a zoonotic disease in humans (93). Because all orthopoxviruses are related immunologically and can be protective against infection by other orthopoxviruses, the cessation of mass vaccinations against smallpox may have allowed humans to become increasingly susceptible to MPXV. Vaccination against smallpox therefore likely provided cross-protection from infection with other orthopoxviruses such as MPXV unintentionally (94, 95). An

outbreak of MPXV related to the western African virus occurred in the United States in 2003. The virus is thought to have been imported from Ghana in a shipment of infected rodents and was transmitted to local prairie dogs that were kept as pets (96). This outbreak marked the first occurrence of human MPXV outside of Africa, where human infections occurred sporadically. No human-to-human transmission nor any human fatalities were observed during the US outbreak, which may be attributed to the lower virulence of the western African MPXV compared to the central African species (97).

A striking difference between the MPXVs and other orthopoxviruses are gene- or domain-inactivating mutations in both orthologs of VACV K3L and E3L, respectively. An early stop-codon found in K3L, as well as deletions of key residues important for interacting with the host protein, PKR, are found in both MPXV species. Furthermore, mutations in the start-codon of the E3L ortholog in MPXV and a 2bp deletion in the N-terminus lead to the functional inactivation of the Zα domain (57). The initiation of translation likely occurs within this domain and results in the production of only the C-terminal dsRNA-binding domain. A recombinant VACV encoding an E3L with the same N-terminal truncation is attenuated in mouse models, but recent work showed that MPXV encodes other proteins that are able to compensate for the loss of this protein domain (98).

Vaccinia virus, horsepox virus and rabbitpox virus

The eradication of smallpox from nature still remains one of the greatest triumphs of the World Health Organization, and the use of VACV as a vaccine in the eradication campaign, has been the driving force for much of the effort to understand its biology (99). For this reason, VACV is the type species of the *Orthopoxvirus* genus and has been the most intensively studied poxvirus. Although the precise origin and natural history of VACV are unknown, the biology of this virus is still relevant to the study of all vertebrate poxviruses and viral diseases more broadly (100). For instance, VACV was the first animal virus to be purified and genetically engineered for use as a vaccine vector for other infectious diseases and recombinant VACVs have been used to develop vaccines against other infectious diseases such as tuberculosis, rabies, vesicular stomatitis virus, and rinderpest in cattle as well as induce cross-reactive immune responses for diseases such as HIV (101-106).

VACV has often been confused with CPXV due to the historical use of the term "cow pox" used by Edward Jenner in his original description of his experiments and observations (107). However, VACV is most closely related to horsepox (HSPV) and rabbitpox viruses (RPXV). The historical and evolutionary relationship of VACV to HSPV and RPXV is not well resolved. Edward Jenner in his own experiments showed that material taken from the "grease" of horses (an infection of horses' heels that may have been caused by a VACV-like poxvirus) directly provided protective immunity against smallpox infection. Additionally because RPXV has only been identified in laboratory rabbit colonies, some believe it is a descendant of a laboratory strain of VACV and do not consider it a separate species (107, 108). Phylogenetic analyses suggest, however, that both HSPV and RPXV are well separated from all of the analyzed VACV strains and likely have an independent evolutionary history (57, 109, 110).

There are numerous strains of VACV that have been developed as vaccine strains over the years, as well as several VACV-related viruses that have been discovered in the environment, some of which are likely to be escaped vaccine strains following the global eradication campaign (111, 112). For instance, VACV-related viruses have caused outbreaks in Brazilian cattle farmers and their herds that are thought to be descendants of vaccine strains of VACV used in the area. Positive PCR tests from the surveillance of local capuchin monkeys (*Cebus paella*) and black-howling monkeys (*Allouata caraya*) as well as successful virus isolation from a wild mouse (*Mus musculus*) during these outbreaks indicate that these species might be natural reservoirs for VACV-like viruses (113, 114).

The most widely used VACV strains for laboratory research are the Western Reserve (WR), which is a mouse adapted derivative of a vaccine strain of VACV, and the Copenhagen strain, which was the first VACV strain to be completely sequenced (115, 116). Each represent the type genomes for the species although extensive passaging in cell culture of these and other VACV strains has led to large variation between VACV genomes mainly due to large deletions. This is particularly apparent in vaccine strains of VACV where attenuation by gene loss was the objective. The four most widely used vaccine strains of VACV for vaccinating against smallpox were EM-63 from Russia, Lister in the United Kingdom, New York City Board of Health (NYCBH) in the United States, and Temple of Heaven (Tian Tan) in China due to the higher safety record of each compared to other VACV strains (99, 111, 117-119). As time went on,

even safer and more attenuated strains were developed. Targeted deletion of 18 non-essential genes from the Copenhagen strain of VACV resulted in the generation of the highly attenuated NYVAC strain (120). Similarly, an alternative approach to attenuation by gene deletion was used to develop the MVA (Modified virus Ankara) and the CVI-78 (derived from NYCBH) vaccine strains by serial passaging the virus in animals or in tissue culture. The MVA vaccine strain, for example, was passaged more than 550 times in chick embryo fibroblasts and accumulated multiple deletions (~30kb of genomic material was lost) that severely restricted its host range (99, 121-125). The efficacy of many of these vaccine strains for protecting against human smallpox is unknown since the virus has been eradicated, and this can no longer be tested. Nevertheless, research continues as the threat of VARV or other orthopoxviruses being used for bioterrorism still exists, and the continued emergence of environmental zoonotic poxviruses such as MPXV remains a possible risk to humans and animals.

The host range of VACV is relatively broad, as indicated by experimental infections of primate, rodent, lagomorph, and ungulate species (95). Moreover, transmission between humans has been observed, which, in immunocompromised individuals, can be fatal (126, 127). In general, the virulence of VACV in humans is much less severe than VARV, and the quest to understand this difference has driven much of the research on this and other poxviruses. While the expanded host range of CPXV can be attributed to the larger set of immunomodulatory genes and genes with host range function, the larger host range of VACV compared to VARV cannot be explained solely by the number of such genes. It is therefore important to look at the interactions between individual host range gene products and the host proteins they serve to regulate to gain a clearer picture of the mechanisms underlying host range in poxviruses.

North American orthopoxviruses

The *Orthopoxvirus* clade can be further subdivided into so-called “old-world” and “new-world” orthopoxviruses. The global distribution of most orthopoxviruses naturally occurs in the eastern hemisphere on the Eurasian and African continents (in the old world), however, there is a subset of closely related poxviruses that are presumed to be endemic to North America. These include the raccoonpox virus (RCPV), skunkpox virus (SKPV), and volepox virus (VPXV). The host range and natural reservoirs for these orthopoxviruses remains largely unknown, although each was isolated from their namesake animal species (128-130). A phylogenetic analysis using nine conserved chordopoxvirus genes placed the North American orthopoxviruses within the

Orthopoxvirus clade, but all three species formed a monophyletic sister group distinct from the formerly described old-world orthopoxviruses, indicating their genetic and evolutionary separation (59).

Clade II Poxviruses

Yatapoxviruses

Viruses within Clade II are comprised of several poxvirus genera that infect a wide range of hosts. The yatapoxviruses, represented by yaba-like disease virus (YLDV), tanapox virus (TPV) and yaba monkey tumor virus (YMTV), are a group of viruses for which few studies have been done to understand the virulence and host range, but all of these viruses are known to infect species of primates including humans. Each virus was isolated from primates in equatorial Africa, but it is not known if primates are the natural hosts for these viruses or even whether they are the only hosts (131, 132). TPV was isolated from humans living in the Tana River basin in Kenya in 1957 and 1962, and a few years later, an outbreak of YLDV occurred in three primate colonies in the US in 1966 (133, 134). YLDV and TPV are closely related to one another exhibiting 98.6% nucleotide identity levels across their genomes and are generally considered to be different strains of the same species, while YMTV is distinct from either antigenically and in its disease presentation (132, 135). YMTV was discovered as the causative agent that induced tumors in rhesus macaques (*Mucaca mulatta*) in Yaba, Nigeria (136). The genome of YMTV is missing 13 ORFs that are found in both TPV and YLDV, which include some genes with putative host range function, although all three viruses appear to be able to infect a similar range of primate species (57, 133, 136-138).

Leporipoxviruses

Aside from the orthopoxviruses, the leporipoxviruses are the second most extensively studied group of poxviruses. The prototype virus from this genus is myxoma virus (MYXV), which is endemic in North and South America. Currently there are two major groups of MYXV recognized: the Californian and South American strains. MYXV infections are restricted to leporid species (lagomorphs including rabbits and hares) for which the genus is named. The South American strains naturally infect the Tapeti rabbit (*Sylvilagus brasiliensis*) causing a mild and self-limited disease in these animals (139, 140). Infection of European rabbits (*Oryctolagus*

cuniculus) by MYXV, by contrast, causes a severe disease known as myxomatosis with lethality rates approaching 100% (141). For this reason, MYXV was used as a biological weapon against invasive European rabbit populations in Australia in the 1950's and later (illegaly) in Europe. Following the introduction of MYXV into these locations, rabbit populations were devastated killing more than 99% of the rabbits. Over time, however, the released strains of MYXV became attenuated in terms of virulence, and the local European rabbit populations simultaneously became more resistant to MYXV infection (3). The sequences of field MYXV isolates has revealed several differences in coding sequences that may explain the reduced virulence of the MYXV over time (142). The majority of observed mutations were located in the ITR, where most immune evasion and host range genes are found, and by analyzing samples collected at different times, the inferred mean evolutionary rate of the MYXV isolates were found to be the highest of any dsDNA virus to date. Because the natural hosts of MYXV are American rabbit species, the switch to the European rabbit host is thought to have driven rapid evolution in this virus particularly in genes that combat the host immune response. To illustrate this point, a single point mutation in the host range gene, M156R, which was found in 13 out of 22 MXYV isolates, was found to attenuate virus replication in cell culture (143). This suggests that in response to the new immune responses of the European rabbit hosts, natural selection for attenuated viruses with this mutation occurred in the field. Attenuation of these viruses presumably prolongs the survival of the animal host and increases the chance of transmission to a subsequent host, which ultimately increases the fitness of the virus.

There are three other less well characterized members of the *Leporipoxvirus* genus: rabbit fibroma virus (RFV), squirrel fibroma virus (SQFV), and hare fibroma virus (FIBV). The complete genome sequence of rabbit fibroma virus was published at the same time as the MYXV genome (144, 145). In the fourth chapter of this thesis, we also present the complete genome sequence of squirrel fibroma virus and discuss the details of its contents more extensively. Both RFV and SQFV are endemic to North America, while FIBV has been primarily identified in Africa and is the only leporipoxvirus to naturally infect species outside of the western hemisphere. The natural hosts of RFV are Eastern cottontail rabbits (*Sylvilagus floridanus*) found in southern US, Central America and northern South America. Like MYXV infection of its natural host, RFV infection of cottontail rabbits causes the formation of cutaneous fibromas, but the disease is otherwise mild and infected rabbits eventually recover. In contrast to MYXV

infection of European rabbits, RFV infection of this species is not severe and rabbits recover from infection within a few weeks (139). While the majority of the leporipoxviruses infect lagomorph species (FIBV infects African hares of the *Lepus* genus), the hosts of the SQFV are species of North American tree squirrels (*Sciurus sp.* and *Tamiasciurus sp.*). Despite its genetic similarities with the other sequenced leporipoxviruses, attempts to infect rabbits with SQFV did not produce disease symptoms or a high virus titer (146).

A characteristic shared by all sequenced leporipoxviruses is that the E3L orthologs lack the N-terminal Zα domain that binds left-handed Z-DNA/Z-RNA and instead encode only the dsRNA-binding domain. While the Zα domain is inactivated and likely non-functional in MPXV, this domain is completely absent from the genomes for all leporipoxviruses. Because all other Clade II poxviruses contain E3L orthologs encoding both the Zα domain and the dsRNA-binding domain, this domain was likely lost in the ancestral leporipoxvirus and may contribute to the relative host range restriction of the viruses in this genus. The loss of the N-terminal Zα domain that is observed in both MPXV and leporipoxviruses represents an interesting example of convergent evolution in very different poxviruses with different host species. Whether the loss of this domain led to an attenuation of these viruses in their natural hosts that resulted in increased transmissibility remains an untested but viable hypothesis.

Cervidpoxviruses, suipoxviruses and capripoxviruses

Both the cervidpoxviruses and the suipoxviruses are represented by a single virus species: deerpox virus (DPV) and swinepox virus (SWPV), respectively. The genomes of two DPV strains have been completely sequenced that exhibit 95% sequence identity at the nucleotide level (147). These viruses have been isolated from wild mule deer (*Odocoileus sp*.) in northwestern US states, although infection of a captive reindeer (*Rangifer tarandus tarandus*) was also reported (148, 149). However, because a high seroprevalence for DPV antibodies was observed in *Odocoileus* deer species that wasn't observed in sympatric elk species (*Cervus sp*.), the host range of this virus is probably not very broad (150). SWPV infections occur worldwide causing a common skin disease in pigs. However, pigs (*Sus scrofa*) are the only known host of SWPV. Although work on host range genes in SWPV is limited, analyses of the genome of SWPV revealed that compared to other Clade II poxviruses, SWPV is missing 13 ORFs that may contribute to the narrow host range of this virus (151). Studies on the K3L ortholog in SWPV

showed that this ortholog is capable of inhibiting human PKR in yeast and cell culture-based assays (152, 153) and preliminary evidence suggests that this viral protein shows a species-specific preference for strongly inhibiting PKR from swine (Peng and Rothenburg, unpublished).

The genus *Capripoxviridae* contains three closely related members: sheeppox virus (SPPV), goatpox virus (GTPV), and lumpy skin disease virus (LSDV). These viruses naturally infect sheep, goats, and cattle, respectively, of north equatorial Africa and parts of Asia although some SPPV and GTPV isolates can infect both sheep and goats (154, 155). These viruses are of high interest to agricultural and veterinary communities as infections by capripoxviruses have led to serious economic losses. Mortality rates for SPPV and GTPV are near 100% for their respective hosts, and although LSDV mortality rates are often much lower (~1%), they can occasionally reach 75% (154). The genomes of the capripoxviruses display approximately 96% sequence identity with one another and each possess a similar set of immunomodulatory genes (156, 157). A study of African wildlife indicated a relatively low prevalence for these viruses in the wild, although, because of their high virulence, this group of viruses is still closely watched due to the risks they pose. Nevertheless, the host range for these viruses is probably relatively narrow, and human infections have not been reported.

Poxvirus immune evasion by host range genes

Poxvirus pathogens are excellent at hijacking and taking over their host cells due to the expression of an impressive arsenal of immunomodulatory genes that inhibit and subvert host responses. Poxvirus genes that modulate the host response and control virulence are generally located near the termini of poxvirus genomes and are most variable between species. Many of these genes are dispensable for virus replication in cell culture, but viruses that have been engineered to lack them are often attenuated in infection models. Poxvirus genes that are important for viral replication in a subset of cells or host animals and genes that are important for differences in poxvirus host range are referred to as host range genes (12). To date, approximately 15 genes have been identified that possess host range function in different poxvirus species as deletion of these genes leads to replication defects in some, but not all, otherwise permissive cells (13). These genes can be grouped into distinct gene families, although interestingly, not a single host range gene family has been identified that is present in all poxviruses (57). Instead, most of these gene families actually show evidence for multiple

independent lineage-specific inactivation events, such as the inactivation of the K3L orthologs in MPXV and ECTV and the loss of the N-terminal domains of E3L orthologs in MPXV and leporipoxviruses. The major targets of poxvirus host range genes are the key mediators of innate immune response including interferon and complement pathways as well as the apoptotic and inflammatory responses. In the following section, both host innate immune pathways and the host range genes that interact with them will be discussed.

Poxviral antagonism of the interferon response

Interferon (IFN) responses are strategically and systematically targeted by all poxviruses, as this host defense constitutes one of the most potent barriers to infection. IFN induces the expression of antiviral genes within the infected cell and also promotes T helper cell responses (158-160). IFN signaling occurs through IFN receptors (IFNARs), which bind extracellular IFN at the cell surface to mediate the recruitment and activation of intracellular Janus kinases (JAKs) and the phosphorylation of specific pairs of signal transducers and activators of transcription (STATs) (161). Phosphorylated STAT dimers translocate to the nucleus or activate interferon response factors (IRFs) to induce transcription of several interferon-stimulated genes (ISGs) involved in establishing an antiviral state (162, 163). Multiple IFN family genes are found in all vertebrates, which underscores the importance of this response for controlling virus infection from a very early point in vertebrate evolution. IFN proteins were originally discovered by their ability to interfere with virus replication (164). The critical importance of their activity was later confirmed in IFNAR-deficient mice, which exhibited an extreme susceptibility to viral infection and often serve as animal models of infection when suitable animal models cannot be used (165, 166). IFN family genes are categorized as either type I or type II based on structural homology, the receptors they use and the signaling pathways they trigger (167, 168). Type I IFN proteins are further sub-divided into IFN-α, -β, -ε -κ, -ω, and -ν, which all bind to and signal through the IFN-α/β receptors (167, 169-172). IRF3 and IRF7 are key transcriptional regulators of type I IFN induction (173-175).

IFN-γ is the only recognized type II IFN protein, which differs considerably from the type I IFNs in structure and signals through a distinct receptor (176). Type II IFN-γ plays a critical role in limiting poxvirus infection (165, 177). To overcome the antiviral effect of IFN-γ, several poxviruses encode viral IFN-γ receptor homologs that competitively bind IFN-γ to

prevent signaling (Fig. 1.2) (178-180). In MYXV, the IFN-γ receptor homolog called M-T7 specifically binds to rabbit IFN-γ while IFN-γ receptor homologs from orthopoxviruses possess a broader specificity for binding IFN-γ from different species, likely reflecting the evolutionary history of the orthopoxviruses with their hosts (179, 181-183). M-T7 in MYXV was also shown to bind a broad spectrum of chemokines to modulate the immune response, although this activity was not species-specific and may serve to supplement the IFN-γ binding function (184). Like the IFN-γ receptor homologs, many poxviruses also encode a protein that is similar to the cellular IFN-α/β receptor (185). The best characterized of these comes from VACV (B18R in VACV-WR). This protein contains three immunoglobulin domains and inhibits IFN–α/β signaling by competitive binding of IFN-α/β from various mammalian species (186-188). Both of these gene families in poxviruses aid in limiting the IFN-mediated establishment of the antiviral state.

VACV C7L has also been shown to inhibit the activity of type I interferon signaling via IRF-1, which interferes with the expression of ISGs and the establishment of the antiviral state (189) (Fig. 1.2). VACV C7L was identified as a host range gene due to the fact that it restored viral replication of a K1L deficient VACV in human MRC-5 and swine LLC-PK1 cells but not rabbit RK13 cells (190). C7L orthologs are found in all orthopoxviruses and Clade II poxviruses, however, the molecular mechanism of its host range function is currently unknown (191, 192). In leporipoxviruses, the C7L ortholog has been duplicated twice and is present in three tandem copies (M062R, M063R, and M064R) (57). From targeted gene knockouts of each copy, only deletion of M064R did not lead to a defect in host range, but it was still found to be a virulence factor for the virus (193). Deletion of M063R, on the other hand, dramatically reduced MYXV replication in rabbit cell lines, but did not affect replication in monkey cells (BGMK and BSC-40) and only moderately affected replication in human and murine cells (HOS and 3T3, respectively) (194). Similarly, a deficiency in M062 led to replication defects of MYXV in several cell lines except some human cell lines and BSC-40 cells (195). The M062 protein was shown to specifically interact with the rabbit version of the antiviral protein, SAMD9, which may explain its host range function for MYXV (196) (Fig. 1.2).

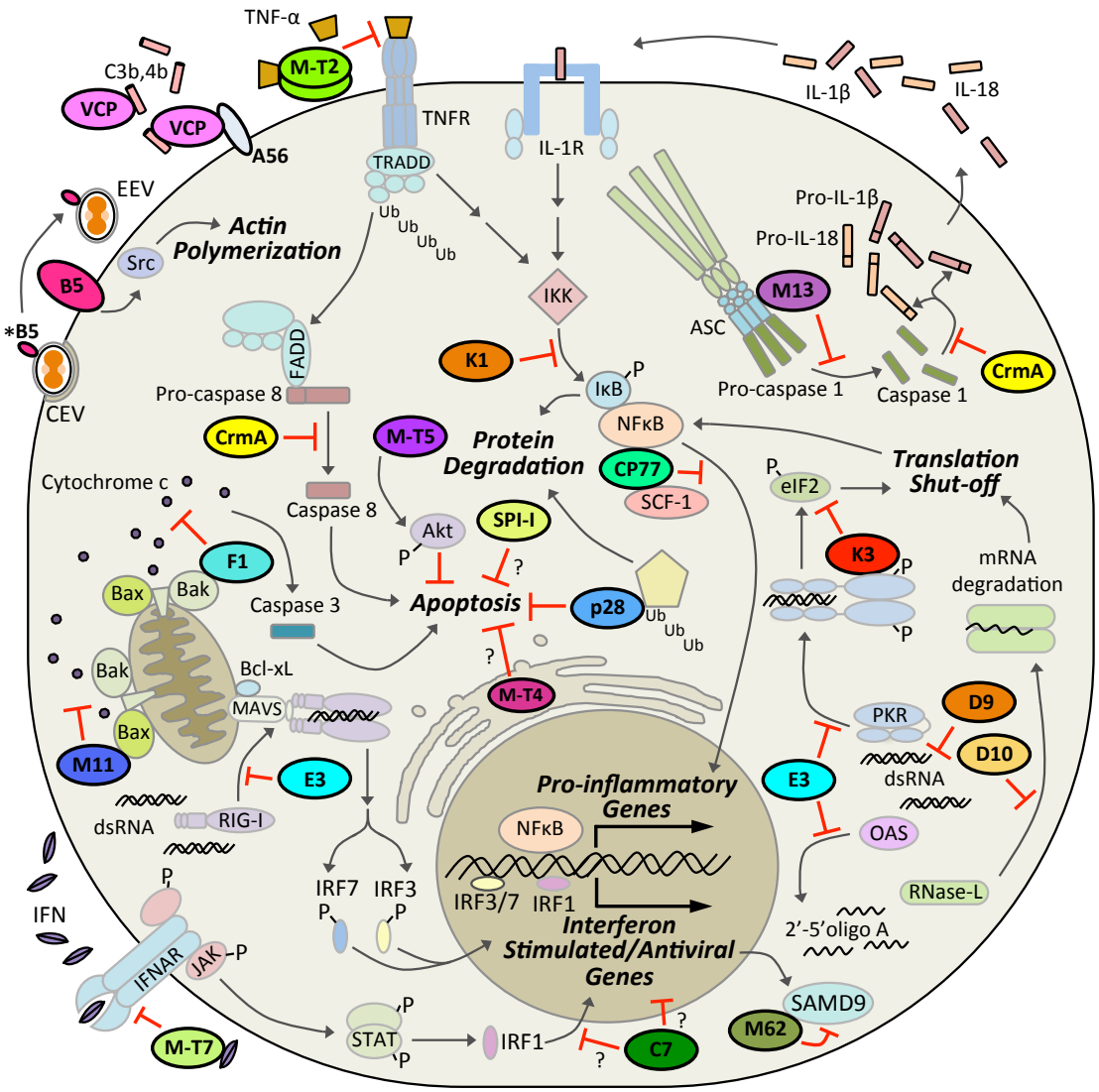

Figure 1.2 Molecular interactions of host range factors in poxviruses.

*The host range function of genes encoded by poxviruses can be attributed to several interactions with specific host proteins. The specificity of these interactions with their host targets can either restrict or expand the range of hosts in which the virus can replicate. Abbreviations used: dsRNA = double stranded RNA; MAVS = mitochondrial antiviral signaling protein (also known as IPS-1/Cardiff/VISA); TNFR = tumor necrosis factor receptor; IRF (1,3,7) = interferon response factor; CEV = cell associated enveloped virus; EEV = extracellular enveloped virus; Ub = ubiquitin; SCF-1 = Skp1:Cullin-1:F-box ubiquitin ligase complex; eIF2 = eukaryotic translation initiation factor 2; IFNAR = interferon receptor; IFN = interferon; Bcl-xL = B-cell lymphoma extra large; FADD = Fas-associated Death domain protein; TRADD = TNFR-1 associated Death domain protein; Organelles and proteins not drawn to scale. * B5 is present on both cellular and EEV membranes (here shown in two sizes) and promotes the transition from CEV to EEV during viral replication. Modified after* (14).

Poxviral defenses against cellular inflammation and host complement

Several other signaling pathways also stimulate the induction of ISGs via interleukin-mediated or tumor necrosis factor (TNF)-mediated signal transduction and activation of the pro-inflammatory transcription factor, NFκB (197). NFκB comprises an important family of transcription factors that regulate the innate interferon and inflammatory responses, including apoptosis (198). In uninfected cells, NFκB is bound to its inhibitor, IκB, which prevents NFκB from traveling to the nucleus (197). A kinase complex identified as the IκB kinase (IKK) complex is responsible for phosphorylating IκB following its own activation, which is then degraded by the proteasome (199). The degradation of IκB releases NFκB and allows it to translocate to the nucleus where it stimulates the transcription of an array of antiviral and pro-inflammatory genes including type I IFN (200).

The MVA vaccine strain of VACV contains multiple genomic deletions and has been useful for identifying the importance of various poxvirus genes for host range through complementation experiments. The K1L gene is partially deleted in MVA and insertion of the full-length K1L in MVA restored virus replication in rabbit RK13 cells, but not in other cells normally permissive to VACV replication (124). Deletion of K1L from VACV-Cop similarly resulted in reduced replication in RK13 cells, but not in human, monkey, or pig cell lines (190). Cells infected with this virus induce a rapid shutdown of protein synthesis suggesting K1L may act upstream of cellular proteins that inhibit protein translation, and further studies indicated K1L inhibits the activation of the NFκB pathway (201, 202). Deletion of K1L in VACV resulted in an increase in IκBα degradation and led to an increase in activated NFκB and NFκB transcriptional activity (202) (Fig. 1.2). K1L orthologs are found in all orthopoxviruses except VARV, CMLV and TATV where early stop-codons and short indels result in the inactivation of the ORF. Interestingly, these gene inactivations occurred independently in each of these three viruses, suggesting the deletion of this gene may play a role in restricting poxvirus host range as these three viruses exhibit some of the most restricted host ranges of all poxviruses (57).

TNF is a pro-inflammatory cytokine induced by NFκB activity that is primarily secreted by macrophages and activated T-cells (203). Several poxviruses also encode decoy homologs of the TNF receptor that function by sequestering extracellular TNF (204-207). The best-studied poxvirus TNF receptor homologs are the T2-like proteins encoded by leporipoxviruses (Fig. 1.2). M-T2 from MYXV binds rabbit TNF comparably to the cellular rabbit TNF receptor and is

important for MYXV pathogenesis (204, 205). An M-T2 deficient MYXV replicated well in RK13 cells but showed a replication defect in RL-5 cells (205, 208). Like the viral mimics of the IFN receptors, M-T2-like proteins are likely to have a large effect on virus host range as the ligands they bind from different species often display great variability in sequence. M-T2 was shown to specifically interact with rabbit TNFα, but showed no ability to interact with TNFα from human or mouse origin, and a T2-like protein from VARV (CrmB) was better able to inhibit human TNF than mouse or rat, which correlates with the host range of these viruses (209, 210).

Cellular inflammation is also associated with the activity of a group of proteins that form complexes of initiator proteins called inflammasomes (211). Inflammasomes are distinct protein complexes made up of a family of proteins called NOD-like receptors (NLRs), although recently other sensor proteins have been associated with different inflammasome complexes in response to different stimuli (212-216). These NLRs recognize and respond to different stimuli generated by viruses, bacteria and toxins to induce an inflammatory response (217, 218). Once activated, NLRs oligomerize and subsequently recruit and activate inflammatory proteases like caspase-1 (219). The activation of caspase-1 requires proteolytic processing of its pro-domain, and this process is mediated by ASC (adaptor protein apoptosis-associated speck-like protein containing a CARD), which enables interactions between related domains on the NLR and the unprocessed pro-caspase-1 (220). The release of cleaved caspase-1 allows it to act on several cytokines, including pro-interleukin (IL)-1β (221). IL-1β, as well as IL-18, belongs to the IL-1 family of cytokines that regulate T-cell responses and activates natural killer (NK) cells in response to IFN-γ signaling or cellular inflammation (222). Both proteins are cleaved from a precursor pro-IL form into a shorter active form by the IL-1β-converting enzyme (ICE) and are then secreted from the cell (223).

MYXV encodes a small protein called M013L that contains a pyrin domain like those found in inflammasome NLRs that mediate their interaction (224). M013L was shown to inhibit the activation of caspase-1 in human THP-1 cells, and M013L proteins from MYXV as well as those from the related RFV were observed to physically interact with the adaptor protein, ASC, which contains a similar pyrin domain (224, 225) (Fig. 1.2). Deletion of M013L impaired MYXV replication in rabbit RL5 cells and primary blood lymphocytes and monocytes, but had no effect on MYXV replication in rabbit RK13 cells, indicating a role for this gene in the cell

tropism of MYXV and possibly also the host range. Orthologs of this gene are only found in Clade II poxviruses, although loss of this gene probably occurred independently in the capripoxviruses and in the yatapoxvirus YMTV, as each of these viruses lacks an M013L ortholog, but they are not directly related phylogenetically (57).

In addition, poxvirus caspase inhibitors such as CrmA in CPXV (SPI-2 in VACV) inhibit the cleavage and secretion of these IL-1 family cytokines to modulate their inflammatory effects (226) (Fig. 1.2). Other poxviral serine protease inhibitors (serpins) also play important roles in regulating inflammation, apoptosis and complement activation (227, 228). Three serpin proteins are encoded by orthopoxviruses, which target caspases including caspase-1, as well as other caspases and host complement factors. Deletion of the serpin, SPI-1 from RPXV and VACV impaired virus replication in human cells (RPXV and VACV) or pig cells (RPXV), but did not affect replication in other cells (229, 230). This host range activity of the poxvirus serpins has only been shown for SPI-1, but it remains likely that the other serpins also contribute to the host range of poxviruses.

The complement system is an ancient arm of the innate immune system and is targeted by several pathogens including poxviruses (231). In response to an invading pathogen, complement convertases initiate a series of enzymatic reactions via classical and alternative pathways that result in the destruction of the infected cell. VACV encodes a complement control protein (VCP) that is localized on the surface of infected cells in association with another VACV protein, A56, and which has been shown to interfere with the complement cascade at multiple points (232, 233) (Fig. 1.2). VACV VCP is made up of four short consensus repeats (SCR) that are homologous to the basic units of mammalian complement regulators (234, 235). A protein related to VCP, called B5R has been identified as a host range gene because it was inactivated in an attenuated vaccine strain of VACV (LC16m8), which cannot replicate in Vero cells, but replicates well in rabbit RK13 cells (235). Complementation of B5R in this strain increased plaque size and restored replication of this virus to that of the parent virus strain. Additionally, a strain of RPXV lacking B5R produced smaller plaques in RK13, CV1 and Rat2 cells, indicating viral spread was diminished, but the virus was still able to replicate in Vero cells even without plaque formation (236). Unlike VCP, which is a virulence factor for VACV that binds complement factors, B5R interacts with Src kinase to phosphorylate another VACV surface protein to induce actin polymerization required for cell-to-cell spread (237) (Fig. 1.2). All

orthopoxviruses and Clade II viruses encode an ortholog of VCP with different numbers of SCR domains, and all orthopoxviruses except MPXV and TATV encode an ortholog of B5R (57). Although only B5R has been attributed with a host range function, VCP orthologs were shown to inhibit complement in a virus and host species-specific manner. The VCP ortholog from VARV inhibited complement factors, such as C3b and C4b, from human and baboon better than VACV VCP, which was a better inhibitor of guinea pig, cat, and dog complement proteins (238, 239). The species-specificity of VCP activity in these viruses correlated with their host range, and therefore VCP likely also contributes partially to the host range of these viruses.

Induction and inhibition of apoptosis by poxviruses

Apoptosis is a form of programmed cell death in which defective or unwanted cells are removed from an organism (240). Apoptosis is also an effective mechanism for getting rid of virus-infected cells and thus can function as a form of innate immunity (241). A key event in the induction of the apoptotic response is the activation of a family of pro-apoptotic caspases (242). These caspases are often targeted by viruses, including poxviruses, to prevent the initiation of apoptosis. MOCV, for example, prevents the activation of the initiator caspase, caspase-8 that signals apoptosis from Fas or TNF ligand binding and subsequent signaling cascades (243) Additionally, CrmA from CPXV, which inhibits the pro-inflammatory ICE activity, can inhibit granzyme B-mediated apoptosis, initiated by diverse stimuli including TNF ligand binding (244-246).

Several poxvirus proteins that interfere with apoptotic signaling have been characterized in MYXV. M011L from MYXV prevents the release of cytochrome c from mitochondria that stimulates apoptosis by inhibiting the loss of inner mitochondrial membrane potential (247) (Fig. 1.2). VACV F1L fulfills a similar function in orthopoxviruses through sequestration of the mitochondrial membrane proteins Bax and Bak (248-253). M011L and F1L are structurally related to the cellular Bcl-2 family proteins, which are localized to mitochondrial membranes (254, 255). Additionally, MYXV expresses an endoplasmic reticulum (ER)-localized protein (M-T4) that inhibits apoptosis by an unknown mechanism (256, 257). M-T2, which acts as an extracellular TNF receptor homolog in MYXV also functions as an intracellular inhibitor of apoptosis (208, 258).

The M-T5 protein of MYXV has also been linked to the inhibition of apoptosis and exhibits homology with CP77 from CPXV (CHOhr) (259, 260). These two proteins are members of largest family of poxvirus proteins, which encode ankyrin repeat domains (ANK) that mediate protein-protein interactions (261). Most of theses proteins also encode F-box-like domains in their C-terminus (also known as Pox protein Repeats of Ankyrin C-terminal domains, PRANC) (262, 263). CPXV CP77 and M-T5 are the only two PRANC proteins with identified host range function (259, 264). CP77 is required to rescue VACV replication in non-permissive CHO cells, which otherwise induces apoptosis via TNFα-mediated activation of NFκB (265). CP77 likely binds to p65 of NFκB and the cellular SCF E3 ligase complex, which leads to the degradation of this important transcription factor (Fig. 1.2). CP77 has also been shown to rescue replication of ECTV in poorly permissive hamster and rabbit cells (266). MYXV encodes two copies of M-T5 in its ITR, and it is essential for pathogenesis in rabbits (259). Deletion of M-T5 led to a reduction of viral replication in rabbit RL5 cells and a subset of human tumor cells, however, no defect was observed in rabbit RK13 cells (267). The defect in replication was correlated with a reduction of Akt phosphorylation, so M-T5 is thought to inhibit apoptosis through interactions with Akt (Fig. 1.2).

Another family of host range genes that affects apoptosis is the p28 family for which ECTV p28 is the prototype member. ECTV p28 encodes a unique combination of N-terminal KilA-N and C-terminal RING domains (268). The mechanism of the host range function of p28 is not well understood, but it is suggested that the ubiquitin ligase activity of the RING domain is important for targeting host proteins for degradation to prevent the induction of apoptosis (269, 270) (Fig. 1.2).

Cellular sensors of double-stranded RNA and poxviral evasion strategies

Virus infection induces IFN production through the detection of viral pathogen-associated molecular patterns (PAMPs) by host pattern-recognition receptors (PRRs). This initial sensing by the host is the first obstacle a virus must overcome in order to successfully replicate in a given host. PRRs can sense components of the viral envelope such as glycoproteins, the viral genome itself or products generated during virus replication such as double-stranded (ds) RNA. Double-stranded RNA is a particularly potent danger signal for the cell, as it is not a normal constituent of the cellular cytoplasmic environment. Double-stranded RNA is generated

following infection with most viruses including not only dsRNA viruses, but also DNA viruses like poxviruses, which actually generate a large amount of dsRNA due to the accumulation of overlapping transcripts, particularly late in infection (35). Several cellular proteins can sense and are activated by dsRNA because it is strong indicator of infection by a broad range of viruses. Two major groups of antiviral dsRNA sensors that are found in most vertebrate cells and that are important regulators of poxvirus replication and host range are the RIG-I-like receptors (RLRs), and the 2'-5'-oligoadenylate synthetases (OASs).

The RIG-I-like receptor (RLR) family is comprised of RIG-I, melanoma differentiation-associated gene 5 (MDA5), and laboratory of genetics and physiology 2 (LGP2). RIG-I and MDA5 consist of two N-terminal caspase recruitment domains (CARDs), a DExD/H box RNA helicase domain and a C-terminal repressor domain, while LGP2 lacks the CARD domains necessary for antiviral activity (271, 272). Both RIG-I and MDA5 recognize distinct forms of cytoplasmic dsRNA. RIG-I recognizes short dsRNA molecules with 5' triphosphates, while longer dsRNA molecules activate MDA5 (273, 274). The helicase domains of RIG-I and MDA5 are important for sensing these viral RNA molecules, but it is the CARD domains that are responsible for triggering the intracellular antiviral signaling cascades through direct interactions with the mitochondrial antiviral sensor protein, MAVS (also known as IPS-1, VISA or CARDIF) (275, 276). Signaling by MAVS leads to the phosphorylation and nuclear translocation of IRF-3 and IRF-7 and subsequently, the induction of several ISGs (277). The 2'-5'-oligoadenylate synthetase proteins (OASs) are a family of IFN-induced antiviral restriction factors that also sense and respond to viral dsRNA (278-280). Activated OAS family proteins synthesize 2'-5'-phosphodiester-linked oligoadenylate molecules that activate the latent effector protein RNase L (281). The endoribonuclease activity of activated RNase L causes the degradation of cellular and viral mRNAs (single-stranded RNA) thereby preventing protein translation and restricting viral replication (282).

Two genes in VACV, called D9 and D10, have been implicated in preventing the accumulation of dsRNA to avoid detection by these PRRs. D9 and D10 are decapping enzymes that hydrolyze the 5' cap of mRNA transcripts (283, 284), but their inactivation in VACV leads to a dramatic increase in dsRNA accumulated during infection of several different cell types (285). Inactivation of both D9 and D10 in the same virus led to replication defects in monkey (BSC-1 and Vero) and human (HeLa, MRC-5, and A549) cells, but not in Syrian hamster BHK-

21 or murine MEF cells and therefore together provide a host range function. Individual deletion of either D9 or D10, however, only led to moderate effects on virus replication, so their cooperation is important to this host range function although no evidence was found that D9 and D10 directly interact with each other (286, 287). By tightly regulating viral mRNA stability, it was proposed that the decapping activity of D9 and D10 control the levels of dsRNA generated by complementary transcripts during infection, which was required for preventing the antiviral activity of RNase L and the phosphorylation of IRF-3 in some host cells.

Despite the activity of D9 and D10, poxvirus replication does produce a great deal of dsRNA during post-DNA replicative stages of infection. VACV E3L prevents the activation of host sensors such as RIG-I and OAS by binding dsRNA, which leads to a block in IRF-3 and IRF-7 activation and IFN-α/β production (288-290). VACV E3L is a multifunctional host range gene that is critically important for antagonizing the IFN response to allow the replication of poxviruses in most cells (291-293) (Ch.2). VACV E3L consists of an N-terminal Z-DNA binding domain (Zα) and a C-terminal dsRNA-binding domain. Deletion of E3L from VACV leads to replication defects in cells from several species, but not in chicken embryonic fibroblasts, BHK-21, or RK13 cells (290, 294).

RNA-dependent protein kinase, PKR

There are many host proteins involved in mediating an immune response against viral infection, and the orchestration of their activities together is necessary to give host cells the advantage in most host-virus interactions. Inhibition of one or more of these proteins is required in order for viruses to successfully replicate within a given host cell. The focus of the work in this thesis is on a single host protein that is a key mediator of many aspects of the innate immune response to virus infection that have been discussed in this chapter. The RNA-dependent protein kinase, PKR, is a pattern recognition receptor that detects viral dsRNA in the cytoplasm but also has a dual function as an antiviral effector to restrict viral replication. Activated PKR causes a shutdown of cellular protein translation, which induces the expression of NFκB regulated IFN and inflammatory cytokines (295), and the activation of PKR has also been associated with the induction of apoptosis following cellular stress such as during a virus infection (296).

PKR is expressed in all vertebrate cells and is composed of two N-terminal dsRNA-binding domains and a C-terminal kinase domain, which are connected by a flexible linker

region of variable length (297). Latent PKR is activated by cytoplasmic dsRNA, which it senses and binds with its two dsRNA-binding domains. For human PKR, the first dsRNA-binding domain exhibits a higher affinity for dsRNA and is more critical for PKR activation (298, 299). Activated PKR forms dimers that catalyze phosphorylation reactions on serine 51 of the alpha subunit of the eukaryotic translation initiation factor 2 (eIF2α) (300, 301). The phosphorylated form of eIF2α binds more tightly with its guanine exchange factor, eIF2B, which prevents the recharging of the GDP-bound eIF2α to its GTP-bound form. This then renders eIF2α incapable of binding Met-tRNA and initiating translation of the mRNA and leads to a shutdown of cap-dependent protein synthesis, including the translation of both cellular and viral proteins. As a consequence of PKR's central role in the innate immune response, many viruses have evolved mechanisms to subvert its antiviral activities (302). The continued antagonism by viral inhibitors, including inhibitors encoded by poxviruses, has driven the rapid evolution of PKR, and positive selection at specific residues involved in the interactions with these viral proteins has been identified in PKR from certain vertebrate lineages (153, 303).

As a dsRNA-binding protein, VACV E3L also inhibits the activation and activity of PKR in addition to RIG-I and OAS (304-307) (Fig. 1.2). Because E3L inhibits several PRRs that detect dsRNA, it is not clear which targets of E3L are responsible for its host range function or what the molecular mechanisms are for this function. There is strong evidence, however, to suggest that PKR is the main target of E3L at least in some cell types (308) (Ch. 2). In the second and third chapters of this thesis, the host range function of E3L for VACV replication in hamster host cells is investigated in more detail with the aim of uncovering the molecular mechanism responsible for the defect in host range caused by deletion of E3L from VACV.

In addition to E3L, many poxviruses also encode a second inhibitor of PKR called K3L in VACV. K3L shares structural homology with the S1 domain of eIF2α, the target of PKR, and therefore K3L competitively binds activated PKR as a pseudosubstrate to inhibit its activity (309, 310) (Fig. 1.2). Like E3L, deletion of K3L from VACV impaired virus replication in a subset of mammalian cells (murine L929 and hamster BHK-21 cells), but did not affect replication in others (human HeLa and rabbit RK13 cells) (290, 311, 312). K3L from VACV and its ortholog from MYXV, M156R, have been shown to exhibit species-specificity in their inhibitory interactions with PKR (143, 153, 303). Because K3L sequences from different poxviruses are highly variable (as low as 21% protein sequence identity between different species) and PKR

from the species they infect are also quite divergent (~60% protein sequence identity between human and mouse PKR), we hypothesized that differences in their interactions are responsible for the observed host range function of K3L, and that K3L orthologs have evolved to specifically inhibit PKR of their respective hosts. In addition to analyzing the host range function of E3L, in this thesis the host range function of VACV K3L for virus replication in different host cells is also examined and discussed (Chs. 2 and 3).

Although the natural host of VACV is unknown, its relationship to other orthopoxviruses and infection studies in different animal models and host cells suggest that the natural host of the VACV ancestor was likely a small mammal, such as a rodent. As previously mentioned, a host range defect in VACV replication was identified in Syrian hamster BHK-21 cells from the deletion of K3L, but not E3L (290), therefore the analyses into the host range function of these viral proteins in this thesis focus on their interactions with host PKR proteins from the Syrian hamster and related hamster species. The Syrian hamster (*Mesocricetus auratus*) is a widely used model organism for bacterial and viral infection due to the ease of raising this animal in captivity. Other hamster species have also been or are still used in scientific research, such as the Chinese hamster (*Cricetulus griseus*), although many hamster species were not easy to keep or breed. All Syrian hamsters used in research laboratories up to 1971 originated from a single female hamster and her litter that were dug up in the early 1930s by a naturalist in northern Syria, and this species is found only in a small region of this area (Fig. 1.3). Meanwhile, the related Turkish hamster (*Mesocricetus brandtii*) has a much broader home territory that overlaps with the Syrian hamster's, although it is still relatively small compared to the geographic range covered by the Chinese hamster in northern East Asia or the Armenian hamster (also known as the migratory hamster, *Cricetulus migratorius*) across broad tracts of the Asian continent. Old-world orthopoxviruses like VACV, are likely to have been present across several regions of Asia for a long time, therefore it is possible that their geographic boundaries overlapped with these hamster species. If these viruses were maintained in small mammals, it is possible that the hamster species may have encountered and evolved alongside VACV-like or other related orthopoxviruses.

The concerted effort of host antiviral genes is important for preventing virus infection, and in the same way small species-specific differences can lead to changes in host susceptibility, the unique cooperative activities of several viral proteins also dictate the range of hosts a virus

can infect. Poxviruses have a tremendous coding capacity compared to other viruses, and as a family, poxviruses encode a remarkable array of genes, the products of which for many appear to have co-evolved in their respective hosts to specifically counteract components of the immune response. The fourth chapter of this thesis is a genomic analysis of a poorly characterized poxvirus of the *Leporipoxvirus* genus that exhibits a very different host range from the other better-characterized leporipoxviruses. The detailing of the genome of the SQFV along with the characterization of some of its potential host range genes is an important first step in understanding how each of the genes encoded by this poxvirus contributes to its host tropism and species-specific virulence. Additionally, a study of its evolutionary relationship to other poxviruses serves to support the overarching goal of this thesis, which is to understand the genetic and molecular determinants of host range in poxviruses.

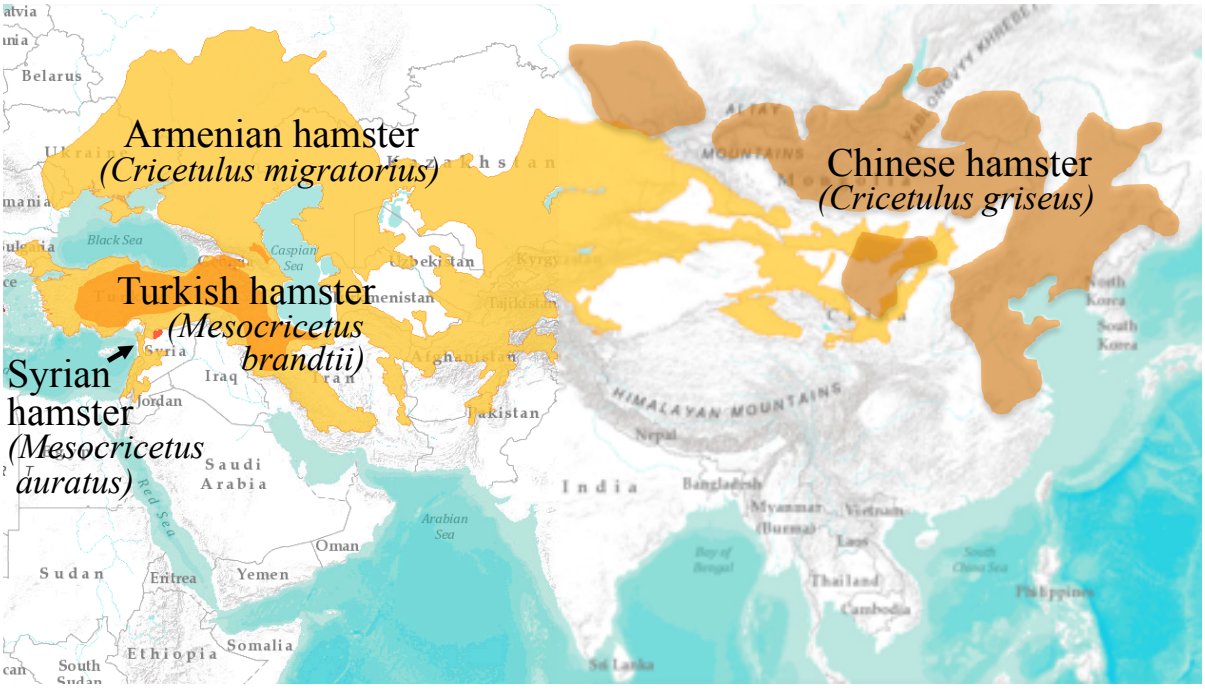

Figure 1.3 Hamster home territories.

The territory ranges of the four hamster species used in this thesis are pictured (IUCN Red List). The Syrian hamster originates from a very small region of northern Syria (red), while the other hamsters are found across broader areas of the Middle East and Asia.

References

1. Jones KE, Patel NG, Levy MA, Storeygard A, Balk D, Gittleman JL, Daszak P (2008) Global trends in emerging infectious diseases. *Nature* 451(7181):990–993.

2. Karesh WB, Dobson A, Lloyd-Smith JO, Lubroth J, Dixon MA, Bennett M, Aldrich S, Harrington T, Formenty P, Loh EH, Machalaba CC, Thomas MJ, Heymann DL (2012) Ecology of zoonoses: natural and unnatural histories. *Lancet* 380(9857):1936–1945.

3. Fenner F (2000) Adventures with poxviruses of vertebrates. *FEMS Microbiol Rev*. 24(2):123-133.

4. Essbauer S, Pfeffer M, Meyer H (2010) Zoonotic poxviruses. *Vet Microbiol* 140(3-4):229–236.

5. Dales S, Siminovitch KA (1961) The development of vaccinia virus in Earle's L strain cells as examined by electron microscopy. *J Biophys Biochem Cytol* 10:475–503.

6. Munyon W, Paoletti E, Grace JT (1967) RNA polymerase activity in purified infectious vaccinia virus. *Proc Natl Acad Sci USA* 58(6):2280–2287.

7. Gubser C, Hué S, Kellam P, Smith GL (2004) Poxvirus genomes: a phylogenetic analysis. *J Gen Virol* 85(Pt 1):105–117.

8. Moss B (2006) Poxvirus entry and membrane fusion. *Virology* 344(1):48–54.

9. Hsiao J-C, Chung C-S, Chang W (1999) Vaccinia virus envelope D8L protein binds to cell surface chondroitin sulfate and mediates the adsorption of intracellular mature virions to cells. *J Virol* 73:8750–8761.

10. Chung CS, Hsiao JC, Chang YS, Chang W (1998) A27L protein mediates vaccinia virus interaction with cell surface heparan sulfate. *J Virol* 72(2):1577–1585.

11. Moss B (2016) Membrane fusion during poxvirus entry. *Semin Cell Dev Biol* S1084-9521(16):30210–30215.

12. McFadden G (2005) Poxvirus tropism. *Nat Rev Micro* 3(3):201–213.

13. Werden SJ, Rahman MM, McFadden G (2008) Poxvirus host range genes. *Adv Virus Res* 71:135–171.

14. Haller SL, Peng C, McFadden G, Rothenburg S (2014) Poxviruses and the evolution of host range and virulence. *Infect Genet Evol* 21:15–40.

15. Esposito JJ, Knight JC (1985) Orthopoxvirus DNA: a comparison of restriction profiles and maps. *Virology* 143(1):230–251.

16. Upton C, Slack S, Hunter AL, Ehlers A, Roper RL (2003) Poxvirus orthologous clusters: toward defining the minimum essential poxvirus genome. *J Virol* 77(13):7590–7600.

17. Seet BT, Johnston JB, Brunetti CR, Barrett JW, Everett H, Cameron C, Sypula J, Nazarian SH, Lucas A, McFadden G (2003) Poxviruses and Immune Evasion. *Annu Rev Immunol* 21(1):377–423.

18. Lefkowitz EJ, Wang C, Upton C (2006) Poxviruses: past, present and future. *Virus Res* 117(1):105–118.

19. Mitsuhashi W, Miyamoto K, Wada S (2014) The complete genome sequence of the Alphaentomopoxvirus Anomala cuprea entomopoxvirus, including its terminal hairpin loop sequences, suggests a potentially unique mode of apoptosis inhibition and mode of DNA replication. *Virology* 452-453:95–116.

20. Thézé J, Takatsuka J, Gallais J, Doucet D, Arif B, Nakai M, Herniou EA (2013) New insights into the evolution of Entomopoxvirinae from the complete genome sequences of four entomopoxviruses infecting Adoxophyes honmai, Choristoneura biennis, Choristoneura rosaceana, and Mythimna separata. *J Virol* 87(14):7992–8003.

21. Massung RF, Liu LL, Qi J, Knight JC, Yuran TE, Kerlavage AR, Parsons JM, Venter JC, Esposito JJ (1994) Analysis of the Complete Genome of Smallpox Variola Major Virus Strain Bangladesh-1975. *Virology* 201(2):215–240.

22. Fenner F (1958) The biological characters of several strains of vaccinia, cowpox and rabbitpox viruses. *Virology* 5(3):502–529.

23. Qin L, Evans DH (2014) Genome scale patterns of recombination between coinfecting vaccinia viruses. *J Virol* 88(10):5277–5286.

24. Pickup DJ, Ink BS, Parsons BL, Hu W, Joklik WK (1984) Spontaneous deletions and duplications of sequences in the genome of cowpox virus. *Proc Natl Acad Sci USA* 81(21):6817–6821.

25. Upton C, Macen JL, Maranchuk RA, DeLange AM (1988) Tumorigenic poxviruses: fine analysis of the recombination junctions in malignant rabbit fibroma virus, a recombinant between Shope fibroma virus and myxoma virus. *Virology*. 166(1):229-239.

26. Yao X-D, Evans DH (2003) High-frequency genetic recombination and reactivation of orthopoxviruses from DNA fragments transfected into leporipoxvirus-infected cells. *J Virol* 77(13):7281–7290.

27. Evans DH, Stuart D, McFadden G (1988) High levels of genetic recombination among cotransfected plasmid DNAs in poxvirus-infected mammalian cells. *J Virol* 62(2):367–375.

28. Baroudy BM, Venkatesan S, Moss B (1982) Incompletely base-paired flip-flop terminal loops link the two DNA strands of the vaccinia virus genome into one uninterrupted polynucleotide chain. *Cell* 28(2):315–324.

29. DeLange AM (1989) Identification of temperature-sensitive mutants of vaccinia virus that are defective in conversion of concatemeric replicative intermediates to the mature linear DNA genome. *J Virol* 63(6):2437–2444.

30. Garcia AD, Moss B (2001) Repression of vaccinia virus Holliday junction resolvase inhibits processing of viral DNA into unit-length genomes. *J Virol* 75(14):6460–6471.

31. Eckert D, Williams O, Meseda CA, Merchlinsky M (2005) Vaccinia Virus Nicking-Joining Enzyme Is Encoded by K4L (VACWR035). *J Virol* 79(24):15084–15090.

32. Afonso CL, Tulman ER, Lu Z, Oma E, Kutish GF, Rock DL (1999) The genome of Melanoplus sanguinipes entomopoxvirus. *J Virol* 73(1):533–552.

33. Bawden AL, Glassberg KJ, Diggans J, Shaw R, Farmerie W, Moyer RW (2000) Complete genomic sequence of the Amsacta moorei entomopoxvirus: analysis and comparison with other poxviruses. *Virology* 274(1):120–139.

34. Da Silva M, Upton C (2005) Host-derived pathogenicity islands in poxviruses. *Virology* 2:30.

35. Bayliss CD, Condit RC (1993) Temperature-Sensitive Mutants in the Vaccinia Virus A18R Gene Increase Double-Stranded RNA Synthesis as a Result of Aberrant Viral Transcription. *Virology* 194(1):254–262.

36. Baldick CJ, Moss B (1993) Characterization and temporal regulation of mRNAs encoded by vaccinia virus intermediate-stage genes. *J Virol* 67(6):3515–3527.

37. Yang Z, Maruri-Avidal L, Sisler J, Stuart CA, Moss B (2013) Cascade regulation of vaccinia virus gene expression is modulated by multistage promoters. *Virology* 447(1-2):213–220.

38. Moss B (2013) Poxvirus DNA replication. *Cold Spring Harb Perspect Biol* 5:a010199.

39. Broyles SS, Moss B (1988) DNA-dependent ATPase activity associated with vaccinia virus early transcription factor. *J Biol Chem* 263(22):10761–10765.

40. Broyles SS, Fesler BS (1990) Vaccinia virus gene encoding a component of the viral early transcription factor. *J Virol* 64(4):1523–1529.

41. Gershon PD, Moss B (1990) Early transcription factor subunits are encoded by vaccinia virus late genes. *Proc Natl Acad Sci USA* 87(11):4401–4405.

42. Keck JG, Baldick CJ, Moss B (1990) Role of DNA replication in vaccinia virus gene expression: a naked template is required for transcription of three late trans-activator genes. *Cell* 61(5):801–809.

43. Sanz P, Moss B (1999) Identification of a transcription factor, encoded by two vaccinia virus early genes, that regulates the intermediate stage of viral gene expression. *Proc Natl Acad Sci USA* 96(6):2692–2697.

44. Vos JC, Stunnenberg HG (1988) Derepression of a novel class of vaccinia virus genes upon DNA replication. *EMBO J* 7(11):3487–3492.

45. Cochran MA, Puckett C, Moss B (1985) In vitro mutagenesis of the promoter region for a vaccinia virus gene: evidence for tandem early and late regulatory signals. *J Virol* 54(1):30–37.

46. Rosel JL, Earl PL, Weir JP, Moss B (1986) Conserved TAAATG sequence at the transcriptional and translational initiation sites of vaccinia virus late genes deduced by structural and functional analysis of the HindIII H genome fragment. *J Virol* 60(2):436–449.

47. Moss B, Shisler JL (2001) Immunology 101 at poxvirus U: Immune evasion genes. *Semin Immunol* 13(1):59–66.

48. Husain M, Moss B (2005) Role of receptor-mediated endocytosis in the formation of vaccinia virus extracellular enveloped particles. *J Virol* 79(7):4080–4089.

49. Hiller G, Weber K (1985) Golgi-derived membranes that contain an acylated viral polypeptide are used for vaccinia virus envelopment. *J Virol* 55(3):651–659.

50. Payne LG (1980) Significance of extracellular enveloped virus in the in vitro and in vivo dissemination of vaccinia. *J Gen Virol* 50(1):89–100.

51. Bratke KA, McLysaght A, Rothenburg S (2013) A survey of host range genes in poxvirus genomes. *Infect Genet Evol* 14:406–425.

52. Afonso PP, Silva PM, Schnellrath LC, Jesus DM, Hu J, Yang Y, Renne R, Attias M, Condit RC, Moussatche N, Damaso CR (2012) Biological characterization and next-generation genome sequencing of the unclassified Cotia virus SPAn232 (Poxviridae). *J Virol* 86(9):5039–5054.

53. Hautaniemi M, Ueda N, Tuimala J, Mercer AA, Lahdenpera J, McInnes CJ (2010) The genome of pseudocowpoxvirus: comparison of a reindeer isolate and a reference strain. *J Gen Virol* 91(Pt 6):1560–1576.

54. Zhao G, Droit L, Tesh RB, Popov VL, Little NS, Upton C, Virgin HW, Wang D

(2011) The Genome of Yoka Poxvirus. *J Virol* 85(19):9657–9657.

55. Emerson GL, Li Y, Frace MA, Olsen-Rasmussen MA, Khristova ML, Govil D, Sammons SA, Regnery RL, Karem KL, Damon IK, Carroll DS (2009) The phylogenetics and ecology of the orthopoxviruses endemic to North America. *PLoS ONE* 4(10):e7666.

56. Gjessing MC, Yutin N, Tengs T, Senkevich T, Koonin E, Ronning HP, Alarcon M, Yiving S, Lie K-I, Saure B, Tran L, Moss B, Dale OB (2015) Salmon Gill Poxvirus, the Deepest Representative of the Chordopoxvirinae. *J Virol* 89(18):9348–9367.

57. Afonso CL, Tulman ER, Delhon G, Lu Z, Viljoen GJ, Wallace DB, Kutish GF, Rock DL (2006) Genome of crocodilepox virus. *J Virol* 80(10):4978–4991.

58. Lopesode S, Lacerda JP, Fonseca FG, Castro DP, Forattini OP, Rabello EX (1965) Cotia virus: A new agent isolated from sentinel mice in Sao Paulo, Brazil. *Am J Trop Med Hyg* 14:156–157.

59. Zeller HG, Karabatsos N, Calisher CH, Digoutte JP (1989) Electron microscopy and antigenic studies of uncharacterized viruses. I. Evidence suggesting the placement of viruses in families Arenaviridae, Paramyxoviridae, or Poxviridae. *Arch Virol* 108(3-4):191–209.

60. Bolte AL, Meurer J, Kaleta EF (1999) Avian host spectrum of avipoxviruses. *Avian Pathol* 28(5):415–432.

61. Afonso CL, Tulman ER, Lu Z, Zsak L, Kutish GF, Rock DL (2000) The genome of fowlpox virus. *J Virol* 74(8):3815–3831.

62. Tulman ER, Afonso CL, Lu Z, Zsak L, Kutish GF, Rock DL (2004) The genome of canarypox virus. *J Virol* 78(1):353–366.

63. Boyle DB (2007) Genus avipoxvirus. *Poxviruses*. 217-251.

64. Jarmin S, Manvell R, Gough RE, Laidlaw SM, Skinner MA (2006) Avipoxvirus phylogenetics: identification of a PCR length polymorphism that discriminates between the two major clades. *J Gen Virol* 87(Pt 8):2191–2201.

65. Bugert JJ (2007) Genus Molluscipoxvirus. *Poxviruses*. 89-112.

66. Moss B, Shisler JL, Xiang Y, Senkevich TG (2000) Immune-defense molecules of molluscum contagiosum virus, a human poxvirus. *Trends Microbiol* 8(10):473–477.

67. Senkevich TG, Koonin EV, Bugert JJ, Darai G, Moss B (1997) The genome of molluscum contagiosum virus: analysis and comparison with other poxviruses. *Virology* 233(1):19–42.

68. Delhon G, Tulman ER, Afonso CL, Lu Z, de la Concha-Bermejillo A, Lehmkuhl

HD, Piccone ME, Kutish GF, Rock DL (2004) Genomes of the parapoxviruses ORF virus and bovine papular stomatitis virus. *J Virol* 78(1):168–177.

69. Fleming SB, Mercer AA (2007) Genus parapoxvirus. *Poxviruses*. 127-165.

70. Hosamani M, Scagliarini A, Bhanuprakash V, McInnes CJ, Singh RK (2009) Orf: an update on current research and future perspectives. *Expert Rev Anti Infect Ther* 7(7):879–893.

71. Riley JC (2010) Smallpox and American Indians revisited. *J Hist Med Allied Sci* 65(4):445–477.

72. Babkina IN, Babkin IV, Le U, Ropp S, Kline R, Damon IK, Esposito JJ, Sandakhchiev LS, Shchelkunov SN (2004) Phylogenetic comparison of the genomes of different strains of variola virus. *Dokl Biochem Biophys* 398:316–319.

73. Esposito JJ, Sammons SA, Frace AM, Osborne JD, Olsen-Rasmussen M, Zhang M, Govil D, Damon IK, Kline R, Laker M, Li Y, Smith GL, Meyer H, Leduc W, Wohlhueter RM (2006) Genome sequence diversity and clues to the evolution of variola (smallpox) virus. *Science* 313(5788):807–812.

74. Duraffour S, Meyer H, Andrei G, Snoeck R (2011) Camelpox virus. *Antiviral Res* 92(2):167–186.

75. Bera BC, Shanmugasundaram K, Barua S, Venkatesan G, Virmani N, Riyesh T, Gulati BR, Bhanuprakash V, Vaid RK, Kakker NK, Malik P, Bansal M, Gadvi S, Singh RV, Yadav V, Sardarilal, Nagarajan G, Balamurugan V, Hosamani M, Pathak KML, Singh RK (2011) Zoonotic cases of camelpox infection in India. *Vet Microbiol* 152(1-2):29–38.

76. Kriz B (1982) A study of camelpox in Somalia. *J Comp Pathol* 92(1):1–8.

77. Jezek Z, Kriz B, Rothbauer V (1983) Camelpox and its risk to the human population. *J Hyg Epidemiol Microbiol Immunol* 27(1):29–42.

78. Damon IK, Esposito JJ (2003) *Poxvirus infections* (Manual of clinical microbiology). 1583-1591.

79. Gubser C, Smith GL (2002) The sequence of camelpox virus shows it is most closely related to variola virus, the cause of smallpox. *J Gen Virol* 83(Pt 4):855–872.

80. Lourie B, Nakano JH, Kemp GE, Setzer HW (1975) Isolation of poxvirus from an African Rodent. *J Infect Dis* 132(6):677–681.

81. Babkin IV, Babkina IN (2012) A retrospective study of the orthopoxvirus molecular evolution. *Infect Genet Evol* 12(8):1597–1604.

82. Babkin IV, Shchelkunov SN (2008) Molecular evolution of poxviruses. *Russ J*

Genet 44(8):895–908.

83. Hughes AL, Irausquin S, Friedman R (2010) The evolutionary biology of poxviruses. *Infect Genet Evol* 10(1):50–59.

84. Firth C, Kitchen A, Shapiro B, Suchard MA, Holmes EC, Rambaut A (2010) Using Time-Structured Data to Estimate Evolutionary Rates of Double-Stranded DNA Viruses. *Mol Biol Evol* 27(9):2038–2051.

85. McLysaght A, Baldi PF, Gaut BS (2003) Extensive gene gain associated with adaptive evolution of poxviruses. *Proc Natl Acad Sci USA* 100(26):15655–15660.

86. Hendrickson RC, Wang C, Hatcher EL, Lefkowitz EJ (2010) Orthopoxvirus genome evolution: the role of gene loss. *Viruses* 2(9):1933–1967.

87. Marennikova SS, Gashnikov PV, Zhukova OA, Riabchikova EI, Strel'tsov VV, Riazankina OI, Chekunova EV, Ianova NN, Shchelkunov SN (1996) The biotype and genetic characteristics of an isolate of the cowpox virus causing infection in a child. *Zh Mikrobiol Epidemiol Immunobiol* (4):6–10.

88. Chantrey J, Meyer H, Baxby D, Begon M, Bown KJ, Hazel SM, Jones T, Montgomery WI, Bennett M (1999) Cowpox: reservoir hosts and geographic range. *Epidemiol Infect* 122(03):455–460.

89. Bennett M, Gaskell CJ, Gaskell RM, Baxby D, Gruffydd-Jones TJ (1986) Poxvirus infection in the domestic cat: some clinical and epidemiological observations. *Vet Rec* 118(14):387–390.

90. Likos AM, Sammons SA, Olson VA, Frace AM, Li Y, Olsen-Rasmussen M, Davidson W, Galloway R, Khristova ML, Reynolds MG, Zhao H, Carroll DS, Curns A, Formenty P, Esposito JJ, Regnery RL, Damon IK (2005) A tale of two clades: monkeypox viruses. *J Gen Virol* 86(Pt 10):2661–2672.

91. Parker S, Nuara A, Buller RML, Schultz DA (2007) Human monkeypox: an emerging zoonotic disease. *Future Microbiol* 2(1):17–34.

92. Chen N, Li G, Liszewski MK, Atkinson JP, Jahrling PB, Feng Z, Schriewer J, Buck C, Wang C, Lefkowitz EJ, Esposito JJ, Harms T, Damon IK, Roper RL, Upton C, Buller RML (2005) Virulence differences between monkeypox virus isolates from West Africa and the Congo basin. *Virology* 340(1):46–63.

93. Di Giulio DB, Eckburg PB (2004) Human monkeypox. *Lancet Infect Dis* 4(4):199.

94. Hammarlund E, Lewis MW, Carter SV, Amanna I (2005) Multiple diagnostic techniques identify previously vaccinated individuals with protective immunity against monkeypox. *Nature Med*. 11(9):1005-1011.

95. Fenner F (1989) Risks and benefits of vaccinia vaccine use in the worldwide

smallpox eradication campaign. *Res Virol* 140(5):465–6– discussion 487–91.

96. Croft DR, Sotir MJ, Williams CJ, Kazmierczak JJ, Wegner MV, Rausch D, Graham MB, Foldy SL, Wolters M, Damon IK, Karem KL, Davis JP (2007) Occupational Risks during a Monkeypox Outbreak, Wisconsin, 2003. *Emerging Infect Dis* 13(8):1150–1157.

97. Reed KD, Melski JW, Graham MB, Regner RL, Sotir MJ, Wegner MV, Kazmierczak JJ, Stratman EJ, Li Y, Fairley JA, Swain GR, Olson VA, Sargent EK, Kehl SC, Frace MA, Kline R, Foldy SL, Davis JP, Damon IK (2004) The detection of monkeypox in humans in the Western Hemisphere. *N Engl J Med* 350(4):342–350.

98. Arndt WD, Cotsmire S, Trainor K, Harrington H, Hauns K, Kibler KV, Huynh TP, Jacobs BL (2015) Evasion of the Innate Immune Type I Interferon System by Monkeypox Virus. *J Virol* 89(20):10489–10499.

99. Regnery DC (1987) Isolation and partial characterization of an orthopoxvirus from a California vole (Microtus californicus). Brief report. *Arch Virol* 94(1-2):159–162.

100. Knight JC, Goldsmith CS, Tamin A, Regner RL, Regnery DC, Esposito JJ (1992) Further analyses of the orthopoxviruses volepox virus and raccoon poxvirus. *Virology* 190(1):423–433.

101. Alexander AD, Flyger V, Herman YF, McConnell SJ, Rothstein N, Yager RH (1972) Survey of wild mammals in a Chesapeake Bay area for selected zoonoses. *J Wildl Dis* 8(2):119–126.

102. Fenner F, Henderson DA, Arita I, Jezek Z, Ladnyi ID (1988) *Smallpox and its Eradication: The Pathogenesis, Immunology, and Pathology of Smallpox and Vaccinia* (World Health Organization).

103. Smith GL (2007) Genus Orthopoxvirus: vaccinia virus. *Poxviruses*. 1-45.

104. Panicali D, Davis SW, Weinberg RL, Paoletti E (1983) Construction of live vaccines by using genetically engineered poxviruses: biological activity of recombinant vaccinia virus expressing influenza virus hemagglutinin. *Proc Natl Acad Sci USA* 80(17):5364–5368.

105. Wiktor TJ, Macfarlan RI, Reagan KJ, Dietzschold B, Curtis PJ, Wunner WH, Kieny MP, Lathe R, Lecocq JP, Mackett M (1984) Protection from rabies by a vaccinia virus recombinant containing the rabies virus glycoprotein gene. *Proc Natl Acad Sci USA* 81(22):7194–7198.

106. Mackett M, Yilma T, Rose JK, Moss B (1985) Vaccinia virus recombinants: expression of VSV genes and protective immunization of mice and cattle. *Science* 227(4685):433–435.

107. Giavedoni L, Jones L, Mebus C, Yilma T (1991) A vaccinia virus double recombinant expressing the F and H genes of rinderpest virus protects cattle against rinderpest and causes no pock lesions. *Proc Natl Acad Sci USA* 88(18):8011–8015.

108. Yewdell JW, Bennink JR, Smith GL, Moss B (1985) Influenza A virus nucleoprotein is a major target antigen for cross-reactive anti-influenza A virus cytotoxic T lymphocytes. *Proc Natl Acad Sci USA* 82(6):1785–1789.

109. Cooney EL, Collier AC, Greenberg PD, Coombs RW, Zarling J, Arditti DE, Hoffman MC, Hu SL, Corey L (1991) Safety of and immunological response to a recombinant vaccinia virus vaccine expressing HIV envelope glycoprotein. *Lancet* 337(8741):567–572.

110. Jenner E (1798) An Inquiry into the causes and effects of variole vaccinae, a disease discovered in some of the western counties of England, particularly Gloucerstershire, and known by the name of cowpox. (London: Sampson Low).

111. Chapman JL, Nichols DK, Martinez MJ, Raymond JW (2010) Animal models of orthopoxvirus infection. *Vet Pathol* 47(5):852–870.

112. Li G, Chen N, Roper RL, Feng Z, Hunter A, Danila M, Lefkowitz EJ, Buller RML, Upton C (2005) Complete coding sequences of the rabbitpox virus genome. *J Gen Virol* 86(Pt 11):2969–2977.

113. Tulman ER, Delhon G, Afonso CL, Lu Z, Zsak L, Sandybaev NT, Kerembekova UZ, Zaitsev VL, Kutish GF, Rock DL (2006) Genome of horsepox virus. *J Virol* 80(18):9244–9258.

114. Henderson DA, Moss B (1999) Recombinant vaccinia virus vaccines. *Vaccines*.

115. Yadav S, Hosamani M, Balamurugan V, Bhanuprakash V, Singh RK (2010) Partial genetic characterization of viruses isolated from pox-like infection in cattle and buffaloes: evidence of buffalo pox virus circulation in Indian cows. *Arch Virol* 155(2):255–261.

116. Abrahão JS, de Souza Trindade G, Ferreira JMS, Campos RK, Bonjardim CA, Ferreira PCP, Kroon EG (2009) Long-lasting stability of Vaccinia virus strains in murine feces: implications for virus circulation and environmental maintenance. *Arch Virol* 154(9):1551–1553.

117. Abrahão JS, Silva-Fernandes AT, Lima LS, Campos RK, Guedes MIMC, Cota MMG, Assis FL, Borges IA, Souza-Junior MF, Lobato ZIP, Bonjardim CA, Ferreira PCP, de Souza Trindade JS, Kroon EG (2010) Vaccinia Virus Infection in Monkeys, Brazilian Amazon. *Emerging Infect Dis* 16(6):976–979.

118. Parker RF, Bronson LH, Green RH (1941) Further Studies Of The Infectious Unit Of Vaccinia. *J Exp Med* 74(3):263–281.

119. Goebel SJ, Johnson GP, Perkus ME, Davis SW, Winslow JP, Paoletti E (1990) The complete DNA sequence of vaccinia virus. *Virology*. 179(1):247-266, 517-563.

120. Marennikova SS, Svet-Moldavskaia IA, Mal'tseva NM (1969) Laboratory markers of the reactogenicity of smallpox vaccines. *Vopr Virusol* 14(5):579–584.

121. Horgan ES, Hasbeb MA (1939) Cross immunity experiments in monkeys between variola, alastrim and vaccinia. *J Hyg*. 39(6):615-637.

122. Rivers TM, Technical Assistance of S. M. Ward (1931) Cultivation of Vaccine Virus for Jennerian Prophylaxis in Man. *J Exp Med* 54(4):453–461.

123. Tartaglia J, Perkus ME, Taylor J, Norton EK, Audonnet JC, Cox WI, Davis SW, van der Hoeven J, Meignier B, Riviere M (1992) NYVAC: a highly attenuated strain of vaccinia virus. *Virology* 188(1):217–232.

124. Mayr A, Hochstein-Mintzel V, Stickl H (1975) Passage history, properties, and applicability of the attenuated vaccinia virus strain MVA. *Infection*. 6-14.

125. Stickl H, Hochstein-Mintzel V, Mayr A (1974) MVA vaccination against smallpox: clinical tests with an attenuated live vaccinia virus strain (MVA). *Dtsch Med Wochenschr* 99:2386–2392.

126. Antoine G, Scheiflinger F, Dorner F, Falkner FG (1998) The Complete Genomic Sequence of the Modified Vaccinia Ankara Strain: Comparison with Other Orthopoxviruses. *Virology* 244(2):365–396.

127. Meyer H, Sutter G, Mayr A (1991) Mapping of deletions in the genome of the highly attenuated vaccinia virus MVA and their influence on virulence. *J Gen Virol* 72 (Pt 5):1031–1038.

128. Carroll MW, Overwijk WW, Chamberlain RS, Rosenberg SA, Moss B, Restifo NP (1997) Highly attenuated modified vaccinia virus Ankara (MVA) as an effective recombinant vector: a murine tumor model. *Vaccine* 15(4):387–394.

129. Mayr A, Danner K (1978) Vaccination against pox diseases under immunosuppressive conditions. *Dev Biol Stand* 41:225–234.

130. Lane JM, Ruben FL, Neff JM, Millar JD (1969) Complications of Smallpox Vaccination, 1968. *N Engl J Med* 281(22):1201–1208.

131. Downie AW (1972) The epidemiology of tanapox and yaba virus infections. *J Med Microbiol* 5(4):Pxiv.

132. Downie AW, España C (1972) Comparison of Tanapox virus and Yaba-like viruses causing epidemic disease in monkeys. *J Hyg (Lond)* 70(1):23–32.

133. Downie AW, Taylor-Robinson CH, Caunt AE, Nelson GS, Manson-Bahr PE,

Matthews TC (1971) Tanapox: a new disease caused by a pox virus. *Br Med J* 1(5745):363–368.

134. España C (1971) Review of some outbreaks of viral disease in captive nonhuman primates. *Lab Anim Sci* 21(6):1023–1031.

135. Downie AW, España C (1973) A comparative study of Tanapox and Yaba viruses. *J Gen Virol.* 19(1):37-49.

136. Bearcroft WG, Jamieson MF (1958) An outbreak of subcutaneous tumours in rhesus monkeys. *Nature* 182(4629):195–196.

137. Brunetti CR, Amano H, Ueda Y, Qin J, Miyamura T, Suzuki T, Li X, Barrett JW, McFadden G (2003) Complete genomic sequence and comparative analysis of the tumorigenic poxvirus Yaba monkey tumor virus. *J Virol* 77(24):13335–13347.

138. Casey HW, Woodruff JM, Butcher WI (1967) Electron microscopy of a benign epidermal pox disease of rhesus monkeys. *Am J Pathol* 51(3):431–446.

139. Barrett JW, McFadden G (2007) Genus Leporipoxvirus. *Poxviruses.* 183-201.

140. Stanford MM, McFadden G, Karupiah G, Chaudhri G (2007) Immunopathogenesis of poxvirus infections: forecasting the impending storm. *Immunol Cell Biol* 85(2):93–102.

141. Kerr PJ, Ghedin E, DePasse JV, Fitch A, Cattadori IM, Hudson PJ, Tscharke DC, Read AF, Holmes EC (2012) Evolutionary History and Attenuation of Myxoma Virus on Two Continents. *PLoS Pathog* 8(10):e1002950.

142. Kerr PJ, Rogers MB, Fitch A, DePasse JV, Cattador IM, Twaddle AC, Hudson PJ, Tscharke DC, Read AF, Holmes EC, Ghedin E (2013) Genome scale evolution of myxoma virus reveals host-pathogen adaptation and rapid geographic spread. *J Virol* 87(23):12900–12915.

143. Peng C, Haller SL, Rahman MM, McFadden G, Rothenburg S (2016) Myxoma virus M156 is a specific inhibitor of rabbit PKR but contains a loss-of-function mutation in Australian virus isolates. *Proc Natl Acad Sci USA*. 113(14):3855-3860. doi:10.1073/pnas.1515613113.

144. Willer DO, McFadden G, Evans DH (1999) The complete genome sequence of shope (rabbit) fibroma virus. *Virology* 264(2):319–343.

145. Cameron C, Hota-Mitchell S, Chen L, Barrett J, Cao JX, Macaulay C, Willer DO, Evans DH, McFadden G (1999) The complete DNA sequence of myxoma virus. *Virology* 264(2):298–318.

146. Kilham L, Herman CM, Fisher ER (1953) Naturally occurring fibromas of grey squirrels related to Shope's rabbit fibroma. *Exp Biol Med.* 82(20099):298-301.

147. Afonso CL, Delhon G, Tulman ER, Lu Z, Zsak A, Becerra VM, Zsak L, Kutish GF, Rock DL (2004) Genome of Deerpox Virus. *J Virol* 79(2):966–977.

148. Williams ES, Becerra VM, Thorne ET, Graham TJ, Owens JM, Nunamaker CE (1985) Spontaneous poxviral dermatitis and keratoconjunctivitis in free-ranging mule deer (Odocoileus hemionus) in Wyoming. *J Wildl Dis* 21(4):430–433.

149. Moerdyk-Schauwecker M, Eide K, Bildfell R, Baker RJ, Black W, Graham D, Thompson K, Crawshaw G, Rohrmann GF, Jin L (2009) Characterization of Cervidpoxvirus isolates from Oregon, California, and eastern Canada. *J Vet Diagn Invest* 21(4):487–492.

150. Jin L, McKay A, Green R, Xu L, Bildfell R (2013) Serosurvey for antibody to deerpox virus in five cervid species in Oregon, USA. *J Wildl Dis* 49(1):186–189.

151. Afonso CL, Tulman ER, Lu Z, Zsak L, Osorio FA, Balinsky C, Kutish GF, Rock DL (2002) The genome of swinepox virus. *J Virol* 76(2):783–790.

152. Kawagishi-Kobayashi M, Cao C, Lu J, Ozato K, Dever TE (2000) Pseudosubstrate Inhibition of Protein Kinase PKR by Swine Pox Virus C8L Gene Product. *Virology* 276(2):424–434.

153. Rothenburg S, Seo EJ, Gibbs JS, Dever TE, Dittmar K (2009) Rapid evolution of protein kinase PKR alters sensitivity to viral inhibitors. *Nat Struct Mol Biol* 16(1):63–70.

154. Babiuk S, Bowden TR, Boyle DB, Wallace DB, Kitching RP (2008) Capripoxviruses: an emerging worldwide threat to sheep, goats and cattle. *Transbound Emerg Dis* 55(7):263–272.

155. Diallo A, Viljoen GJ (2007) Genus capripoxvirus. *Poxviruses*. 167-182.

156. Tulman ER, Afonso CL, Lu Z, Zsak L, Kutish GF, Rock DL (2001) Genome of lumpy skin disease virus. *J Virol* 75(15):7122–7130.

157. Tulman ER, Afonso CL, Lu Z, Zsak L, Sur JH, Sandybaev NT, Kerembekova UZ, Zaitsev VL, Kutish GF, Rock DL (2002) The Genomes of Sheeppox and Goatpox Viruses. *J Virol* 76(12):6054–6061.

158. Sen GC (2001) Viruses and interferons. *Annu Rev Microbiol* 55:255–281.

159. Samuel CE (2001) Antiviral actions of interferons. *Clin Microbiol Rev* 14:778.

160. Smith GL, Symons JA, Alcamí A (1998) Poxviruses: interfering with interferon. *Sem Virol*. 8(5):409-418.

161. Schindler C, Levy DE, Decker T (2007) JAK-STAT signaling: from interferons to cytokines. *J Biol Chem* 282(28):20059–20063.

162. Schoggins JW, Rice CM (2011) Interferon-stimulated genes and their antiviral effector functions. *Curr Opin Virol* 1(6):519–525.

163. Schneider WM, Chevillotte MD, Rice CM (2014) Interferon-stimulated genes: a complex web of host defenses. *Annu Rev Immunol* 32:513–545.

164. Isaacs A, Lindenmann J (1957) Virus interference. I. The interferon. *Proc R Soc Lond, B, Biol Sci* 147(927):258–267.

165. Müller U, Steinhoff U, Reis LF, Hemmi S, Pavlovic J, Zinkernagel RM, Aguet M (1994) Functional role of type I and type II interferons in antiviral defense. *Science* 264(5167):1918–1921.

166. Rossi SL, Tesh RB, Azar SR, Muruato AE, Hanley KA, Auguste AJ, Langsjoen RM, Paessler S, Vasilakis N, Weaver SC (2016) Characterization of a Novel Murine Model to Study Zika Virus. *Am J Trop Med Hyg* 94(6):1362–1369.

167. Pestka S, Krause CD (2006) Interferon and Related Receptors. *The Interferons*. (Wiley-VCH Verlag GmbH & Co. KGaA, Weinheim, FRG), pp 113–140.

168. Shuai K, Schindler C, Prezioso VR, Darnell JE (1992) Activation of transcription by IFN-gamma: tyrosine phosphorylation of a 91-kD DNA binding protein. *Science* 258(5089):1808–1812.

169. Darnell JE Jr, Kerr IM, Stark GR (1994) Jak-STAT pathways and transcriptional activation in response to IFNs and other extracellular signaling proteins. *Science* 264:1415.

170. Pestka S, Langer JA, Zoon KC (1987) Interferons and their actions. *Annu Rev Biochem* 56:727–777.

171. Sen GC, Lengyel P (1992) The interferon system. A bird's eye view of its biochemistry. *J Biol Chem*. 267(8):5017-5020.

172. Stark GR, Kerr IM, Williams BRG, Silverman RH, Schreiber RD (1998) How Cells Respond To Interferons. *Annu Rev Biochem* 67(1):227–264.

173. Lin R, Heylbroeck C, Pitha PM, Hiscott J (1998) Virus-dependent phosphorylation of the IRF-3 transcription factor regulates nuclear translocation, transactivation potential, and proteasome-mediated degradation. *Mol Cell Biol* 18(5):2986–2996.

174. Sato M, Tanaka N, Hata N, Oda E, Taniguchi T (1998) Involvement of the IRF family transcription factor IRF-3 in virus-induced activation of the IFN-beta gene. *FEBS Letters* 425(1):112–116.

175. Sato M, Tanaka N, Oda E, Taniguchi T (1998) Positive feedback regulation of type I IFN genes by the IFN-inducible transcription factor IRF-7. *FEBS Letters* 441(1):106–110.

176. Gray PW, Goeddel DV (1982) Structure of the human immune interferon gene. *Nature.* 298(5877):859-863.

177. Huang S, Hendriks W, Althage A, Hemmi S, Bluethmann H, Kamijo R, Vilcek J, Zinkernagel RM, Aguet M (1993) Immune response in mice that lack the interferon-gamma receptor. *Science* 259(5102):1742–1745.

178. Upton C, Mossman K, McFadden G (1992) Encoding of a homolog of the IFN-gamma receptor by myxoma virus. *Science* 258(5086):1369–1372.

179. Mossman K, Upton C, McFadden G (1995) The myxoma virus-soluble interferon-gamma receptor homolog, M-T7, inhibits interferon-gamma in a species-specific manner. *J Biol Chem* 270(7):3031–3038.

180. Alcamí A, Smith GL (1995) Vaccinia, cowpox, and camelpox viruses encode soluble gamma interferon receptors with novel broad species specificity. *J Virol*. 69(8):4633-4639.

181. Mossman K, Barry M, McFadden G (1995) Interferon-gamma receptors encoded by poxviruses *Viroceptors, Virokines and Related Immune Modulators Encoded by DNA Viruses* 41-54.

182. Symons JA, Tscharke DC, Price N, Smith GL (2002) A study of the vaccinia virus interferon-gamma receptor and its contribution to virus virulence. *J Gen Virol* 83(Pt 8):1953–1964.

183. Puehler F, Weining KC, Symons JA, Smith GL, Sta (1998) Vaccinia virus-encoded cytokine receptor binds and neutralizes chicken interferon-gamma. *Virology* 248(2):231–240.

184. Lalani AS, Graham K, Mossman K, Rajarathnam K, Clark-Lewis I, Kelvin D, McFadden G (1997) The purified myxoma virus gamma interferon receptor homolog M-T7 interacts with the heparin-binding domains of chemokines. *J Virol* 71(6):4356–4363.

185. Colamonici OR, Domanski P, Sweitzer SM, Larner A, Buller RM (1995) Vaccinia virus B18R gene encodes a type I interferon-binding protein that blocks interferon alpha transmembrane signaling. *J Biol Chem* 270(27):15974–15978.

186. Symons JA, Alcamí A, Smith GL (1995) Vaccinia virus encodes a soluble type I interferon receptor of novel structure and broad species specificity. *Cell* 81(4):551–560.

187. Liptáková H, Kontseková E, Alcamí A, Smith GL, Kontsek P (1997) Analysis of an interaction between the soluble vaccinia virus-coded type I interferon (IFN)-receptor and human IFN-alpha1 and IFN-alpha2. *Virology* 232(1):86–90.

188. Vancová I, La Bonnardiere C, Kontsek P (1998) Vaccinia virus protein B18R

inhibits the activity and cellular binding of the novel type interferon-delta. *J Gen Virol* 79 (Pt 7):1647–1649.

189. Meng X, Schoggins J, Rose L, Cao J, Ploss A, Rice CM, Xiang Y (2012) C7L family of poxvirus host range genes inhibits antiviral activities induced by type I interferons and interferon regulatory factor 1. *J Virol* 86(8):4538–4547.

190. Perkus ME, Goebel SJ, Davis SW, Johnson GP (1990) Vaccinia virus host range genes. *Virology*.

191. Hughes AL, Friedman R (2005) Poxvirus genome evolution by gene gain and loss. *Mol Phylogenet Evol* 35(1):186–195.

192. Bratke KA, McLysaght A (2008) Identification of multiple independent horizontal gene transfers into poxviruses using a comparative genomics approach. *BMC Evol Biol.* 8(1):67-80.

193. Liu J, Wennier S, Moussatche N, Reinhar M, Condit R, McFadden G (2012) Myxoma virus M064 is a novel member of the poxvirus C7L superfamily of host range factors that controls the kinetics of myxomatosis in European rabbits. *J Virol* 86(9):5371–5375.

194. Barrett JW, Alston LR, Wang F, Stanford MM, Gilbert PA, Gao X, Jimenez J, Villeneuve D, Forsyth P, McFadden G (2007) Identification of host range mutants of myxoma virus with altered oncolytic potential in human glioma cells. *J Neurovirol* 13(6):549–560.

195. Liu J, Wennier S, Zhang L, McFadden G (2011) M062 is a host range factor essential for myxoma virus pathogenesis and functions as an antagonist of host SAMD9 in human cells. *J Virol* 85(7):3270–3282.

196. Liu J, McFadden G (2015) SAMD9 is an innate antiviral host factor with stress response properties that can be antagonized by poxviruses. *J Virol* 89(3):1925–1931.

197. Hayden MS, Ghosh S (2008) Shared principles in NF-κB signaling. *Cell* 132:344–362.

198. Ghosh S (1999) Regulation of inducible gene expression by the transcription factor NF-κB. *Immunol Res*. 19(2-3):183-190.

199. DiDonato JA, Hayakawa M, Rothwarf DM, Zandi E, Karin M (1997) A cytokine-responsive IkappaB kinase that activates the transcription factor NF-kappaB. *Nature* 388(6642):548–554.

200. Lenardo MJ, Fan CM, Maniatis T, Baltimore D (1989) The involvement of NF-kappa B in beta-interferon gene regulation reveals its role as widely inducible mediator of signal transduction. *Cell* 57(2):287–294.

201. Ramsey-Ewing AL, Moss B (1996) Complementation of a vaccinia virus host-range K1L gene deletion by the nonhomologous CP77 gene. *Virology* 222(1):75–86.

202. Shisler JL, Jin X-L (2004) The vaccinia virus K1L gene product inhibits host NF-kappaB activation by preventing IkappaBalpha degradation. *J Virol* 78(7):3553–3560.

203. Smith CA, Farrah T, Goodwin RG (1994) The TNF receptor superfamily of cellular and viral proteins: activation, costimulation, and death. *Cell* 76(6):959–962.

204. Smith CA, Davis T, Wignall JM, Din WS, Farrah T, Upton C, FcFadden G, Goodwin RG (1991) T2 open reading frame from the Shope fibroma virus encodes a soluble form of the TNF receptor. *Biochem Biophys Res Commun* 176(1):335–342.

205. Upton C, Macen JL, Schreiber M, McFadden G (1991) Myxoma virus expresses a secreted protein with homology to the tumor necrosis factor receptor gene family that contributes to viral virulence. *Virology* 184(1):370–382.

206. Xu X, Nash P, McFadden G (2000) Myxoma virus expresses a TNF receptor homolog with two distinct functions. *Virus Genes* 21(1-2):97–109.

207. Cunnion KM (1999) Tumor necrosis factor receptors encoded by poxviruses. *Mol Genet Metab* 67(4):278–282.

208. Macen JL, Graham KA, Lee SF, Schreiber M, Boshkov L, McFadden G (1996) Expression of the Myxoma Virus Tumor Necrosis Factor Receptor Homologue and M11L Genes Is Required to Prevent Virus-Induced Apoptosis in Infected Rabbit T Lymphocytes. *Virology* 218(1):232–237.

209. Schreiber M, McFadden G (1994) The myxoma virus TNF-receptor homologue (T2) inhibits tumor necrosis factor-alpha in a species-specific fashion. *Virology* 204(2):692–705.

210. Alejo A, Ruiz-Arguello MB, Ho Y, Smith VP, Saraiva M, Alcami A (2006) A chemokine-binding domain in the tumor necrosis factor receptor from variola (smallpox) virus. *Proc Natl Acad Sci USA* 103(15):5995–6000.

211. Guo H, Callaway JB, Ting JP-Y (2015) Inflammasomes: mechanism of action, role in disease, and therapeutics. *Nature Med* 21(7):677–687.

212. Bürckstümmer T, Baumann C, Bluml S, Dixit E, Durnberger G, Jahn H, Planyavsky M, Bilban M, Colinge J, Bennet KL, Superti-Furga G (2009) An orthogonal proteomic-genomic screen identifies AIM2 as a cytoplasmic DNA sensor for the inflammasome. *Nat Immunol* 10(3):266–272.

213. Fernandes-Alnemri T, Yu J-W, Datta P, Wu J, Alnemri ES (2009) AIM2 activates the inflammasome and cell death in response to cytoplasmic DNA. *Nature* 458(7237):509–513.

214. Hornung V, Ablasser A, Charrel-Dennis M, Bauernfeind F, Horvath G, Caffrey DR, Latz E, Fitzgerald KA (2009) AIM2 recognizes cytosolic dsDNA and forms a caspase-1-activating inflammasome with ASC. *Nature* 458(7237):514–518.

215. Kerur N, Veettil M, Sharma-Walia N, Bottero V, Sadagopan S, Otageri P, Chandran B (2011) IFI16 acts as a nuclear danger sensor and induces the inflammasome in response to Kaposi's sarcoma associated herpesvirus (KSHV) infection (157.8). *J Immunol* 186.

216. Roberts TL, Idris A, Dunn JA, Kelly GM (2009) HIN-200 proteins regulate caspase activation in response to foreign cytoplasmic DNA. *Science.* 323(5917):1057-1060.

217. Boyden ED, Dietrich WF (2006) Nalp1b controls mouse macrophage susceptibility to anthrax lethal toxin. *Nature Genet* 38(2):240–244.

218. Franchi L, McDonald C, Kanneganti TD, Amer A, Nunez G (2006) Nucleotide-Binding Oligomerization Domain-Like Receptors: Intracellular Pattern Recognition Molecules for Pathogen Detection and Host Defense. *J Immunol* 177(6):3507–3513.

219. Yazdi AS, Guarda G, D'Ombrain MC, Drexler SK (2010) Inflammatory caspases in innate immunity and inflammation. *J Innate Immun* 2(3):228–237.

220. Yang X, Chang HY, Baltimore D (1998) Essential role of CED-4 oligomerization in CED-3 activation and apoptosis. *Science*. 281(5381):1355-1357.

221. Martinon F, Burns K, Tschopp J (2002) The inflammasome: a molecular platform triggering activation of inflammatory caspases and processing of proIL-β. *Mol Cell*. 10:417-426.

222. Nakanishi K, Yoshimoto T, Tsutsui H, Okamura H (2001) Interleukin-18 regulates both Th1 and Th2 responses. *Annu Rev Immunol* 19:423–474.

223. Gu Y, Kuida K, Tsutsui H, Ku G, Hsiao K, Fleming MA, Hayashi N, Higashino K, Okamura H, Nakanishi K, Kurimoto M, Tanimoto T, Flavell RA, Sato V, Harding MW, Livingston DJ, Su MS-S (1997) Activation of Interferon-gamma Inducing Factor Mediated by Interleukin-1beta Converting Enzyme. *Science* 275(5297):206–209.

224. Johnston JB, Barrett JW, Nazarian SH, Goodwin M, Ricuttio D, Wang G, McFadden G (2005) A Poxvirus-Encoded Pyrin Domain Protein Interacts with ASC-1 to Inhibit Host Inflammatory and Apoptotic Responses to Infection. *Immunity* 23(6):587–598.

225. Dorfleutner A, Talbott SJ, Bryan NB, Funya KN, Rellick SL, Reed JC, Shi X, Rojanasakul Y, Flynn DC, Stehlik C (2007) A Shope Fibroma virus PYRIN-only protein modulates the host immune response. *Virus Genes* 35(3):685–694.

226. Ray CA, Black, RA, Kronheim SR, Greenstreet TA, Sleath PR, Salvesen GS,

Pickup DJ (1992) Viral inhibition of inflammation: cowpox virus encodes an inhibitor of the interleukin-1 beta converting enzyme. *Cell* 69(4):597–604.

227. Silverman GA (2001) The Serpins Are an Expanding Superfamily of Structurally Similar but Functionally Diverse Proteins. Evolution, Mechanism of Inhibition, Novel Functions, and a Revised Nomenclature. *J Biol Chem* 276(36):33293–33296.

228. van Gent D, Sharp P, Morgan K, Kalsheker N (2003) Serpins: structure, function and molecular evolution. *Int J Biochem Cell Biol* 35(11):1536–1547.

229. Ali AN, Turner PC, Brooks MA, Moyer RW (1994) The SPI-1 gene of rabbitpox virus determines host range and is required for hemorrhagic pock formation. *Virology* 202(1):305–314.

230. Shisler JL, Isaacs SN, Moss B (1999) Vaccinia virus serpin-1 deletion mutant exhibits a host range defect characterized by low levels of intermediate and late mRNAs. *Virology* 262(2):298–311.

231. Favoreel HW, van de Walle G, Nauwynck HJ, Pensaert MB (2003) Virus complement evasion strategies. *J Gen Virol* 84(1):1–15.

232. DeHaven BC, Girgis NM, Xiao Y, Hudson PN, Olson VA, Damon IK, Isaacs SN (2010) Poxvirus Complement Control Proteins Are Expressed on the Cell Surface through an Intermolecular Disulfide Bridge with the Viral A56 Protein. *J Virol* 84(21):11245-11254.

233. Girgis NM, DeHaven BC, Fan X, Viner KM, Shamim M, Isaacs SN (2008) Cell surface expression of the vaccinia virus complement control protein is mediated by interaction with the viral A56 protein and protects infected cells from complement attack. *J Virol* 82(9):4205–4214.

234. Engelstad M, Howard ST, Smith GL (1992) A constitutively expressed vaccinia gene encodes a 42-kDa glycoprotein related to complement control factors that forms part of the extracellular virus envelope. *Virology* 188(2):801–810.

235. Takahashi-Nishimaki F, Funahashi S, Miki K, Hashizume S, Sugimoto M (1991) Regulation of plaque size and host range by a vaccinia virus gene related to complement system proteins. *Virology* 181(1):158–164.

236. Martinez-Pomares L, Stern RJ, Moyer RW (1993) The ps/hr gene (B5R open reading frame homolog) of rabbitpox virus controls pock color, is a component of extracellular enveloped virus, and is secreted into the medium. *J Virol* 67(9):5450–5462.

237. Newsome TP, Scaplehorn N, Way M (2004) SRC mediates a switch from microtubule- to actin-based motility of vaccinia virus. *Science* 306(5693):124–129.

238. Rosengard AM, Liu Y, Nie Z, Jimenez R (2002) Variola virus immune evasion

design: expression of a highly efficient inhibitor of human complement. *Proc Natl Acad Sci USA* 99(13):8808–8813.

239. Yadav VN, Pyaram K, Ahmad M, Sahu A (2012) Species selectivity in poxviral complement regulators is dictated by the charge reversal in the central complement control protein modules. *J Immunol* 189(3):1431–1439.

240. Roulston A, Marcellus RC, Branton PE (1999) Viruses and apoptosis. *Annu Rev Microbiol* 53:577–628.

241. Everett H, McFadden G (1999) Apoptosis: an innate immune response to virus infection. *Trends Microbiol* 7(4):160–165.

242. Hengartner MO (2000) The biochemistry of apoptosis. *Nature* 407(6805):770–776.

243. Bertin J, Armstrong RC, Ottilie S, Martin DA, Wang Y, Banks S, Wang GH, Senkevich TG, Alnemri ES, Moss B, Lenardo MJ, Tomaselli KJ, Cohen JI (1997) Death effector domain-containing herpesvirus and poxvirus proteins inhibit both Fas- and TNFR1-induced apoptosis. *Proc Natl Acad Sci USA* 94(4):1172–1176.

244. Quan LT, Caputo A, Bleackley RC, Pickup DJ, Salvesen GS (1995) Granzyme B is inhibited by the cowpox virus serpin cytokine response modifier A. *J Biol Chem* 270(18):10377–10379.

245. Tewari M, Telford WG, Miller RA, Dixit VM (1995) CrmA, a poxvirus-encoded serpin, inhibits cytotoxic T-lymphocyte-mediated apoptosis. *J Biol Chem* 270(39):22705–22708.

246. Enari M, Hug H, Nagata S (1995) Involvement of an ICE-like protease in Fas-mediated apoptosis. *Nature* 375(6526):78–81.

247. Everett H, Barry M, Lee SF, Sun X, Graham K, Stone J, Bleackley RC, McFadden G (2000) M11L: a novel mitochondria-localized protein of myxoma virus that blocks apoptosis of infected leukocytes. *J Exp Med* 191(9):1487–1498.

248. Wasilenko ST, Stewart TL, Meyers AFA, Barry M (2003) Vaccinia virus encodes a previously uncharacterized mitochondrial-associated inhibitor of apoptosis. *Proc Natl Acad Sci USA* 100(24):14345–14350.

249. Su J, Wang G, Barrett JW, Irvine TS, Gao X, McFadden G (2006) Myxoma Virus M11L Blocks Apoptosis through Inhibition of Conformational Activation of Bax at the Mitochondria. *J Virol* 80(3):1140–1151.

250. Taylor JM, Quilty D, Banadyga L, Barry M (2006) The vaccinia virus protein F1L interacts with Bim and inhibits activation of the pro-apoptotic protein Bax. *J Biol Chem* 281(51):39728–39739.

251. Wang G, Barrett JW, Nazarian SH, Everett H, Gao X, Bleackley C, Colwill K,

Moran MF, McFadden G (2004) Myxoma virus M11L prevents apoptosis through constitutive interaction with Bak. *J Virol* 78(13):7097–7111.

252. Wasilenko ST, Banadyga L, Bond D, Barry M (2005) The vaccinia virus F1L protein interacts with the proapoptotic protein Bak and inhibits Bak activation. *J Virol* 79(22):14031–14043.

253. Postigo A, Cross JR, Downward J, Way M (2006) Interaction of F1L with the BH3 domain of Bak is responsible for inhibiting vaccinia-induced apoptosis. *Cell Death Differ* 13(10):1651–1662.

254. Douglas AE, Corbett KD, Berger JM, McFadden G, Handel TM (2007) Structure of M11L: A myxoma virus structural homolog of the apoptosis inhibitor, Bcl-2. *Protein Sci* 16(4):695–703.

255. Kvansakul M, Yang H, Fairlie WD, Czabotar PE, Fischer SF, Perugini MA, Huang DCS, Colman PM (2008) Vaccinia virus anti-apoptotic F1L is a novel Bcl-2-like domain-swapped dimer that binds a highly selective subset of BH3-containing death ligands. *Cell Death Differ* 15(10):1564–1571.

256. Hnatiuk S, Barry M, Zeng W, Liu L, Lucas A, Percy D, McFadden G (1999) Role of the C-terminal RDEL motif of the myxoma virus M-T4 protein in terms of apoptosis regulation and viral pathogenesis. *Virology* 263(2):290–306.

257. Barry M, Hnatiuk S, Mossman K, Lee SF, Boshkov L, McFadden G (1997) The myxoma virus M-T4 gene encodes a novel RDEL-containing protein that is retained within the endoplasmic reticulum and is important for the productive infection of lymphocytes. *Virology* 239(2):360–377.

258. Schreiber M, Sedger L, McFadden G (1997) Distinct domains of M-T2, the myxoma virus tumor necrosis factor (TNF) receptor homolog, mediate extracellular TNF binding and intracellular apoptosis inhibition. *J Virol* 71(3):2171–2181.

259. Mossman K, Lee SF, Barry M, Boshkov L, McFadden G (1996) Disruption of M-T5, a novel myxoma virus gene member of poxvirus host range superfamily, results in dramatic attenuation of myxomatosis in infected European rabbits. *J Virol* 70(7):4394–4410.

260. Ink BS, Gilbert CS, Evan GI (1995) Delay of vaccinia virus-induced apoptosis in nonpermissive Chinese hamster ovary cells by the cowpox virus CHOhr and adenovirus E1B 19K genes. *J Virol* 69(2):661–668.

261. Mosavi LK, Cammett TJ, Desrosiers DC, Peng Z-Y (2004) The ankyrin repeat as molecular architecture for protein recognition. *Protein Sci* 13(6):1435–1448.

262. Mercer AA, Fleming SB, Ueda N (2005) F-box-like domains are present in most poxvirus ankyrin repeat proteins. *Virus Genes* 31(2):127–133.

263. Sonnberg S, Seet BT, Pawson T, Fleming SB, Mercer AA (2008) Poxvirus ankyrin repeat proteins are a unique class of F-box proteins that associate with cellular SCF1 ubiquitin ligase complexes. *Proc Natl Acad Sci USA* 105(31):10955–10960.

264. Spehner D, Gillard S, Drillien R, Kirn A (1988) A cowpox virus gene required for multiplication in Chinese hamster ovary cells. *J Virol* 62(4):1297–1304.

265. Chang S-J, Hsiao J-C, Sonnberg S, Chiang C-T, Yang M-H, Tzou D-L, Mercer AA, Chang W (2009) Poxvirus host range protein CP77 contains an F-box-like domain that is necessary to suppress NF-kappaB activation by tumor necrosis factor alpha but is independent of its host range function. *J Virol* 83(9):4140–4152.

266. Chen W, Drillien R, Spehner D, Buller R (1992) Restricted replication of ectromelia virus in cell culture correlates with mutations in virus-encoded host range gene. *Virology*. 187(2):433-442.

267. Wang G, Barrett JW, Stanford M, Werden SJ, Johnston JB, Gao X, Sun M, Cheng JQ, McFadden G (2006) Infection of human cancer cells with myxoma virus requires Akt activation via interaction with a viral ankyrin-repeat host range factor. *Proc Natl Acad Sci USA* 103(12):4640–4645.

268. Iyer LM, Koonin EV, Aravind L (2002) Extensive domain shuffling in transcription regulators of DNA viruses and implications for the origin of fungal APSES transcription factors. *Genome Biol* 3(3):research0012.1.

269. Huang J, Huang Q, Zhou X, Shen MM, Yen A, Yu SX, Dong G, Qu K, Huang P, Anderson EM, Daniel-Issakani S, Buller RML, Payan DG, Lu HH (2004) The Poxvirus p28 Virulence Factor Is an E3 Ubiquitin Ligase. *J Biol Chem* 279(52):54110–54116.

270. Nerenberg BTH, Taylor J, Bartee E, Gouveia K, Barry M, Fruh K (2005) The poxviral RING protein p28 is a ubiquitin ligase that targets ubiquitin to viral replication factories. *J Virol* 79(1):597-601.

271. Yoneyama M, Kikuchi M, Matsumoto K, Imaizumi T, Miyagishi M, Taira K, Foy E, Loo YM, Gale M, Akira S, Yonehara S, Kato A, Fujita T. (2005) Shared and Unique Functions of the DExD/H-Box Helicases RIG-I, MDA5, and LGP2 in Antiviral Innate Immunity. *J Immunol* 175(5):2851–2858.

272. Yoneyama M, Kikuchi M, Natsukawa T, Shinobu N (2004) The RNA helicase RIG-I has an essential function in double-stranded RNA-induced innate antiviral responses. *Nat Immunol* 5(7):730-737.

273. Kato H, Takeuchi O, Mikamo-Satoh E, Hirai R, Kawai T, Matsushita K, Hiiragi A, Dermody TS, Fujita T, Akira S (2008) Length-dependent recognition of double-stranded ribonucleic acids by retinoic acid-inducible gene-I and melanoma differentiation-associated gene 5. *J Exp Med* 205(7):1601–1610.

274. Hornung V, Ellegast J, Kim S, Brzozka K, Jung A (2006) 5'-Triphosphate RNA is the Ligand for RIG-I. *Science* 314:935–936.

275. Kawai T, Akira S (2006) Innate immune recognition of viral infection. *Nat Immunol*. 7(2):131-137.

276. Potter JA, Randall RE, Taylor GL (2008) Crystal structure of human IPS-1/MAVS/VISA/Cardif caspase activation recruitment domain. *BMC Struct Biol* 8:11.

277. Seth RB, Sun L, Ea C-K, Chen ZJ (2005) Identification and characterization of MAVS, a mitochondrial antiviral signaling protein that activates NF-kappaB and IRF 3. *Cell* 122(5):669–682.

278. Benech P, Vigneron M, Peretz D, Revel M, Chebath J (1987) Interferon-responsive regulatory elements in the promoter of the human 2“,5-”oligo(A) synthetase gene. *Mol Cell Biol* 7(12):4498–4504.

279. Hovanessian AG, Kerr IM (1979) The (2'-5') oligoadenylate (pppA2'-5'A2“-5”A) synthetase and protein kinase(s) from interferon-treated cells. *Eur J Biochem* 93(3):515–526.

280. Williams BR, Kerr IM, Gilbert CS, White CN, Ball LA (1978) Synthesis and breakdown of pppA2'p5'A2“p5”A and transient inhibiton of protein synthesis in extracts from interferon-treated and control cells. *Eur J Biochem* 92(2):455–462.

281. Dong B, Silverman RH (1995) 2-5A-dependent RNase molecules dimerize during activation by 2-5A. *J Biol Chem* 270(8):4133–4137.

282. Clemens MJ, Vaquero CM (1978) Inhibition of protein synthesis by double-stranded RNA in reticulocyte lysates: Evidence for activation of an endoribonuclease. *Biochem Biophys Res Commun* 83(1):59–68.

283. Parrish S, Resch W, Moss B (2007) Vaccinia virus D10 protein has mRNA decapping activity, providing a mechanism for control of host and viral gene expression. *Proc Natl Acad Sci USA* 104(7):2139–2144.

284. Parrish S, Moss B (2007) Characterization of a second vaccinia virus mRNA-decapping enzyme conserved in poxviruses. *J Virol* 81(23):12973–12978.

285. Liu S-W, Katsafanas GC, Liu R, Wyatt LS, Moss B (2015) Poxvirus decapping enzymes enhance virulence by preventing the accumulation of dsRNA and the induction of innate antiviral responses. *Cell Host & Microbe* 17(3):320–331.

286. Liu SW, Wyatt LS, Orandle MS, Minai M, Moss B (2013) The D10 Decapping Enzyme of Vaccinia Virus Contributes to Decay of Cellular and Viral mRNAs and to Virulence in Mice. *J Virol* 88(1):202–211.

287. Parrish S, Moss B (2006) Characterization of a vaccinia virus mutant with a deletion of the D10R gene encoding a putative negative regulator of gene expression. *J Virol* 80(2):553–561.

288. Rivas C, Gil J, Mělková Z, Esteban M, Diaz-Guerra M (1998) Vaccinia virus E3L protein is an inhibitor of the interferon (i.f.n.)-induced 2-5A synthetase enzyme. *Virology* 243(2):406–414.

289. Xiang Y, Condit RC, Vijaysri S, Jacobs B, Williams BRG, Silverman RH (2002) Blockade of Interferon Induction and Action by the E3L Double-Stranded RNA Binding Proteins of Vaccinia Virus. *J Virol* 76:5251–5259.

290. Langland JO, Jacobs BL (2002) The Role of the PKR-Inhibitory Genes, E3L and K3L, in Determining Vaccinia Virus Host Range. *Virology* 299(1):133–141.

291. Perdiguero B, Esteban M (2009) The Interferon System and Vaccinia Virus Evasion Mechanisms. *J Interferon Cytokine Res* 29(9):581–598.

292. Rahman MM, Liu J, Chan WM, Rothenburg S, McFadden G (2013) Myxoma virus protein M029 is a dual function immunomodulator that inhibits PKR and also conscripts RHA/DHX9 to promote expanded host tropism and viral replication. *PLoS Pathog* 9(7):e1003465.

293. Haig DM, McInnes CJ, Thomson J, Wood A, Bunyan K, Mercer A (1998) The orf virus OV20.0L gene product is involved in interferon resistance and inhibits an interferon-inducible, double-stranded RNA-dependent kinase. *Immunology* 93(3):335–340.

294. Beattie E, Kauffman EB, Martinez H, Perkus ME, Jacobs BL, Paoletti E, Tartaglia J (1996) Host-range restriction of vaccinia virus E3L-specific deletion mutants. *Virus Genes* 12(1):89–94.

295. García MA, Meurs EF, Esteban M (2007) The dsRNA protein kinase PKR: virus and cell control. *Biochimie* 89(6-7):799–811.

296. Gil J, Esteban M (2000) Induction of apoptosis by the dsRNA-dependent protein kinase (PKR): mechanism of action. *Apoptosis* 5(2):107–114.

297. Meurs E, Chong K, Galabru J, Thomas NS, Kerr IM, Williams BR, Hovanessian AG (1990) Molecular cloning and characterization of the human double-stranded RNA-activated protein kinase induced by interferon. *Cell* 62(2):379–390.

298. Wu S, Kaufman RJ (1996) Double-stranded (ds) RNA binding and not dimerization correlates with the activation of the dsRNA-dependent protein kinase (PKR). *J Biol Chem* 271(3):1756–1763.

299. Tian B, Mathews MB (2000) Functional Characterization of and Cooperation between the Double-stranded RNA-binding Motifs of the Protein Kinase PKR. *J*

Biol Chem 276(13):9936–9944.

300. Dey M, Cao C, Dar AC, Tamura T, Ozato K, Sicheri F, Dever TE (2005) Mechanistic link between PKR dimerization, autophosphorylation, and eIF2alpha substrate recognition. *Cell* 122(6):901–913.

301. Dar AC, Dever TE, Sicheri F (2005) Higher-Order Substrate Recognition of eIF2α by the RNA-Dependent Protein Kinase PKR. *Cell* 122(6):887–900.

302. Langland JO, Cameron JM, Heck MC, Jancovich JK, Jacobs BL (2006) Inhibition of PKR by RNA and DNA viruses. *Virus Res* 119(1):100–110.

303. Elde NC, Child SJ, Geballe AP, Malik HS (2009) Protein kinase R reveals an evolutionary model for defeating viral mimicry. *Nature* 457(7228):485–489.

304. Davies MV, Chang H-W, Jacobs BL, Kaufman RJ (1993) The E3L and K3L Vaccinia Virus Gene Products Stimulate Translation through Inhibition of the Double-Stranded RNA-Dependent Protein Kinase by Different Mechanisms. *J Virol* 67:1688–1692.

305. Chang H-W, Watson JC, Jacobs BL (1992) The E3L gene of vaccinia virus encodes an inhibitor of the interferon-induced, double-stranded RNA-dependent protein kinase. *Proc Natl Acad Sci USA* 89:4825–4829.

306. Sharp TV, Moonan F, Romashko A, Joshi B, Barber GN, Jagus R (1998) The vaccinia virus E3L gene product interacts with both the regulatory and the substrate binding regions of PKR: implications for PKR autoregulation. *Virology* 250(2):302–315.

307. Smith EJ, Marie I, Prakash A, Garcia-Sastre A, Levy DE (2001) IRF3 and IRF7 10 phosphorylation in virus-infected cells does not require double-stranded RNA-dependent 11 protein kinase R or Ikappa B kinase but is blocked by Vaccinia virus E3L protein. *J Biol* 12:8951-8957.

308. Zhang P, Jacobs BL, Samuel CE (2008) Loss of Protein Kinase PKR Expression in Human HeLa Cells Complements the Vaccinia Virus E3L Deletion Mutant Phenotype by Restoration of Viral Protein Synthesis. *J Virol* 82(2):840–848.

309. Carroll K, Elroy-Stein O, Moss B, Jagus R (1993) Recombinant vaccinia virus K3L gene product prevents activation of double-stranded RNA-dependent, initiation factor 2 alpha-specific protein kinase. *J Biol Chem* 268(17):12837–12842.

310. Dar AC, Sicheri F (2002) X-Ray Crystal Structure and Functional Analysis of Vaccinia Virus K3L Reveals Molecular Determinants for PKR Subversion and Substrate Recognition. *Mol Cell* 10:295–305.

311. Beattie E, Tartaglia J, Paoletti E (1991) Vaccinia Virus-Encoded eIF2alpha Homolog Abrogates the Antiviral Effect of Interferon. *Virology* 183:419–422.

312. Shors ST, Beattie E, Paoletti E, Tartaglia J, Jacobs BL (1998) Role of the vaccinia virus E3L and K3L gene products in rescue of VSV and EMCV from the effects of IFN-alpha. *J Interferon Cytokine Res* 18(9):721–729.

Chapter 2 - Host range functions of vaccinia virus E3L and K3L are mediated by species-specific PKR inhibition

Haller, S.L.[1]; Peng, C.[1]; Senkevich, T.[2]; Moss, B.[2]; Rothenburg, S.[1]

1. *Division of Biology, Kansas State University, Manhattan, KS 66506, USA*
2. *Laboratory of Viral Diseases, NIAID/NIH, Bethesda, MD 20892, USA*

Keywords: host range, vaccinia virus, interferon, PKR, E3L and K3L

Abstract

Poxviruses exhibit wide variations in host range and some, such as vaccinia virus (VACV), have a broad host range and are able to infect multiple species. Protein kinase R (PKR) is an antiviral protein that suppresses general translation during virus infection and whose rapid evolution is attributed to its interactions with several viral inhibitors. VACV encodes two inhibitors of PKR: E3L and K3L, which were identified as host range genes. Whereas K3L was shown to be necessary for VACV replication in Syrian hamster cells, E3L was essential for replication in cells from other species. To determine the molecular basis for the host range function of E3L and K3L, we used a luciferase reporter transfection assay in PKR-deficient HeLa cells to measure interactions between these inhibitors and PKRs from different rodent species. Our results show a surprising variability in the sensitivity of PKR from even closely related species to both E3L and K3L. We found that PKR from Syrian and Chinese hamsters were sensitive to inhibition by K3L, while Armenian hamster PKR was resistant to K3L but sensitive to inhibition by E3L. In addition, infections of different species' cells with VACV lacking E3L and/or K3L correlated the sensitivity of each species' PKR to E3L or K3L with the replication of VACV mutants and the phosphorylation of PKR's substrate, eIF2α. Our results show that the host range function of E3L and K3L can be explained by species-specific differences in the sensitivity of PKR to these VACV inhibitors.

Significance

Vaccinia virus (VACV) E3L and K3L are known to contribute to the host range of the virus, but the molecular explanation for their host range function has not been determined. In this work we identify species-specific inhibition of PKR as the molecular explanation for the host range function of VACV E3L and K3L, and by validating and extending previous analyses to include closely related hamster species, this work will significantly impact our understanding of viral protein interactions with host innate immune response proteins, which can be surprisingly and critically different even between closely related species. An unexpected significance of this work is the first characterization of a PKR that is resistant to VACV E3L, which would not be predicted by the current model of E3L inhibition by binding excess double-stranded (ds) RNA. This finding and the identification of a closely related PKR that resists inhibition by K3L, provides a framework for the mechanistic characterization of PKR inhibition by K3L as well as E3L, which is not yet completely understood. Additionally in this study, we generated a molecular tool to investigate species-specific interactions with viral PKR inhibitors in the context of an isogenic host cell that in the future will be useful for developing informative studies of virus host range.

Introduction

Poxviruses are large double-stranded (ds) DNA viruses that exclusively replicate in the cytoplasm of infected host cells. The entry of poxviruses into a host cell utilizes receptors ubiquitous in most species and is therefore species-independent (1). The successful replication of poxviruses in their hosts is therefore dependent on their ability to evade the host's innate immune responses within the host cell. As a family, poxviruses exhibit wide variation in host range sizes (2). Through the use of deletion mutants and recombinant viruses, a number of viral genes that are necessary for replication in some hosts but not in others have been identified and are labeled as host range genes. Vaccinia virus (VACV) is the prototypic member of the *Orthopoxvirus* genus, which includes the human-restricted variola virus (VARV), the causative agent of smallpox. In contrast to VARV, VACV exhibits a very broad host range and can infect multiple host species. Two host ranges genes that are well conserved in the genomes of all orthopoxviruses and most poxviruses are called E3L and K3L in VACV.

E3L and K3L have been shown to suppress interferon induced responses of the host, and both inhibit the host early response protein, PKR (3, 4). PKR is an antiviral kinase that is expressed at basal levels in most vertebrate cells. PKR encodes two dsRNA-binding domains in its N-terminus and a kinase domain in its C-terminus, which are connected by a linker region of variable length (5). During virus infection, dsRNA is produced in the cytoplasm of the host cells as a byproduct of viral replication. PKR senses and binds this dsRNA, which induces a conformational change that allows the protein to dimerize with another PKR molecule and become autophosphorylated, which is necessary for its complete activation (6, 7). Activated PKR then phosphorylates the alpha subunit of eIF2 (eIF2α), which leads to a general shutdown of cap-dependent protein translation and prevents viral replication in infected cells. The kinase domain of PKR has been shown to be evolving more rapidly than that of other eIF2α kinases, which is likely due to antagonistic interactions it has with several viral inhibitors including VACV E3L and K3L (8, 9).

E3L is a major interferon (IFN) antagonist of VACV, and in human cells, the inhibition of PKR is the key factor involved in the response to IFN treatment, which would otherwise limit the translation of intermediate and late viral gene transcripts (10). The ability of E3L to bind and sequester viral dsRNA from cellular proteins such as PKR is thought to be critical for E3L's host range function as the replacement of dsRNA-binding proteins from other viruses or even bacteria

have been shown to partially rescue replication of an E3L deleted VACV in mouse and human cell lines, and the deletion of the dsRNA-binding motif from E3L abolishes its ability to inhibit host PKR (11-15). K3L, on the other hand, is a pseudosubstrate inhibitor of PKR. It shares homology with the S1 domain of eIF2α, the major substrate of PKR, and can bind activated PKR to prevent its activity (16).

In 2002, Langland and Jacobs showed that E3L was required for VACV replication in human HeLa cells while being dispensable for virus replication in Syrian hamster BHK-21 cells using VACV mutants deleted for E3L or K3L. In the same study they also showed that K3L was required for replication in the BHK-21 cells, but was not required for replication in HeLa cells. The authors proposed that different levels of PKR expressed in each cell line and differences in the amount of dsRNA generated during infection explained the differential requirement for E3L and K3L in these cells, however, the molecular explanation for the observed host range functions of E3L and K3L remains unclear. Based on previous work in which we correlated the sensitivity of mouse and human PKR to inhibition by VACV K3L with its requirement for VACV infection of cells from the same species (8), we hypothesized that in cells from different species, such as in human HeLa and S. hamster BHK-21 cells, E3L and K3L interact with PKR differently, and that this interaction is responsible for their observed host range functions of E3L and K3L in the different cell lines.

Using a sensitive cell-based luciferase assay to measure the interaction of PKR with these viral antagonists, we were able to assess the sensitivity of PKR from different host species to inhibition by E3L or K3L. Our analyses uncovered an unexpected variation in the sensitivity of PKR from four related hamster species and identified two opposing instances of PKR resistance to inhibition by both viral proteins, which were confirmed in several different assays. Furthermore, the inability of E3L and K3L to inhibit PKR from these species correlated with replication of mutant VACVs lacking E3L or K3L in cells from the corresponding hamster species as well as the phosphorylation of eIF2α by the endogenous PKR proteins. Additionally, increasing PKR expression with IFN stimulation increased the differences in replication of the single-deletion VACV mutants, which could be rescued in BHK-21 cells by knocking-down PKR. Together, these results strongly support the conclusion that species-specific inhibition of PKR by VACV E3L and K3L mediate their host range functions, which contributes to the large host range of this virus.

Methods

Cell lines, viruses, yeast strains and plasmids

Mouse (BALB/C) 3T3 (ATCC CRL-1658; kindly provided by Dr. Stephen K. Chapes), rat NRK (ATCC CRL-6509), mouse C3HA (kindly provided by Dr. Stephen K. Chapes), mouse L929 (ATCC CCL-1; kindly provided by Dr. Stephen K. Chapes), European rabbit RK13 (ATCC CCL-37; kindly provided by Dr. Bernard Moss), Syrian hamster BHK-21 (ATCC CCL-10), Syrian hamster HaK (ATCC CCL-15), Armenian hamster AHL-1 (ATCC CCL-195), Chinese hamster Don (ATCC CCL-16), Chinese hamster V79-4 (ATCC CCL-93), human HeLa control and HeLa-PKRkd (both kindly provided by Dr. Charles Samuel) were maintained in Dulbecco's Modified Essential Medium (DMEM, Life Technologies) supplemented with 5% fetal bovine serum (FBS, Fischer) and 25µg/ml gentamycin (Quality Biologicals). RK13+E3L+K3L cells (17) were grown in media additionally supplemented with 500µg/ml geneticin (G418) and 300µg/ml zeocin (Life Technologies) and stably express VACV E3L and K3L. Human embryonic kidney 293-T-REx cells (Invitrogen) were grown in media further supplemented with 100µg/ml zeocin and 15µg/ml blasticidin (Life Technologies), and Flp-In ready HeLa-PKRkd cells were grown in media supplemented with 100µg/ml zeocin and 10µg/ml blasticidin. Chinese hamster CHO-K1 (ATCC CCL-61; kindly provided by Dr. Anna Zolkiewska) cells were grown in Roswell Park Medical Institute (RPMI, Life Technologies) media supplemented with 10% FBS and 25µg/ml gentamycin. All cells were incubated at 37˚C, 5% CO_2. The HeLa-PKRkd cells stably express shRNA to knock down endogenous human PKR expression, and the HeLa control cells stably express non-specific shRNA (18). Viruses used include the wild-type VC-2 (VACV-Copenhagen) and its derivatives, VC-R1 (ΔE3L, (19)), vp872 (ΔK3L, (3)), and VC-R2 (ΔE3LΔK3L, (20)). Both VC-R1 and VC-R2 express a destabilized EGFP gene from the E3L locus under control of the native E3L promoter.

PKR from the indicated species and VACV-WR E3L and K3L were cloned into the pSG5 mammalian expression vector (Stratagene) for transient expression driven by the SV40 promoter as described in (8). The cloning of knock-down resistant human PKR, mouse PKR, rat PKR, European rabbit PKR, Syrian hamster PKR, and Chinese hamster PKR into the pSG5 plasmid was described previously (8, 21, 22). Armenian hamster PKR was cloned from AHL-1 cells using primers located outside of the open reading frame (ORF) (C42: GGG CGA CGC

GAT CTC AGA GTC AGC ACC CGA AGC AAA AGT CGA ATC CT and C40: GGA AAA AAA AGT ACA ATG TTC CCC CTT ATT CCA TCT CAG ATT TTA G) and cloned into the pCR2.1-TOPO-TA (Invitrogen) vector for amplification and sequencing. Primers were designed to sub-clone the PKR ORF into pSG5 with SacI and XhoI restriction sites (C47: TAA GAG CTC GCC ACC ATG GCC AGT GAT ACA CCG GG and C48: AAT CTC GAG TCA CTA ACG TGT GTG TCT TTT CTG TAT C). Turkish hamster PKR was cloned from cDNA generated from total RNA isolated from the testes of a Turkish hamster (*Mesocricetus brandtii*, kindly donated by Bob Johnston and Frank Castelli (Cornell University)). The same primers used to amplify the A. hamster PKR ORF were used and the primers used to sub-clone the Turkish hamster PKR were BA70 mbPKR SacI-1F: GTA CGA GCT CGC CAC CAT GGC CAG TGA TAC ACC C and BA71 mbPKR XhoI-2R: CTG TCT CGA GTC ACT AAT GTG TGT ATC GTT TCT GTA CTT CTG. Protein sequence alignments and protein sequence identities of the PKRs were obtained using ClustalW in MegAlign (DNAStar, Inc.). For transfections, plasmids were prepared using the Nucleobond Xtra Midi Endotoxin Free DNA preparation kit (Macherey-Nagel).

All yeast strains were amplified on YEPD plates and maintained on synthetic minimal media plates (SD) at 30˚C. The generation of the yeast strains stably transformed with empty vector (pRS305, J673), VACV E3L (J659), or VACV K3L-H47R (J674) at the LEU2 locus were described previously (8). Syrian hamster PKR (pN1) and Armenian hamster PKR (pN2) were cloned into the pYX113 (R&D Systems) vector, which encodes the GAL-CYC1 hybrid promoter and the selectable marker URA3 as previously described for human PKR (8).

Virus infections and interferon and siRNA treatments

For all virus infections, sonicated virus samples were diluted in DMEM (or RPMI) supplemented with 2.5% FBS to perform infections at the indicated multiplicities of infection (MOI). For each of the cell lines used, $5.0x10^5$ cells were plated in 6-well plates one day before infection, and infections were performed in duplicate unless otherwise noted. The growth media was removed from each well before adding the diluted virus inoculum and incubating it for one hour at 37˚C. After the incubation period, the inoculum was removed, cells were washed twice with phosphate buffered saline (PBS), and fresh growth media was replaced. Virus was collected at the indicated times post infection by scraping cells directly into the media and submitting the

lysates to three rounds of freeze/thaw cycles followed by sonication (2x15s) in a cup sonicator. Virus titers were measured in plaque forming units per ml (pfu/ml) by counting plaques formed on RK13+E3L+K3L cells (17). Fluorescent images from VC-R2 infected cells were taken on an inverted microscope (Leica) with Q-Image software (300ms exposure).

Cells were pre-treated with human interferon-alpha (hsIFNα) or mouse interferon-α1 (mmIFNα1, pbl interferon source) 17-24 hours prior to collecting RNA or infecting with viruses. For all experiments with human IFNα, 500 units/ml were used to pre-treat cells. For experiments with mouse IFNα1, BHK-21 cells were either pre-treated with 5, 500, or 1000 units/ml for infections with VC-R1 and VC-R2 or BHK-21, AHL-21, and V79-4 cells were pre-treated with 50 units/ml mmIFNα1 for infections with all four viruses. Cells were treated with 5 units/ml mmIFNα1 before collecting RNA for RT-PCR analysis.

Four siRNA duplexes (21nt) were designed to target Syrian hamster PKR or Armenian hamster PKR (Dharmacon, Table 2.1). BHK-21 cells were left untreated or transfected in 6-well plates with 50nM or 100nM siRNA diluted in siRNA buffer (60mM KCl, 6mM HEPES, 20μM MgCl2, pH 7.4) using GenMute (SignaGen) or Lipofectamine RNAiMAX (Invitrogen) siRNA transfection reagents according to the manufacturers instructions. The media in each well was changed after 24 hours, and the cells were infected with the four VACV strains at an MOI=1 at 48 hours post transfection or at an MOI=0.01 24 hours post transfection. Virus lysates from two replicate infections were collected after 30 hours and titered on RK13+E3L+K3L cells. Fluorescent and bright field images were taken at 24 and 48 hours post infection (hpi) using an inverted fluorescent microscope (Leica).

	Sense	Antisense
Duplex 1	GGAAUUAGCUGAACAAAUAUU	UAUUUGUUCAGCUAAUUCCUU
Duplex 2	CACCAGAACGAUAGAGUAAUU	UUACUCUAUGCUUCUGGUGUU
Duplex 3	CCACAUGACAGAAGGUUUAUU	UAAACCUUCUGUCAUGUGGUU
Duplex 4	GGAAAGUAGACAAUGAUUUUU	AAAUCAUUGUCUACUUUCCUU

Table 2.1 Sequences of hamster PKR siRNA duplexes.

Four siRNA target sequences were designed to target S. hamster or A. hamster PKR using the Dharmacon siDESIGN Center (dharmacon.gelifesciences.com).

Human PKR was knocked-down in the 293-T-REx cells by transfecting 10nM, 50nM, or 100nM of Human EIF2AK2 (5610) siRNA (Dharmacon, ON-TARGETplus-SMARTpool) or 100nM of the pooled hamster PKR siRNA duplexes in 6-well plates as described. Protein lysates were collected 24 hours post transfection in 1% SDS for Western blot analysis.

Luciferase assay for PKR inhibition

The luciferase assay for inhibition of PKR activity was described previously (8, 22). Briefly, $5x10^4$ HeLa-PKRkd cells were seeded 24 hours before transfection in 24-well plates. For each transfection, 0.05µg of firefly luciferase encoding plasmid (pGL3promoter, Promega), 0.2µg PKR encoding plasmids (pSG5), and 0.4µg VACV E3L or VACV K3L were transfected using GenJet-Hela (Signagen) in triplicate. For titration experiments, VACV E3L was co-transfected at the indicated concentrations and the total amount of plasmid transfected was kept constant with additional empty vector (pSG5). Cell lysates were harvested 48 hours after transfection using mammalian lysis buffer (Goldbio), and the luciferase activity was determined by measuring light in a luminometer (Berthold) after adding luciferin substrate (Promega). Luciferase activity from vector control transfections were compared to transfections with only PKR encoding plasmids to assess the PKR activity for each species, which was then used to normalize co-transfections of the corresponding PKR with each viral inhibitor.

For luciferase assays of VACV infected cells, $5x10^4$ HeLa-PKRkd cells seeded in 24-well plates were co-transfected in triplicate with 0.3µg of either S. hamster or A. hamster PKR and 0.05µg firefly luciferase. Twenty-four hours post transfection, cells were infected with VC-R2, VC-R1 or vp872 (MOI=1) and lysates were collected 24 hours post infection. Relative luciferase activity was calculated by normalizing results for transfections with each PKR to those infected with VC-R2 (no PKR inhibitors).

Yeast assay for PKR inhibition

Yeast stably expressing VACV E3L (J659), VACV K3L-H47R (J674), or empty vector (J673) were transformed with empty vector or vectors encoding human PKR, S. hamster PKR, or A. hamster PKR using the Lithium acetate/polyethylene glycol method. Four independent transformed clones were picked from each transformation and colony purified on SD plates. Purified colonies were then streaked on SD or galactose plates (S-Gal, contains 2% galactose and all essential amino acids except uracil) to induce PKR expression and grown for seven days.

Generation of hamster PKR-expressing HeLa cell lines

The generation of stable PKR-expressing cells from HeLa-PKRkd cells were performed as described previously with a few differences (22). Briefly, knock-down resistant human PKR, S. hamster PKR and A. hamster PKR were cloned into a stable transfection vector (pEGFP-N1, Clontech) encoding either the endogenous human PKR promoter used by Peng et al. (22) or the SV40 promoter instead of the CMV promoter/enhancer in the original plasmid. The promoter sequences are followed by the intron of the rabbit β-globin gene from pSG5 and a multiple cloning site with two in-frame FLAG tag sequences inserted so that the cloned PKRs are tagged C-terminally. HeLa-PKRkd cells were transfected using GenJet HeLa (SignaGen) according to the manufacturers instructions and cultured with 1μg/ml geneticin (G418, Invitrogen). Geneticin-resistant cells were grown for two or three weeks under selection before isolating individual clones by seeding cells at a low density (0.3 or 1 cell/well) into 96-well plates and amplifying colonies from single cells. PKR expression was monitored from the polyclonal cell populations as well as the single colony isolates by detecting PKR with FLAG antibodies (abm) and comparing expression to the reconstituted HeLa hs-14 cells expressing FLAG tagged PKR at levels comparable to endogenous PKR in HeLa control cells. Individual clones were also screened for endogenous PKR expression with human PKR antibodies.

Generation of tetracycline-inducible Flp-In HeLa cells

HeLa-PKRkd cells were used to generate line of cells where endogenous PKR is knocked down so that other species PKR can be incorporated and their expression controlled using the T-REx Flp-In system (Tet-On, Invitrogen). In this system, the addition of the antibiotic tetracycline or doxycycline de-represses expression of the gene-of-interest, which is inserted into a single site within the genome. HeLa-PKRkd cells were stably transfected with the pFRT/lacZeo plasmid (10μg) encoding the target site and cultured in media containing 100μg/ml zeocin (Life Technologies) to select for stable integrations. Twenty single cell clones were isolated and tested for expression of β-galactosidase (expressed constitutively from a CMV promoter as a fusion gene with Zeocin in the target site) by Western blot. To pick clones with a single target site integration, qPCR of the LacZ gene was performed from genomic DNA and compared to qPCR results with genomic DNA isolated from 293-T-REx cells, which have a single Flp-In integration site (Invitrogen). Two clones with qPCR results similar to the 293-T-REx cells were then

amplified and stably transfected with pcDNA6/TR, which expresses the Tet repressor from a human CMV promoter, and cultured with 10µg/ml blasticidin (Life Technologies).

Generation of tetracycline-inducible hamster PKR-expressing 293 cells

Syrian hamster and A. hamster PKR were cloned into the pcDNA5/FRT/TO expression vector with two C-terminal FLAG tag sequences. Human 293-T-REx cells (Invitrogen) were stably transfected with each hamster PKR plasmid according to the manufacturers instructions and polyclonal pools of the stably transfected cells were selected by their resistance to hygromycin. Each hamster PKR was induced from the polyclonal cells with different concentrations of either tetracycline (Amresco) or doxycycline (Clontech) for 24 hours and their expression was analyzed by Western blot.

Quantitative PCR and RT-PCR analyses

Genomic DNA from 293-T-REx cells (Invitrogen), HeLa-PKRkd cells and 20 single colony isolates of zeocin-resistant HeLa-PKRkd cells was isolated and used as template for quantitative PCR (qPCR) analyses. Quantitative PCR was performed using the BioRad CFX96 Touch Real-Time PCR Detection System with iQ-SYBR Green Supermix (BioRad) to probe for Flp-In insertion site copy number. Primers were designed to amplify 150 base pairs of the LacZ gene present in the LacZ-Zeocin fusion gene marker in the Flp-In site (BA218 LacZ-1F: CAT TCG CCA TTC AGG CTG and BA210 LacZ-1R: GCC GTC GTT TTA CAA CGT C). Genomic DNA template concentrations were varied in a two-fold dilution series for each qPCR. Three technical replicates of each qPCR were performed and the means and standard deviations of the cycle threshold values (Cq) were calculated. The cycle threshold was manually adjusted to 60 relative light units (RLU) in the BioRad software program to generate the reported Cq values. Melt curve analyses were performed after each run to verify the purity of the products generated by each qPCR and samples were run on 1% agarose gels for visual confirmation. The qPCR program used with final melt curve analysis is: 95˚C, 3 min.; (95˚C, 15 sec.; 58˚C, 30 sec) 40 cycle repeats; 65˚C-95˚C, 0.5˚C/s increment.

RNA was collected from IFN treated or untreated cells grown in 6-well plates 17-24 hours after treatment using TRIzol (Thermo Fisher). A cDNA library of expressed genes was then generated using SuperScript III reverse transcriptase and oligo-dT primers (Invitrogen). Primers used to amplify S. hamster PKR from BHK-21 and Hak cells for RT-PCR analysis were

BA16 maPKR NheI-1F TCG CTA GCA TGG CCA GTG ATA CTC CC and BA26 maPKR XhoI-1R TAA TCT CGA GAT GTG TGT GTC GTT TCT GTA CTT C. Primers used to amplify A. hamster PKR from AHL-1 cells were BA14 cmiPKR NheI-1F ACT GCT AGC ATG GCC AGT GAT ACA CCG G and BA27 cmiPKR XhoI-1R TAA TCT CGA GAC GTG TGT GTC TTT TCT GTA TCT C. Primers used to amplify C. hamster PKR from V79-4 cells were C49 cgrPKR-1F TAA GAG CTC GCC ACC ATG GCC AGT GAT ACA CCG GGT TTC TAC ATG GAC and C50 cgrPKR-1R AAT CTC GAG TCA CTA AAG TGT GTG TCT TTT CTG TAT CTC. Primers used to amplify eIF2α from all cell lines were rodent eIF2α-1F GTA GTG ATG GTG AAT GTA AGA TCC and rodent eIF2α-2R CAT CAC ATA CCT GGG TGG AG. Mean band intensities were quantified with the Kodak-4000MM Image Station software. The ratios of PKR to total eIF2α were calculated and for normalized ratios, IFN-treated band ratios were normalized to band ratios for untreated cells.

Western blotting

Protein lysates were collected from confluent monolayers of cells grown in 6-well plates in 1% sodium dodecyl-sulfate (SDS) in PBS and sonicated 2x5s to shear genomic DNA. Lysates from transfected cells were collected 48 hours post transfection in 1% SDS. Lysates from cells infected with wild-type VC-2 (Copenhagen), VC-R1 (ΔE3L), vp872 (ΔK3L), or VC-R2 (ΔE3LΔK3L) (MOI = 5) were collected at 6 hours post infection (hpi) in 1% SDS for analyzing phosphorylation of eIF2α. All protein lysates were separated on 10% polyacrylamide gels and blotted on polyvinyl difluoride (PVDF, GE Healthcare) membranes. Blotted membranes were blocked with either 5% non-fat milk or 5% BSA (for rabbit anti-human PKR and rabbit anti-phospho-eIF2α) before being incubated with mouse or rabbit anti-human PKR (HL71/10, R&D Systems; D7F7, Cell Signaling), mouse anti-D (FLAG, abm), rabbit anti-phospho-eIF2α (Ser51, BioSource International), rabbit anti-total eIF2α (Santa Cruz Biotechnology), mouse anti-β-actin (Sigma-Aldrich), or mouse anti-β-galactosidase (Promega) diluted in TBST buffer (20M Tris, 150mM NaCl, 0.1% Tween 20, pH 7.4). Membranes were incubated overnight at 4˚C in the primary antibody, washed with TBST, and then incubated for 1hr at room temperature with the secondary antibody conjugated to horseradish peroxidase (goat anti-rabbit-HRP or goat anti-mouse-HRP, Open Biosystems; donkey anti-rabbit-HRP or donkey anti-mouse-HRP, Life Technologies). The membranes were then washed with TBST to remove excess secondary

antibody, and proteins were detected with Proto-Glo ECL detection buffers (National Diagnostics). Images were taken using the Kodak-4000MM Image Station, and mean band intensities were quantified with the Kodak Image Station software. The standard deviations of the ratios of phosphorylated eIF2α to total eIF2α for each sample were calculated from two independent Western blots.

Results

E3L and K3L are differentially required for VACV replication in cell culture

Vaccinia virus (VACV) encodes several regulators of the antiviral response, and two of these genes E3L and K3L, have been shown to be differentially required for VACV replication in cells from different species and are therefore labeled as host range genes. Both VACV E3L and K3L positively impacted virus replication in mouse L929 cells, but only VACV K3L was required for virus replication in BHK-21 hamster cells while VACV E3L was required for virus replication in human HeLa cells (23, 24). In these studies, VACV lacking either E3L or K3L was compared to the parental virus. To further test the importance of VACV E3L and K3L for virus replication in other species' cells and extend previous analyses, we used wild type VACV (Copenhagen) and mutant viruses lacking the genes for E3L (VC-R1), K3L (vp872) as well as a VACV mutant lacking both E3L and K3L (VC-R2) to infect different rodent and rabbit cell lines (Fig 2.1). As previously observed, deletion of either E3L or K3L from VACV reduced virus replication in murine L929 cells, suggesting both are important for replication in these cells. VACV did not, however, replicate to high titers in the L929 cells, so we also tested BALB/C-3T3 and C3HA murine cells. Additionally, we tested VACV replication in rat NRK cells and European (E.) rabbit RK13 cells. In the murine cell lines, deletion of K3L resulted in a 4.1-10-fold reduction in virus titer, but deletion of K3L only marginally impaired virus replication in the E. rabbit RK13 cells and rat NRK cells. Deletion of E3L, however, had a severe impact on virus replication in all cell lines tested with significant reductions in titer in BALB/C-3T3, NRK, and RK13 cells and dramatic reductions in both C3HA and L929. The presence of either E3L or K3L was required for VACV replication in all of the tested cell lines as deletion of both genes prevented replication of VC-R2 above input levels. We were able to rescue the replication of the VACV mutants in RK13 cells by ectopically expressing E3L and K3L (Fig 2.2A). Wild type RK13 cells (RK13wt) and RK13 cells engineered to stably express E3L and K3L from VACV

(RK13+E3L+K3L) were infected with the three mutant viruses and the wild-type VACV. The expression of E3L and K3L in the RK13 cells significantly increased replication of VC-R1 and VC-R2, which both exhibited the largest defect in replication in the wild type RK13 cells. The slight reduction in titer that we consistently observed for vp872 compared to VC-2 in the wild type cells (~2.2-fold) was also completely eliminated in the RK13+E3L+K3L cells. These results suggest that E3L and K3L are both important for VACV replication in murine cells and that E3L is critical for VACV replication in mammalian cells from several species.

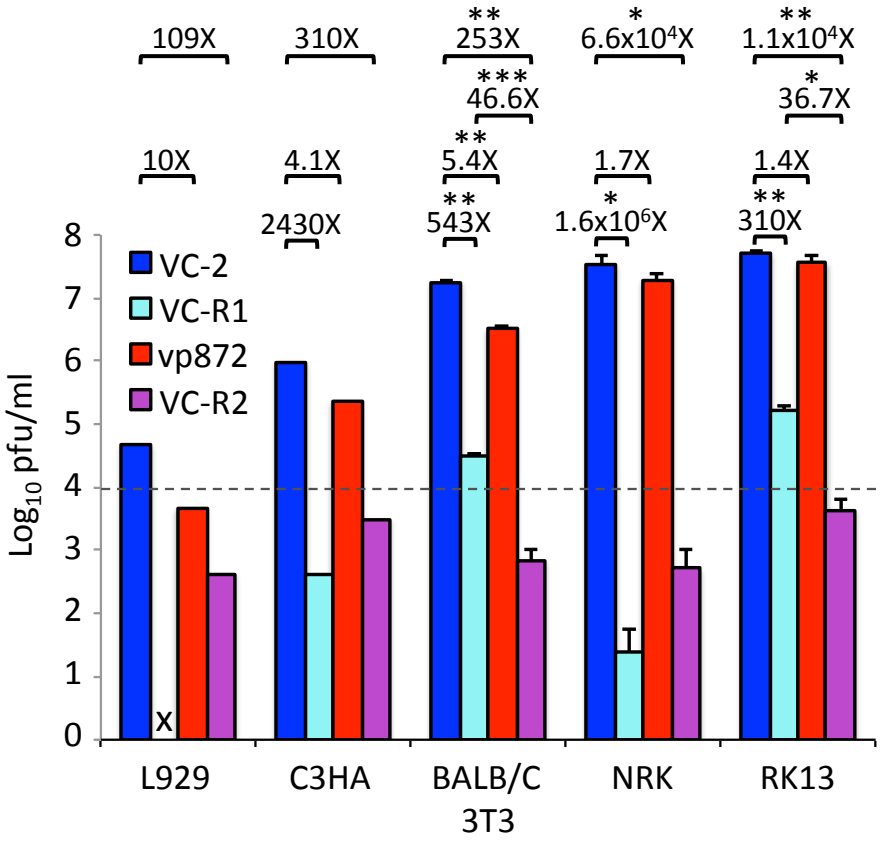

Figure 2.1 VACV E3L and K3L are differentially required for replication in cell culture.
*Different rodent or rabbit cells were infected with VACV-Cop or its derivatives lacking E3L (VC-R1), K3L (vp872) or both (VC-R2) at an MOI=0.01. Virus samples were collected from each infection at 30 hours post infection (hpi) and titers were measured in RK13+E3L+K3L cells by standard plaque assay. Error bars indicate the standard deviation of two independent replicate infections. Titers for C3HA and L929 cells represent results from a single infection. Titers indicated with an "x" were below the detection limit (<10pfu/ml) The dashed line represents the level of input virus. Fold differences between the indicated virus titers are shown above the graph. P-values were calculated using the Student's t-test. *p<0.05; **p<0.005; ***p<0.0005.*

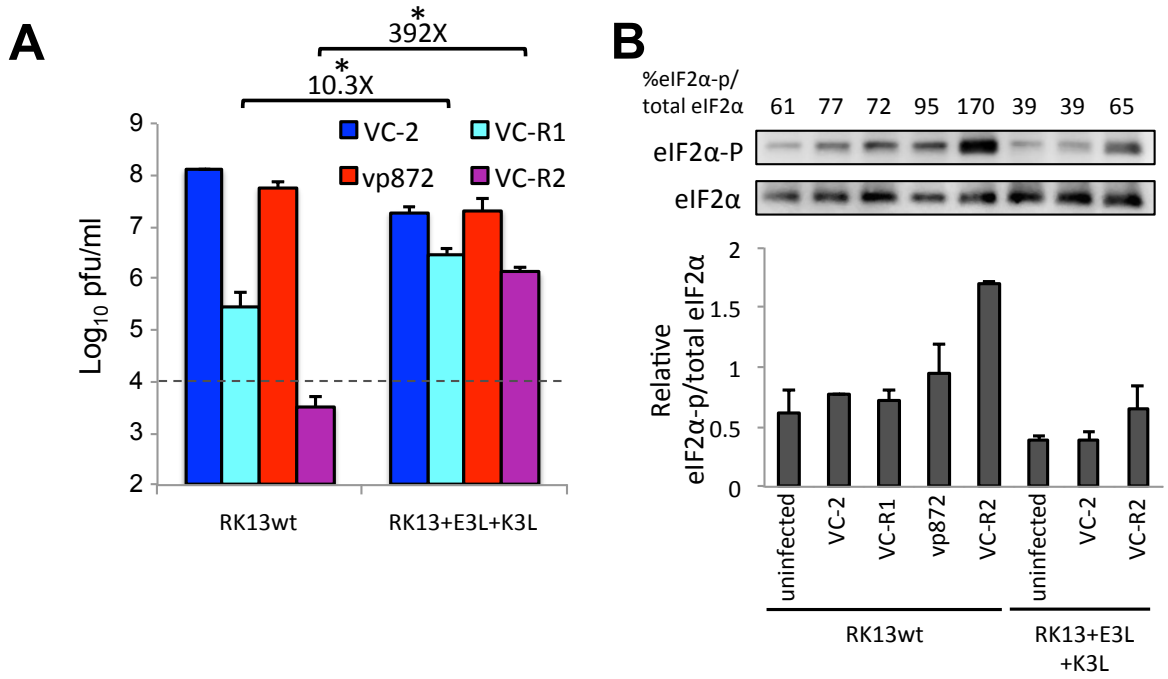

Figure 2.2 VACV E3L and K3L inhibition of PKR is required for VACV replication in RK13 cells. *Wild type RK13 or RK13+E3L+K3L cells were infected with VACV-Cop or its derivatives lacking E3L (VC-R1), K3L (vp872) or both (VC-R2) at an MOI=0.01. Virus samples were collected from each infection at 30 hours post infection (hpi, A). The dashed line represents the level of input virus, and fold differences in virus titer are indicated above the graph. Wild type RK13 or RK13+E3L+K3L cells were mock infected or infected with the indicated vaccinia viruses at an MOI=5. Cell lysates were collected 6 hours post infection and analyzed by Western blot (B). Membranes were probed for phosphorylated eIF2α (eIF2α-P; B, top panel), and then stripped and re-probed for total eIF2α (B, bottom panel). Band intensities for each were measured and the ratios of phosphorylated eIF2α to total eIF2α were calculated as a percentage. The average ratios of two independent blots are indicated above the panels in B and are represented in the bar graph below. Error bars indicate the standard deviation of two replicate experiments. P-values were calculated using the Student's t-test. *p<0.05* (19).

PKR inhibition by E3L and K3L is important for VACV replication

Both E3L and K3L have been shown to inhibit the antiviral interferon (IFN) response (14). One IFN-stimulated gene that interacts with both E3L and K3L is the RNA-dependent protein kinase, PKR. We tested the activity of PKR during VACV infection by detecting phosphorylation of its substrate eIF2α in infected RK13 cells as well as in RK13+E3L+K3L

cells (Fig 2.2B). The severe attenuation of VC-R2 in the wild-type RK13 cells correlated with high levels of phosphorylated eIF2α, whereas the wild-type virus as well as the single deletion mutant viruses suppressed eIF2α phosphorylation to levels close to uninfected cells. The rescue of VC-R2 in the RK13+E3L+K3L cells also correlated with a reduction in the levels of phosphorylated eIF2α similar to that observed in uninfected RK13 cells.

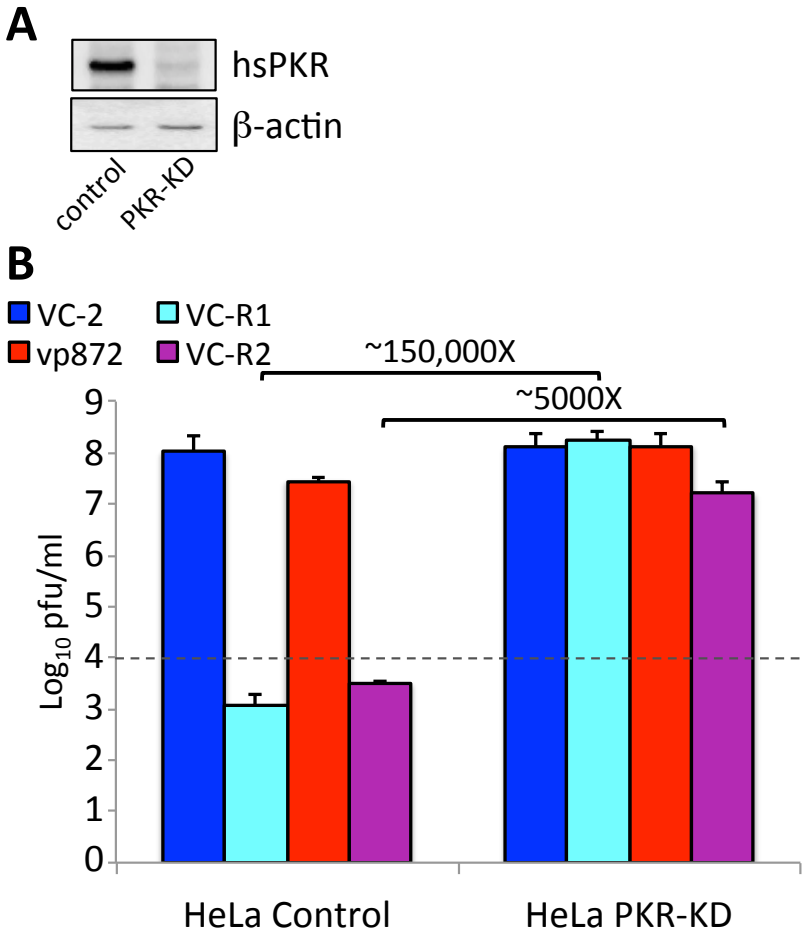

Figure 2.3 PKR inhibition is a critical barrier to VACV replication in HeLa cells.

Protein lysates from HeLa control cells stably expressing control shRNA (18) *and Hela-PKRkd cells were probed for PKR expression (A). HeLa-PKRkd cells or HeLa-control cells were infected with VACV-Cop or its derivatives lacking E3L (VC-R1), K3L (vp872) or both (VC-R2) at an MOI=0.01 (B). Virus samples were collected from each infection at 30 hours post infection (hpi) and titers were measured on RK13+E3L+K3L cells by standard plaque assays. Error bars indicate the standard deviation of two independent replicate infections. The dashed line represents the level of input virus.*

In contrast to expressing E3L and K3L ectopically, we also infected cells where the endogenous PKR is stably knocked down, and found that replication of the mutant viruses was also rescued. HeLa cells stably expressing shRNA against human PKR exhibit nearly complete suppression of PKR expression (Fig. 2.3A) (18). Wild type VACV replicates to high titers in HeLa cells, but deletion of E3L completely restricted virus replication (Fig. 2.3B) (23), which we also observed with the virus deleted for both E3L and K3L. Depletion of endogenous PKR in HeLa cells allowed both VC-R1 and VC-R2 to replicate to levels comparable or close, respectively, to VC-2 suggesting inhibition of PKR activity by E3L is the greatest barrier to VACV replication in human HeLa cells.

The rescue of the mutant virus' replication in cells overexpressing E3L and K3L or in cells depleted for PKR suggests that antagonism of PKR by E3L and/or K3L is important for VACV replication in several different host cells. To investigate the molecular basis for the relative importance and differential requirement of E3L and K3L for VACV replication in the host cells that we tested, we used a luciferase reporter assay. We used this assay, which is based on the PKR-mediated translational suppression of luciferase expression in HeLa-PKRkd cells, to test inhibition of PKR from the corresponding host species (8). In these cells, we transiently co-transfected a plasmid encoding luciferase with plasmids encoding PKR cloned from human, mouse, rat or E. rabbit cells along with plasmids encoding either VACV E3L or K3L (Fig. 2.4A and B). Consistent with previous work, human PKR was sensitive to inhibition by E3L, as indicated by the increase in luciferase activity relative to transfections with this PKR alone, but it was only weakly inhibited by K3L. Similarly rat PKR was only sensitive to inhibition by E3L and was resistant to inhibition by K3L. The relative insensitivity of human and rat PKR to K3L inhibition correlated with the absolute requirement of E3L for VACV replication in cells from these two host species (Figs. 2.1 and 2.3). In contrast, mouse and E. rabbit PKR were completely inhibited by both E3L and K3L. VC-R1 replicated in murine BALB-C/3T3 and E. rabbit RK13 to titers above input levels, which were 36.7-46.6 times greater than those reached by VC-R2 in the same cells (Fig. 2.1). This indicated that in these cells, K3L was still important for virus replication. In the RK13 cells, VC-R1 also suppressed phosphorylation of eIF2α with K3L alone to levels comparable to VC-2 infected cells (Fig. 2.2B). Together these results suggest that PKR inhibition by E3L and/or K3L is necessary for VACV replication in multiple host cells, and the

differential dispensability of K3L for VACV replication correlated with species-specific inhibition of PKR by K3L.

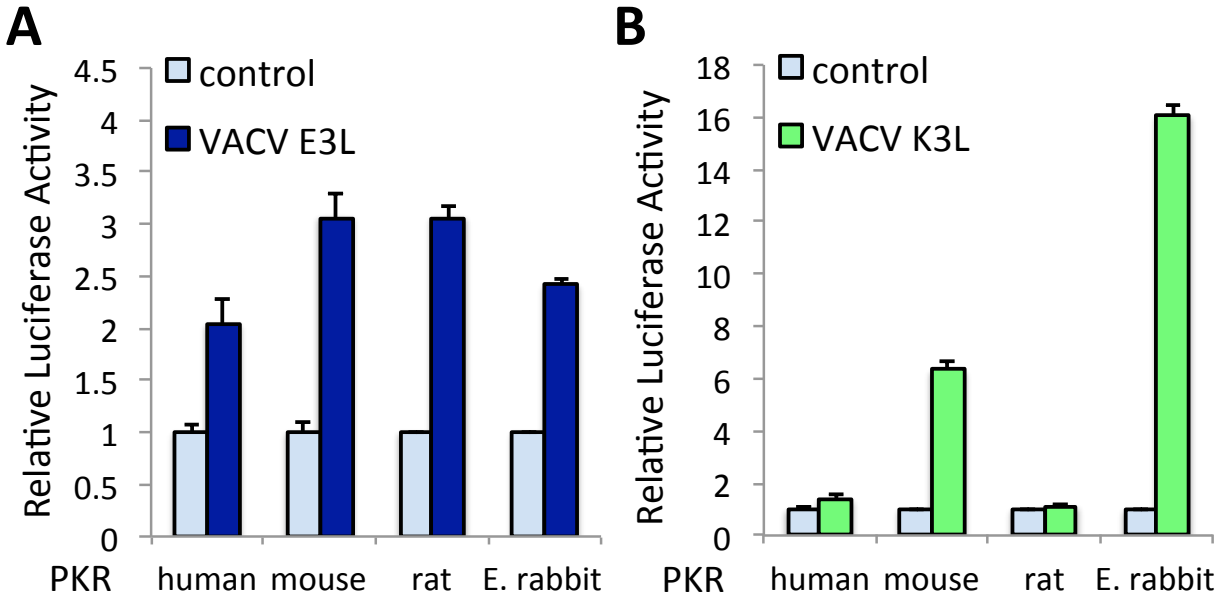

Figure 2.4 PKR inhibition by VACV E3L and K3L.

HeLa-PKRkd cells were transfected with plasmids encoding firefly luciferase (0.05μg), PKR from the indicated species (0.2μg) and VACV E3L or K3L (0.4μg). Relative luciferase activity for each transfection was determined by normalizing measured light units to PKR-only transfected cells. Error bars indicate the standard deviations for three replicate transfections.

Syrian hamster PKR from BHK-21 cells is resistant to inhibition by VACV E3L

Considering the broadly observed requirement for E3L during VACV infection in many of the cell lines that we tested, including not only the rodent and rabbit cells, but also cells from dog, cow, camel, pig and sheep species (Peng, C., unpublished), we were intrigued by the previous results observed by Langland and Jacobs (23) that E3L was dispensable for VACV replication in BHK-21 cells and that deletion of K3L instead restricted virus replication. Knowing that inhibition of PKR by E3L is a critical barrier to VACV infection in other cells, we hypothesized that in infections with the E3L-deleted VACV, K3L can inhibit PKR from BHK-21 cells and overcome the host shut-off induced by its activity, but when K3L is deleted from the virus, E3L is unable to suppress PKR activity sufficiently. We previously showed that the sensitivity of mouse, rat, and human PKR to inhibition by VACV K3L correlated with its

requirement during VACV infection of cells from the same species (Fig. 2.4) (8). To test our hypothesis, we used the same luciferase assay for PKR inhibition and co-transfected plasmids encoding mouse PKR or Syrian (S.) hamster PKR cloned from BHK-21 cells as well as a plasmid encoding VACV E3L in increasing concentrations (Fig. 2.5). As was observed previously, mouse PKR was sensitive to E3L inhibition, and this sensitivity was dose dependent with higher levels of relative luciferase activity indicating increased levels of inhibition by E3L. Interestingly, S. hamster PKR exhibited no sensitivity to E3L inhibition and was resistant even when high amounts of E3L plasmid were co-transfected. The complete resistance of S. hamster PKR to inhibition by VACV E3L was particularly striking considering that the generally accepted mechanism of E3L inhibition of PKR by binding excess dsRNA would not predict a species-specific response. These results, however, are consistent with our hypothesis and explain the unusual dispensability of E3L for VACV replication in S. hamster BHK-21 cells.

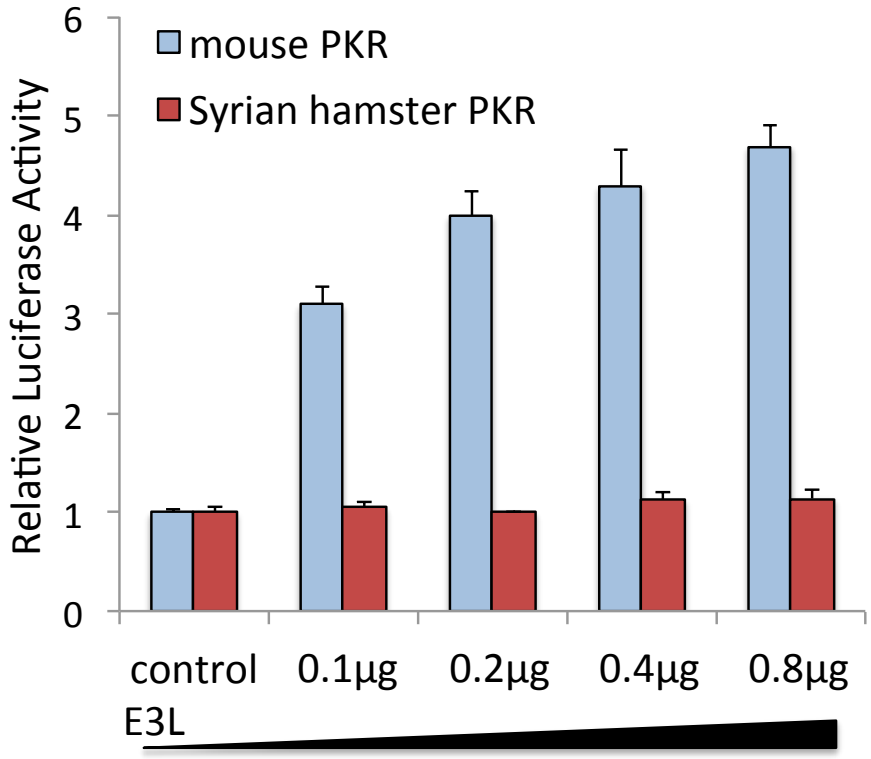

Figure 2.5 Syrian hamster PKR is resistant to inhibition by VACV E3L.

HeLa-PKRkd cells were transfected with plasmids encoding firefly luciferase (0.05µg), mouse or Syrian hamster PKR (0.2µg) and VACV E3L at the indicated concentrations. Relative luciferase activity for each transfection was determined by normalizing measured light units to PKR-only transfected cells. Error bars indicate the standard deviations for three replicate transfections.

VACV E3L and K3L exhibit differential inhibition of PKR from hamster species

To determine if this phenomenon was unique to S. hamster PKR or whether PKR from other hamster species also shared this trait, we cloned PKR into expression plasmids from three additional hamster species: the Turkish (T.) hamster (*Mesocricetus brandtii*), the Armenian (A.) hamster (*Cricetulus migratorius*), and the Chinese (C.) hamster (*Cricetulus griseus*). Compared to human PKR, which has been used most frequently to characterize PKR activity and function, the four hamster PKRs, including that from S. hamster (*Mesocricetus auratus*), share a much higher sequence identity with each other (Figs 2.6 and 2.7). A protein sequence alignment of the hamster PKRs with human PKR revealed several regions of the protein unique to the hamster species (highlighted in purple) as well as some regions that are well conserved between humans and hamsters (highlighted in blue). PKR from the two *Mesocricetus* hamster species shared a higher amino acid sequence identity (97.3%) to each other than to PKR from the *Cricetulus* species (80.6-83%), while PKR from the A. hamster and C. hamster shared a slightly lower identity (89.9%) with each other.

H.s.	*M.a.*	*M.b.*	*C.m.*	*C.g.*	% amino acid identity
	62.7	62.0	61.9	62.7	Human PKR (*Homo sapiens*)
		97.3	82.1	83.0	S. Hamster PKR (*Mesocricetus auratus*)
			80.6	81.7	T. Hamster PKR (*Mesocricetus brandtii*)
				89.9	A. Hamster PKR (*Cricetulus migratorius*)
					C. Hamster PKR (*Cricetulus griseus*)

Figure 2.6 Percent sequence identiies of the hamster PKRs and human PKR.

The amino acid sequences of human PKR, Syrian hamster PKR, Turkish hamster PKR, Armenian hamster PKR, and Chinese hamster PKR were aligned by Clustal W (MegAlign, DNAStar, Inc.), and the percent amino acid sequence identities are listed for each PKR pair. H.s = human PKR; M.a. = S. hamster PKR; M.b. = T. hamster PKR; C.m. = A. hamster PKR; C.g. = C. hamster PKR.

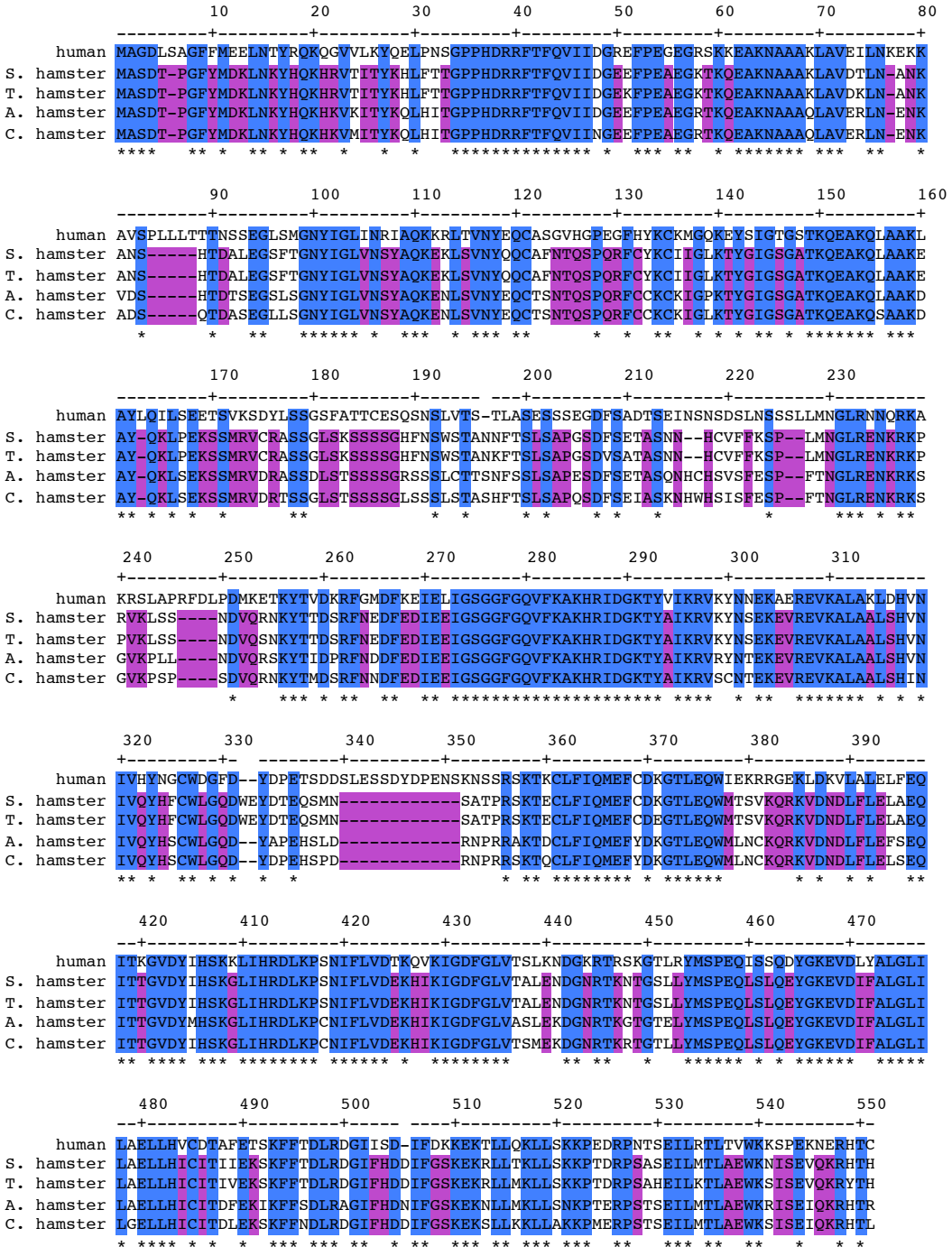

Figure 2.7 Protein sequence alignment of hamster PKRs with human PKR.

The amino acid sequences of human PKR, Syrian hamster PKR, Turkish hamster PKR, Armenian hamster PKR, and Chinese hamster PKR were aligned by Clustal W (MegAlign, DNAStar, Inc.). Conserved residues are highlighted in blue and indicated with an asterisk. Residues conserved in the four hamster PKRs are highlighted in purple. Residues are numbered according to human PKR.

We tested the four hamster PKRs as well as human and mouse PKR for comparison in the luciferase transfection assay for their sensitivities to VACV E3L inhibition (Fig 2.8A). Human and mouse PKR were inhibited by E3L, confirming previous results and correlating with the importance of this gene product for VACV replication in human and mouse cells (8, 23, 24). Additionally, both A. hamster and C. hamster PKR were also sensitive to inhibition by E3L, but importantly T. hamster PKR, like S. hamster PKR, was resistant to E3L inhibition. These results suggest that PKR resistance to VACV E3L is not unique to the S. hamster but is shared by at least one other *Mesocricetus* hamster species. Interestingly, resistance to E3L inhibition appears to be uncommon. We also tested 17 other mammalian PKRs for sensitivity to E3L, and only the S. hamster and T. hamster PKR were not inhibited (Peng, C., unpublished).

To understand the role of K3L inhibition of PKR in these species, we tested the same human, mouse, and hamster PKRs with VACV K3L in the luciferase assay (Fig. 2.8B). Again confirming previous results, human PKR was found to be largely insensitive to inhibition by K3L and mouse PKR was efficiently inhibited. Whereas S. hamster and T. hamster PKR were resistant to E3L inhibition, both exhibited sensitivity to inhibition by K3L. Contrary to this, the PKRs from the *Cricetulus* hamster species exhibited very different sensitivities to K3L. PKR from the C. hamster was inhibited well by K3L as illustrated by the high levels of luciferase activity, whereas A. hamster PKR was completely resistant to K3L inhibition. We also compared the expression of transfected FLAG-tagged S. hamster PKR and A. hamster PKR with human PKR using anti-FLAG antibodies and found them to be expressed to comparable levels (Fig 2.9A). Remarkably, in testing their expression in co-transfection with either FLAG-tagged E3L or K3L from VACV, we observed a correlation between an increase in the transfected gene expression and inhibition of PKR by either E3L or K3L. Co-transfection of VACV E3L and S. hamster PKR, for example, resulted in no increase in S. hamster or T. hamster PKR expression (Fig. 2.9A and B), but co-transfection of K3L with S. hamster PKR resulted in an increase in the overall levels of both PKR and K3L likely due to a reduction in the translational suppression mediated by PKR that occurs following transfection. Together, the resistance of S. hamster PKR to E3L inhibition and the sensitivity of it to K3L inhibition, therefore, further explain the previous observation that VACV lacking K3L did not replicate well in BHK-21 cells.

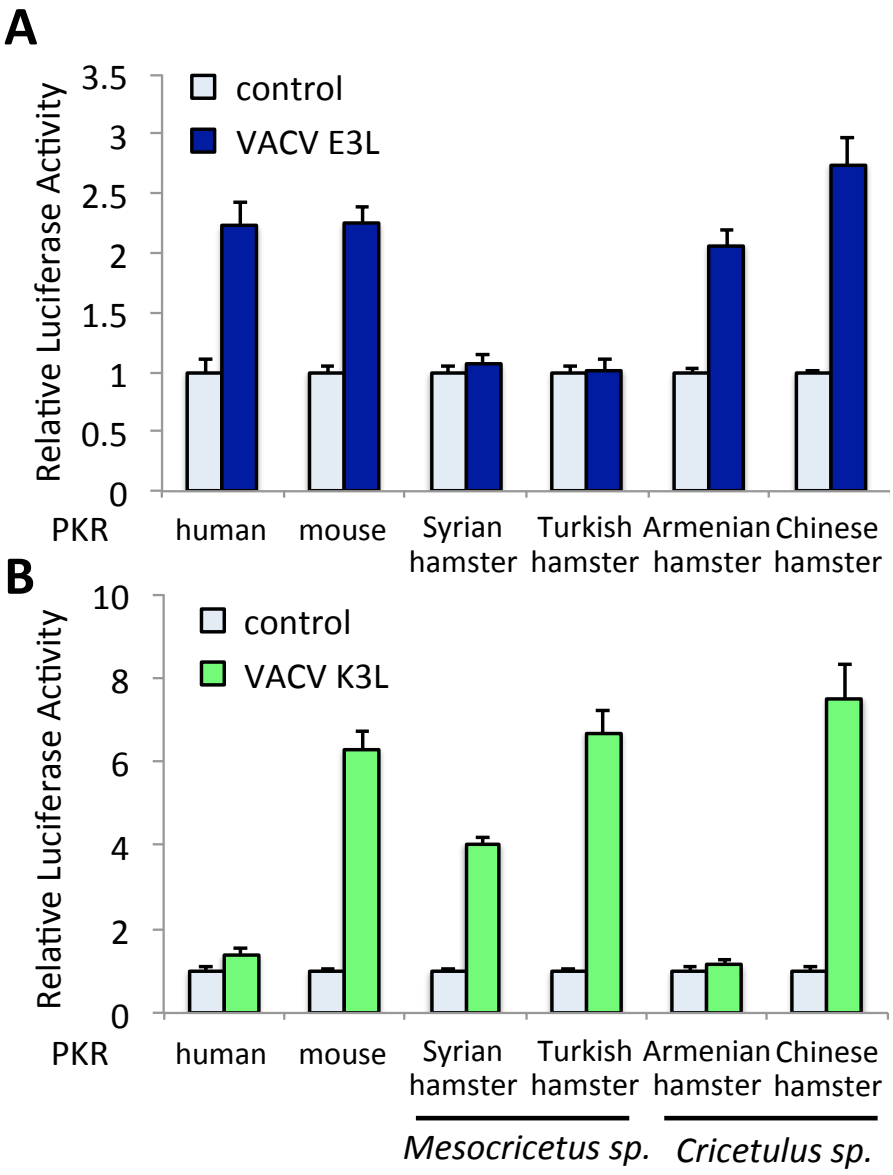

Figure 2.8 Species-specific PKR inhibition by VACV E3L and K3L.

*HeLa-PKRkd cells were transfected with plasmids encoding firefly luciferase (0.05μg), PKR from the indicated species (0.2μg) and VACV E3L (**A**) or VACV K3L (**B**, 0.4μg). Relative luciferase activity for each transfection was determined by normalizing measured light units to PKR-only transfected cells. Error bars indicate the standard deviations for three replicate transfections.*

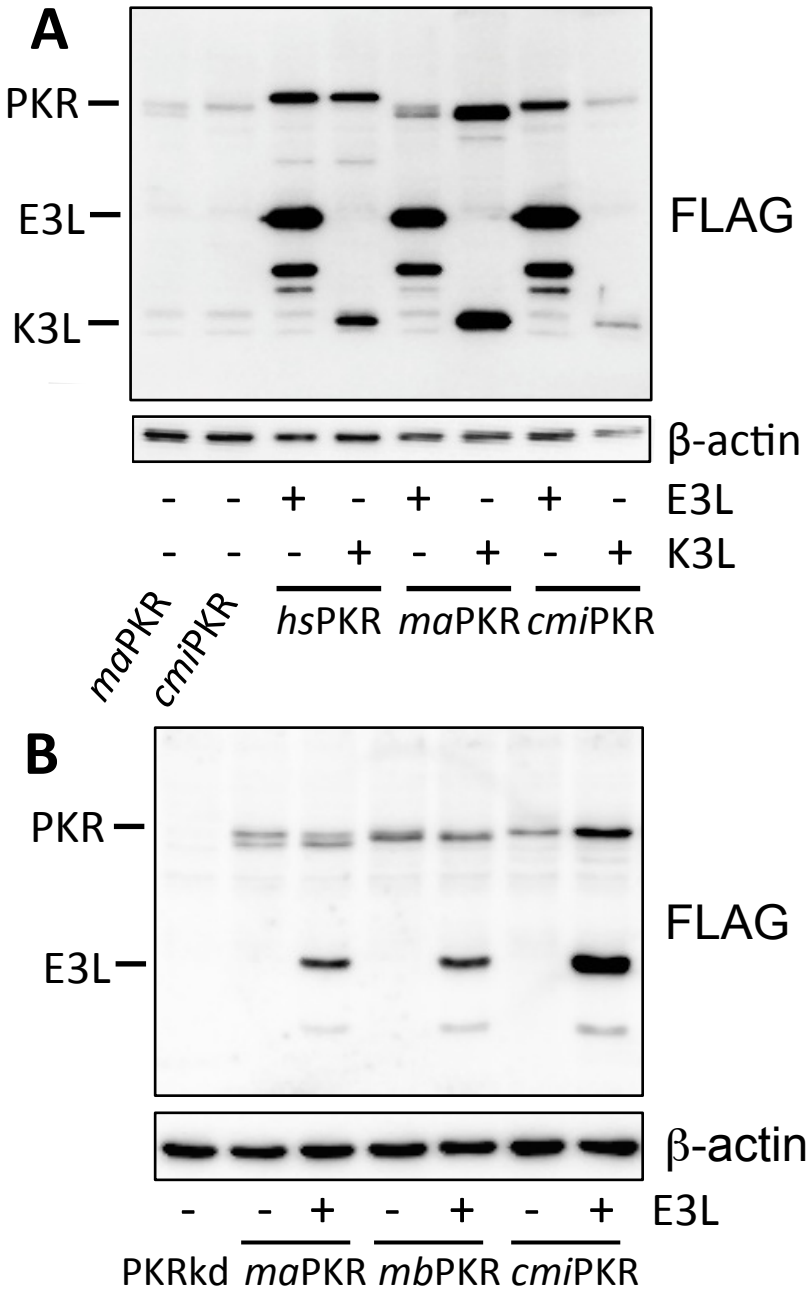

Figure 2.9 Co-transfection of PKR from different species with VACV E3L and K3L.

HeLa-PKRkd cells were transfected with plasmids encoding FLAG-tagged PKR from the indicated species (1μg) with or without FLAG-tagged VACV K3L or E3L (1μg). 1% SDS protein lysates were collected and analyzed by Western blot for gene expression 24 hours post transfection with anti-FLAG antibodies (top panels) or anti-β-actin as a loading control (bottom panels). All of the PKRs were expressed to similar levels, but expression of each PKR increased as well as the viral inhibitor when PKR was inhibited. ma = S. hamster; cmi = A. hamster; hs = human; mb = T. hamster.

The species-specific resistances of the S. hamster PKR and A. hamster PKR to inhibition by VACV E3L and K3L, respectively, was further confirmed in a yeast growth assay in which the expression and activity of PKR suppresses translation and arrests yeast growth under PKR expression inducing conditions (Fig. 2.10A-C). Plasmids encoding human PKR, S. hamster PKR, or A. hamster PKR were transformed into control yeast strains or yeast strains stably expressing VACV E3L or VACV K3L-H47R, which was identified in a mutation screen for better inhibitors of PKR in yeast (H47R, (25)). We also tested the inhibition of PKR by K3L-H47R in the luciferase assay and found that it inhibits the tested PKRs similarly to wild type VACV K3L (Fig. 2.11). Expression of both hamster PKRs and human PKR in yeast prevented yeast growth compared to yeast transformed with the empty vector (Fig 2.10A). Yeast growth was rescued when human PKR was transformed into E3L or K3L-H47R expressing cells (Fig. 2.10B and C), indicating human PKR was inhibited by both viral inhibitors. When S. hamster PKR was expressed, however, yeast growth was only rescued in K3L-H47R expressing cells, and no yeast growth was observed in E3L expressing cells. Similarly, only co-expression of A. hamster PKR with E3L resulted in yeast growth, which correlated with our previous results in the luciferase assay. However, similar to what we consistently observed in the luciferase assay, inhibition of PKR by K3L elicited more robust results than inhibition of PKR by E3L, which may be due to differences in the mode of PKR inhibitory activity for each protein (3, 24).

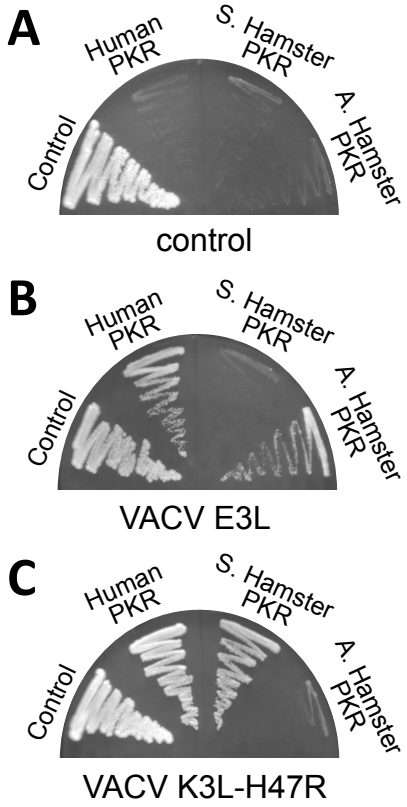

Figure 2.10 Species-specific PKR inhibition by VACV E3L and K3L in yeast.

Plasmids encoding human, S. hamster, or A. hamster PKR under the control of a yeast GAL-CYC1 hybrid promoter were transformed into yeast strains stably expressing the empty vector (control, A), VACV E3L (B), or VACV K3L-H47R (C) from the LEU2 locus. Transformants were colony-purified under non-inducing conditions and then streaked on SC-Gal plates to induce PKR expression for 7 days. Representative results are shown for 4 independent transformations.

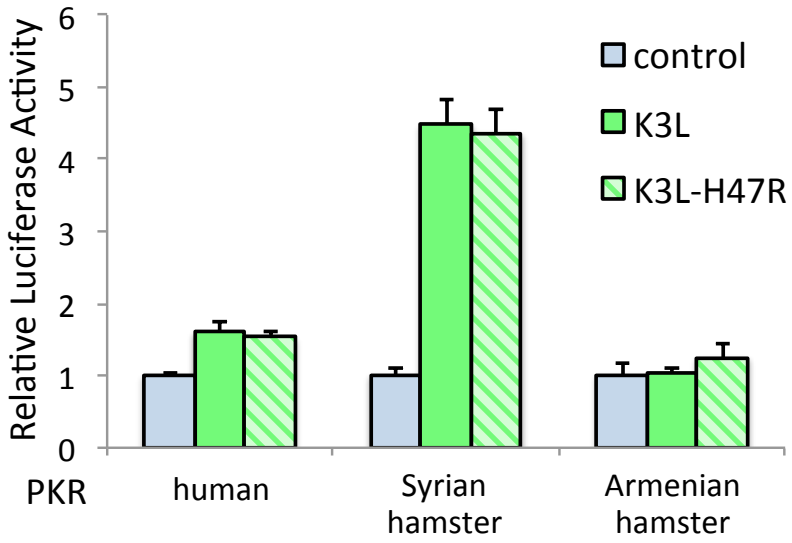

Figure 2.11 VACV K3L-H47R inhibits PKR similarly to VACV K3L.

HeLa-PKRkd cells were transfected with plasmids encoding firefly luciferase (0.05µg), PKR from the indicated species (0.2µg) and VACV K3L or VACV K3L-H47R (0.4µg). Relative luciferase activity for each transfection was determined by normalizing measured light units to PKR-only transfected cells. Error bars indicate the standard deviations for three replicate transfections.

To determine if the resistant phenotypes of S. hamster and A. hamster PKR would also be observed during virus infection, we transfected HeLa-PKRkd cells with plasmids encoding each PKR and luciferase and subsequently infected the cells with VC-R2, VC-R1, or vp872 (Fig 2.12). The luciferase activity measured from the infected cell lysates further confirmed the results from our transient co-transfection experiments. In cells transfected with S. hamster PKR and infected with VC-R1 (encodes only K3L), we observed higher luciferase activity than in cells infected with vp872 (encodes only E3L) or VC-R2 (no PKR inhibitors). Similarly, higher luciferase activity was observed in vp872 infected cells expressing A. hamster PKR, suggesting that the activity of this PKR on the translation of luciferase was more inhibited when E3L was expressed from vp872 than in either VC-R2 or VC-R1 infections where no E3L was present.

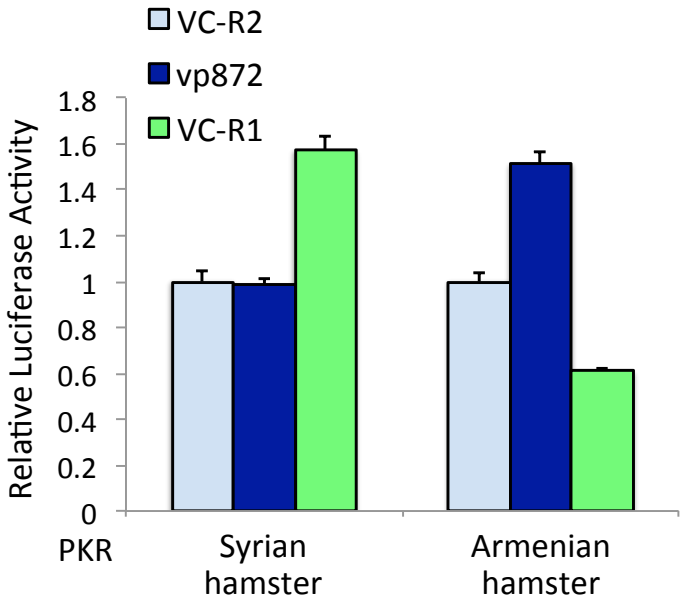

Figure 2.12 Ectopic expression of hamster PKR in VACV infected cells.

HeLa-PKRkd cells in 24-well plates were transfected with either S. hamster or A. hamster PKR (0.3µg) and infected with VACV-Cop mutants lacking E3L, K3L, or both (MOI = 1) after 24hrs. Relative luciferase activity was obtained 48hrs post transfection by normalizing the results to those from wells infected with VC-R2 (lacks E3L and K3L). Error bars represent the standard deviation for three replicate transfections/infections.

Requirement for E3L or K3L for VACV replication in hamster cells correlates with PKR inhibition and eIF2α phosphorylation

Having identified the two hamster PKRs from S. hamster and A. hamster as showing opposing sensitivities to inhibition by VACV E3L and K3L, as well as C. hamster PKR that was sensitive to inhibition by both VACV inhibitors, we wanted to test if these observed PKR sensitivities correlated with virus replication in cells from these species with our mutant VACV strains. We first needed to test the susceptibility of different hamster species cell lines to infection with the wild type VACV as well as test for the requirement of E3L and K3L in each cell line. We infected five hamster cell lines with VC-2 and VC-R2 at a low multiplicity of infection (MOI) to observe multi-cycle replication (Fig. 2.13). BHK-21 cells derived from a S. hamster and AHL-1 cells derived from an A. hamster were both permissive to VACV infection, but VC-R2 was unable to replicate above levels of input in either cell line. While the most commonly used C. hamster cell line is CHO, VACV infection of C. hamster CHO cells results in

an abortive infection in the absence of a cowpox virus protein, CP77 (26, 27). In agreement with the previous reports, neither wild type VC-2 nor VC-R2 could replicate in our CHO cells. Because it was not clear if the inability of VACV to replicate in CHO cells had a cell-type-specific or a species-specific base, we tested two additional C. hamster cells lines, Don and V79-4, for their ability to support VACV replication. VC-2 replicated in both additional C. hamster cell lines, although not to the same level as in either BHK-21 or AHL-1 cells within 48 hours. The deletion of E3L and K3L also restricted VC-R2 replication in both Don and V79-4 cells suggesting their importance for VACV replication in these cells. We decided to use the V79-4 C. hamster cells in subsequent experiments because they grew more similarly to the BHK-21 and AHL-1 cells whereas the Don cells grew more slowly.

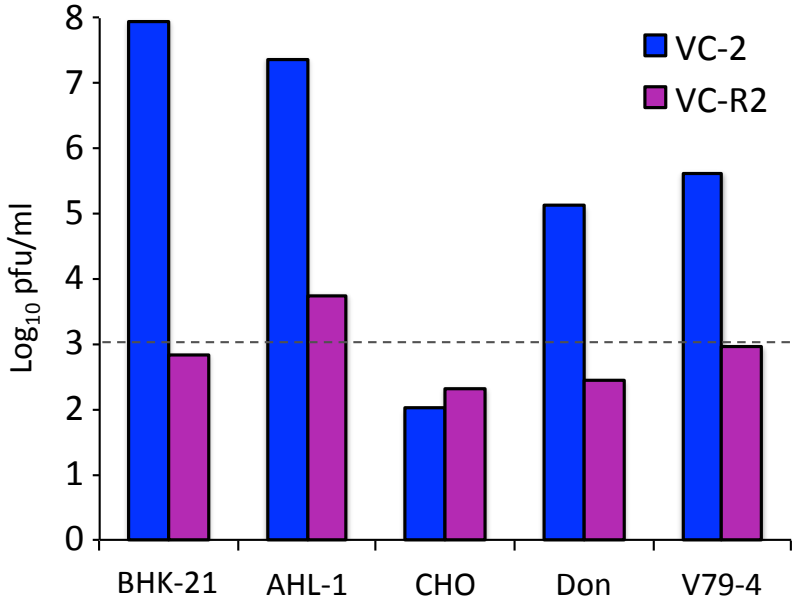

Figure 2.13 VACV replication in hamster cells.

Cells derived from S. hamster (BHK-21), A. hamster (AHL-1), and C. hamsters (CHO, Don, V79-4) were infected with wild-type VACV-Cop (VC-2) or VC-R2 lacking E3L and K3L at an MOI=0.001. Virus was collected after 48hrs, and the dashed line represents the level of input virus. VC-2 replicates in BHK-21 and AHL-1 cells whereas the mutant VC-R2 is highly attenuated. Because VACV cannot replicate in C. hamster CHO cells without the expression of CPXV CP77, two other C. hamster cell lines were tested, in which VC-2 was able to replicate.

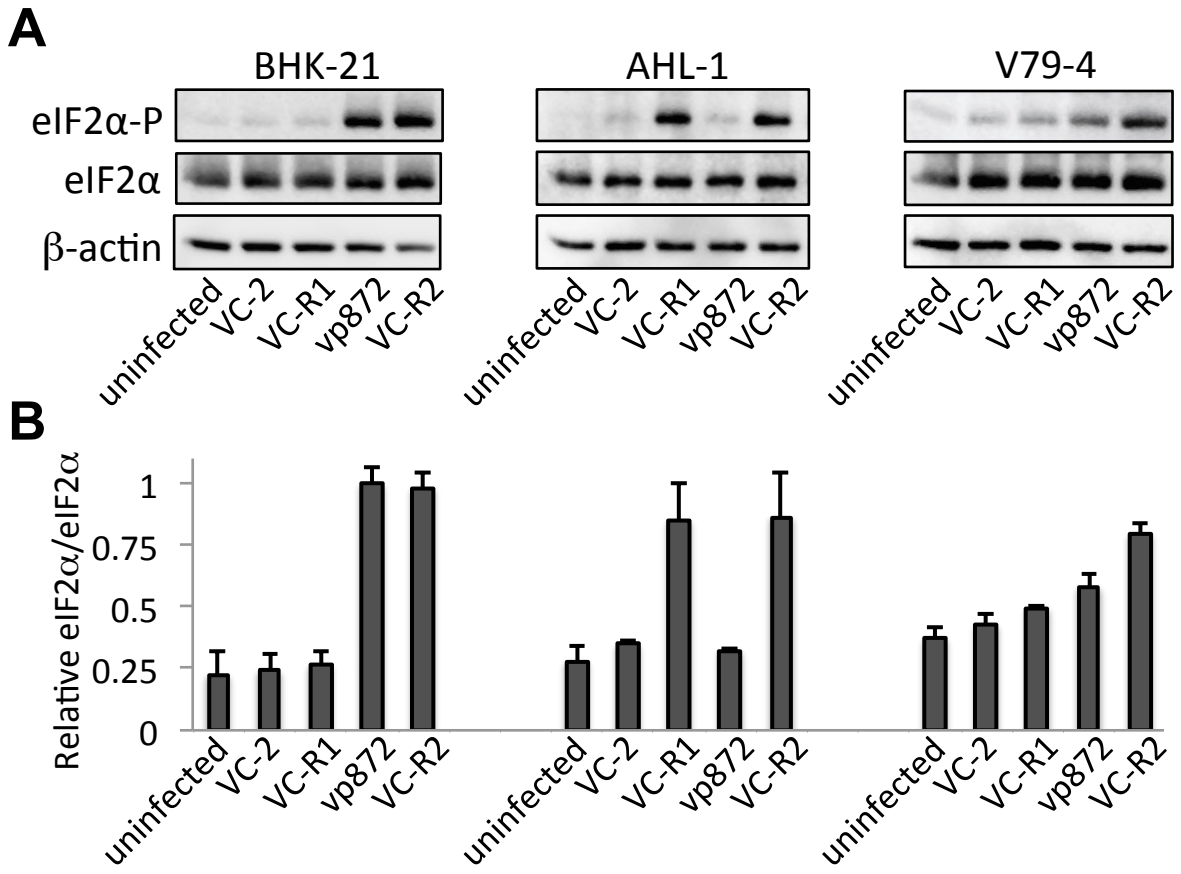

Figure 2.14 Phosphorylation of eIF2α in mutant VACV infected hamster cells.

Three hamster cell lines were infected with wild type VACV-Cop (VC-2) or mutant viruses lacking E3L (VC-R1), K3L (vp872), or both (VC-R2) at an MOI=5. Protein was collected with 1%SDS at 6hpi and separated by SDS-PAGE. Membranes were probed for phosphorylated eIF2α (Ser-51, top panels), total eIF2α (middle panels), or β-actin (bottom panels) (A). Band intensities for each were measured and the ratios of phosphorylated eIF2α to total eIF2α were calculated and plotted on the graph (B). Error bars indicate the standard deviation of two independent experiments.

To correlate PKR activity in the hamster cell lines during infection with the observed sensitivity of each species' PKR to inhibition by E3L or K3L in our luciferase assay, we analyzed protein lysates from the three hamster species' cells infected with the wild type or mutant VACV strains by Western blot and probed them for phosphorylated eIF2α (eIF2α-P) as well as total eIF2α and β-actin as loading controls (Fig. 2.14A and B). In all three cell lines, a low level of eIF2α-P (low PKR activity) was observed in uninfected and VC-2 infected cells, but

high levels were induced by infection with VC-R2 as expected (Fig. 2.14A, upper panels). Furthermore, in agreement with the observed sensitivities of S. hamster PKR and A. hamster PKR to E3L and K3L, no difference in the levels of eIF2α phosphorylation was observed in S. hamster BHK-21 cells infected with VC-R1 or A. hamster AHL-1 cells infected vp872 compared to uninfected controls (Fig 2.14B). However, strong bands for eIF2α-P were observed in BHK-21 cells infected with vp872 and AHL-1 cells infected with VC-R1, which supports our hypothesis that these viruses lack a good inhibitor of PKR from the respective species. Accordingly, the ratio of eIF2α-P to total eIF2α was lower in V79-4 cells infected with either VC-R1 or vp872 than in cells infected with VC-R2.

To correlate the differences in PKR activity with virus replication in each cell line, we infected cells from each of the three hamster species with all four VACV strains at a relatively high MOI of 1 (Fig. 2.15). We observed a strong correlation between increased PKR activity during infection (high levels of eIF2α-P) and restriction of virus replication. While virus titers resulting from infections with the wild type VC-2 and double-deletion mutant VC-R2 in all of the cells were similar to our previous observations with the low MOI, we observed notable differences in the virus titers reached by the single-deletion mutant viruses in each of the cell lines. These differences correlated both with the PKR activity observed for each cell line as well as the sensitivity of each species' PKR to inhibition by E3L or K3L. In S. hamster BHK-21 cells, VC-R1 replicated nearly as well as VC-2 (~2-fold reduction), while vp872, which lacks K3L, reached titers 3.5 times less than VC-R1 and 7.2 times less than VC-2. Meanwhile, in A. hamster AHL-1 cells, VC-R1 replication was severely restricted. Compared to VC-R1, vp872 replicated significantly better to titers 90 times greater and comparable to those reached by VC-2 (1.6-fold reduction). Both of these results correlated with the observed ability of S. hamster and A. hamster PKR to resist inhibition by E3L and K3L, which we would predict necessitates the presence of the second inhibitor for virus replication. Furthermore, both VC-R1 and vp872 replicated similarly in C. hamster V79-4 cells and slightly less than VC-2 (~2-fold reduction), suggesting the remaining viral PKR inhibitor in either of the single-deletion viruses was sufficient to allow virus replication in these cells. Consistent with this, the level of eIF2α-P in either the VC-R1 or vp872 infected V79-4 cells was slightly increased relative to VC-2 infected cells, which may correspond to the slight reduction in titer we observed for these viruses in the V79-4 cells (Figs. 2.14 and 2.15). These results suggests that the functional redundancy of E3L

and K3L in VACV for inhibiting host PKR may be necessary for maintaining its broad host range and their activity may be synergistic in some species cells, such as in C. hamster cells.

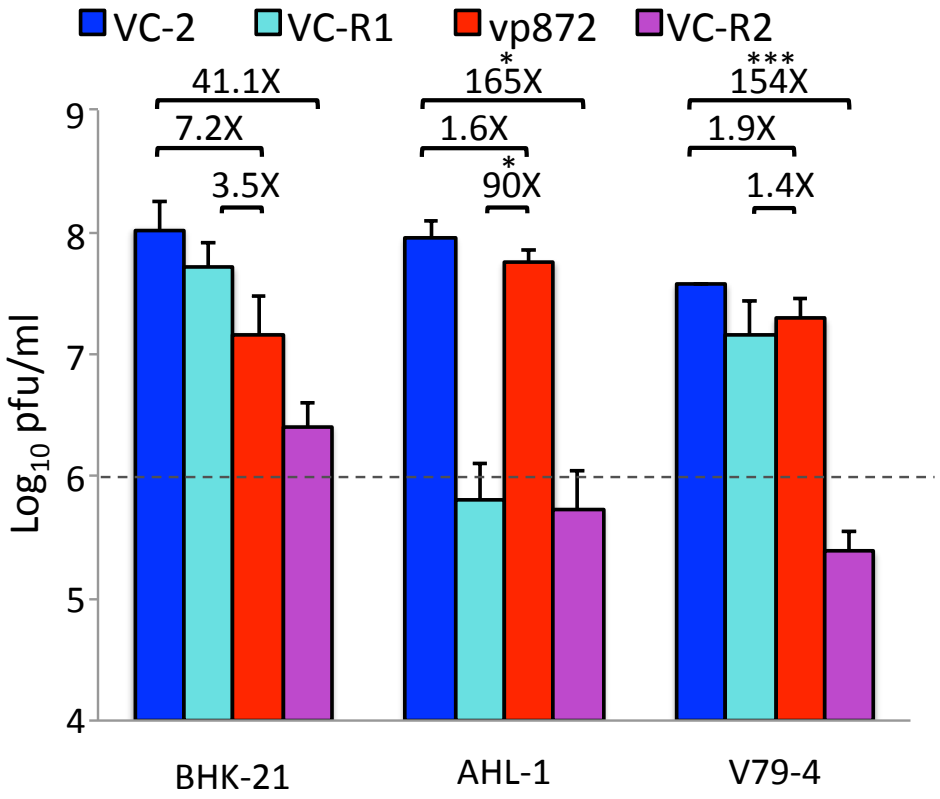

Figure 2.15 VACV mutant replication in hamster cells.

*Three hamster cell lines were infected with wild type VACV-Cop (VC-2) or mutant viruses lacking E3L (VC-R1), K3L (vp872), or both (VC-R2) at an MOI=1 in duplicate. Viruses were collected at 30hpi and titered on RK13+E3L+K3L cells by plaque assay. Error bars indicate the standard deviation of two replicate experiments and fold differences between the single and double-deletion mutant viruses are noted above each. P-values were calculated using the Student's t-test. * $p<0.05$; *** $p<0.0005$.*

Induction or suppression of PKR expression affects VACV replication in hamster cells

The level of eIF2α-phosphorylation observed in BHK-21 cells infected with vp872 was surprising considering this virus was still able to replicate in our BHK-21 cells (Figs. 2.14 and 2.15), which was contrary to previously published results (23). We speculated that our BHK-21 cells expressed lower levels of PKR than other cell lines, so to induce higher expression of PKR, we treated the BHK-21 cells with human interferon alpha (hsIFNα) and measured PKR

expression by RT-PCR, since antibodies against Syrian hamster PKR were not available to measure protein levels (Fig. 2.16A and B). Additionally, to be sure that the differences we observed in VACV replication and eIF2α-phosphorylation were due to species-specific differences and not cell type-specific differences, we included a second S. hamster cell line, HaK, in our analysis.

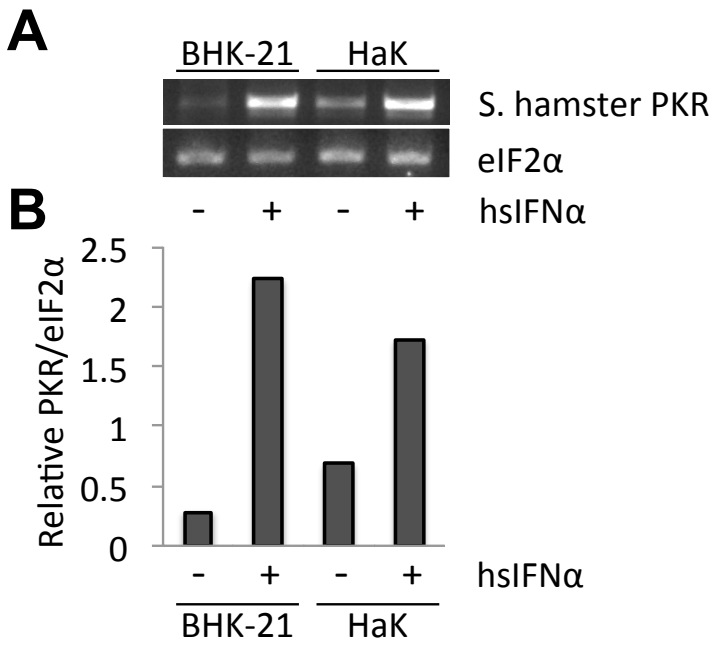

Figure 2.16 Interferon induces PKR expression in Syrian hamster cells.

Two S. hamster cell lines (BHK-21 and HaK) were treated with 500U/ml human interferon-α (hsIFNα) or left untreated. RNA was isolated from each well after 17 hours to generate cDNA for RT-PCR amplification of S. hamster PKR or eIF2α genes (A). Band intensities were measured and plotted as a ratio of PKR to eIF2α (B).

We also performed replication curves of the four VACV strains in the two untreated and IFN treated S. hamster cell lines (Fig 2.17). Treatment with hsIFNα strongly induced PKR expression in both BHK-21 and HaK cells with relative ratios of PKR increasing nearly 8-fold in BHK-21 cells and nearly 2.5-fold in HaK cells (Fig. 2.16B). In the untreated cells, the replication kinetics of the VACV mutants was very similar between the two cell lines (Fig. 2.17). VC-R1 replicated as well as the wild type VACV in both BHK-21 and HaK cells and vp872 replicated in both untreated cell lines to intermediate levels between VC-R2 and VC-R1. Pre-treatment of

BHK-21 cells with hsIFNα, however, slowed the replication of vp872 and increased the fold difference with VC-R1 at 32hpi to 49-times less compared to 17-times less in untreated cells. All four VACV strains were more sensitive to hsIFNα pre-treatment in the HaK cells, but VC-R1 still replicated as well as the wild type VC-2 and neither vp872 nor VC-R2 could replicate in the treated cells.

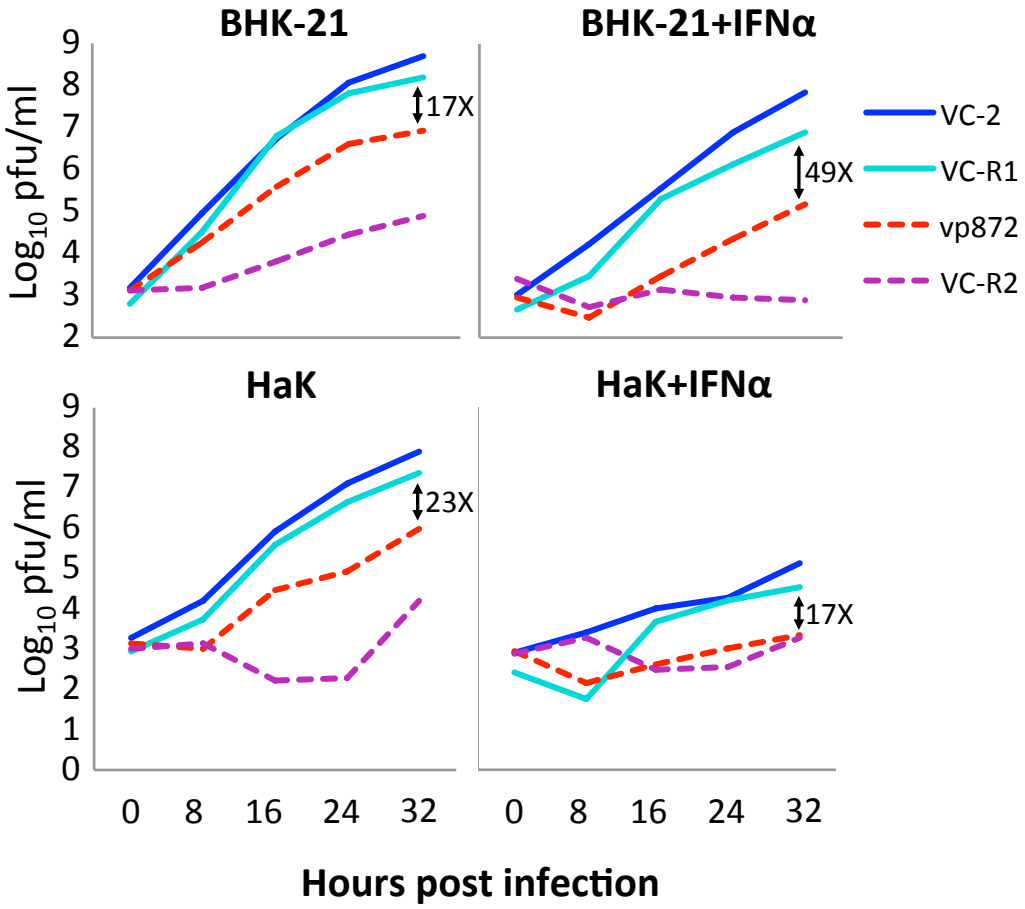

Figure 2.17 VACV replication in interferon treated Syrian hamster cells.

Two S. hamster cell lines (BHK-21 and HaK) were pre-treated with 500U/ml hsIFNα or left untreated. After 17 hours, the cells were infected with VACV-Cop and the mutant VACV strains at an MOI=0.01. Virus was collected at the indicated time points and titered on RK13+E3L+K3L cells by plaque assay. Fold differences between the single-deletion VACV strains at 32hpi is indicated. IFN pre-treatment attenuated the vp872 virus lacking K3L in both S. hamster cell lines.

We additionally treated the AHL-1 cells and V79-4 cells with hsIFNα and compared virus replication with the treated BHK-21 cells (Fig. 2.18). All four VACV strains replicated to

lower titers in the AHL-1 cells pre-treated with hsIFNα, although vp872 was still able to replicate above input levels. Similarly, we again observed a significant difference between VC-R1 and vp872 titers in untreated BHK-21 cells and this difference was increased when cells were pre-treated with hsIFNα. In V79-4 cells, however, virus replication of all of the viruses was only marginally reduced (~2.5-fold reduction on average) with hsIFNα pre-treatment.

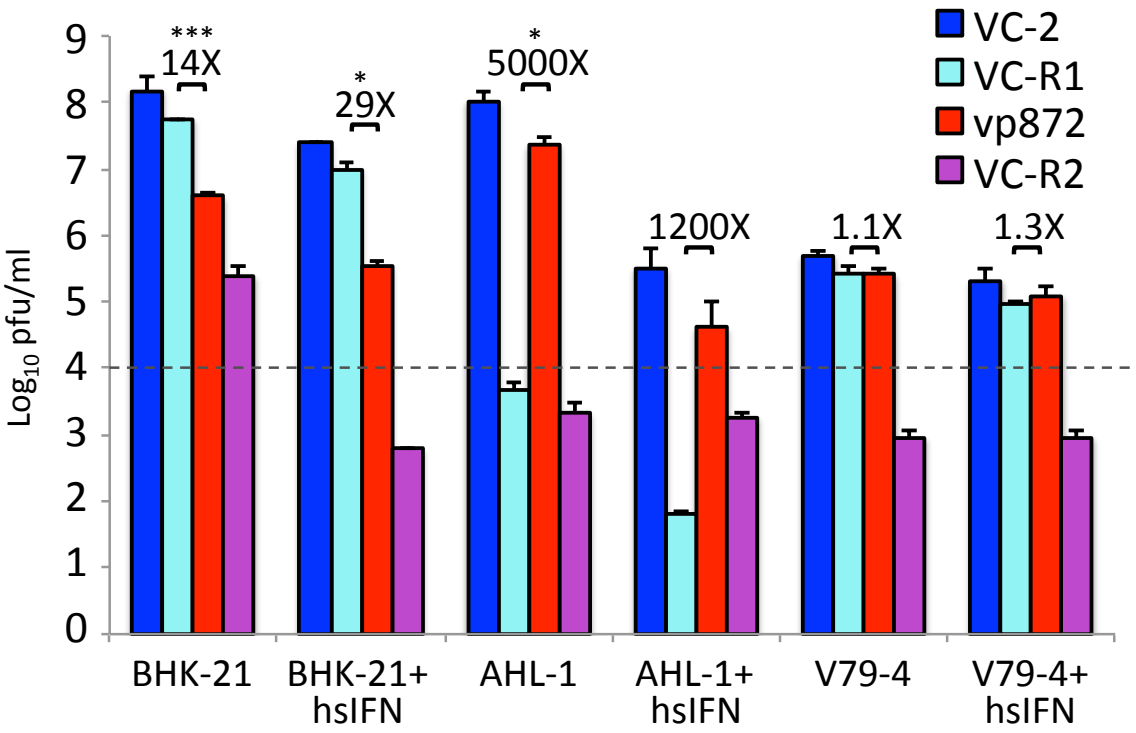

Figure 2.18 VACV replication in human interferon treated hamster cells.

*The three hamster cells were either pre-treated with 500U/ml hsIFNα or left untreated. After 17 hours, the cells were infected with VACV-Cop and the mutant VACV strains at an MOI=0.01. Virus was collected at 30hpi and titered on RK13+E3L+K3L cells by plaque assay. Error bars indicate the standard deviation of two replicate experiments and fold differences between the single deletion mutant VACV strains are noted. P-values were calculated using the Student's t-test. * $p<0.05$, *** $p<0.0005$*

Although the replication of vp872 was reduced in the BHK-21 cells treated with hsIFNα, this virus was still able to moderately replicate despite the increased PKR expression. Because hamsters are more closely related to mice than to humans, we decided to also test murine IFN (mmIFNα1) on BHK-21 cells (Fig. 2.19A-C). The BHK-21 cells were much more sensitive to

mmIFNα1, which induced a high level of PKR expression as detected by RT-PCR even at the lowest concentration tested (5U/ml). This resulted in a 15.2-fold reduction in vp872 virus titers in the mmINFα1 treated BHK-21 cells compared to untreated cells and a 45.7-fold reduction compared to VC-R1 titers in the treated cells. Using similar concentrations of mmIFNα1 to those used with hsIFNα (500U/ml and 1000U/ml), replication of both VC-R1 and vp872 was prevented from reaching titers above the level of input.

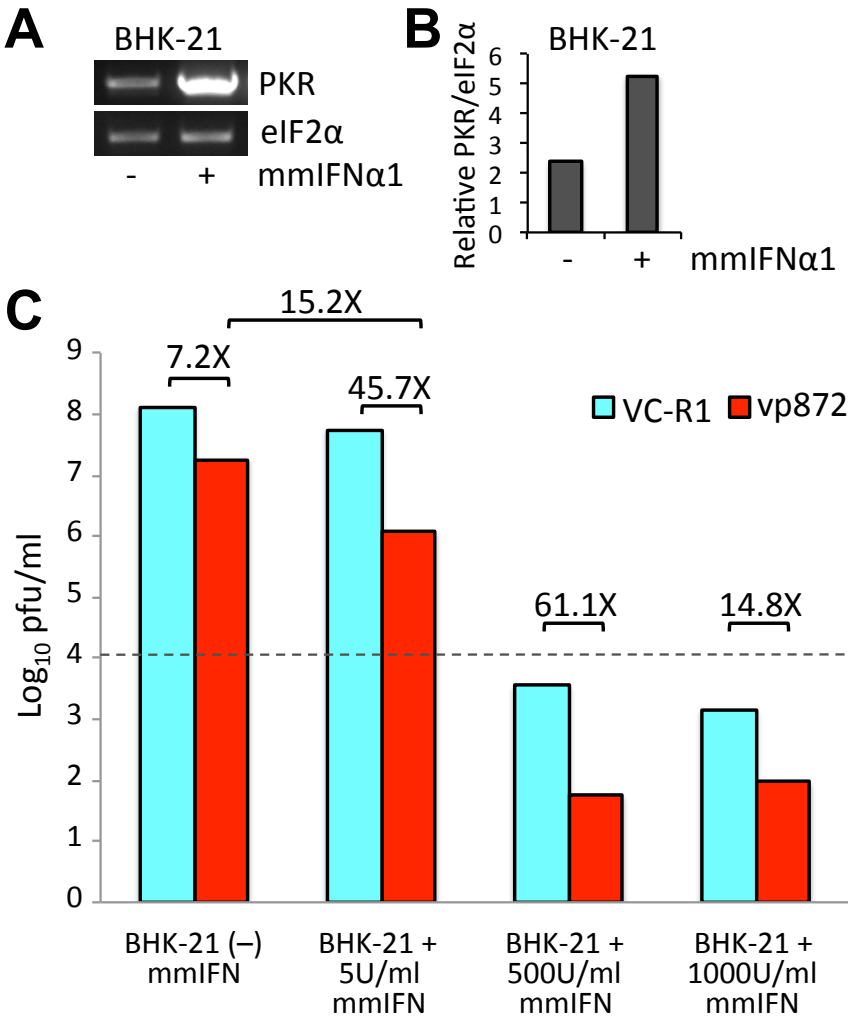

Figure 2.19 Mutant VACV replication in mouse interferon treated BHK-21 cells.

S. hamster PKR and eIF2α genes were amplified by RT-PCR from BHK-21 cells treated with 5U/ml mmIFNα for 17 hours. Band intensities were measured and calculated as a ratio of PKR to eIF2α (A and B). BHK-21 cells were pre-treated with 5U/ml, 500U/ml, or 1000U/ml mmIFNα1 or left untreated. After 24 hours, the cells were infected with VC-R1 or vp872 at an MOI=0.01. Virus was collected at 30hpi and the level of input virus is indicated by the dashed line. Fold differences are noted above the graph (C).

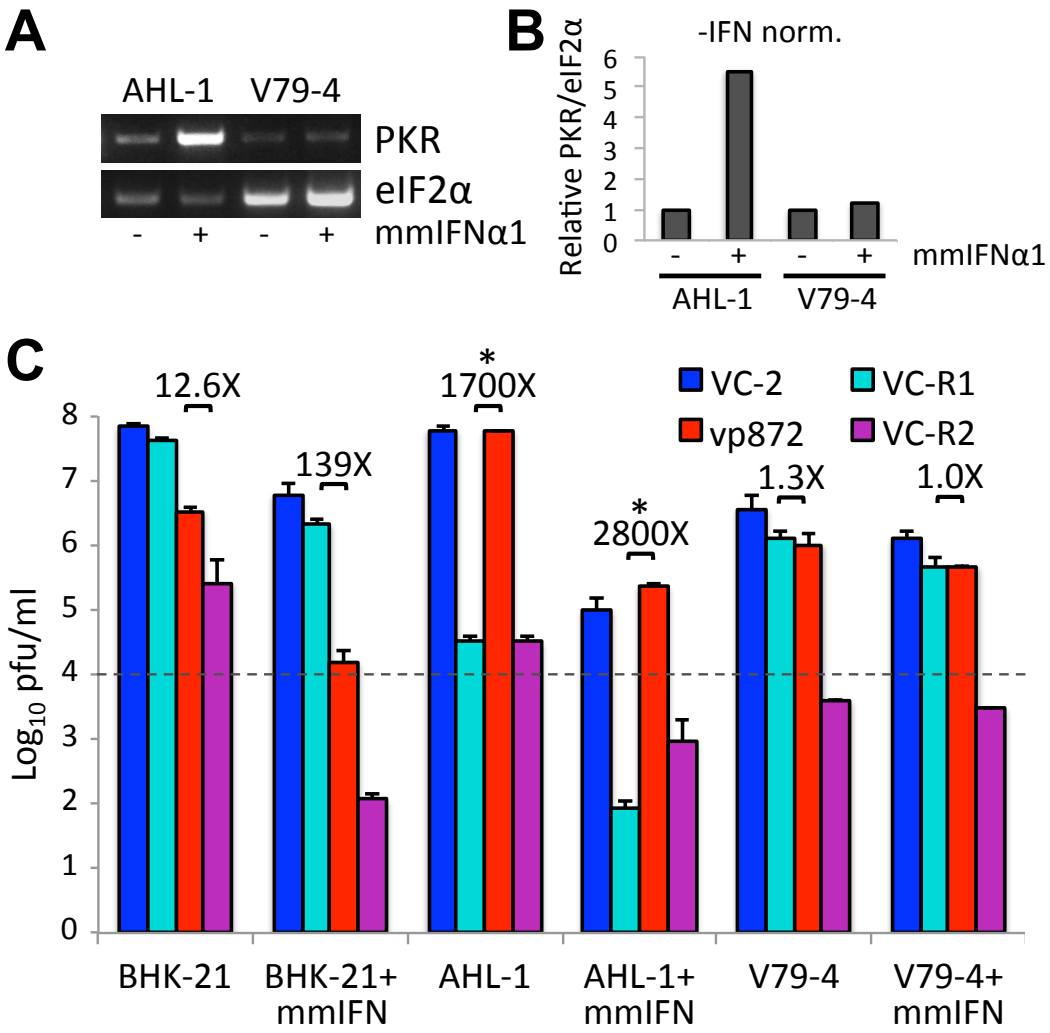

Figure 2.20 Mutant VACV replication in mouse interferon treated hamster cells.

*The A. hamster (AHL-1) and C. hamster (V79-4) cells were pre-treated with 5U/ml mmIFNα1 or left untreated for 17 hours and cDNA was prepared from each for RT-PCR amplification of hamster PKR and eIF2α (A). Band intensities were measured and calculated as a ratio of PKR to eIF2α. The ratios for each were normalized to the untreated sample, which is graphed in B. The three hamster cells were left untreated or pre-treated with 50U/ml mmIFNα1 for 24 hours, and then the cells were infected with the VACVs at an MOI=0.01. Virus was collected at 30hpi and titered on RK13+E3L+K3L cells by plaque assay, and fold differences between the single deletion mutant viruses are noted. Error bars indicate the standard deviation of two replicate experiments. P-values were calculated using the Student's t-test. * $p<0.05$*

Treatment of AHL-1 with mmIFNα1 also resulted in a strong induction of PKR expression as detected by RT-PCR (Fig 2.20A and B), but in the V79-4 cells, expression of PKR was not increased following mmIFNα1 treatment. From these results, we suspected that the V79-4 cells have a deficient IFN response and either lack the IFN receptor or are otherwise defective at some point in the IFN pathway prior to expression of interferon stimulated genes like PKR. Alternatively, but less likely, the murine IFNα1 used in this assay might not be recognized well by the C. hamster IFN receptors. Similar to the hsIFNα pre-treatment, no dramatic change in virus titers was observed when V79-4 cells we pre-treated with mmIFNα1 and infected with the VACV strains (Fig 2.20C). Replication of the VACV strains in both BHK-21 and AHL-1 cells, however, was greatly reduced with mmIFNα1 pre-treatment. The fold reduction in vp872 titers in mmIFNα1 treated BHK-21 cells compared to VC-R1 titers was increased to 139-fold compared to 12.6-fold in untreated cells, and vp872 replicated nearly 2800-times better than VC-R1 in treated AHL-1 cells.

To correspond with the induction and overexpression of PKR in BHK-21 cells treated with IFN, we designed siRNA to target either S. hamster or A. hamster PKR and knock down its expression in BHK-21 as well as the AHL-1 cells. We infected untreated cells and siRNA treated cells with the four VACV strains at an MOI of 0.01 and measured viral titers after 48 hours (Fig. 2.21). In both untreated cell lines, VC-R2 reached titers significantly lower than the wild-type virus (~500-1000X reduction). Treatment with siRNA to knock down PKR expression in both cell lines rescued VC-R2 replication, which reached titers not significantly different from the wild-type virus. Similarly in BHK-21 cells, vp872 titers were increased with siRNA treatment relative to untreated cells and were not significantly different from titers reached by VC-R1, indicating that PKR was successfully knocked down in these cells and that PKR expression and activity correlated with the reduction in vp872 replication in BHK-21 cells. An even greater difference was observed in the AHL-1 cells. VC-R1 replication in untreated AHL-1 cells was restricted compared to vp872 replication (~700X reduction), but replication of VC-R1 was increased significantly with siRNA treatment to titers comparable with both wild-type VC-2 and vp872 viruses.

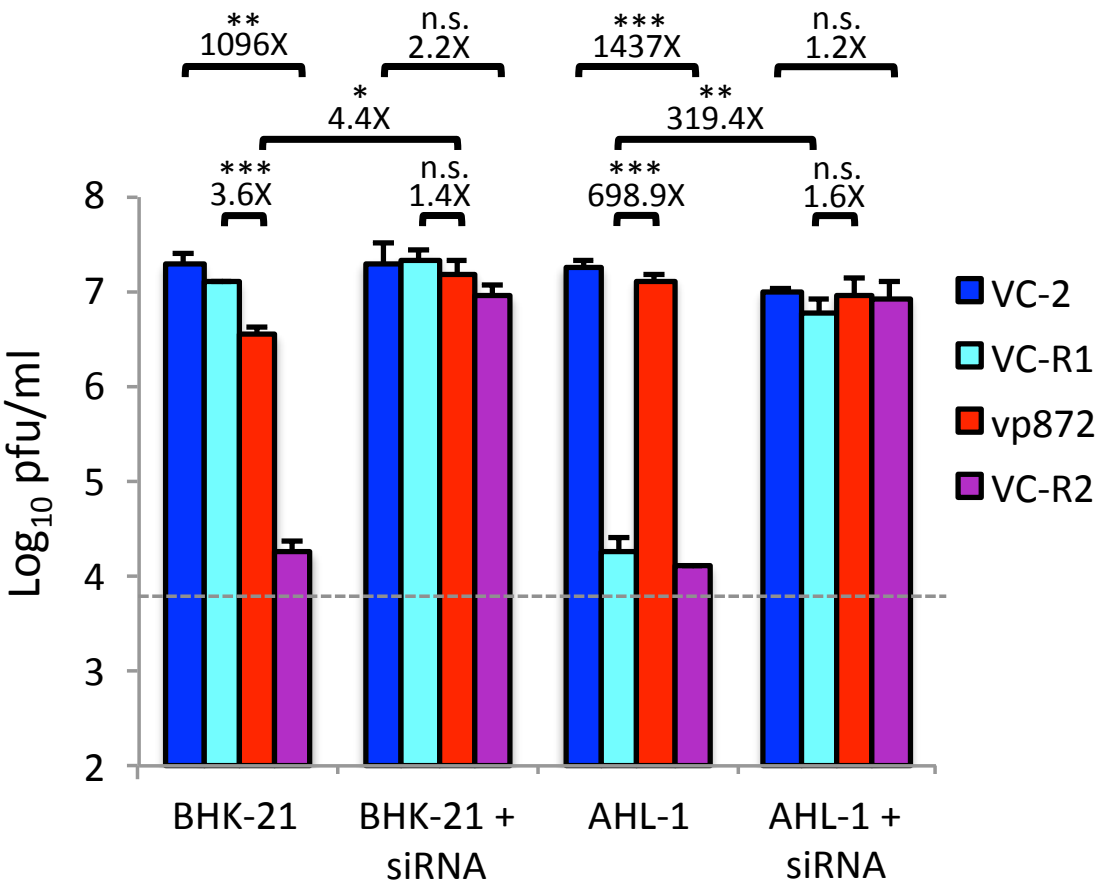

Figure 2.21 siRNA knock-down of PKR in hamster cells.

*A pool of four siRNA oligos targeting hamster PKR were transfected into BHK-21 and AHL-1 cells at 50nM concentration. Twenty-four hours post transfection, untreated cells and siRNA treated cells were infected with wild-type VACV-Cop (VC-2) and its derivatives lacking E3L, K3L, or both. Virus collected after 48 hours was titered on RK13+E3L+K3L cells. Error bars indicate the standard deviation of three replicate infections. Fold differences are shown between the indicated virus infections. Asterisks indicate statistical significance as determined by the Student's t-test. n.s.= $p>0.05$, * $p<0.05$, ** $p<0.005$, *** $p<0.0005$.*

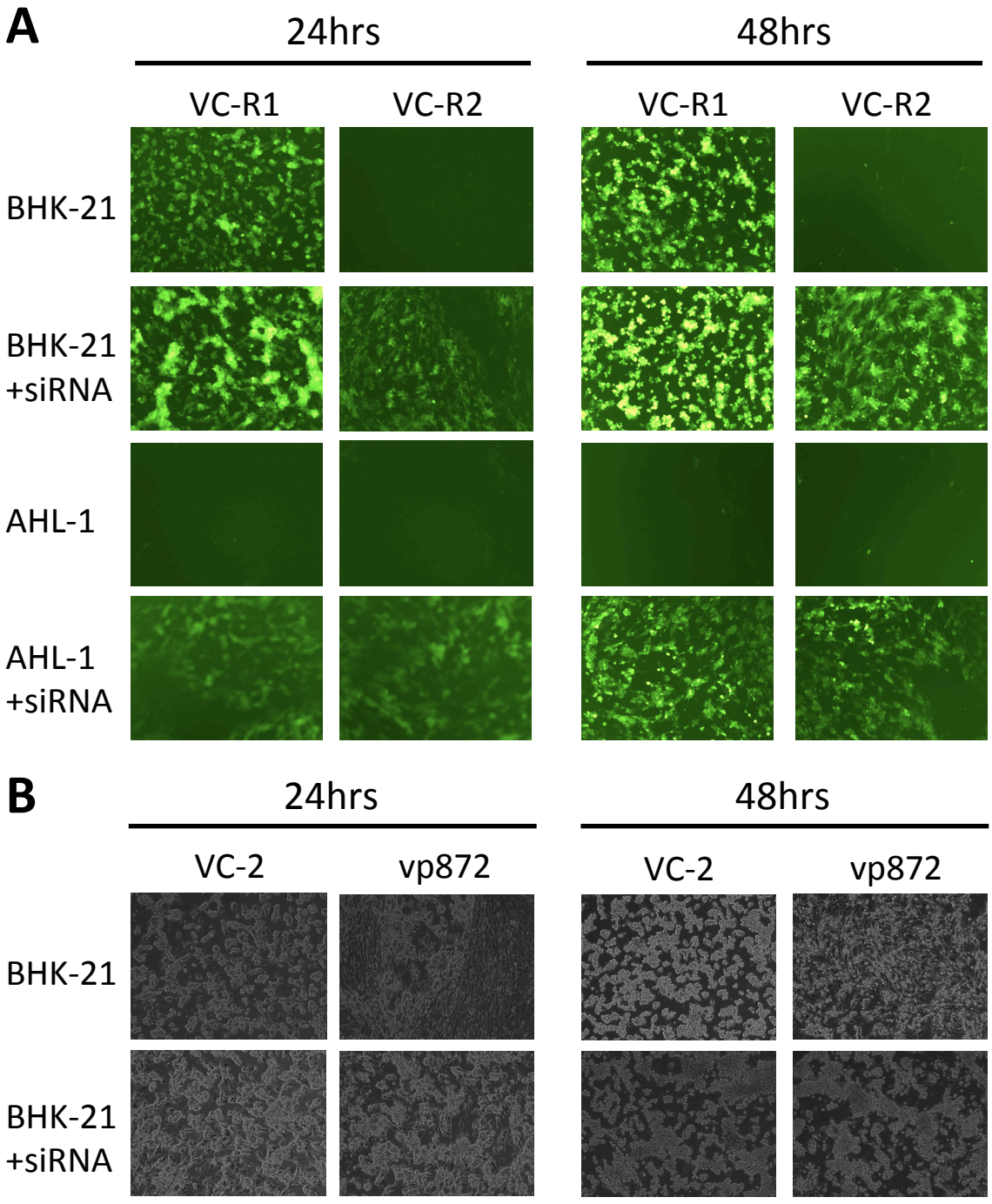

Figure 2.22 siRNA knock-down of PKR in hamster cells rescues mutant VACV replication.

A pool of four siRNA oligos targeting hamster PKR were transfected into BHK-21 and AHL-1 cells at 50nM concentration. Twenty-four hours post transfection, untreated cells and the siRNA treated cells were infected with VC-R1 or VC-R2 at MOI=0.01 (A). Virus replication was monitored at 24hpi and 48hpi by fluorescence imaging (100X magnification, 1000ms exposure). Treated or untreated BHK-21 cells were also infected with VC-2 or vp872 (MOI=0.01) and monitored for CPE by light microscopy (B).

The replication of VC-R1 and VC-R2, which both express GFP from the E3L locus, were also monitored in siRNA treated and untreated cells over 48 hours of infection by fluorescence microscopy (Fig. 2.22A). Very little GFP fluorescence was detected in VC-R2 infected BHK-21 cells after 24hpi or 48hpi, corresponding to the attenuated phenotype of this virus in BHK-21 cells, while GFP fluorescence was observed in VC-R1 infected BHK-21 cells as expected. Knockdown of S. hamster PKR with siRNA resulted in higher levels of GFP expression from VC-R1 and VC-R2 infected BHK-21 cells consistent with the increase in relative titers we observed from the infection (Fig. 2.21). Furthermore, infection with vp872 in the siRNA treated BHK-21 cells also resulted in an increase in cytopathic effect (CPE) compared to untreated cells infected with this virus, particularly after 24hpi, and was similar to that observed from infections with VC-2 (Fig. 2.22B). As expected, no GFP fluorescence was observed from VC-R1 or VC-R2 infections of untreated AHL-1 cells correlating with the inability of these viruses to replicate in these cells. However, when PKR was knocked down in these cells, both VC-R1 and VC-R2 formed large GFP-positive plaques indicative of replication. This data shows a correlation of both the expression and activity of PKR with the replication of VACV lacking E3L and/or K3L in hamster cells, which is consistent with the sensitivity to either inhibitor that we observed for the corresponding PKR from each hamster species.

Generation of hamster PKR expressing cell lines and an inducible-expression system

Our results showed a strong correlation between the sensitivity of PKR from different species to VACV E3L and K3L in reporter assays with eIF2α phosphorylation and virus replication after VACV infection of cell lines. In order to extend these findings, we decided to generate isogenic PKR-expressing cell lines in the HeLa-PKRkd cell background. We previously used this method to compare human and rabbit PKR interactions with the K3L ortholog from myxoma virus (22). Similarly, we cloned both S. hamster and A. hamster PKR into a stable transfection vector to express each PKR from the native human PKR promoter and stably transfected the HeLa-PKRkd cells. Single-cell clones were screened for hamster PKR expression using anti-FLAG antibodies and compared to expression from HeLa-PKRkd cells complemented with human PKR-FLAG (hs-14 cells; a representative sample of the screening is shown in Fig. 2.23A and B). While we were initially able to identify single-cell clones that expressed PKR from each species and also had low endogenous PKR expression, we generally observed very

low expression of the hamster PKRs compared to the control hs-14 cells, which was gradually reduced during subsequent passages (not shown). Additionally, none of the A. hamster PKR-expressing cells were able to restrict replication of VC-R1 or VC-R2 except for clones in which we also observed an increased level of background endogenous human PKR expression. The S. hamster expressing cells that we identified were able to suppress VC-R2 replication, but replication of VC-R1 and vp872 was similar based on GFP-fluorescence of VC-R1 (Fig 2.23B) and CPE caused by vp872 (not shown).

Under the suspicion that the endogenous human PKR promoter may not be ideal for expression of the hamster PKRs in HeLa cells, we sub-cloned both the hamster PKRs as well as human PKR into a stable transfection vector under the control of the constitutive SV40 promoter. Strong expression of each PKR protein was observed from the stably transfected cells at 48 hours post transfection, particularly for human PKR (Fig. 2.24A). After three weeks of passaging the cells under antibiotic selection for the integrated plasmid, however, we observed a dramatic decrease in PKR expression from both of the hamster PKR expressing cell populations as well as the human PKR expressing cells. Nevertheless, the level of human PKR expression after three weeks under selection was similar to that observed from the hs-14 cells expressing human PKR from the endogenous PKR promoter.

When we infected the stably transfected polyclonal cell populations after one passage and after four passages with the four VACV strains, we observed a heavy restriction on replication of all of the VACV strains after one passage post transfection with each of the three PKRs preventing VC-R1 and VC-R2 replication entirely (Fig 2.24B). Cells infected after four rounds of passaging no longer restricted VC-2 replication compared to the vector control transfected cells, but VC-R2 was also able to replicate above input levels for all polyclonal cell lines (Fig 2.24C). While VC-R1 was more restricted in the human PKR and A. hamster PKR-transfected cells as we expected, vp872 was not at all restricted in the polyclonal S. hamster PKR-transfected cells.

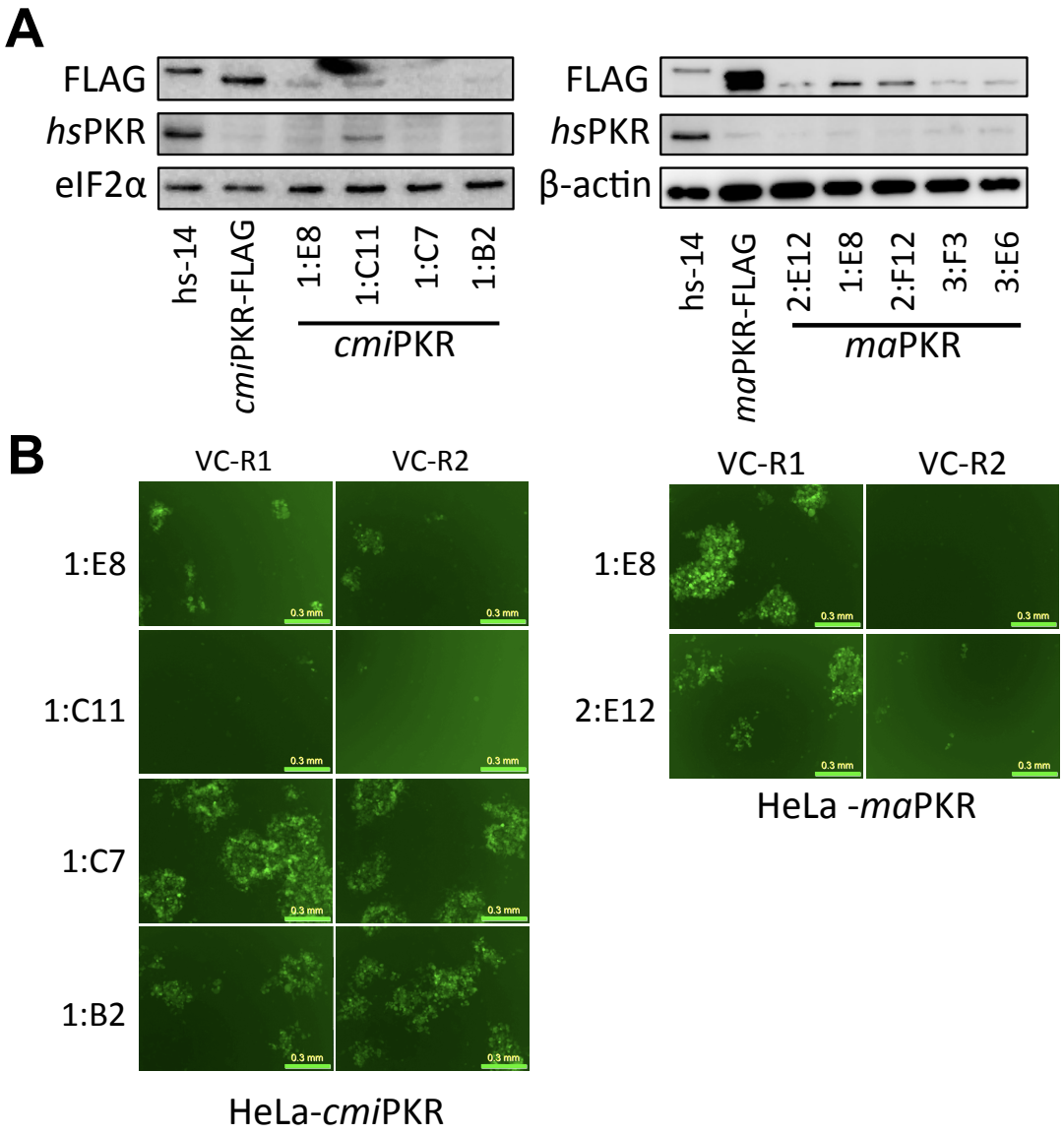

Figure 2.23 Screening of hamster PKR-expressing HeLa cells.

HeLa-PKRkd cells were stably transfected with plasmids encoding FLAG-tagged S. hamster PKR or A. hamster PKR from the native PKR promoter and protein lysates (1% SDS) were collected from single-cell clones for each (A). PKR expression from each clonal cell line was analyzed by Western blot using anti-FLAG antibodies and compared to PKR expression from hs-14 expressing FLAG-tagged human PKR and transiently transfected hamster PKRs (top panel). Membranes were subsequently probed for endogenous human PKR expression with anti-hsPKR antibodies (middle panel) and β-actin or eIF2α as loading control (bottom panel). Each of the single-cell clones were infected with VC-R1 or VC-R2 at MOI = 0.01 and fluorescent plaque formation was observed 24 hours post infection (B). ma = S. hamster; cmi = A. hamster; hs = human.

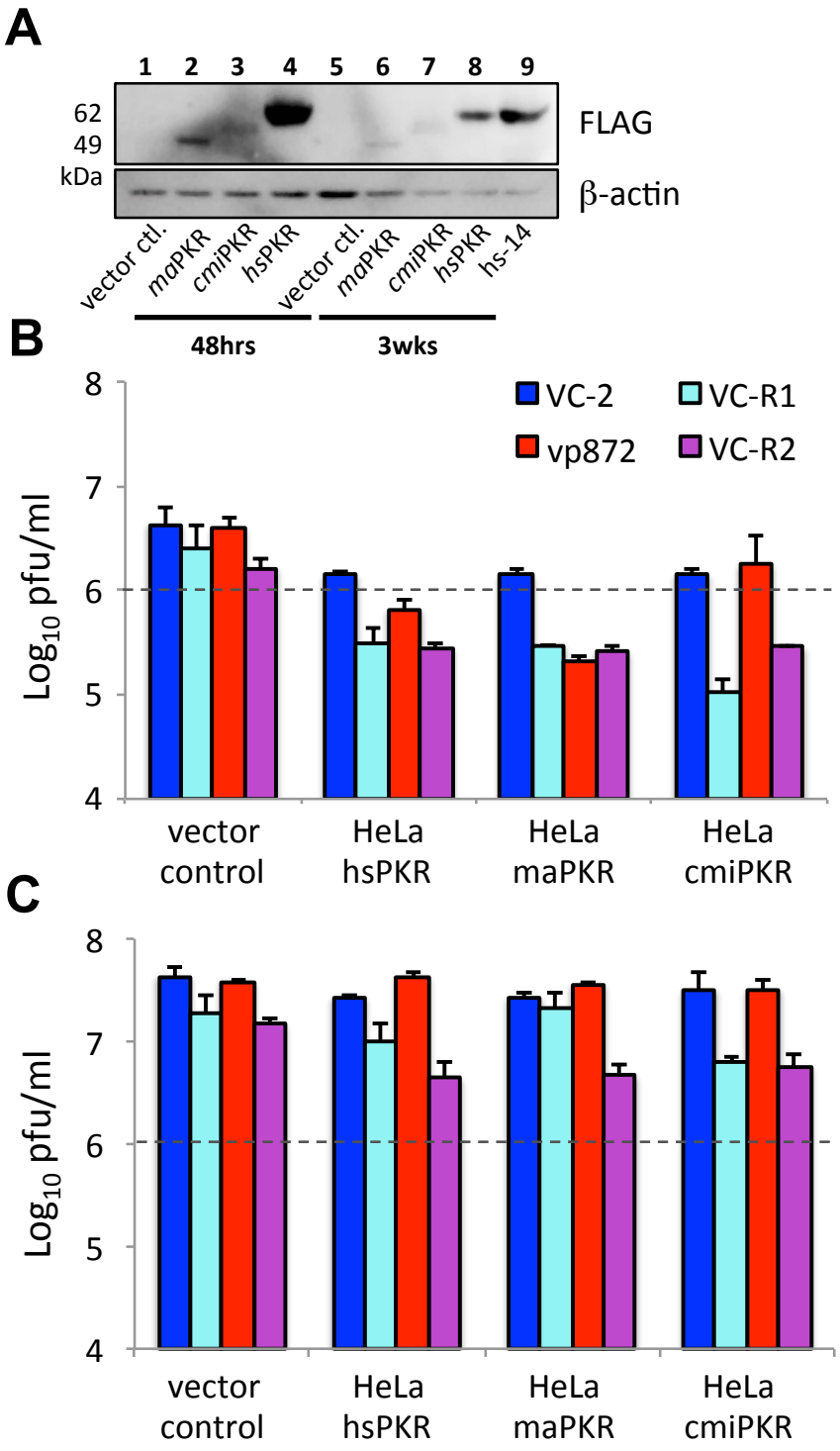

Figure 2.24 Unstable expression from hamster PKR-reconstituted HeLa cells.

HeLa-PKRkd cells were stably transfected with empty vector (control), or plasmids encoding FLAG-tagged knock-down resistant human PKR, S. hamster PKR, or A. hamster PKR driven by the SV40 promoter. Protein lysates were collected from the polyclonal pool of geneticin-resistant cells and probed

for reconstituted PKR expression with anti-FLAG antibodies at 48 hours post transfection and after 3 weeks of geneticin selection (A). At 48 hours (passage 1, B) and after ~3 weeks (passage 4, C), the polyclonal cells were seeded in 6-well plates and infected with the four viruses. Error bars represent the standard deviations of two replicate infections.

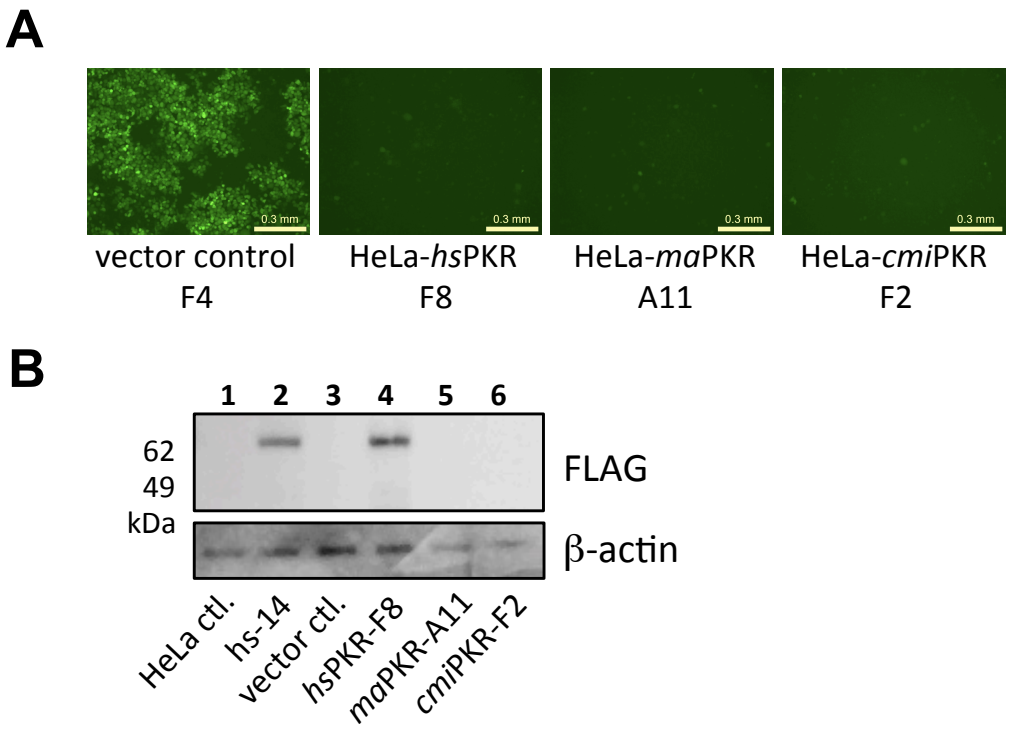

Figure 2.25 PKR-reconstituted HeLa cells suppress VC-R2 but do not express hamster PKR. *Single geneticin-resistant clones were isolated and infected with VC-R2 at MOI=0.01 and monitored for GFP expression after 48 hours (A). VC-R2 replication, as indicated by GFP expression, was reduced in all PKR expressing cell lines compared to the vector control. Protein lysates were collected from the clonal PKR-transfected cells, clonal vector control cells and control HeLa cells (not PKRkd) and probed for PKR expression using anti-FLAG antibodies (B). FLAG-tagged PKR expression was not observed for either hamster PKR-reconstituted clone but was observed from both human PKR-expressing clones tagged with FLAG epitopes.*

We then selected for single cell clones from each of the polyclonal cell populations and screened them for VC-R2 replication and PKR expression using anti-FLAG antibodies (Fig 2.25A and B). While all of the single cell clones that expressed human or hamster PKR restricted VC-R2 replication compared to the vector control cells, we only observed FLAG-tagged PKR

expression from the human PKR clone, which was comparable with hs-14 PKR expression. From these results we concluded that the expression of the hamster PKRs in the HeLa cells might be toxic, which would select against cells expressing high levels of hamster PKR. In addition, our selection for clones that suppress VC-R2 replication may have instead selected for cells that have lost the knockdown of human PKR of the parent cells or otherwise have increased endogenous PKR expression.

In order to overcome the potentially cytotoxic effect of hamster PKR expression, we decided to use a tetracycline-inducible expression system to control PKR expression in the hamster-PKR expressing cells. In this system, the gene for the tetracycline repressor (*TetR*) from *E. coli* is stably expressed from cells and a single gene-of-interest insertion site is integrated into the genome, which has two tetracycline repressor binding sites in the promoter. Integration of the gene-of-interest into this site is mediated by Flp-recombinase from *Saccharomyces cerevisiae*, but expression of the integrated gene is suppressed unless tetracycline or doxycycline is present, which binds the tetracycline repressor and allows for gene transcription (T-REx, Invitrogen).

Using the HeLa-PKRkd cells as the parent cell line, we first transfected the plasmid encoding the insertion site and selected for stable integrations with zeocin. The insertion site expresses a fusion Zeocin-LacZ gene under the control of a constitutive CMV promoter, so we selected twenty single cell clones and screened them for expression of β-galactosidase by Western blot (Fig 2.26A). All twenty clones expressed β-galactosidase to varying degrees and none of the clones exhibited a high background of human PKR expression. To make sure that our cells had only a single integration of the insertion site, we collected genomic DNA from each of the clones and used quantitative (q) PCR with two template concentrations and primers designed to detect a portion of the LacZ gene (Fig 2.26B). We ensured that the designed primers were able to detect a single increase in gene copy-number using genomic DNA prepared from 293-T-REx cells, which have only a single insertion site (Fig. 2.27, Invitrogen). The cycle-threshold values decreased by ~1 cycle with each 2-fold increase in template concentration correlating to a doubling of the target site copy number. We compared the Cq values from qPCR reactions performed with the DNA from the single cell clones to those obtained with the 293-T-REx cell DNA and identified two clones, #4 and #26, that yielded similar results, which indicated they are likely to have only a single integration of the Flp-In insertion site. Both cell lines were subsequently transfected with the plasmid encoding the tetracycline repressor and

selected for stable integration with blasticidin. Into these Flp-In Ready HeLa-PKRkd cells, we will be able to insert the hamster PKRs and test the sensitivity of PKR to VACV E3L and K3L in an isogenic background as well as determine the dose dependent effects of PKR on the requirement for E3L and K3L for VACV infection of cells in this context.

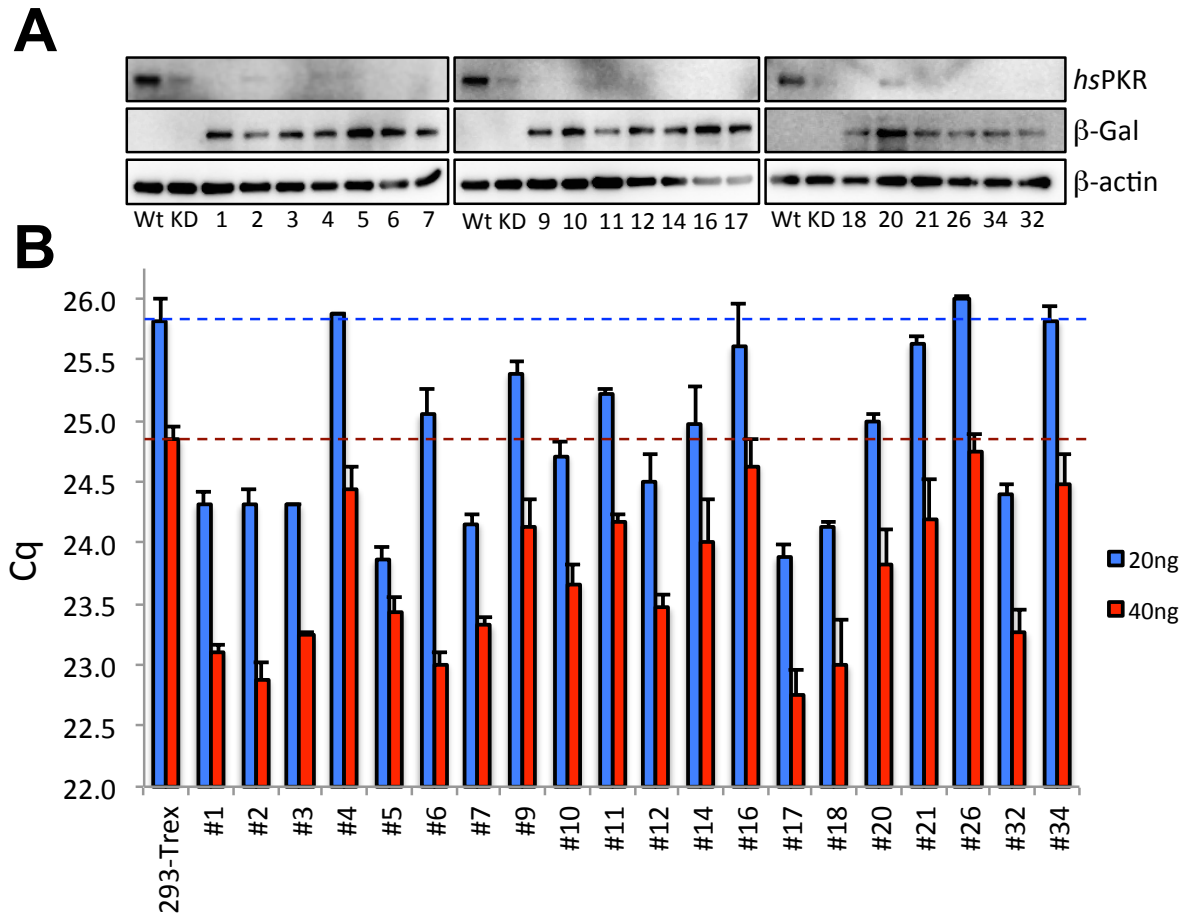

Figure 2.26 Screening HeLa-PKRkd clones for Flp-In site integration.

Protein lysates were collected with 1%SDS from 293-Trex cells, HeLa-PKRkd cells, and 20 single colony isolates (numbered 1 through 34) of HeLa-PKRkd cells stably expressing the Flp-In site for gene-of-interest expression and separated by SDS-PAGE and analyzed for expression endogenous human PKR, b-galactosidase (β-Gal), and β-actin by Western blotting (A). Genomic DNA was collected from 293-Trex cells and the 20 HeLa-PKRkd clones. The gDNA was used as template in two quantities for qPCR with primers amplifying the LacZeo fusion gene to select clones containing a single insertion of the Flp-In site in the genome (B). The dashed lines indicate the cycle threshold value corresponding to single gene copies for each template volume according to the results with 293-Trex cell genomic DNA. Wt = HeLa wild type; KD = HeLa PKRkd.

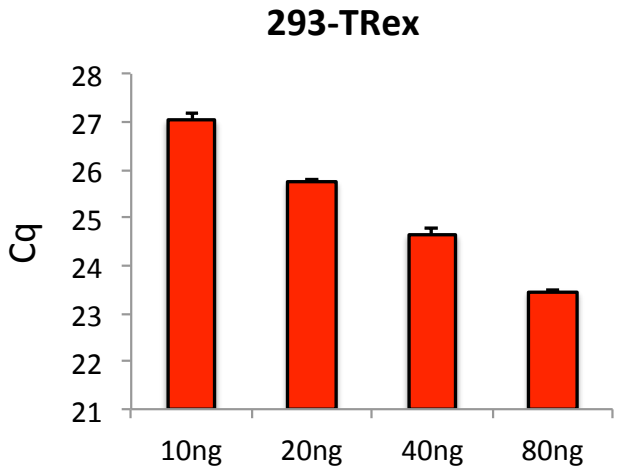

Figure 2.27 Quantitative PCR test for single Flp-In site in 293-T-REx cells.

Genomic DNA was collected from 293-T-REex cells and the gDNA was used as template in four quantities for qPCR with primers amplifying the LacZeo fusion gene. Each doubling of the template DNA reduces the Cq value by ~1 cycle.

To test the induction of gene expression in the T-REx system, we stably transfected both S. hamster and A. hamster PKR into the 293-T-REx cells and assayed for hamster PKR expression following treatment with tetracycline or doxycycline by Western blot (Fig. 2.28). PKR expression was very low in un-induced cells but was strongly induced in the presence of 0.1µg/ml tetracycline or doxycycline. Induction of each PKR was not observed in the presence of lower concentrations of tetracycline; however, the dose-dependent effect on gene expression must lie within the range of 1ng-100ng/ml tetracycline or doxycycline, as no further increase in PKR expression was observed with higher concentrations of each antibiotic. The ability to induce the hamster PKRs from the 293-T-REx cells is a promising proof-of-concept, but their utility for comparing PKR from different species is limited without first knocking-out or knocking-down the expression of the endogenous human PKR. Initial attempts to knock down human PKR in these cells with siRNA did not result in efficient knock-down after 24 hours (Fig. 2.29), but continued optimization of this procedure may allow the use of the hamster PKR-expressing 293 cells in future experiments.

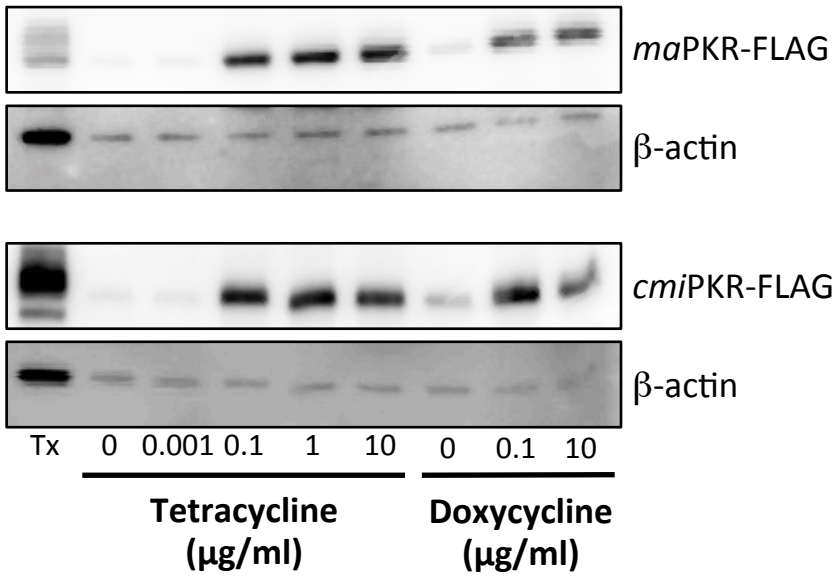

Figure 2.28 293-T-REx cells express hamster PKRs following induction with tetracycline or doxycycline.

FLAG-tagged S. hamster (ma) or A. hamster (cmi) PKR were cloned into 293-T-Rex cells, and their expression was induced with different concentrations of tetracycline or doxycycline as indicated for 24 hours. Protein lysates were collected in 1% SDS and expression was probed by Western blot. Protein collected from HeLa-PKRkd cells transfected with each FLAG-tagged PKR (Tx) was also analyzed for size comparisons.

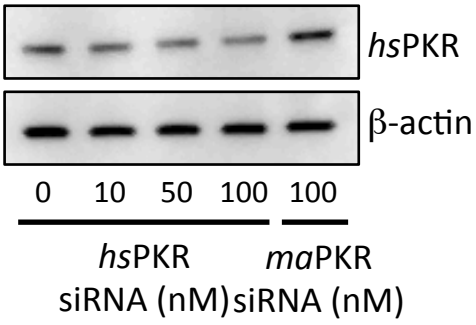

Figure 2.29 siRNA treatment test to knock-down human PKR in 293-T-REx cells.

Protein lysates were collected with 1% SDS from 293-Trex cells that were left untreated or transfected for 24 hours with a pool of four siRNAs targeting human (hs) PKR at different concentrations or pooled siRNAs targeting S. hamster (ma) PKR.

The generation of the Flp-In Ready HeLa-PKRkd cells also provides a useful tool for our lab more generally as we can now express any gene-of-interest in these cells in a PKR-deficient

background and control the expression of each gene by adding tetracycline or doxycycline. This reduces the potential for selecting against highly expressing cells in cases where the exogenous protein is toxic to the cells and has the added benefit that the genomic location of the insertion site is the same between clones, since genomic integration occurs at the Flp-In site.

Discussion

In this study we have demonstrated that E3L and K3L are critical host range factors for VACV replication in a variety of mammalian cell types and that their host range functions can be explained by species-specific inhibition of the host innate immune response protein, PKR. We and others have previously described the host specific nature of VACV K3L inhibition of PKR as well as K3L orthologs in other poxviruses such as myxoma virus (8, 9, 22). Here we extend these analyses to look at interactions between both K3L and E3L of VACV with PKR from closely related hamster species. Although the natural hosts of VACV are unknown, other related orthopoxviruses are thought to be primarily maintained in rodent populations (2, 28), which adds significance to the work done here as the sensitivity of the hamster PKRs to these viral inhibitors has a greater potential to be the result of selective pressure imposed on these rodents by poxviruses or other viruses with similar PKR inhibitors rather than being the result of random differences.

VACV E3L encodes an N-terminal Z-DNA binding domain and a C-terminal dsRNA-binding domain. The dsRNA-binding motif of E3L is highly conserved among dsRNA-binding proteins including PKR and has been shown to be necessary for inhibition of PKR (15, 29, 30), although the N-terminal domain of E3L was also found to be necessary to inhibit the IFN response in mouse cells (31). PKR was identified as the key host factor modulating E3L in human Huh7 cells in response to IFN treatment (10) and is the most important protein in determining the restriction of VACV lacking E3L in HeLa cells (Fig 2.3B) (18).

Our results confirmed previous studies that identified an essential role for E3L in the replication of VACV in several different cell lines. Due to the near universal requirement of E3L for VACV replication in host cells, we found the observation by Langland and Jacobs in 2002 that VACV lacking E3L can replicate in BHK-21 cells intriguing. The authors suggested that variable expression of endogenous PKR and differing levels of dsRNA generated during infection of the different cell lines could explain the dispensability of E3L. While we don't

exclude the effects of these cell-type-specific differences, we propose that the major difference explaining the ability of the E3L-deleted VACV to replicate in BHK-21 cells is the species-specific resistance of S. hamster PKR to E3L inhibition. We showed the resistance of S. hamster PKR to inhibition by VACV E3L in our luciferase transfection assay, in a yeast growth assay, as well as in virus infected cells where levels of transfected PKR were kept constant and we would not expect differences in amounts of dsRNA generated.

Using the same highly sensitive cell culture-based transfection assay for PKR inhibition in cells deficient in endogenous PKR, we were able to compare the sensitivity of PKR from several different species to both viral inhibitors from VACV. The gene product of VACV K3L is comprised of an S1-fold homologous to the S1 domain of PKR's substrate, eIF2α. K3L acts as a pseudosubstrate inhibitor by binding PKR to block its activity (16, 32). We observed a remarkable variability in the ability of K3L to inhibit PKR from even closely related species. In particular, the resistance of the A. hamster PKR to K3L was unique among all the hamster PKRs tested, while PKR from the C. hamster of the same genus was very sensitive to K3L inhibition. The resistance of A. hamster PKR to K3L inhibition was observed in several different assays as with the S. hamster PKR, and their opposing sensitivities to both PKR inhibitors from VACV provides an opportunity to investigate the resistance of each to the respective VACV inhibitors more mechanistically.

Our identification of the resistance of S. hamster PKR to inhibition by VACV E3L was unexpected considering the broad requirement of E3L for VACV replication in many cell lines and the mode of E3L inhibition of PKR by binding dsRNA. However, the identification of a second resistant PKR from a T. hamster (*Mesocricetus brandtii*) suggests that resistance to inhibition by E3L and potentially other viral dsRNA-binding proteins may be a novel innovation that arose in the *Mesocricetus* hamster lineage. Many viruses encode proteins that bind dsRNA to prevent activation of antiviral cellular proteins such as PKR (33). Such a general characteristic of this innate immune response protein would undoubtedly favor individuals with resistant PKRs during virus infection. The presence of both E3L and K3L in VACV and many other poxviruses therefore highlights the importance of having two genes with overlapping functions in order to maintain a broad host range.

Most mammalian cell lines are permissive for VACV replication, however, C. hamster ovary cells (CHO) are one of the few for which VACV cannot replicate. VACV requires the

expression of a host range protein from cowpox virus called CP77 to replicate in CHO cells, which prevents the host shutoff of protein synthesis and the induction of apoptosis to allow for virus replication (26, 34). From this study, we determined that this requirement is not specific to all C. hamster cells, but is instead a characteristic specific to this cell line. Wild-type VACV replicated in two other C. hamster cell lines that we tested (Fig. 2.13), which allowed us to compare replication of our mutant viruses in a cell line from this species to their replication in cell lines derived from the two other hamster species.

By infecting cell lines derived from each hamster species with our VACV mutants lacking E3L and/or K3L, we were able to see a strong correlation between PKR sensitivity to inhibition by E3L and K3L, as determined in the luciferase and yeast assays, and high levels of phosphorylated eIF2α indicative of increased PKR activity, and restriction of replication of the mutant viruses in each cell line. We showed that VC-R1, which displayed a severe host range defect in most cell lines tested, replicated in two different S. hamster cell lines comparably to the wild type virus, and vp872, which lacks K3L, exhibited delayed replication kinetics and reached lower titers compared to the E3L-deleted virus. Additionally, in S. hamster BHK-21 cells, IFN stimulation and the concomitant induction of PKR expression resulted in an increase in the attenuation of vp872. This correlation supports the important role of PKR inhibition in VACV replication and the inability of E3L to inhibit PKR from the S. hamster. It is notable, however, that vp872 titers in the BHK-21 cells were always higher than VC-R2 titers in all of our experiments. This suggests that E3L may perform other necessary functions for the virus besides inhibition of PKR that allows for some replication in these cells. There is evidence to suggest that the N-terminal Z-DNA binding domain of E3L is involved in regulating host gene expression and can act independently of the C-terminal dsRNA-binding domain to inhibit activation of IRF3 (interferon response factor 3), which induces the expression of several ISGs (15). Furthermore, E3L can interfere with the activation of the OAS/RNaseL pathway (in BHK-21 cells, (23)), and E3L is able to suppress cytokine induction through both PKR-dependent and PKR-independent pathways (35). Nevertheless, the relative resistance of VC-R1 in BHK-21 cells to either human or murine IFN pre-treatment in our experiments and the subsequent increase in PKR expression supports our initial hypothesis for the species-specific resistance of S. hamster PKR to inhibition by VACV E3L. This along with the fact that VACV also encodes K3L, which

is otherwise able to inhibit S. hamster PKR, explains the previously observed dispensability of E3L for VACV in these cells.

In addition, the replication of vp872 in the A. hamster AHL-1 cells mirrored the dispensability of K3L that was reported for VACV replication in human HeLa cells (23). Human PKR was only weakly inhibited by VACV K3L, but VACV is able to replicate in human cell lines because human PKR can be inhibited by VACV E3L (Figs. 2.3 and 2.4; (8)). Similarly both A. hamster and rat PKR are resistant to inhibition by VACV K3L, while VACV E3L can inhibit PKR from both species (Figs. 2.4 and 2.8). Likewise, the sensitivities of these species' PKRs correlated with the inability of the E3L-deleted VACV to replicate in cells derived from these host species, while deletion of K3L had little to no negative effect on virus replication (Figs. 2.1 and 2.15). Knocking down A. hamster PKR in the AHL-1 cells also resulted in a rescue of virus replication for both VC-R1 and VC-R2 as indicated by GFP expression, which suggests that inhibition of PKR is a critical factor for VACV replication in these hamster cells and that VACV E3L is required for this function unless PKR expression is suppressed (Fig. 2.22). Altogether, these results indicate that the host range function of VACV K3L is due to species-specific inhibition of PKR from different host species, and that unlike with E3L, PKR resistance to inhibition by K3L has evolved multiple times in different mammalian species.

We were also able to increase the susceptibility of BHK-21 cells to infection with vp872 as well as VC-R2 by knocking down S. hamster PKR, which increased virus induced CPE or GFP expression for each. This suggests that PKR is the major restricting host factor for these viruses and that the attenuation of vp872 in BHK-21 cells is due to a defect in PKR inhibition. The rescue of VC-R1 replication in BHK-21 cells following siRNA knockdown of S. hamster PKR suggests that this PKR may be activated to a low degree in untreated BHK-21 cells infected with VC-R1, although in these cells we only observed a low level of eIF2α-phosphorylation (Fig 2.14). Recent work suggests that PKR may induce the expression of ISGs independent of eIF2α-phosphorylation mediated by interactions with other PRR's such as RIG-I or MDA5 in response to different viruses (36). It remains possible that some of the reduction in VC-R1 replication that we observed relative to VC-2 may be explained by such interactions, although this remains to be tested.

Despite our previous success in engineering HeLa cells that express FLAG-tagged human or rabbit PKR (22), we encountered surprising difficulties using the same methods to create

HeLa cells that express hamster PKR stably. We surmise that the hamster PKRs were not stably expressed in HeLa cells because their activity is toxic to the cells. In cells where each hamster PKR was under the control of the endogenous human PKR promoter, the expression of PKR was generally low in single-cell clones relative to the hs-14 cells expressing human PKR at levels comparable with control cells. It is, however, possible that their expression was higher at earlier passages and that highly expressing clones were selected against over time, since we observed a similar reduction of PKR expression from cells expressing the hamster PKRs from a constitutive SV40 promoter (Fig 2.24). Further evidence for this comes from a recent publication, where the use of S. hamster PKR was suspended and replaced with human PKR for biochemical analyses due to the high toxicity of the hamster PKR in the bacteria used to generate the protein (37). The reason for the unstable hamster PKR expression is not clear, but our solution to use an inducible expression system for generating the hamster PKR expressing cells in turn yielded a useful molecular tool to investigate species-specific interactions with other viral PKR inhibitors in the context of an isogenic host cell that in the future will be useful for developing informative studies of virus host range.

Author contributions

The experiments in this study were conceived and designed by S.L.H. and S.R. Experiments were performed by S.L.H., C.P., T.S. and S.R. and were supervised by B.M. and S.R. The paper was written by S.L.H and S.R, and T.S. and B.M. critically examined the manuscript.

References

1. Chung CS, Hsiao JC, Chang YS, Chang W (1998) A27L protein mediates vaccinia virus interaction with cell surface heparan sulfate. *J Virol* 72(2):1577–1585.

2. Haller SL, Peng C, McFadden G, Rothenburg S (2014) Poxviruses and the evolution of host range and virulence. *Infect Genet Evol* 21:15–40.

3. Beattie E, Tartaglia J, Paoletti E (1991) Vaccinia Virus-Encoded eIF2alpha Homolog Abrogates the Antiviral Effect of Interferon. *Virology* 183:419–422.

4. Beattie E, Denzler KL, Tartaglia J, Perkus ME, Paoletti E, Jacobs BL (1995) Reversal of the interferon-sensitive phenotype of a vaccinia virus lacking E3L by expression of the reovirus S4 gene. *J Virol* 69:499–505.

5. Meurs E, Chong K, Galabru J, Thomas NS, Ker IM, Williams BR, Hovanessian AG (1990) Molecular cloning and characterization of the human double-stranded RNA-activated protein kinase induced by interferon. *Cell* 62(2):379–390.

6. Dey M, Mann BR, Anshu A, Mannan MA-U (2014) Activation of protein kinase PKR requires dimerization-induced cis-phosphorylation within the activation loop. *J Biol Chem* 289(9):5747–5757.

7. Hovanessian AG (2007) On the discovery of interferon-inducible, double-stranded RNA activated enzymes: The 2′–5′oligoadenylate synthetases and the protein kinase PKR. *Cytokine Growth Factor Rev* 18(5-6):351–361.

8. Rothenburg S, Seo EJ, Gibbs JS, Dever TE, Dittmar K (2009) Rapid evolution of protein kinase PKR alters sensitivity to viral inhibitors. *Nat Struct Mol Biol* 16(1):63–70.

9. Elde NC, Child SJ, Geballe AP, Malik HS (2009) Protein kinase R reveals an evolutionary model for defeating viral mimicry. *Nature* 457(7228):485–489.

10. Arsenio J, Deschambault Y, Cao J (2008) Antagonizing activity of vaccinia virus E3L against human interferons in Huh7 cells. *Virology* 377(1):124–132.

11. Guerra S, Agaitua F, Martinez-Sobrido L, Esteban M, Garcia-Sastre A, Rodriguez D (2011) Host-Range Restriction of Vaccinia Virus E3L Deletion Mutant Can Be Overcome In Vitro, but Not In Vivo, by Expression of the Influenza Virus NS1 Protein. *PLoS ONE* 6(12):e28677.

12. Chang H-W, Uribe LH, Jacobs BL (1995) Rescue of vaccinia virus lacking the E3L gene by mutants of E3L. *J Virol* 69:6605–6608.

13. Shors T, Kibler KV, Perkins KB, Seidler-Wulff R, Banaszak MP, Jacobs BL (1997) Complementation of Vaccinia Virus Deleted of the E3L Gene by Mutants of E3L. *Virology* 239:269–276.

14. Beattie E, Denzler KL, Tartaglia J, Perkus ME, Paoletti E, Jacobs BL (1995) Reversal of the Interferon-Sensitive Phenotype of a Vaccinia Virus Lacking E3L by Expression of the Reovirus S4 Gene. *J Virol* 69:499–505.

15. Langland JO, Kash JC, Carter V, Thomas MJ, Katze MG, Jacobs BL (2006) Suppression of Proinflammatory Signal Transduction and Gene Expression by the Dual Nucleic Acid Binding Domains of the Vaccinia Virus E3L Proteins. *J Virol* 80(20):10083–10095.

16. Dar AC, Sicheri F (2002) X-Ray Crystal Structure and Functional Analysis of Vaccinia Virus K3L Reveals Molecular Determinants for PKR Subversion and Substrate Recognition. *Mol Cell* 10:295–305.

17. Rahman MM, Liu J, Chan WM, Rothenburg S, McFadden G (2013) Myxoma virus protein M029 is a dual function immunomodulator that inhibits PKR and also conscripts RHA/DHX9 to promote expanded host tropism and viral replication. *PLoS Pathog* 9(7):e1003465.

18. Zhang P, Jacobs BL, Samuel CE (2008) Loss of Protein Kinase PKR Expression in Human HeLa Cells Complements the Vaccinia Virus E3L Deletion Mutant Phenotype by Restoration of Viral Protein Synthesis. *J Virol* 82(2):840–848.

19. Hand ES, Haller SL, Peng C, Rothenburg S, Hersperger AR (2015) Ectopic expression of vaccinia virus E3 and K3 cannot rescue ectromelia virus replication in rabbit RK13 cells. *PLoS ONE* 10(3):e0119189.

20. Brennan G, Kitzman JO, Rothenburg S, Shendure J, Geballe AP (2014) Adaptive gene amplification as an intermediate step in the expansion of virus host range. *PLoS Pathog* 10(3):e1004002.

21. Seet BT, Johnston JB, Brunettie CR, Barrett JW, Everett H, Cameron C, Sypula J, Nazarian SH, Lucas A, McFadden G (2003) Poxviruses and Immune Evasion. *Annu Rev Immunol* 21(1):377–423.

22. Peng C, Haller SL, Rahman MM, McFadden G, Rothenburg S (2016) Myxoma virus M156 is a specific inhibitor of rabbit PKR but contains a loss-of-function mutation in Australian virus isolates. *Proc Natl Acad Sci USA*. 113(14):3855-3860. doi:10.1073/pnas.1515613113.

23. Langland JO, Jacobs BL (2002) The Role of the PKR-Inhibitory Genes, E3L and K3L, in Determining Vaccinia Virus Host Range. *Virology* 299(1):133–141.

24. Beattie E, Paoletti E, Tartaglia J (1995) Distinct Patterns of IFN Sensitivity Observed in Cells Infected with Vaccinia K3L- and E3L- Mutant Viruses. *Virology* 210(2):254–263.

25. Kawagishi-Kobayashi M, Silverman JB, Ung TL, Dever TE (1997) Regulation of the Protein Kinase PKR by the Vaccinia Virus Pseudosubstrate Inhibitor K3L Is Dependent on Residues Conserved between the K3L Protein andthe PKR Substrate eIF2alpha. *Mol Cell Biol* 17:4146–4158.

26. Spehner D, Gillard S, Drillien R, Kirn A (1988) A cowpox virus gene required for multiplication in Chinese hamster ovary cells. *J Virol* 62(4):1297–1304.

27. Hsiao J-C, Chung C-S, Drillien R, Chang W (2004) The cowpox virus host range gene, CP77, affects phosphorylation of eIF2 alpha and vaccinia viral translation in apoptotic HeLa cells. *Virology* 329(1):199–212.

28. Essbauer S, Pfeffer M, Meyer H (2010) Zoonotic poxviruses. *Vet Microbiol* 140(3-4):229–236.

29. Chang HW, Watson JC (1992) The E3L gene of vaccinia virus encodes an inhibitor of the interferon-induced, double-stranded RNA-dependent protein kinase. *Proc Natl Acad Sci USA* 89:4825-4829.

30. Chang HW, HH UL, Jacobs BL (1995) Rescue of vaccinia virus lacking the E3L gene by mutants of E3L. *J Virol* 69(10):6605-6608.

31. White SD, Jacobs BL (2012) The Amino Terminus of the Vaccinia Virus E3 Protein Is Necessary To Inhibit the Interferon Response. *J Virol* 86(10):5895–5904.

32. Davies MV, Chang H-W, Jacobs BL, Kaufman RJ (1993) The E3L and K3L Vaccinia Virus Gene Products Stimulate Translation through Inhibition of the Double-Stranded RNA-Dependent Protein Kinase by Different Mechanisms. *J Virol* 67:1688–1692.

33. Alcamí A, Symons JA, Smith GL (2000) The vaccinia virus soluble alpha/beta interferon (IFN) receptor binds to the cell surface and protects cells from the antiviral effects of IFN. *J Virol* 74(23):11230–11239.

34. Ink BS, Gilbert CS, Evan GI (1995) Delay of vaccinia virus-induced apoptosis in nonpermissive Chinese hamster ovary cells by the cowpox virus CHOhr and adenovirus E1B 19K genes. *J Virol* 69(2):661–668.

35. Myskiw C, Arsenio J, van Bruggen R, Deschambault Y, Cao J (2009) Vaccinia Virus E3 Suppresses Expression of Diverse Cytokines through Inhibition of the PKR, NF- B, and IRF3 Pathways. *J Virol* 83(13):6757–6768.

36. Pham AM, Santa Maria FG, Lahiri T, Friedman E, Marie IJ, Levy DE (2016) PKR Transduces MDA5-Dependent Signals for Type I IFN Induction. *PLoS Pathog* 12(3):e1005489.

37. Husain B, Mayo C, Cole JL (2016) Role of the Interdomain Linker in RNA-Activated Protein Kinase Activation. *Biochemistry* 55(2):253–261.

Chapter 3 - Molecular mechanisms of species-specific PKR resistance to vaccinia virus E3L and K3L

Haller, S.L.[1]; Peng, C.[1]; Vipat, S.[1]; Tazi, L.[1]; Rothenburg, S.[1]

1. *Division of Biology, Kansas State University, Manhattan, KS 66506, USA*

Keywords: E3L, K3L, positive selection, PKR resistance, dsRNA–binding proteins

Abstract

Vaccinia virus (VACV), the prototype poxvirus, can infect several host species including rodents, cattle, and humans and therefore has a very broad host range. To maintain this broad host range, VACV encodes several host range genes that are important for overcoming host defenses. Two host range genes encoded by VACV called E3L and K3L target PKR, a critical mediator of the host interferon response, at different steps during its activation and activity. Our previous work and work from others has shown that the redundant roles of E3L and K3L for VACV are critically important for VACV to maintain its broad host range and its ability to infect many different species. Deletion of E3L, for example, prevented virus replication in cells derived from an Armenian hamster, whose PKR is resistant to inhibition by K3L, while deletion of K3L highly attenuated virus replication in Syrian hamster derived cells, whose PKR is resistant to inhibition by E3L. Using the inverse relationship of these two hamster PKRs with VACV E3L and K3L, we designed a set of experiments using a cell culture-based luciferase assay to investigate the critical components of each that contribute to their ability to resist inhibition by either VACV protein. From this analysis, we uncovered further support for the interaction of K3L with residues in the helix αG of PKR's kinase domain, which has likely also driven positive selection in PKR during rodent and lagomorph evolution. Additionally, we determined that the interaction with VACV E3L is more complex and involved interactions with multiple domains in PKR. However, mutations that interfere with dimer formation restored E3L's ability to inhibit PKR from the S. hamster and mutations that are predicted to abolish dsRNA-binding in PKR prevented E3L from inhibiting otherwise sensitive PKRs. These results provided evidence to support a model of E3L inhibition that depends on PKR's ability to bind dsRNA and form inactive hetero-dimers via dsRNA bridging or by disrupting PKR dimers.

Significance

Protein kinase R (PKR) is a key mediator of the interferon-induced antiviral response. Its activation by double-stranded RNA during virus infection leads to a shutdown of protein translation and viral replication. For this reason, many viruses have evolved proteins and mechanisms to overcome the activity of this protein. Vaccinia virus (VACV) encodes two inhibitors of PKR, E3L and K3L that inhibit PKR at different steps in its activation and activity. At the same time, PKR in different species have been shown to exhibit differential sensitivities to these inhibitors, for which the molecular explanations are not yet completely understood. In this study we performed a mechanistic analysis of two PKRs from related species that are resistant to inhibition by E3L or K3L. Our results confirmed previous reports of the importance of the αG helix in the kinase domain of PKR for interactions with K3L and provide evidence for a general resistance mechanism to viral dsRNA-binding protein inhibitors by S. hamster PKR. This resistance can be attributed to interdomain interactions involved in PKR dimerization and activation. The study of this novel innovation in S. hamster PKR to overcome viral PKR inhibition by VACV E3L is significant because it challenges the conventional model for E3L inhibition of PKR by sequestration and provides further evidence to support the hetero-dimerization model for the PKR inhibitory function of E3L, which continues to be an area of intense research.

Introduction

The RNA-dependent protein kinase (PKR) is a critical component of the antiviral innate immune response in vertebrates (1, 2). PKR recognizes intracellular double-stranded (ds) RNA generated during a virus infection, which leads to its activation via dimerization and autophosphorlylation reactions (3-5). Active PKR then phosphorylates the alpha subunit of the eukaryotic translation initiation factor 2 (eIF2α), locking eIF2 in a GDP-bound state that is incapable of binding Met-tRNA to initiate protein translation. This causes a general shutdown in cellular cap-dependent protein translation and halts virus replication as viruses critically depend on cellular translation machinery to replicate in host cells (6).

Vaccinia virus (VACV) is the prototype member of the poxvirus family, which collectively exhibits wide variation in host range. Vaccinia virus can infect several host species including rodents, cattle, and humans, and it therefore has a very broad host range. To maintain this broad host range, VACV encodes several host range genes that are important for overcoming host defenses. Two host range genes encoded by VACV called E3L and K3L target PKR at different steps during its activation and activity (7, 8). Our work and work from others has shown that the redundant roles of E3L and K3L for VACV are critically important for VACV to maintain its broad host range and its ability to infect different species (Ch. 2) (9, 10). K3L contains an S1 domain that is homologous to the PKR binding domain of PKR's substrate, eIF2α, and directly binds to the kinase domain of PKR, thereby blocking the interaction of activated PKR with eIF2α (7, 11, 12). The E3L gene encodes an N-terminal Z-DNA-binding domain (Zα) that plays some role in the pathogenesis of VACV *in vivo* as well as a C-terminal dsRNA-binding domain whose function is critical for suppression of the interferon response in VACV infected cells (13, 14). The exact mechanism of E3L's interactions with PKR is less well understood, but it is generally accepted that the binding of dsRNA is necessary for E3L's host range function and inhibition of PKR activity, although recent work has suggested the possibility of a role for E3L's immune antagonism that is independent of dsRNA binding (15).

PKR is composed of two N-terminal dsRNA-binding domains (RBDs) that are linked to a C-terminal kinase domain by a flexible region of variable length (linker region). The kinase domain of PKR, like other cellular kinases, can be further divided into a smaller N-terminal lobe (N-lobe) and a larger, C-terminal lobe (C-lobe). The N-lobe is made up of five anti-parallel β sheets (β1- β5) flanked by two α helices (α1 and α2). This lobe is involved in direct interactions

between the two PKR molecules of an active dimer. The C-lobe is mostly helical in structure with 8 α helices (αD to αJ) and two pairs of short anti-parallel β sheets (β7- β8 and β6- β9). Three helices form the core of the C-lobe (αE, αF, and αH), while αD, αG, and αJ are more exposed on the surface of the enzyme. The helix αG forms the interaction interface with the substrate of PKR, eIF2α (16). Residues within this helix have been shown to be important in interactions with viral pseudosubstrate inhibitors of PKR, such as VACV K3L (17, 18). These interactions have influenced the rapid evolution of the PKR kinase domain, which shows strong signatures for positive selection in primates and vertebrates.

In the previous chapter, we described two closely related hamster PKRs that exhibited opposing resistances to inhibition by either VACV E3L or K3L. While Armenian (A.) hamster PKR was resistant to inhibition by VACV K3L, Syrian (S.) hamster PKR was resistant to inhibition by VACV E3L and both were sensitive to the remaining viral inhibitor. This observation provided a framework for us to investigate the mechanism of each PKR's resistance to either inhibitor, which also unexpectedly allowed us to examine aspects of PKR's activation that are targeted by viral inhibitors more generally. We generated a series of domain exchanges in either hamster PKR as well as deletion and point mutations to uncover the regions and residues important for their ability to resist inhibition by E3L and K3L using our cell culture-based luciferase for PKR inhibition. Our results confirmed previous reports of the importance of the helix αG in the kinase domain of PKR for interactions with K3L and provided evidence for a general resistance mechanism to viral dsRNA-binding protein inhibitors by S. hamster PKR, which could be attributed to interdomain interactions involved in PKR dimerization and activation by dsRNA.

Methods

Cell lines and plasmids

HeLa-PKRkd (kindly provided by Dr. Charles Samuel) cells were maintained at 37˚C, 5% CO_2 in Dulbecco's Modified Essential Medium (DMEM, Life Technologies) supplemented with 5% fetal bovine serum (FBS, Fischer) and 25μg/ml gentamycin (Quality Biologicals).

PKR from the indicated species and viral inhibitors were cloned into the pSG5 mammalian expression vector (Stratagene) for transient expression driven by the SV40 promoter as described by Rothenburg, et al. (17). Plasmids encoding VACV-Western Reserve (WR) E3L and K3L were described previously (Ch. 2). The E3L ortholog from VARV was generated by mutating residues in VACV E3L to match the sequence of VARV E3L and then cloned into pSG5. Sequences for Us11 and σ3 were derived from Herpes Simplex virus-1 and mammalian reovirus Type 1 Lang S4 gene (σ3 protein), which were kindly provided by Ian Mohr and Cathy Miller, respectively. The cloning of knock-down resistant human PKR, and PKR from European rabbit, mouse, rat, Syrian hamster, and Armenian hamster species into the pSG5 plasmid was described previously (17, 19, 20) (Ch. 2). Guinea pig PKR was cloned from 104C1 cells (ATCC CRL-1405, *Cavia porcellus*), and chicken PKR was cloned from cDNA prepared from a whole 14-day chicken embryo (*Gallus gallus*). Hybrid PKR constructs or deletion mutant PKRs were generated using two- or three-step fusion PCR to join segments of each PKR gene with overlapping ends into a single open reading frame (ORF). Point mutations were generated by site-directed mutagenesis PCR using the PfuUltra High-Fidelity DNA polymerase (Invitrogen). PCR was performed with primers containing the intended mutations flanked by 15-20 nucleotides identical to the template up- and downstream of the mutations. All ORFs were cloned into the pSG5 mammalian expression vector (Stratagene) driven by the SV40 promoter and each construct was sequenced to confirm the absence of other mutations. Nucleotide sequences for PKR genes analyzed in the positive selection analysis were obtained from Genbank (described in Table 3.1) or were derived from PKR sequences amplified from tissue samples in this analysis. Protein sequence alignments of the PKRs were obtained using ClustalW in MegAlign (DNAStar, Inc.). For transfection assays, plasmids were prepared using the NucleoBond Xtra Midi Endotoxin Free plasmid preparation kit (Macherey-Nagel).

Luciferase assay for PKR inhibition

The luciferase assay for inhibition of PKR activity was described previously (17, 20). Briefly, $5x10^4$ HeLa-PKRkd cells were seeded 24 hours before transfection in 24-well plates. For each transfection, 0.05µg of firefly luciferase encoding plasmid (pGL3promoter, Promega), PKR encoding plasmids (pSG5), and plasmids encoding each viral inhibitor or S. hamster dsRBDs were transfected at the indicated concentrations using GenJet-Hela (Signagen) in triplicate. For titration experiments the total amount of plasmid transfected was kept constant with additional empty vector (pSG5). Cell lysates were harvested 48 hours after transfection using mammalian lysis buffer (Goldbio), and the luciferase activity was determined by measuring light in a luminometer (Berthold) after adding luciferin substrate (Promega). PKR activity for each mutant construct was determined by comparing the luciferase activity for each PKR with vector control transfections. For PKR activity values in Table 3.5, the vector normalized PKR activity for each PKR mutant was subsequently normalized to S. hamster PKR activities within each experiment and the average and standard deviation of the normalized activity was determined from at least two independent experiments. For most experiments shown, the relative luciferase activity for each co-transfection with a PKR inhibitor was normalized to transfections with each PKR construct alone to show the relative amount of inhibition.

Phylogenetic and positive selection analysis

Nucleotide sequences of 7 rodent or 12 rodent and lagomorph species PKRs (Table 3.1) were aligned using MUSCLE (21) and poorly aligned regions were trimmed using G-blocks (version 0.91b, (22)). A maximum likelihood tree was generated from theses alignments using PhyML v3 with nodal support assessed via 100 pseudo-replicates of bootstrapping (23). Model selection for the phylogenetic analysis was determined using ModelTest (24) The dN/dS rates (ω) were estimated using the codon-based nested models M1 (neutral)/M2 (selection) and M7 (beta)/M8 (beta and ω), as implemented in PAML v4 (Phylogenetic Analysis by Maximum Likelihood, (25)). Using a Bayesian approach (Bayes Empirical Bayes, BEB), amino acid residues with posterior probabilities above 0.900 ($p<0.10$) for positive selection ($\omega>1$) in either model were screened, and residues with posterior probabilities above 0.950 ($p<0.05$) in either rodent or rodent and lagomorph (*Glires*) PKR sequences were considered to be under positive selection for this analysis. Residues under positive selection in the kinase domain were projected

onto the PKR-eIF2α structure (PDB 2A1A, (16)) using human PKR coordinates in MacPyMol (26).

Species name	Common name	Gene Abbr.	Accession number
Mesocricetus auratus	Syrian hamster	*ma*PKR	NM_001281945.1
Mesocricetus brandtii	Turkish hamster	*mb*PKR	unpublished
Cricetulus migratorius	Armenian hamster	*cmi*PKR	unpublished
Cricetulus griseus	Chinese hamster	*criP*KR	KT272869.1
Mus musculus	house mouse	*mm*PKR	NM_011163
Rattus norvegicus	brown rat	*rn*PKR	XM_008764426.1
Cavia porcellus	Guinea pig	*cpo*PKR	KT272870.1
Heterocephalus glaber	naked mole rat	*hg*PKR	XM_004839297.2
Ictidomys tridecemlineatus	13-lined ground squirrel	*it*PKR	XM_005336548.2
Oryctolagus cuniculus	European rabbit	*oc*PKR	KT272867.1
Sylvilagus floridanus	cottontail rabbit	*sf*PKR	unpublished
Sylvilagus bachmani	brush rabbit	*sb*PKR	unpublished

Table 3.1. Gene sequences used in the positive selection analysis.

Rodent (top 7) and lagomorph (last 3) species PKR sequences were collected from GenBank (NCBI) or were cloned from cells or tissue from the indicated species in this study.

Results

Syrian hamster PKR is resistant to dsRNA-binding proteins from different viruses

In the previous chapter, we described the resistance of Syrian (S.) hamster PKR and Turkish (T.) hamster PKR, both from *Mesocricetus* hamster species, to inhibition by vaccinia virus (VACV) E3L and confirmed the importance of this resistance to virus replication in cells from these species. The resistance of S. and T. hamster PKR was surprising and unexpected considering the conventional mode of E3L inhibition by binding and sequestering dsRNA (8, 27). To investigate the molecular mechanism of this resistance, we focused only on S. hamster PKR since it shares a high sequence identity with T. hamster PKR and first asked whether this resistance is restricted to VACV E3L or if it was also able to resist inhibition by E3L orthologs from other poxviruses. Using the same cell culture-based luciferase reporter assay that was used in the previous chapter to detect PKR inhibition, we co-transfected plasmids encoding PKR from mouse and Armenian (A.) hamster, which we previously identified as sensitive to VACV E3L

inhibition, and S. hamster PKR with E3L from VACV as well as orthologs from variola virus (VARV), myxoma virus (MYXV), yaba monkey tumor virus (YMTV), sheeppox virus (SPPV), and swinepox virus (SWPV) (Fig 3.1). Both mouse and A. hamster PKR were sensitive to inhibition by E3L orthologs from VACV, VARV and MYXV, but S. hamster PKR activity was not affected by any of these proteins.

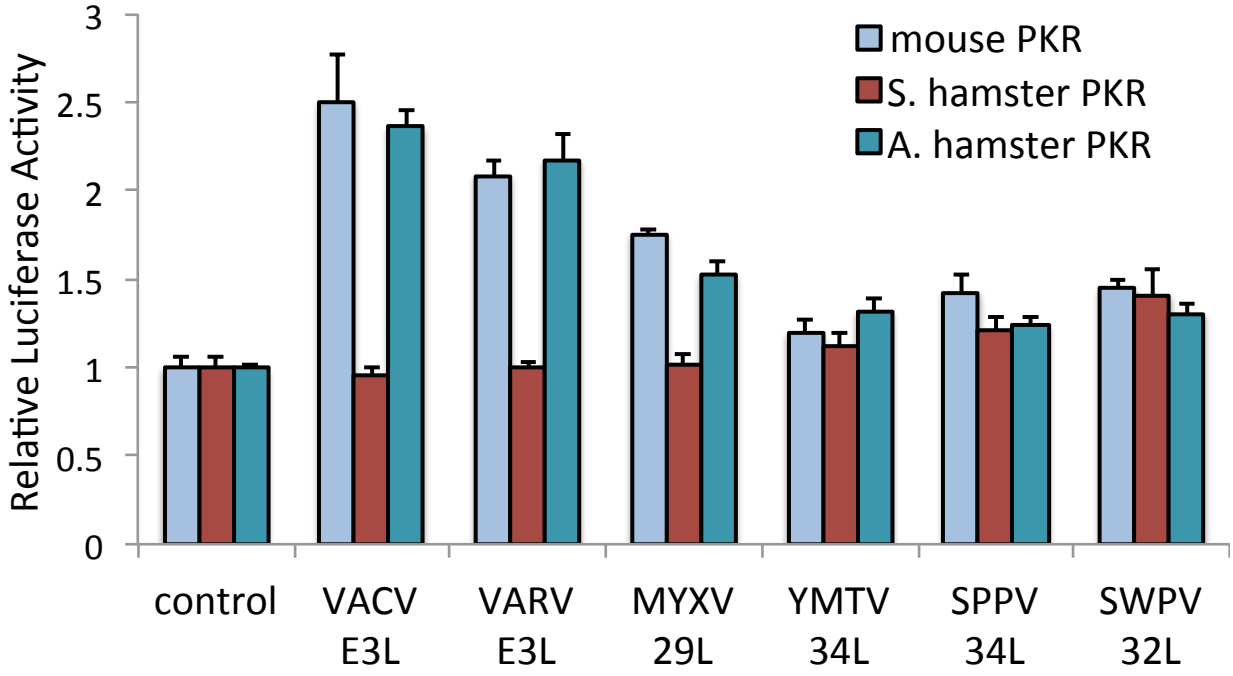

Figure 3.1 Syrian hamster PKR is resistant to other E3L orthologs from poxviruses.
HeLa-PKRkd cells were co-transfected with plasmids encoding firefly luciferase (0.05μg) and PKR from the indicated species (0.2μg), and E3L orthologs from the indicated viruses (0.4μg). Relative luciferase activity was determined by normalizing measured light units to PKR-only transfected cells. Error bars indicate the standard deviations for three replicate transfections. VACV= vaccinia virus; VARV= variola virus; MYXV= myxoma virus; YMTV= yaba monkey tumor virus; SPPV= sheeppox virus; SWPV= swinepox virus.

M029L, the E3L ortholog from MYXV, lacks the N-terminal Zα Z-DNA-binding domain found in both E3L proteins from VACV and VARV and encodes only a domain orthologous to the C-terminal dsRNA-binding domain of E3L (28). Previous work has suggested a role for the N-terminal Zα domain for the anti-immune function of E3L for VACV (13, 14). While the Zα domain in VACV E3L may perform other anti-immune functions for VACV, our results for

M029L inhibition of these PKRs imply that only a dsRNA-binding domain is required for PKR inhibition. Furthermore, the resistance of S. hamster PKR to all of these inhibitors suggests there is a similar interaction between these PKRs and orthologous E3L proteins for which we observed PKR inhibition. E3L orthologs from YMTV, SPPV and SWPV, which are from related Clade II poxviruses, were also tested, but these viral proteins exhibited no or only minimal inhibitory activities in this assay against the tested PKRs (Fig. 3.1). These data are in agreement work showing that these orthologs cannot fully rescue the replication of an E3L-deleted VACV (29).

The replication of recombinant VACV viruses lacking E3L could be partially rescued with dsRNA-binding proteins from other viruses or bacteria (30-32). To determine if the resistance of S. hamster PKR was unique to orthologous poxvirus proteins, or if this phenomenon extended to other viral dsRNA-binding proteins, we tested the ability of Us11 from Herpes Simplex virus 1 (HSV-1) and σ3 from mammalian reovirus to inhibit S. hamster PKR in the luciferase assay along with human, mouse and A. hamster PKR for comparison (Fig 3.2A). Us11 is a dsRNA binding protein that interacts with PKR physically to block its activation, which requires its basic residue-rich RNA-binding domain (33, 34). Reovirus σ3 is a structural protein that also binds dsRNA and can inhibit PKR activity, which, similar to E3L and Us11, requires its ability to bind dsRNA
(32, 35, 36). Neither Us11 nor σ3 share sequence homology with E3L, but both have been shown to partially rescue the replication of an E3L-deleted VACV (37). In the luciferase assay, both Us11 and σ3 inhibited PKR from human, mouse and A. hamster, but the S. hamster PKR was not inhibited by either. In fact, of eight different mammalian and avian PKRs tested, only the S. hamster PKR was resistant to both σ3 and Us11 (Fig 3.2A and B). Interestingly, PKR from other species, such as rat and chicken, were relatively insensitive to inhibition by either σ3 or Us11 compared to the other tested PKRs suggesting that perhaps the development of resistance to viral dsRNA-binding inhibitors may be more common than has been previously appreciated. Furthermore, these results suggest that S. hamster PKR is more broadly resistant to inhibition by various dsRNA-binding proteins, which represents a unique innovation that evolved to overcome virus infection by many different viruses.

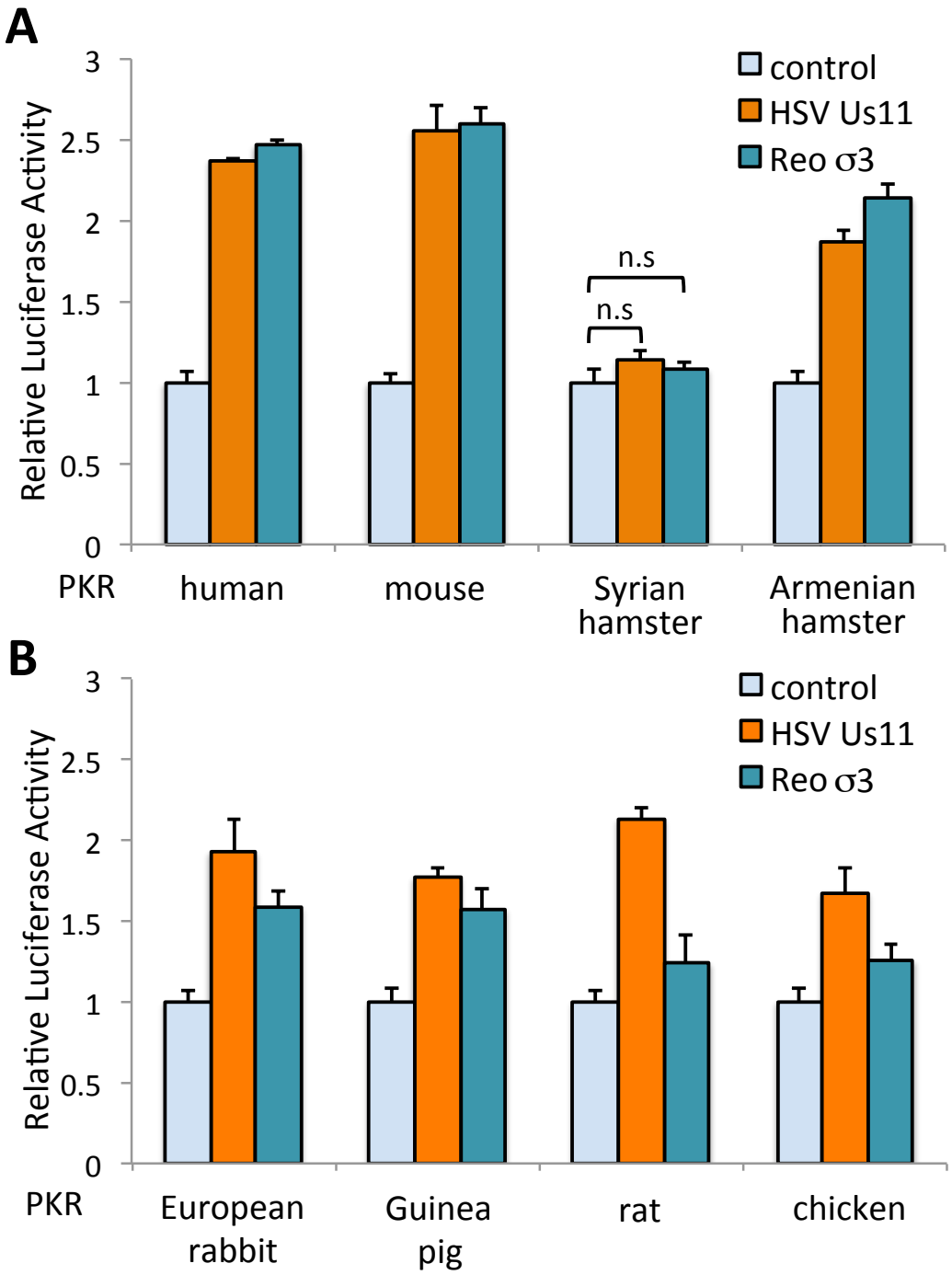

Figure 3.2 Syrian hamster PKR is resistant to other viral dsRNA-binding proteins.

HeLa-PKRkd cells were co-transfected with plasmids encoding firefly luciferase (0.05μg) and PKR from the indicated species (0.2μg), and Herpes Simplex virus-1 (HSV) Us11 or mammalian reovirus (Reo) σ3 (0.4μg). Relative luciferase activity for each transfection was determined by normalizing measured light units to PKR-only transfected cells. Error bars indicate the standard deviations for three replicate transfections. P-values were calculated with Student's t-test. n.s.= $p>0.05$

Domain swapping of hamster PKRs reveals regions important for resistance to VACV E3L and K3L

To investigate the molecular basis for the resistance of S. hamster PKR to inhibition by dsRNA-binding inhibitors, we focused on its interaction with VACV E3L. In addition, to build off our previous findings that another PKR from the closely related A. hamster is resistant to the second PKR inhibitor encoded by VACV, K3L, we decided to use the opposing resistances of each PKR to construct a series of hybrid PKRs of the two by swapping protein domains (described in Figs. 3.3 and 3.13) to test in the luciferase assay, taking advantage of the relatively high-throughput capacity of this assay. This allowed us to determine the regions within each protein important for their resistance to E3L or K3L, thereby giving us insight into the molecular mechanism of their interactions.

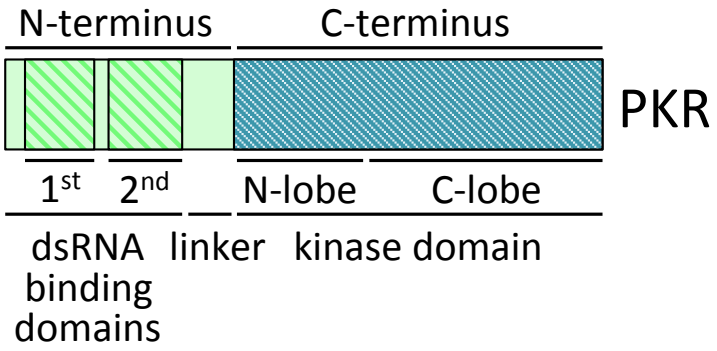

Figure 3.3 Domain map of PKR.

The two N-terminal dsRNA-binding domains (broad green stripes), linker region and kinase domain (thin blue stripes) are shown on the domain map. In domain exchange experiments, the N-terminus included the linker region and the C-terminus included the entire kinase domain after that. The kinase domain was further subdivided into N-terminal and C-terminal lobes (N- and C-lobe, respectively).

Hybrid PKRs of S. hamster PKR and mouse PKR, which is sensitive to both E3L and K3L inhibition, or A. hamster PKR were generated by exchanging the first 241 amino acids of either PKR (N-terminus) with the C-terminal kinase domain of the other species' PKR protein sequence. For both sets of hybrids, exchange of the kinase domain significantly altered sensitivity to VACV K3L without changing the activity of each hybrid PKR (Table 3.5), while exchange of the N-terminus, encoding both dsRNA-binding domains (RBDs) and the variable

linker region, significantly altered sensitivity to VACV E3L (Fig 3.4A and B). The resistance of A. hamster PKR to VACV K3L was completely transferred to the hybrid PKR encoding the kinase domain of A. hamster (*ma*/*cmi* PKR, #5), supporting previous data that the kinase domain of PKR is involved in direct interactions with this viral inhibitor (12, 17, 18). Meanwhile, exchange of the N-terminus of S. hamster PKR significantly reduced the sensitivity of the same hybrid PKR relative to A. hamster PKR, although we consistently observed a slight increase in sensitivity relative to the S. hamster PKR (Fig 3.4B), which was significant when higher ratios of E3L to PKR (4:1) were transfected (Fig 3.5). This suggests that the majority of the resistance phenotype of S. hamster PKR lies in the N-terminus, however, we cannot exclude completely a role for the kinase domain in this interaction. It is interesting, however, in experiments with the same hybrid of S. hamster PKR and mouse PKR (*ma*/*mm* PKR, #21) that we did not see the same increase in sensitivity to E3L (Fig 3.4A), which suggests that subtle differences between the kinase domain sequences of A. hamster and mouse PKR may affect the interaction with VACV E3L.

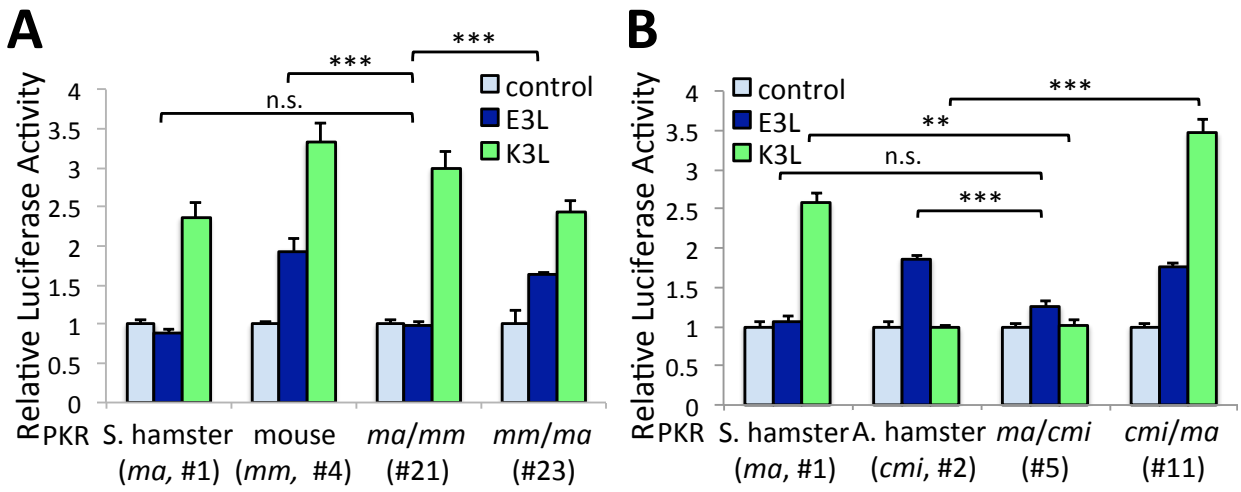

Figure 3.4 Resistance to VACV E3L and K3L lie in N- or C-terminal domains of PKR.

*HeLa-PKRkd cells were co-transfected with plasmids encoding firefly luciferase (0.05µg), PKR or PKR hybrids from the indicated species (0.2µg), and VACV E3L or K3L (0.4µg). Relative luciferase activity for each transfection was determined by normalizing measured light units to PKR-only transfected cells. Error bars indicate the standard deviations for three replicate transfections. Numbers under each species PKR correspond to their number in Table 3.5. ma= S. hamster, mm= mouse, cmi= A. hamster. P-values were calculated with Student's t-test. n.s.= p>0.05, **p<0.005, ***p<0.0005.*

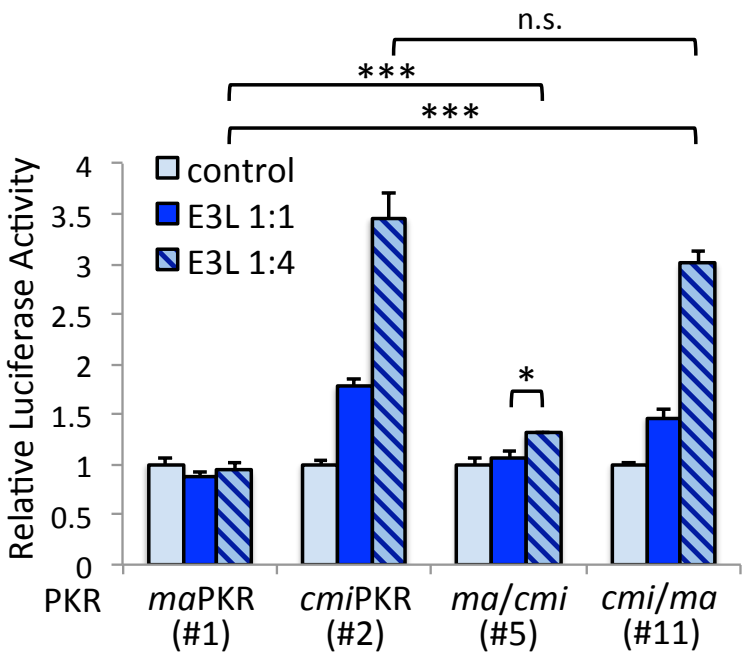

Figure 3.5 The N-terminus of Syrian hamster PKR mostly confers resistance to VACV-E3L. *HeLa-PKRkd cells were co-transfected with plasmids encoding firefly luciferase (0.05µg), PKR or PKR hybrids from the indicated species (0.2µg), and VACV E3L or K3L (0.2µg or 0.8µg). Relative luciferase activity was determined by normalizing measured light units to PKR-only transfected cells. Error bars indicate the standard deviations for three replicate transfections. Numbers under each species PKR correspond to their number in Table 3.5. ma= S. hamster, cmi= A. hamster. P-values were calculated with Student's t-test. n.s.= p>0.05, *p<0.05, ***p<0.0005.*

The kinase domain of PKR is divided into an N-terminal lobe that is involved in the auto-inhibition of latent PKR and a C-terminal lobe that contains the catalytic site (16). To investigate whether either of these regions contributed to the slight sensitivity of the N-terminal S. hamster hybrid PKR (*ma*/*cmi* PKR, #5), we swapped either the N-terminal lobe (N-lobe) or C-terminal lobe (C-lobe) from A. hamster PKR kinase domain into S. hamster PKR and compared it to the hybrid PKR with the entire kinase domain from A. hamster (*ma*/*cmi* PKR, #5) (Fig 3.6). Neither domain lobe conferred a large increase in sensitivity to E3L, but the C-terminal lobe had a slightly greater effect than the N-terminal lobe, which did not affect S. hamster PKR sensitivity to E3L inhibition at all. This suggests that any role for the kinase domain of S. hamster PKR in its resistance to E3L lies in the C-terminal lobe; however, our results suggest that the N-terminus of S. hamster PKR is primarily responsible for the observed resistance to E3L inhibition.

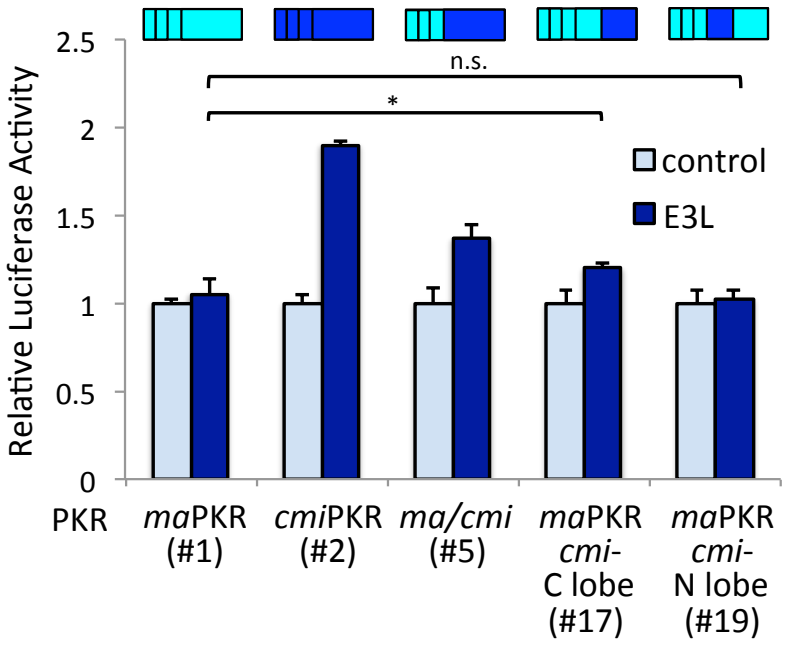

Figure 3.6 Resistance to E3L may involve the kinase domain.

*HeLa-PKRkd cells were co-transfected with plasmids encoding firefly luciferase (0.05µg), PKR or PKR hybrids from the indicated species (0.2µg), and VACV E3L (0.4µg). Relative luciferase activity for each transfection was determined by normalizing measured light units to PKR-only transfected cells. Error bars indicate the standard deviations for three replicate transfections. Small domain maps of each PKR construct are shown above the corresponding data. (cyan = S. hamster; blue = A. hamster). Numbers under each species PKR correspond to their number in Table 3.5. P-values were calculated with Student's t-test. n.s.= p>0.05, *p<0.05; ma= S. hamster; cmi= A. hamster.*

To further fine-map the protein regions in the N-terminus of S. hamster PKR important for the resistance to VACV E3L, we sub-divided the N-terminal region exchanged between S. hamster PKR and A. hamster PKR into each RBD and the linker region and tested their sensitivity to VACV E3L and/or K3L (Figs 3.7 and 3.8). As we saw before, the kinase domain was entirely responsible for PKR sensitivity to VACV K3L inhibition as all hybrids encoding the kinase domain from A. hamster PKR were resistant to K3L inhibition (#5-7). The sensitivity of each hybrid PKR to VACV E3L, on the other hand was different for different combinations of the RBDs and the linker region. A general trend was observed with an increase in sensitivity to E3L for hybrids encoding a larger percentage of the protein and multiple domains from A. hamster PKR than from S. hamster PKR, which again suggests that some cooperation occurs between multiple protein regions to resist E3L inhibition.

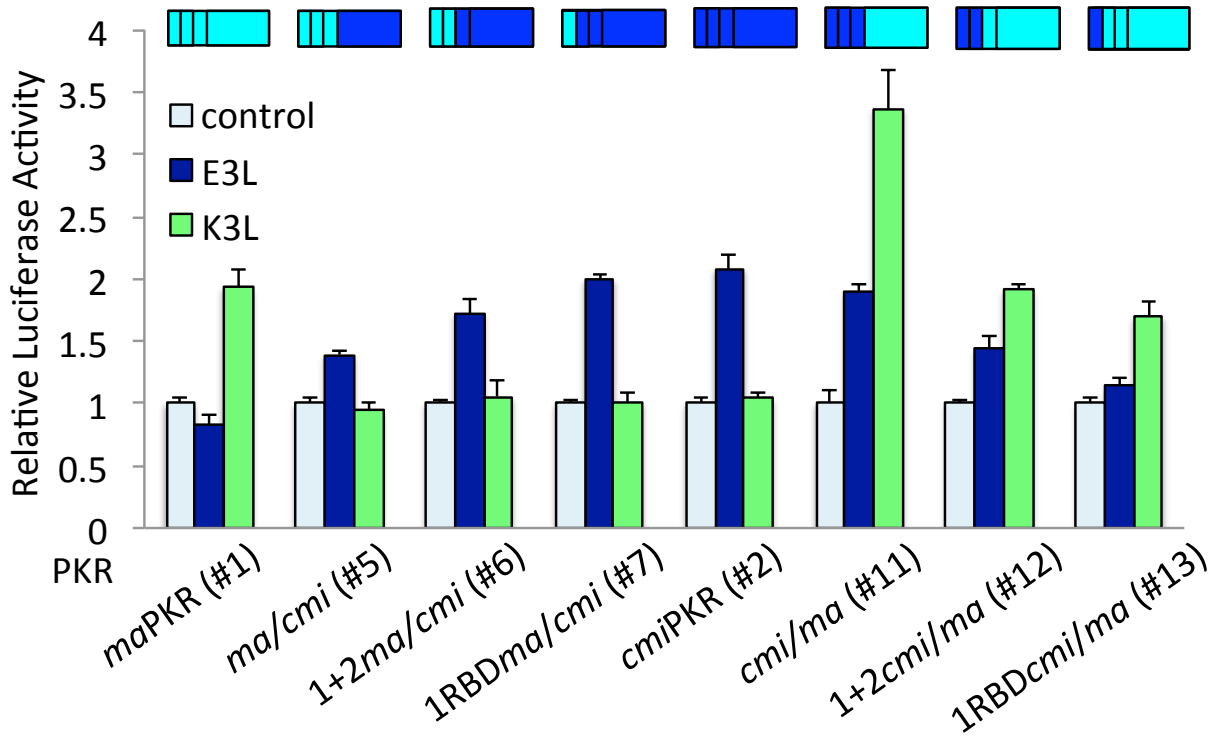

Figure 3.7 Domain exchanges of Syrian hamster and Armenian hamster PKR alter sensitivity of VACV E3L and K3L.

HeLa-PKRkd cells were co-transfected with plasmids encoding firefly luciferase (0.05µg), PKR or PKR hybrids from the indicated species (0.2µg), and VACV E3L or K3L (0.4µg). Relative luciferase activity for each transfection was determined by normalizing measured light units to PKR-only transfected cells. Error bars indicate the standard deviations for three replicate transfections. Numbers after each species PKR correspond to their number in Table 3.5. Small domain maps of each PKR construct are shown above the corresponding data (cyan = S. hamster; blue = A. hamster). ma= S. hamster; cmi= A. hamster; RBD= dsRNA-binding domain.

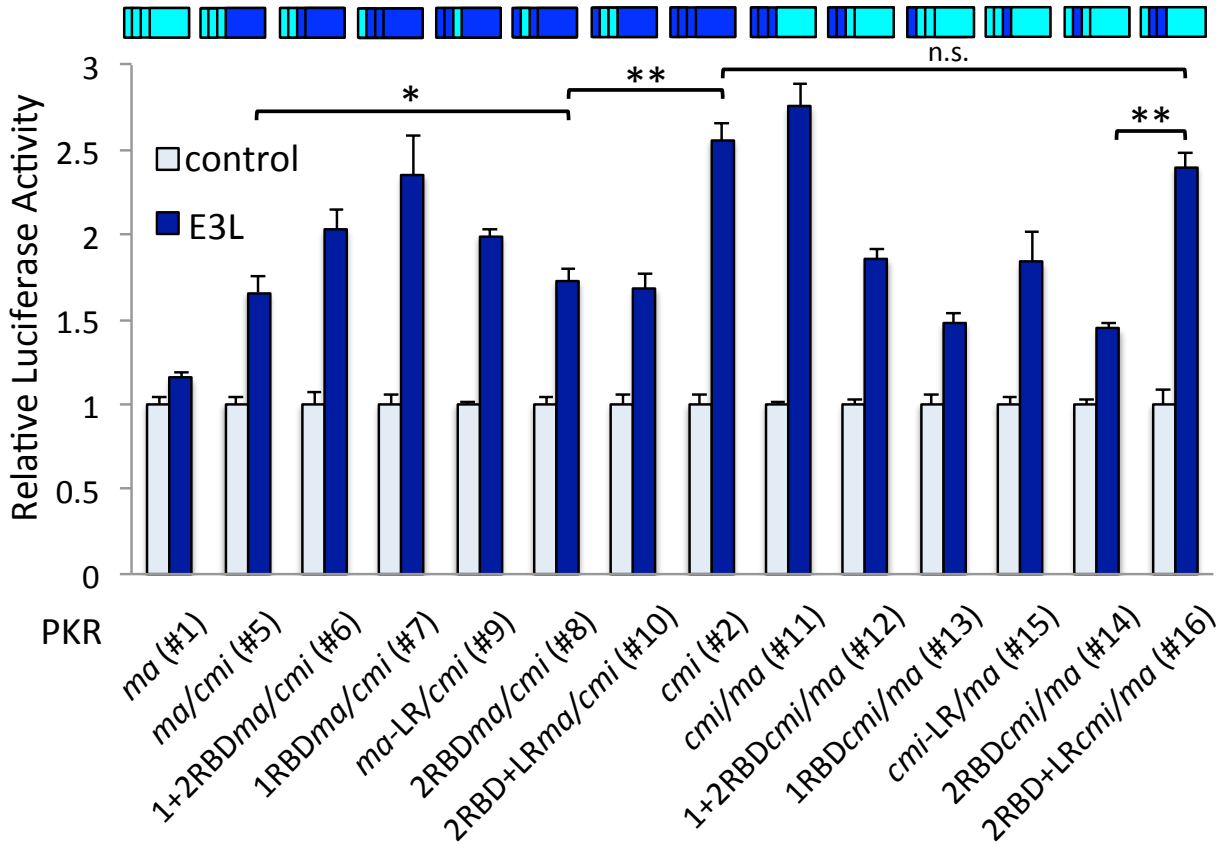

Figure 3.8 Resistance to E3L involves multiple domains.

*HeLa-PKRkd cells were co-transfected with plasmids encoding firefly luciferase (0.05μg), PKR or PKR hybrids from the indicated species (0.2μg), and VACV E3L (0.4μg). Relative luciferase activity for each transfection was determined by normalizing measured light units to PKR-only transfected cells. Error bars indicate the standard deviations for three replicate transfections. Numbers after each species PKR correspond to their number in Table 3.5. Small domain maps of each PKR construct are shown above the corresponding data (cyan = S. hamster; blue = A. hamster). P-values were calculated with Student's t-test. n.s.= p>0.05, *p<0.05, **p<0.005; ma= S. hamster; cmi= A. hamster; RBD= dsRNA-binding domain; LR= linker region.*

The PKR hybrids that were least sensitive to E3L inhibition, however, encoded both the linker region and second RBD from S. hamster PKR, although neither domain alone could completely confer resistance to E3L in A. hamster PKR (Fig 3.8). These two domains were found to cooperatively affect both the sensitivity of S. hamster PKR and the resistance of A. hamster PKR in hybrid constructs. The second RBD from S. hamster PKR significantly reduced

the sensitivity of A. hamster PKR and this hybrid PKR (2RBD*ma*/*cmi*, #8) was as sensitive to E3L as hybrid constructs also encoding the linker region and/or the first RBD of S. hamster PKR (#5 and #10, respectively). This suggests that the second RBD in the N-terminus of S. hamster PKR is primarily responsible for the reduced sensitivity to E3L observed for the N-terminus S. hamster hybrid (*ma*/*cmi* PKR, #5). Complementary exchange of the second RBD in S. hamster PKR with that from A. hamster PKR, however, only marginally increased the sensitivity to E3L inhibition (~1.2X increase from S. hamster PKR). Likewise, the linker region of A. hamster PKR alone did not make S. hamster PKR as sensitive to E3L as the N-terminus A. hamster hybrid (*cmi*/*ma* PKR, #11). However, in combination, the linker region and second RBD from A. hamster PKR created a hybrid PKR that was significantly more sensitive to E3L than the hybrid with only the second RBD from A. hamster PKR and was as sensitive as the wild type A. hamster PKR. Additionally, the importance of the linker region in PKR interactions with E3L was also observed in hybrid PKRs made with mouse and S. hamster PKR (Fig 3.9). PKR hybrids with linker regions originating from mouse PKR were more sensitive to E3L inhibition even when both RBDs were from S. hamster PKR.

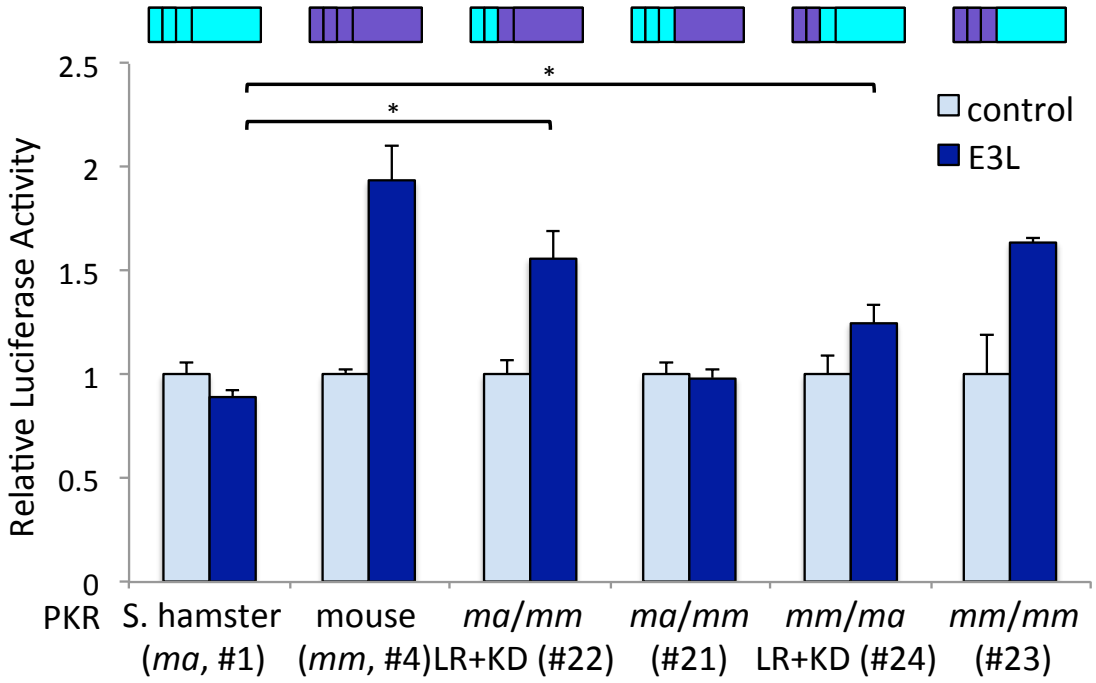

Figure 3.9 Syrian hamster linker region is important for resistance to E3L.

HeLa-PKRkd cells were co-transfected with plasmids encoding firefly luciferase (0.05μg), PKR and PKR hybrids from the indicated species (0.2μg) and VACV E3L (0.4μg). Relative luciferase activity was

*determined by normalizing measured light units to PKR-only transfected cells. Numbers after each species PKR correspond to their number in Table 3.5. Small domain maps of each PKR construct are shown above the corresponding data (cyan = S. hamster; purple = mouse). Error bars indicate the standard deviations for three replicate transfections. P-values were calculated with Student's t-test. *p<0.05 ma= S. hamster; mm-mouse; LR= linker region; KD= kinase domain.*

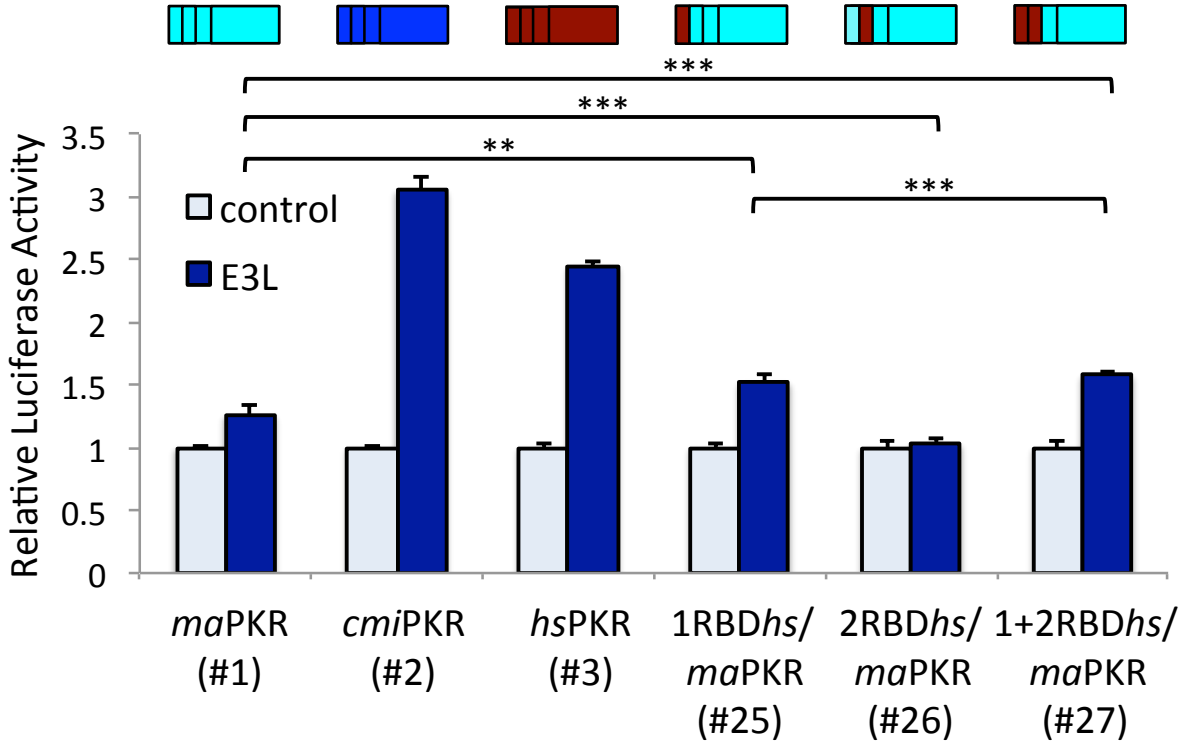

Figure 3.10 First dsRNA-binding domain of human PKR increases Syrian hamster PKR sensitivity to E3L.

*HeLa-PKRkd cells were co-transfected with plasmids encoding firefly luciferase (0.05µg), PKR and PKR hybrids from the indicated species (0.2µg) and VACV E3L (0.4µg). Relative luciferase activity for each transfection was determined by normalizing measured light units to PKR-only transfected cells. Error bars indicate the standard deviations for three replicate transfections. Numbers under each species PKR correspond to their number in Table 3.5. Small domain maps of each PKR construct are shown above the corresponding data (cyan = S. hamster; blue = A. hamster; dark red = human). P-values were calculated with Student's t-test. **p<0.005; ***p<0.0005; ma= S. hamster; cmi= A. hamster, hs= human, RBD= dsRNA-binding domain.*

Because most studies on the function of PKR and its domains have been performed using human PKR, we decided to see if we could confirm our results using hybrids with human PKR. Interestingly, hybrid PKRs generated by swapping the RBDs of S. hamster PKR with those from human PKR, which is also sensitive to E3L inhibition, suggested that the first RBD might also be important for the interaction with E3L (Fig 3.10). However, the sensitivity of these hybrids to E3L inhibition was only marginally increased (~1.2-1.3X increase from S. hamster PKR) or not increased at all, supporting the conclusion that multiple domains of PKR, including the linker region, are involved in the interaction with E3L and the resistance of S. hamster PKR to E3L inhibition.

Residues in the linker region are important for PKR sensitivity to VACV E3L

When we cloned S. hamster PKR from BHK-21 cells, we identified two isoforms that correspond to the full-length protein and a splice variant that is missing 53 amino acids from the linker region. The structure of the linker region connecting the C-terminal kinase domain and the N-terminal RBDs has not been solved, and it is variable in length between PKR from different species. The flexibility of this region is thought to play a role in the conformational change that occurs during PKR activation (38, 39), and from our previous results, we suspected that this region might be involved in the interaction with VACV E3L. We already showed that full length S. hamster PKR was resistant to E3L inhibition, but to test whether the presence of a short version of S. hamster PKR may affect the ability of E3L to inhibit PKR in this species' cells, we cloned the splice variant isoform of S. hamster PKR into the mammalian expression vector and tested its interactions with E3L in the luciferase assay (Fig 3.11). Additionally, we deleted the corresponding region in A. hamster PKR to create an artificial "splice-variant" form (*cmi*PKR-sv, #33) and tested its activity and sensitivity to E3L as well. Deletion of the spliced out linker region residues in either hamster PKR did not affect their activity or their sensitivity to inhibition by E3L. These results support recently published work using deletion mutants of human PKR, which showed that PKR activity and regulation by dsRNA was not affected by deletion of the same region within human PKR (40).

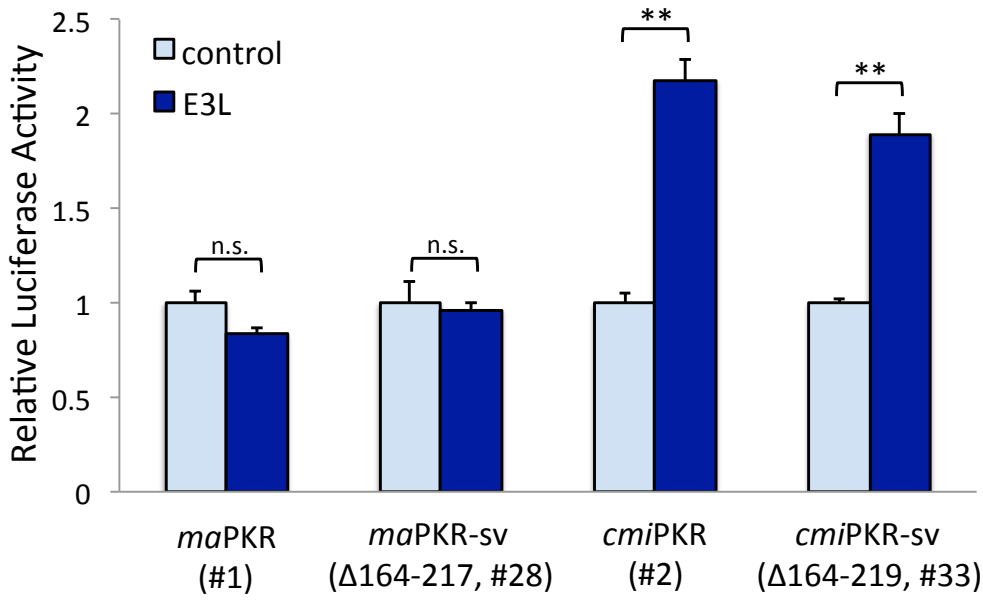

Figure 3.11 Splice variant forms of hamster PKR do not exhibit altered sensitivity to VACV E3L. *HeLa-PKRkd cells were co-transfected with plasmids encoding firefly luciferase (0.05µg), S. hamster or A. hamster PKR with the indicated deletions (0.2µg), and VACV E3L (0.4µg). Relative luciferase activity for each transfection was determined by normalizing measured light units to PKR-only transfected cells. Numbers under each species PKR correspond to their number in Table 3.5. Error bars indicate the standard deviations for three replicate transfections. P-values calculated with Student's t-test. n.s.= p>0.05; **p<0.005; ma= S. hamster; cmi= A. hamster; sv= splice variant.*

The splice variant of S. hamster PKR has the shortest linker region of all of the PKRs that we tested with only 24 amino acids compared to 77 amino acids in the full length protein and 82 amino acids in human PKR. To determine whether the remaining 24 amino acids in the splice variant S. hamster PKR are contributing to the resistance of this PKR to VACV E3L, we generated a series of deletion mutant S. hamster PKRs by deleting 6 amino acids at a time in the remaining linker region and tested if this altered their sensitivity to E3L (Fig. 3.12). Deletion of amino acids 164-223 had no considerable effect on S. hamster PKR sensitivity to E3L, while deletion of the next 6 amino acids caused a significant increase in sensitivity, which we also observed in successive deletion mutants. Deletion of the entire linker region (Δ164-241) resulted in a slight reduction in PKR activity relative to the other mutants (#32). Remarkably this PKR was still able to suppress 74-86% of luciferase translation. These results suggested that residues important for S. hamster PKR resistance to E3L lay between residues 224-229 in the linker

region (indicated in Fig. 3.13). Within this length of amino acids in the linker region, 5 of the 6 amino acids are not conserved across seven rodent species that also exhibit sensitivity to E3L inhibition, but there are only two amino acids that differ between S. hamster PKR and A. hamster PKR. Surprisingly, however, mutation of these two amino acids in full length S. hamster PKR to the corresponding residues in A. hamster PKR (PR228-229SG) or vice versa (SG230-231PR) did not alter the sensitivity of these mutants to inhibition by E3L (Fig 3.23, #55 and #57). It is therefore possible that the significant increase in sensitivity of the linker region deletion mutant primarily resulted from the shortened linker.

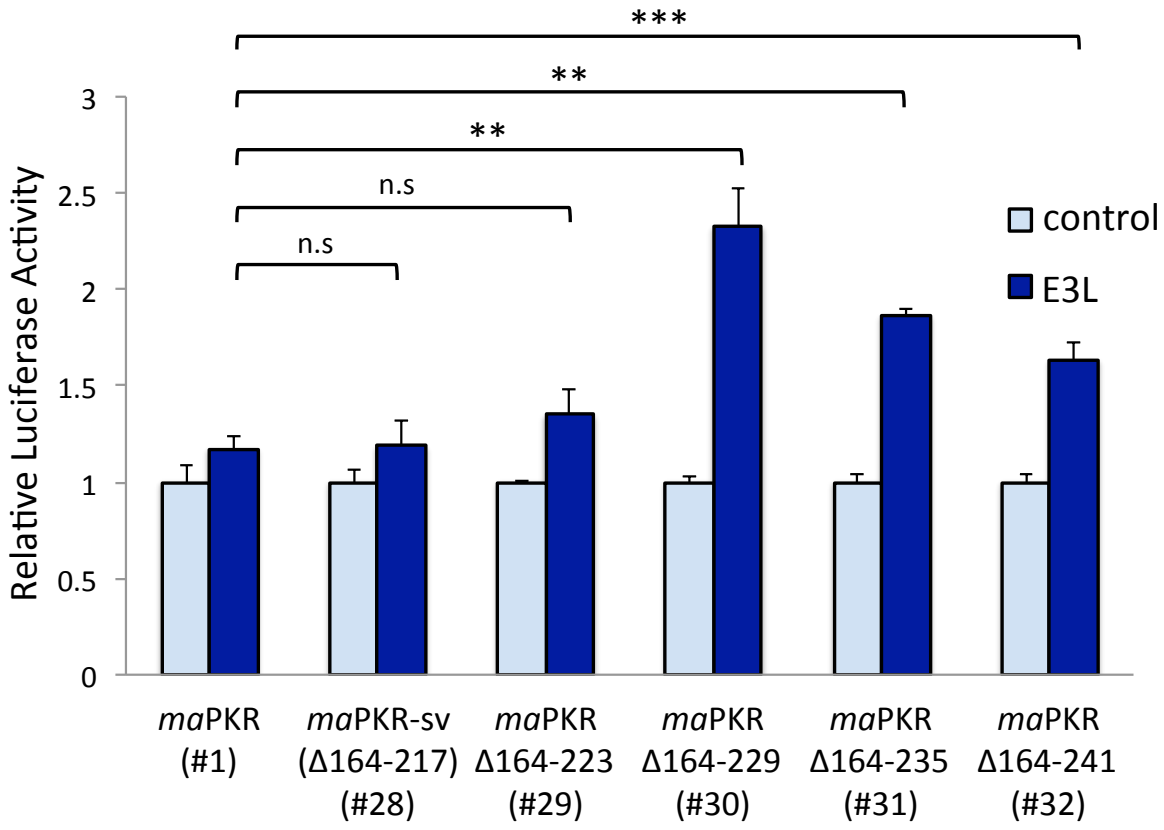

Figure 3.12 Linker region deletion mutants of Syrian hamster PKR are sensitive to E3L.
*HeLa-PKRkd cells were co-transfected with plasmids encoding firefly luciferase (0.05µg), S. hamster PKR with the indicated deletions (0.2µg), and VACV E3L (0.4µg). Relative luciferase activity for each transfection was determined by normalizing measured light units to PKR-only transfected cells. Error bars indicate the standard deviations for three replicate transfections. Numbers under each species PKR correspond to their number in Table 3.5. P-values were calculated with Student's t-test. n.s.= p>0.05, **p<0.005, ***p<0.0005; ma= S. hamster; cmi= A. hamster.*

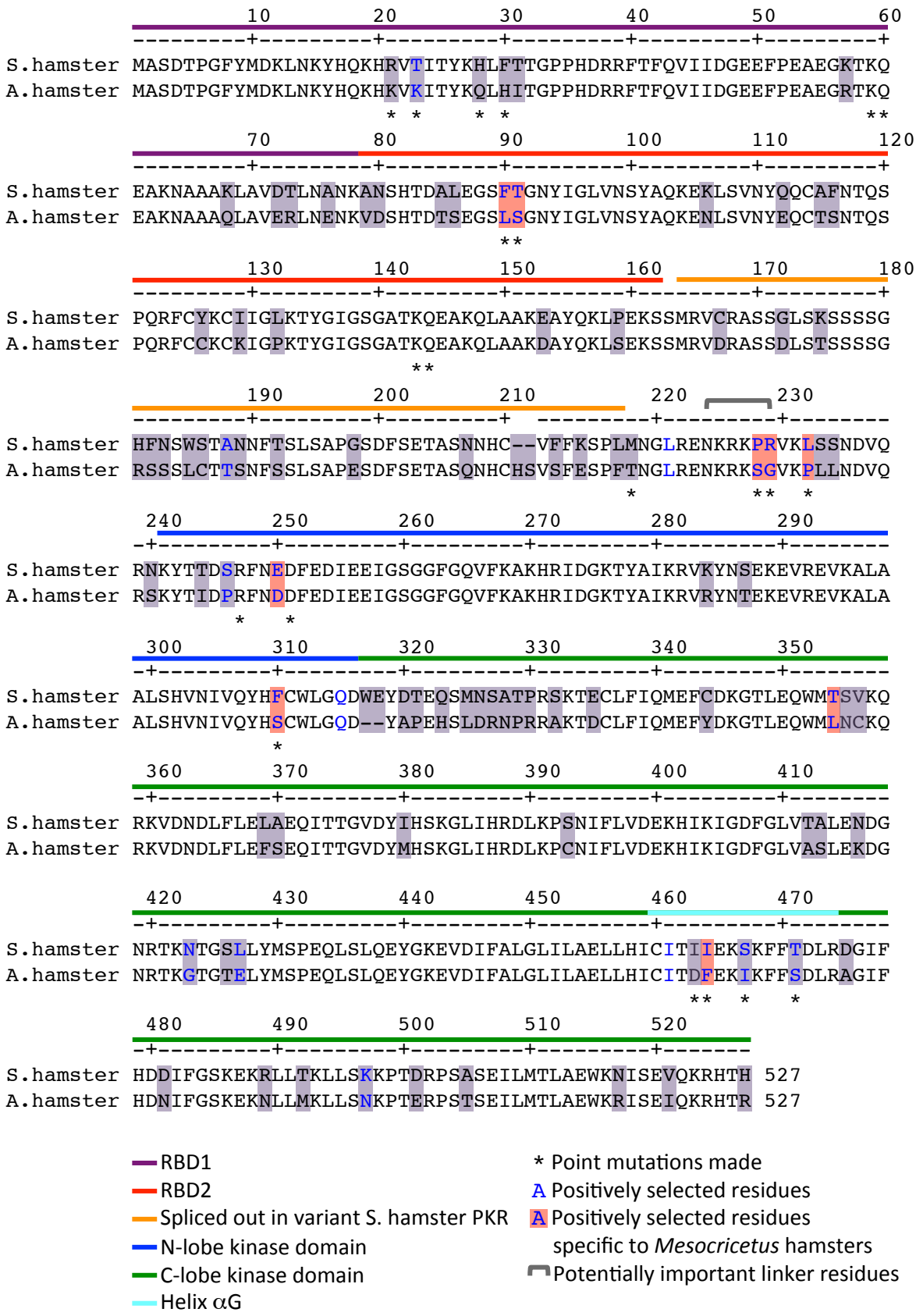
10 20 30 40 50 60
S.hamster MASDTPGFYMDKLNKYHQKHRVTITYKHLFTTGPPHDRRFTFQVIIDGEEFPEAEGKTKQ
A.hamster MASDTPGFYMDKLNKYHQKHKVKITYKQLHITGPPHDRRFTFQVIIDGEEFPEAEGRTKQ
70 80 90 100 110 120
S.hamster EAKNAAAKLAVDTLNANKANSHTDALEGSFTGNYIGLVNSYAQKEKLSVNYQQCAFNTQS
A.hamster EAKNAAAQLAVERLNENKVDSHTDTSEGSLSGNYIGLVNSYAQKENLSVNYEQCTSNTQS
130 140 150 160 170 180
S.hamster PQRFCYKCIIGLKTYGIGSGATKQEAKQLAAKEAYQKLPEKSSMRVCRASSGLSKSSSSG
A.hamster PQRFCCKCKIGPKTYGIGSGATKQEAKQLAAKDAYQKLSEKSSMRVDRASSDLSTSSSSG
190 200 210 220 230
S.hamster HFNSWSTANNFTSLSAPGSDFSETASNNHC--VFFKSPLMNGLRENKRKPRVKLSSNDVQ
A.hamster RSSSLCTTSNFSSLSAPESDFSETASQNHCHSVSFESPFTNGLRENKRKSGVKPLLNDVQ
240 250 260 270 280 290
S.hamster RNKYTTDSRFNEDFEDIEEIGSGGFGQVFKAKHRIDGKTYAIKRVKYNSEKEVREVKALA
A.hamster RSKYTIDPRFNDDFEDIEEIGSGGFGQVFKAKHRIDGKTYAIKRVRYNTEKEVREVKALA
300 310 320 330 340 350
S.hamster ALSHVNIVQYHFCWLGQDWEYDTEQSMNSATPRSKTECLFIQMEFCDKGTLEQWMTSVKQ
A.hamster ALSHVNIVQYHSCWLGQD--YAPEHSLDRNPRRAKTDCLFIQMEFYDKGTLEQWMLNCKQ
360 370 380 390 400 410
S.hamster RKVDNDLFLELAEQITTGVDYIHSKGLIHRDLKPSNIFLVDEKHIKIGDFGLVTALENDG
A.hamster RKVDNDLFLEFSEQITTGVDYMHSKGLIHRDLKPCNIFLVDEKHIKIGDFGLVASLEKDG
420 430 440 450 460 470
S.hamster NRTKNTGSLLYMSPEQLSLQEYGKEVDIFALGLILAELLHICITTIEKSKFFTDLRDGIF
A.hamster NRTKGTGTELYMSPEQLSLQEYGKEVDIFALGLILAELLHICITDFEKIKFFSDLRAGIF
480 490 500 510 520
S.hamster HDDIFGSKEKRLLTKLLSKKPTDRPSASEILMTLAEWKNISEVQKRHTH 527
A.hamster HDNIFGSKEKNLLMKLLSNKPTERPSTSEILMTLAEWKRISEIQKRHTR 527
RBD1
RBD2
Spliced out in variant S. hamster PKR
N-lobe kinase domain
C-lobe kinase domain
Helix αG
* Point mutations made
A Positively selected residues
A Positively selected residues specific to Mesocricetus hamsters
Potentially important linker residues

Figure 3.13 Protein sequence alignment of Syrian and Armenian hamster PKR.

Syrian and Armenian hamster PKR were aligned using ClustalW (DNAStar, Inc.) and different residues are highlighted in purple. The position of each domain outlined in the domain swapping experiments is indicated by colored lines above the alignment. Residues identified in the positive selection analysis are shown in blue with those specific to the Mesocricetus hamster species highlighted in pink. The position of point mutations made in this study are indicated with an asterisk below the alignment.

Positive selection in hamster PKR reveals the molecular basis for PKR resistance to VACV K3L but not VACV E3L

From our domain swapping analysis, we concluded that multiple domains are involved in the resistance to E3L. To investigate whether the importance of the RBDs and the linker region could be narrowed down to differences or combinations of differences at the amino acid level, we sought a different approach to focus our analysis on those amino acids most likely to be involved in interactions with the viral inhibitor. Previous work looking at protein interactions with viral pseudosubstrate inhibitors of PKR identified important residues for these interactions by looking for signs of positive selection at individual residues (17, 18). The premise for this method is that at interaction interfaces between antagonistic proteins, such as between PKR and a viral inhibitor, the evolutionary pressure to change to avoid inhibition will be high enough to be observed as a higher rate of nonsynonymous to synonymous (dN/dS) mutation across evolutionary history. By analyzing two datasets of related PKR sequences from 7 rodent and 12 rodent and lagomorph species, we identified 49 unique amino acids across PKR for which there was a high probability ($p<0.10$) for positive selection to have occurred (Tables 3.1 and 3.2, Figs 3.14 and 3.15). Based on our analyses and the results of previous analyses, we selected 20 of these amino acids with the highest likelihood of positive selection ($p<0.05$) (Table 3.3). These residues were identified in every domain of PKR covering the entire length of the protein, but most were identified in the linker region (5/20) and the kinase domain (13/20) (Fig 3.16). Residue A488/I463 was not identified with a high probability in our analysis, but this residue was previously identified as being important for conferring human and mouse PKR sensitivity to K3L, so we also included it as a candidate residue for positive selection (17). Additionally, 8 out of the 20 were uniquely different in the *Mesocricetus* species PKRs suggesting they are more likely to be important for the resistance of PKRs from this genus (Fig. 3.13).

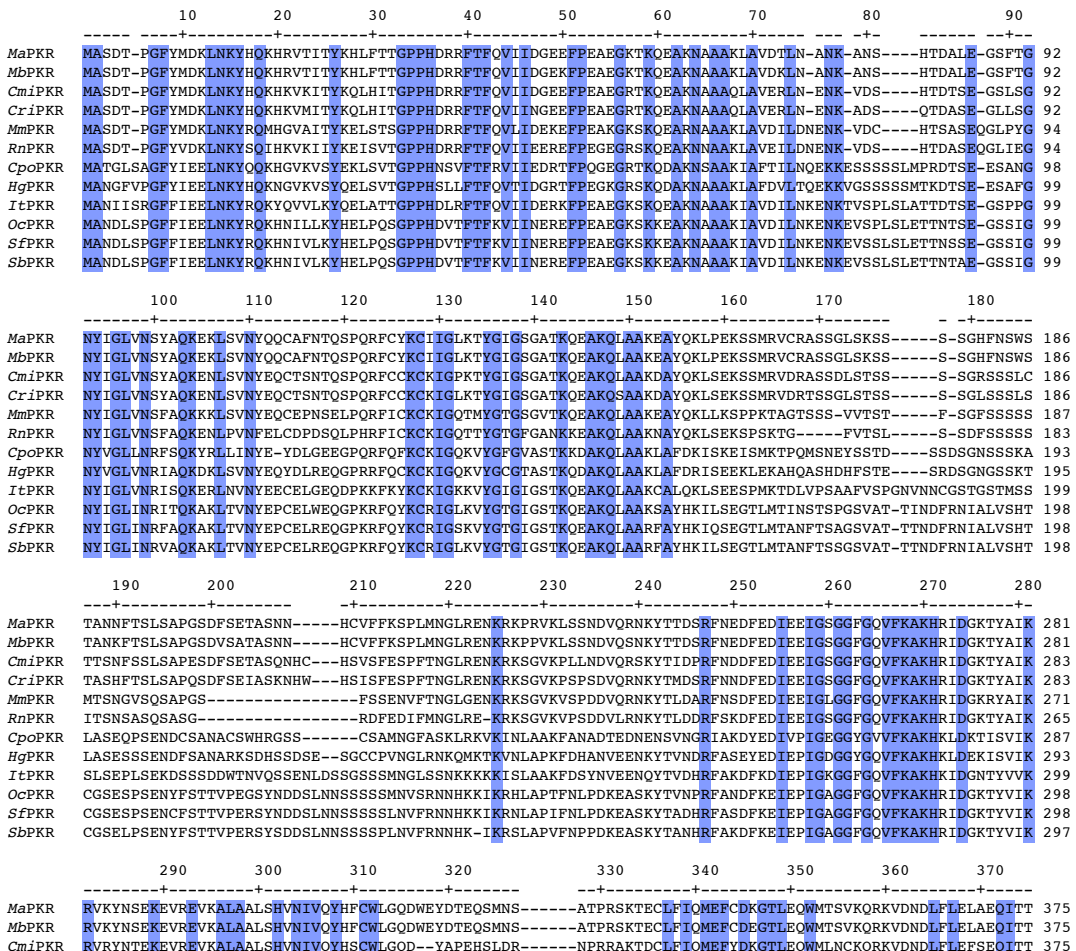

Figure 3.14 Protein sequence alignment of 12 rodent and rabbit PKRs.

Residues conserved in all 12 PKRs examined (100% conserved) are highlighted in blue. Residues are numbered according to S. hamster PKR. Abbreviations of each species PKR are described in Table 3.1.

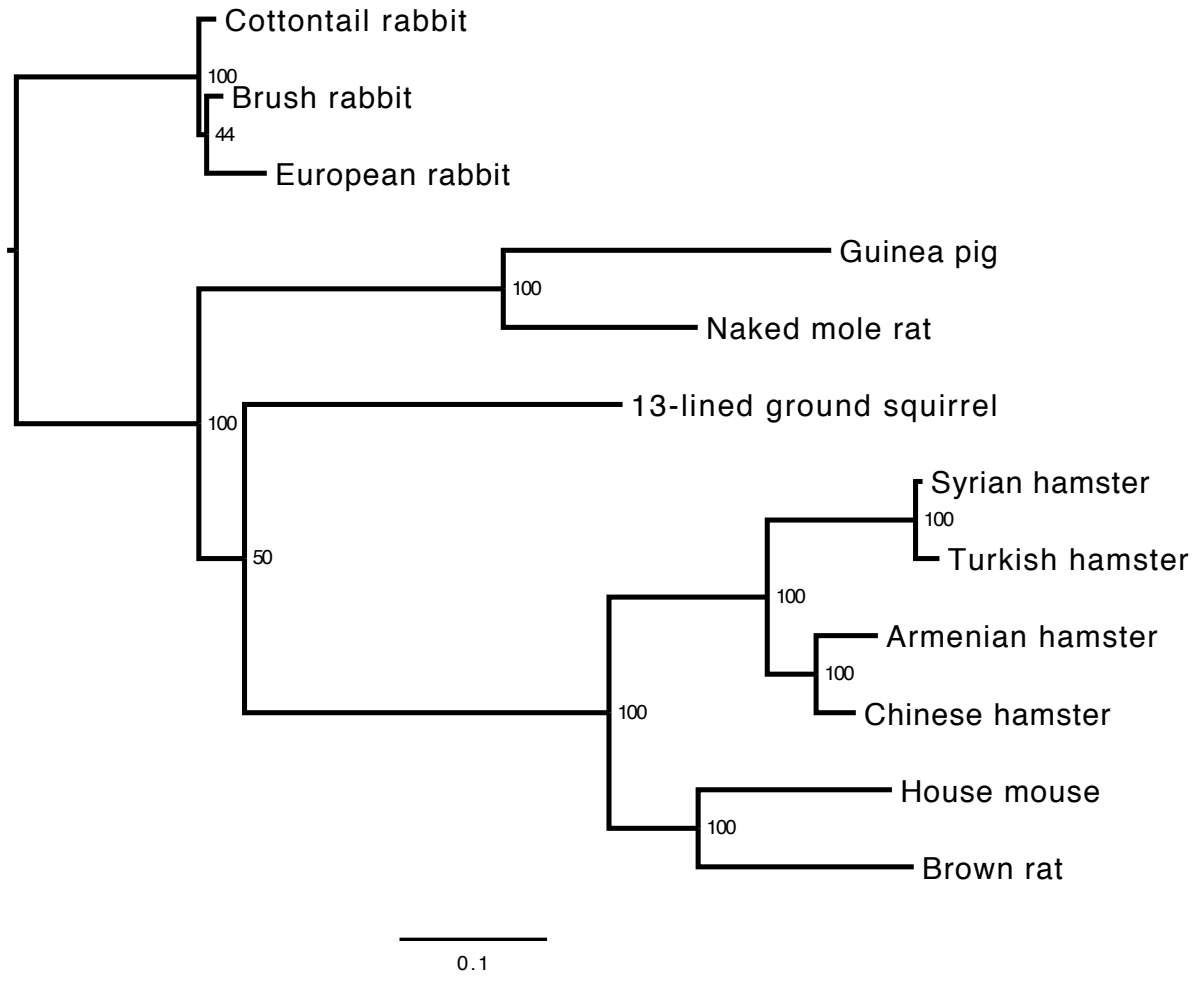

Figure 3.15 Phylogenetic tree of 12 rodent and rabbit PKRs used for positive selection analysis.

A mid-point rooted maximum likelihood tree was constructed from the alignment of the nucleotide sequences for 12 rodent and rabbit PKRs analyzed for positive selection. Bootstrap values for 100 replicates are indicated at branch nodes.

Rodentia 7 seqs.	Residue (*hs/ma*)	PAML-BEB posterior probability
Model 2	V24/T23	0.913
	P31/F30	0.901
	S97/F90	0.926
	T197/N190	0.992
	E379/T354	0.928
	S448/N423	0.964
	L452/L427	0.959
	A488/I463	0.749*
	F489/I464	0.942
	Q516/T492	0.936
Model 8	V24/T23	0.967
	P31/F30	0.966
	S97/F90	0.976
	M98/T91	0.957
	D176/C167	0.916
	Q189/H181	0.928
	S190/F182	0.939
	V194/S186	0.910
	T197/N190	0.998
	E205/G198	0.955
	D211/T204	0.925
	N223/K214	0.956
	S224/S215	0.918
	P245/S234	0.942
	K261/S246	0.951
	M265/E250	0.942
	G325/F310	0.964
	W327/W312	0.903
	D338/M325	0.910
	K360/E335	0.954
	E379/T354	0.976
	R381/V356	0.907
	S448/N423	0.990
	L452/L427	0.988
	D486/I461	0.927
	A488/I463	0.895*
	F489/I464	0.982
	S492/S467	0.943
	T496/T471	0.954
	Q516/T492	0.980
	E524/T500	0.903

Glires 12 seqs.	Residue (*hs/ma*)	PAML-BEB posterior probability
Model 2	V24/T23	0.988
	S97/F90	0.909
	M98/T91	0.991
	S196/A188	0.938
	L232/L221	0.931
	A239/P228	0.974
	K240/R229	0.984
	L243/L232	0.999
	K261/S246	0.989
	M265/E250	0.983
	G325/F310	0.962
	D328/L313	0.903
	F330/Q315	0.991
	T336/Q323	0.944
	D338/M325	0.961
	K352/S327	0.902
	S354/T329	0.939
	S355/P330	0.978
	R356/R331	0.995
	K360/E335	0.995
	E379/T354	0.927
	S448/N423	0.951
	D486/I461	0.935
	F489/I464	0.968
	S492/S467	0.995
	T496/T471	0.928
	K522/K497	0.958
Model 8	V24/T23	0.994
	P31/F30	0.946
	N32/T31	0.948
	S97/F90	0.955
	M98/T91	0.996
	Q139/L132	0.905
	D176/C167	0.931
	C186/S178	0.912
	S196/A188	0.967
	T212/A205	0.900
	S219/C210	0.915
	M229/M218	0.901
	L232/L221	0.964
	P245/S234	0.925
	K261/S246	0.995
	M265/E250	0.992

G325/F310	0.984
D328/L313	0.943
F330/Q315	0.995
T336/Q323	0.975
D338/M325	0.982
D339/N326	0.942
K352/S327	0.958
S354/T329	0.969
S355/P330	0.987
R356/R331	0.996
S357/S332	0.936
K360/E335	0.997
E379/T354	0.964
S448/N423	0.979
L452/L427	0.989
Q463/Q438	0.946
F489/I464	0.986
S492/S467	0.997
T496/T471	0.962
K522/K497	0.978

Table 3.2 Screened residues under positive selection in PKR.

*Residues were identified to be under positive selection in rodent (Rodentia, 7 species sequences) or rodent and rabbit (Glires, 12 species sequences) using two models in the program PAML: Model 2 (selection, ω) and Model 8 (ω&beta). Residues with posterior probabilities greater than 0.900 are listed for each analysis with human (hs) PKR and S. hamster (ma) PKR coordinates. *A488/I463 was identified using both models for rodent PKRs, and not in rodent and rabbit, but the probability of positive selection was below 0.900.*

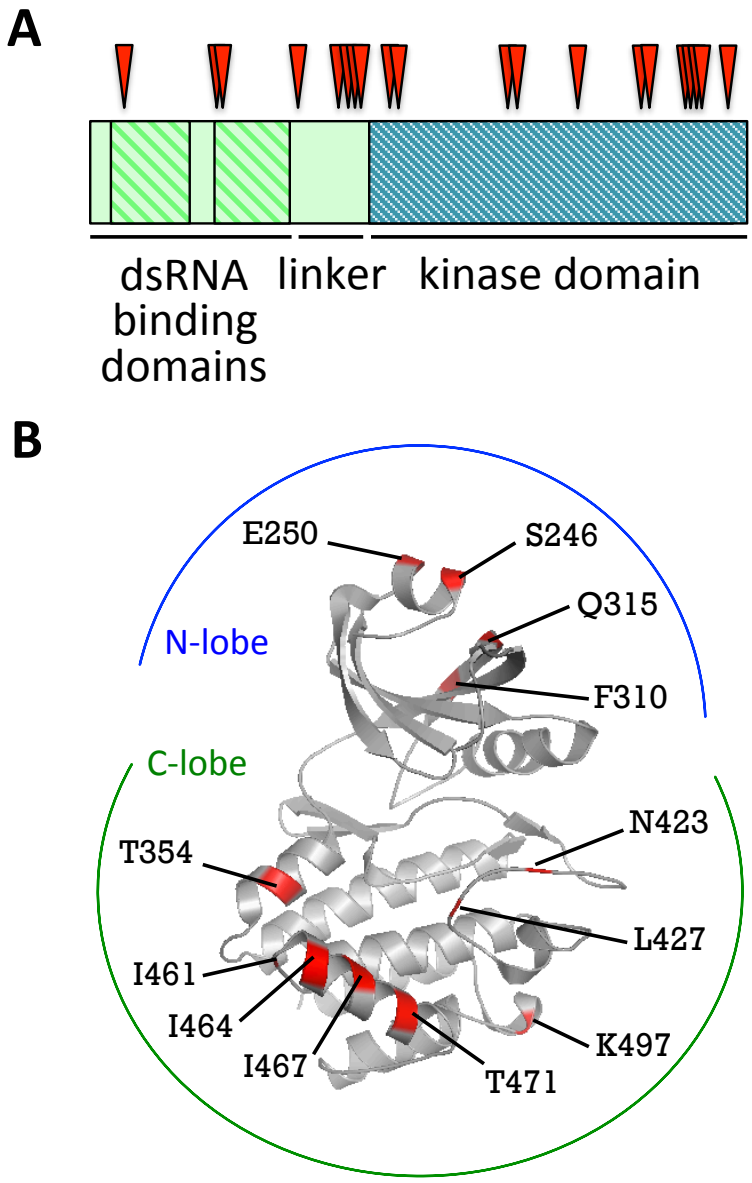

Figure 3.16 Residues under positive selection in rodent/lagomorph PKRs.

The two N-terminal dsRNA-binding domains (broad green stripes), linker region and kinase domain (thin blue stripes) are shown on the domain map. Red arrowheads indicate the position of residues found to be under positive selection in PKR from rodent and lagomorph species (A). A cartoon of the kinase domain of human PKR (PDB 2A19) shows the position of positively selected residues labeled with the S. hamster PKR residue (highlighted in red) (B).

Residue (*hs/ma*)	PAML-BEB (*Glires/Rodentia*:M8)	Other Analyses	Protein Location	Protein Sub-location
V24/T23	***/**	Elde*	RBD1	β1
S97/F90	**/**		RBD2	α3
M98/T91	***/**		RBD2	α3
S196/A188	**/n.s.		Linker	
L232/L221	**/-		Linker	
A239/P228	**/-		Linker	
K240/R229	***/-		Linker	
L243/L232	***/n.s.		Linker	
K261/S246	***/**	Rothenburg*** Elde***	N-lobe	α0
M265/E250	***/*	Elde***	N-lobe	α0
G325/F310	**/**		N-lobe	β4
F330/Q315	***/n.s.	Elde*	N-lobe	β4
E379/T354	**/**	Rothenburg**	C-lobe	αD
S448/N423	**/***	Rothenburg**	C-lobe	loop β9-αEF
L452/L427	**/**		C-lobe	loop β9-αEF
D486/I461	**/*	Rothenburg**	C-lobe	αG
A488/I463	-/n.s.	Rothenburg**	C-lobe	αG
F489/I464	**/**	Elde***	C-lobe	αG
S492/S467	***/*	Elde*	C-lobe	αG
T496/T471	**/**	Elde***	C-lobe	αG
K522/K497	**/n.s.		C-lobe	αI

Table 3.3 Residues in PKR under positive selection.

Residues were identified to be under positive selection in rodent (Rodentia, 7 species sequences) or rodent and rabbit (Glires, 12 species sequences). Residues with posterior probabilities greater than 0.95 ($p<0.05$) from Model 8 (ω&beta) results in one or both analyses are listed with human (hs) PKR and S. hamster (ma) PKR coordinates. For each residue, the domain location and structural sub-location within PKR is indicated as well as whether it was also identified in other similar positive selection analyses (17, 18). *RBD= dsRNA-binding domain, N- and C-lobe= kinase domain. *$p<0.10$, **$p<0.05$, ***$p<0.01$, n.s.= not significant ($p>0.10$), - = not identified.*

The highest concentration of residues under positive selection was found in the C-terminal lobe of the kinase domain in the αG helix. This region of PKR directly contacts eIF2α and has been shown to contribute to the sensitivity of PKR to inhibition by pseudosubstrate inhibitors such as VACV K3L (17, 41). We identified three residues within the helix αG to be under positive selection in rodent and lagomorph species PKR, which were also identified in the previous positive selection analyses on PKR in vertebrate and primate lineages (Fig 3.17). Within this region of PKR, only four amino acid residues differ between S. hamster and A. hamster PKR. These differences coincided with the three positively selected residues we identified at this position in our analyses. Additionally, the fourth differing residue was found to be under positive selection in all vertebrates and was important for contributing to the sensitivity of human and mouse PKR to inhibition by K3L (17). Mutation of each of these four residues individually in S. hamster and A. hamster PKR to the corresponding residue did not completely transfer the sensitivity or resistance of either PKR to inhibition by K3L, but the first two amino acids (amino acids 463 and 464) appeared to have the largest effect (Fig. 3.18). Exchange of all four amino acids in either hamster PKR, however, completely reversed the resistance of A. hamster PKR to K3L inhibition to S. hamster PKR and allowed K3L inhibition of A. hamster PKR. Consistent with the greater individual effect of the first two differing amino acids in the helix αG, mutating both of these residues together also completely reversed the sensitivity to K3L and therefore, entirely account for the resistance of A. hamster PKR to K3L (Fig. 3.19). Meanwhile, mutations in the helix αG did not influence the sensitivity of either hamster PKR to inhibition by E3L (Fig. 3.20).

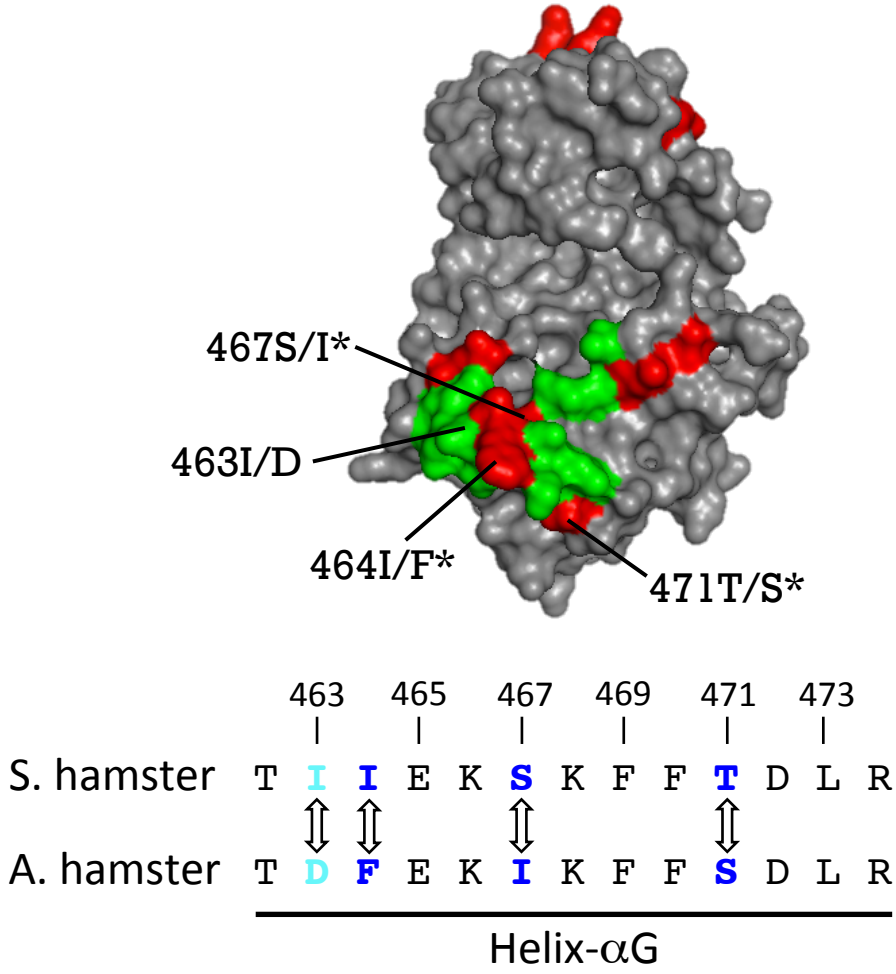

Figure 3.17 Residues under positive selection are clustered on the helix-αG of the PKR kinase domain.

The residues found to be under positive selection in this analysis were projected onto the kinase domain of human PKR (PDB 2A19) and are highlighted in red. Residues contacting eIF2α are highlighted in green. Several positively selected residues cluster near the contact site in the helix-αG, where A. hamster and S. hamster PKR differ at four positions (shown in blue or cyan below). Three of the four amino acids within this helix are under positive selection (shown in blue below and indicated with asterisks above). Residue 463 (highlighted in cyan below) was previously identified to be under positive selection in vertebrates (17).

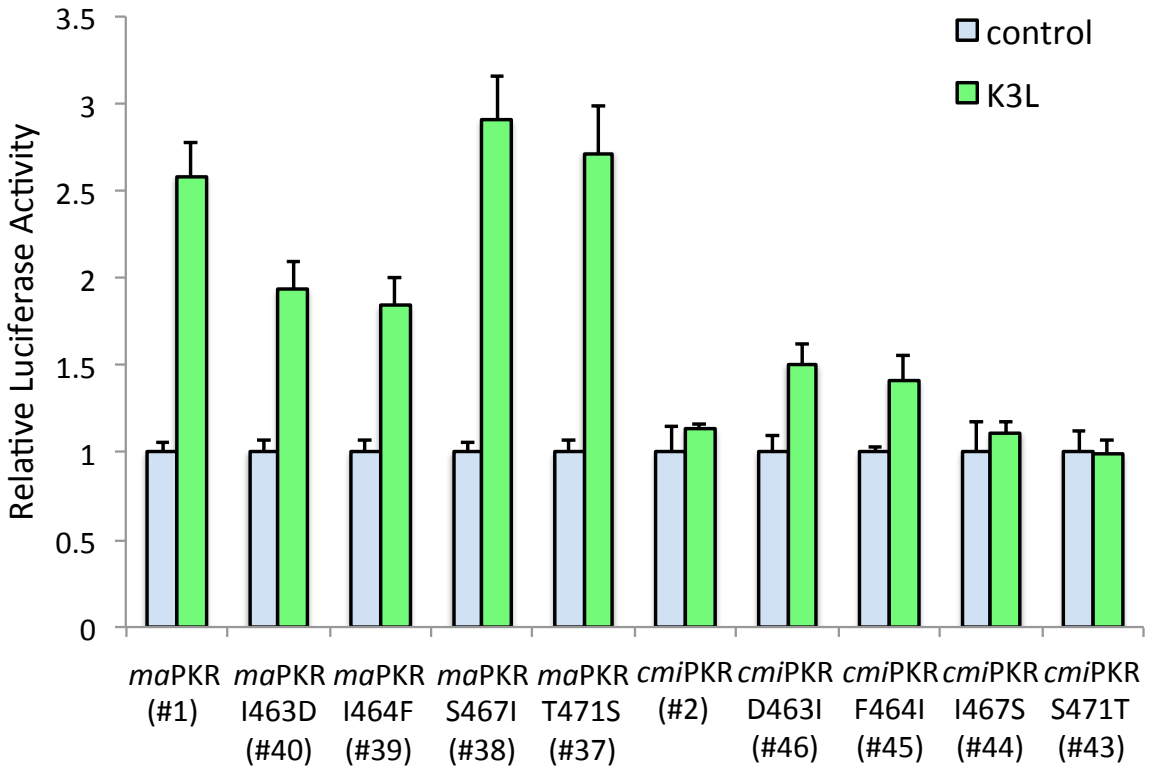

Figure 3.18 Single amino acid exchanges in the helix-αG of the PKR kinase domain.

HeLa-PKRkd cells were co-transfected with plasmids encoding firefly luciferase (0.05μg), PKR with the indicated mutations (0.2μg), and VACV K3L (0.4μg). Relative luciferase activity for each transfection was determined by normalizing measured light units to PKR-only transfected cells. Numbers under each PKR construct correspond to their number in Table 3.5. Error bars indicate the standard deviations for three replicate transfections. ma= S. hamster; cmi= A. hamster.

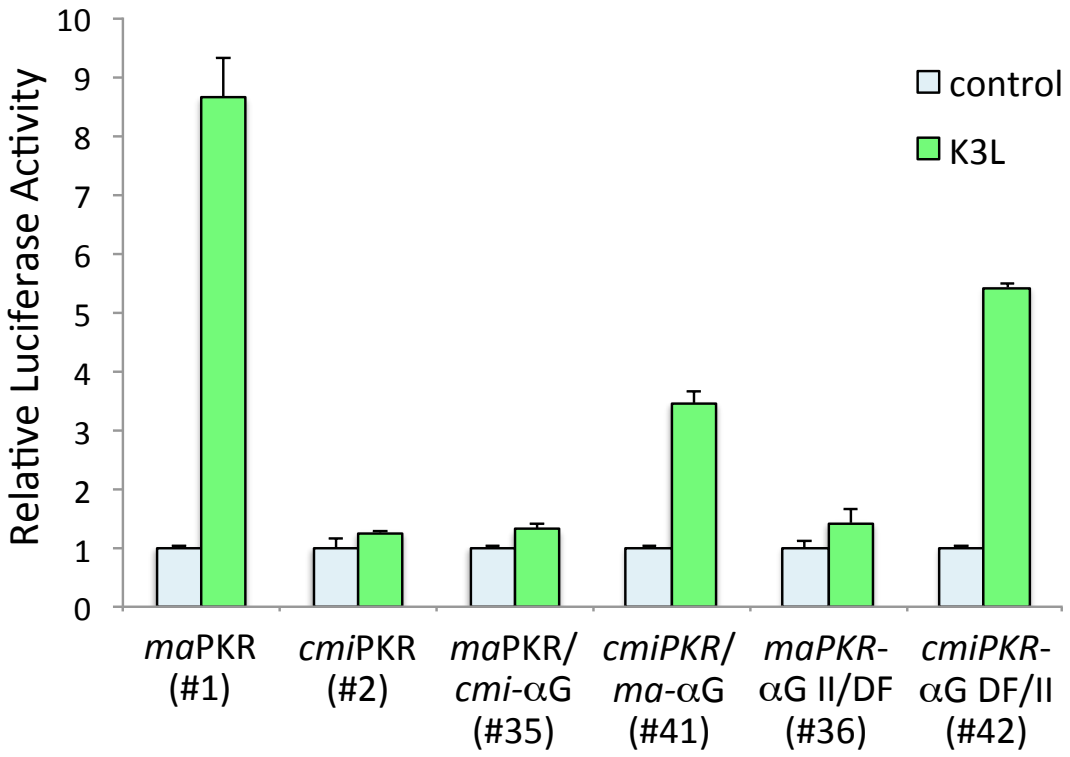

Figure 3.19 Two amino acid exchanges in the helix-αG of the PKR kinase domain alter PKR sensitivity to K3L.

HeLa-PKRkd cells were co-transfected with plasmids encoding firefly luciferase (0.05μg), PKR with either all four residues of the helix-αG mutated (αG) or two mutations (II/DF, DF/II) (0.2μg), and VACV K3L (0.4μg). Relative luciferase activity for each transfection was determined by normalizing measured light units to PKR-only transfected cells. Numbers under each PKR construct correspond to their number in Table 3.5. Error bars indicate the standard deviations for three replicate transfections. ma= S. hamster; cmi= A. hamster.

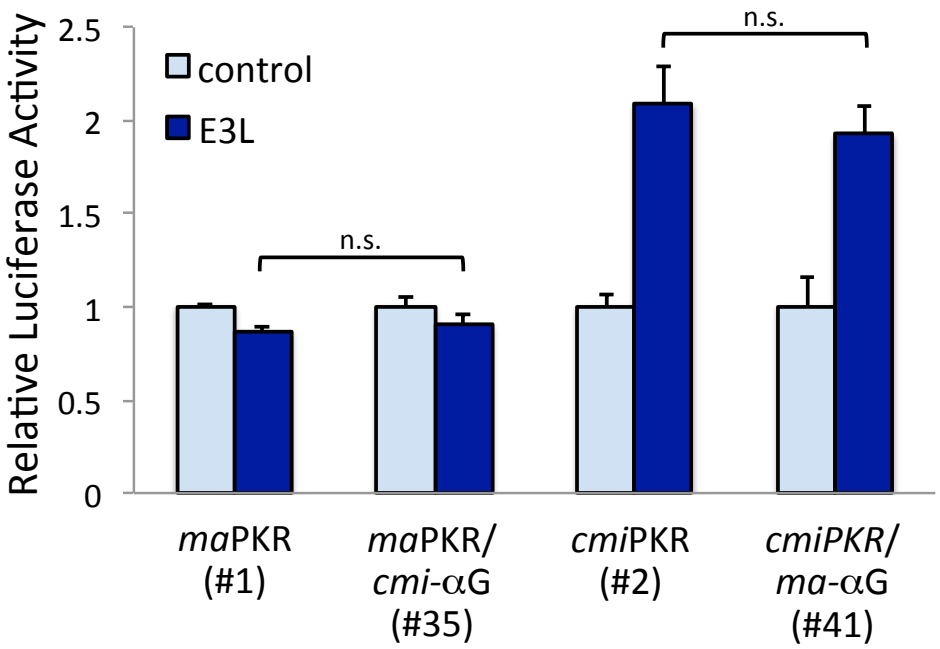

Figure 3.20 Helix-αG mutations do not affect PKR sensitivity to E3L.

HeLa-PKRkd cells were co-transfected with plasmids encoding firefly luciferase (0.05μg), PKR or PKR with the four mutations in the helix-αG (0.2μg), and VACV E3L (0.4μg). Relative luciferase activity for each transfection was determined by normalizing measured light units to PKR-only transfected cells. Numbers under each PKR construct correspond to their number in Table 3.5. Error bars indicate the standard deviations for three replicate transfections. ma= S. hamster; cmi= A. hamster. n.s.=p>0.05.

The identification of positively selected residues in helix αG of PKR in our analyses served as an internal control to validate our results. Therefore, taking the results from our domain swapping and deletion mutant experiments into account we used the same principle to investigate residues potentially involved in interactions with VACV E3L by focusing on positively selected residues found in the N-terminal RBDs and linker region of PKR. We mutated individual positively selected amino acids in S. hamster PKR to the analogous residue found in A. hamster PKR as well as combinations of residues within and between domains and tested their sensitivity to E3L in the luciferase assay (Fig 3.21). We also tagged several PKR constructs with FLAG peptide sequences (only FLAG-tagged versions of some constructs were made) to test their expression by Western blot, which did not affect the relative inhibition by E3L. For many of these point mutations, we also made the corresponding mutations in A. hamster PKR in parallel, which we predicted would reduce the sensitivity of the mutant PKRs to

E3L inhibition. However, none of these individual or combinations of mutations considerably altered the sensitivity of the hamster PKRs (a composite of multiple experiments is shown in Fig 3.21).

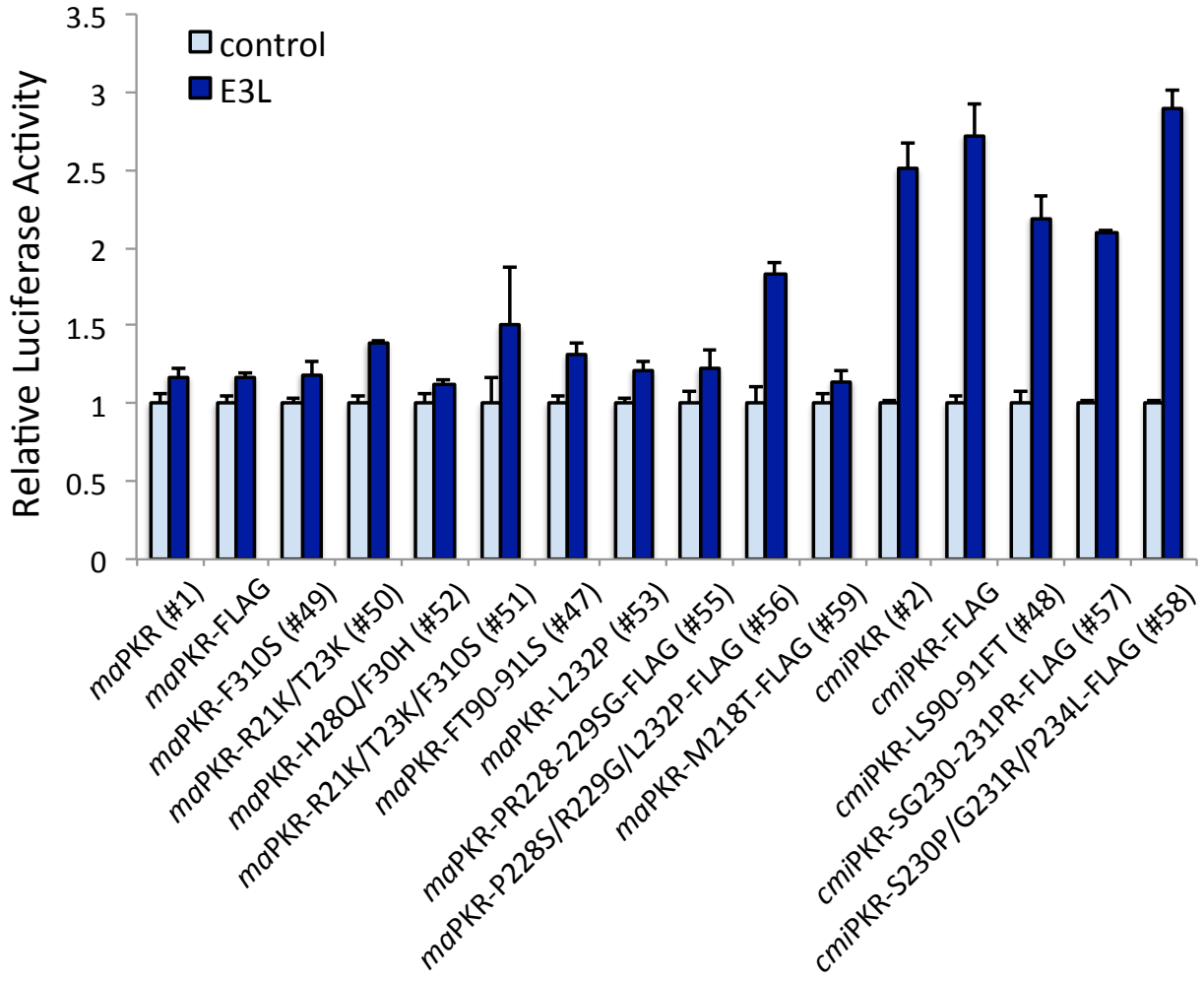

Figure 3.21 Point mutations in hamster PKR do not alter sensitivity to E3L.

HeLa-PKRkd cells were co-transfected with plasmids encoding firefly luciferase (0.05µg), PKR with the indicated mutations (0.2µg), and VACV E3L (0.4µg or 0.8µg). A composite of multiple experiments is shown. Relative luciferase activity for each transfection was determined by normalizing measured light units to PKR-only transfected cells. Numbers under each PKR construct correspond to their number in Table 3.5. Error bars indicate the standard deviations for three replicate transfections. ma= S. hamster; cmi= A. hamster.

A mutant of S. hamster PKR with mutations in the linker region between or near residues 224-229 (*ma*PKR-P228S/R229G/L232P, #56) appeared slightly sensitive to E3L inhibition (note: within a single experiment, the difference is ~1.2X greater than the S. hamster wild-type control), but, the corresponding mutations in A. hamster PKR (#58) did not reduce the sensitivity of this PKR to inhibition by E3L. It is therefore possible that these residues contribute in part to the resistance of S. hamster PKR to E3L inhibition, but they cannot by themselves fully recapitulate this resistance in a PKR sensitive to E3L, such as A. hamster PKR. While we were not able to test all possible mutations and combinations of mutations in S. hamster PKR, we concluded that because the interaction of PKR with E3L is likely to involve multiple residues in different domains, the resistance of S. hamster PKR to E3L is more complicated than PKR interactions with pseudosubstrate inhibitors. We therefore took another approach and analyzed the sensitivity of PKRs that contain mutations in residues that are important for dsRNA-binding or are contributing to PKR homodimerization as these are critical steps in the activation of PKR that might be affected by interactions with E3L.

PKR dsRNA-binding and dimerization affect PKR sensitivity to VACV E3L

There are currently two models that might explain the PKR inhibitory function of E3L: dsRNA sequestration and hetero-dimerization of E3L and PKR. In the sequestration model, E3L binds and sequesters activating dsRNA during virus infections, thereby preventing its detection by latent PKR (10, 14, 27). In the hetero-dimerization model, E3L physically binds PKR to form a hetero-dimer, which prevents the homo-dimerization of PKR that is required for its activation (42, 43). In both models, E3L inhibits PKR before the latter is fully activated. To understand the ability of S. hamster PKR to resist inhibition by E3L, we decided to investigate the early activation steps of S. hamster PKR and look for evidence that might explain this phenomenon.

The first step in PKR activation is the detection of dsRNA via its RBDs. The two RBDs in PKR contain conserved basic residue-rich RNA-binding motifs found in a number of different RNA-binding proteins including VACV E3L (44-47). Mutation of these basic residues in the RNA-binding motif of the first RBD disrupts RNA binding and abolishes human PKR activity (48, 49). Making similar mutations in S. hamster and A. hamster PKR significantly reduced activity levels of both suggesting dsRNA binding is necessary for PKR activation in our luciferase assay as well (Fig 3.22). Alanine substitutions made to abolish RNA binding in the

second RBD of each PKR had a more modest effect on PKR activity than similar mutations in the first RBD. We observed decreases in the translational suppression of the second RBD mutants for each PKR by an average of 2-3-fold compared to 4-6-fold for mutations in the first RBD indicating that, like human PKR, the ability of the first RBD to bind dsRNA is principally important for S. hamster and A. hamster PKR activation. Interestingly, in contrast to what we observed for the hamster PKRs, mutations in both RBDs of human PKR resulted in an unexpected increase in PKR activity relative to the single-domain mutations that we cannot explain.

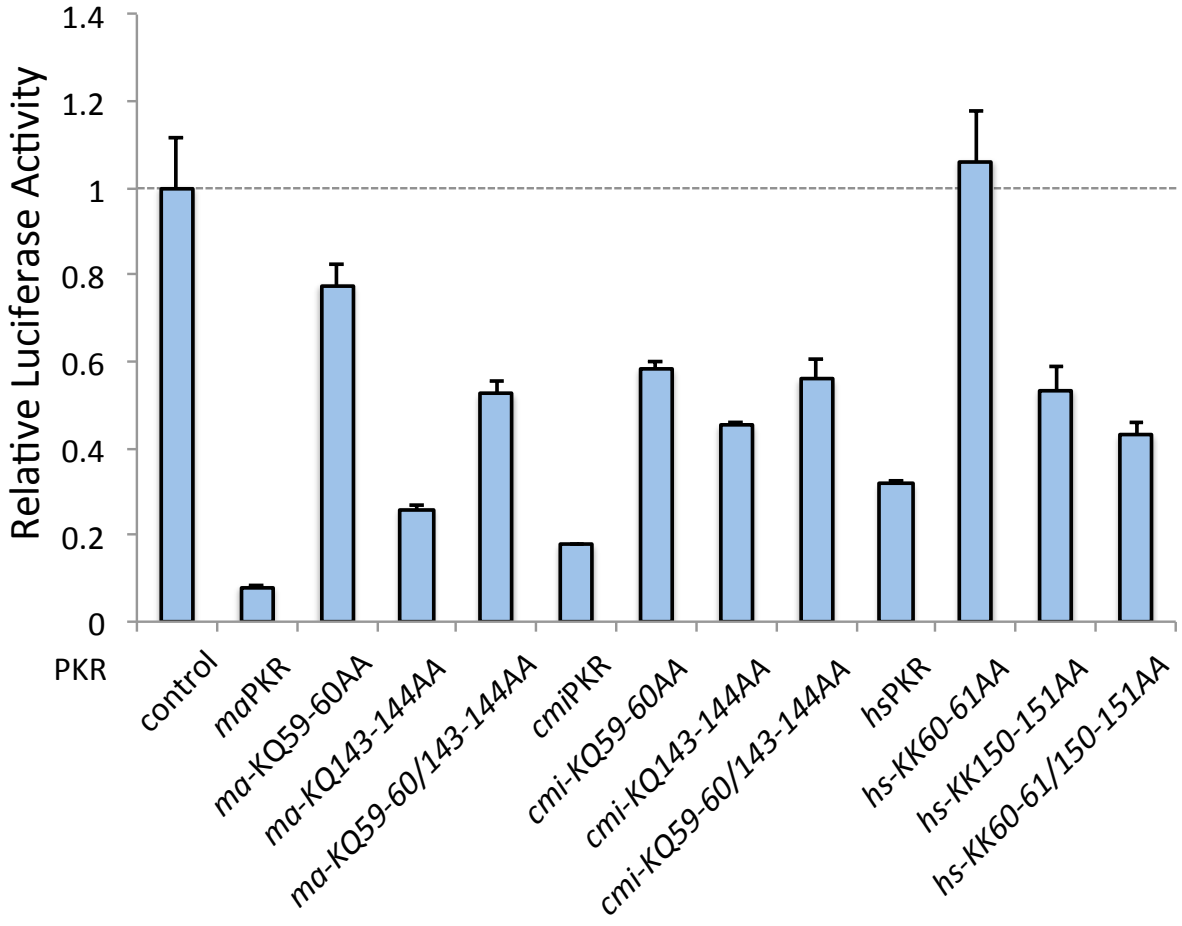

Figure 3.22 Residues important for dsRNA-binding in the first dsRNA-binding domain are most important for PKR activity.

HeLa-PKRkd cells were co-transfected with firefly luciferase (0.05µg) and PKR with the indicated mutations (0.2µg). Relative luciferase activity was normalized to vector-only transfected cells. Error bars indicate the standard deviations for three replicate transfections. The dashed line indicates the control background level of luciferase translation without PKR. ma= S. hamster; cmi= A. hamster; hs= human.

To know if these PKR mutations affected the sensitivity to E3L inhibition, we looked at the relative luciferase activity in co-transfections with VACV E3L (Fig 3.23). Remarkably, E3L was unable to inhibit any of the RNA-binding mutant PKRs, even mutants with higher PKR activity, suggesting that dsRNA binding is required for E3L's inhibitory interactions with PKR. Mutation of dsRNA-binding residues in S. hamster PKR had no effect on E3L inhibition, as these mutants were resistant like the wild type protein.

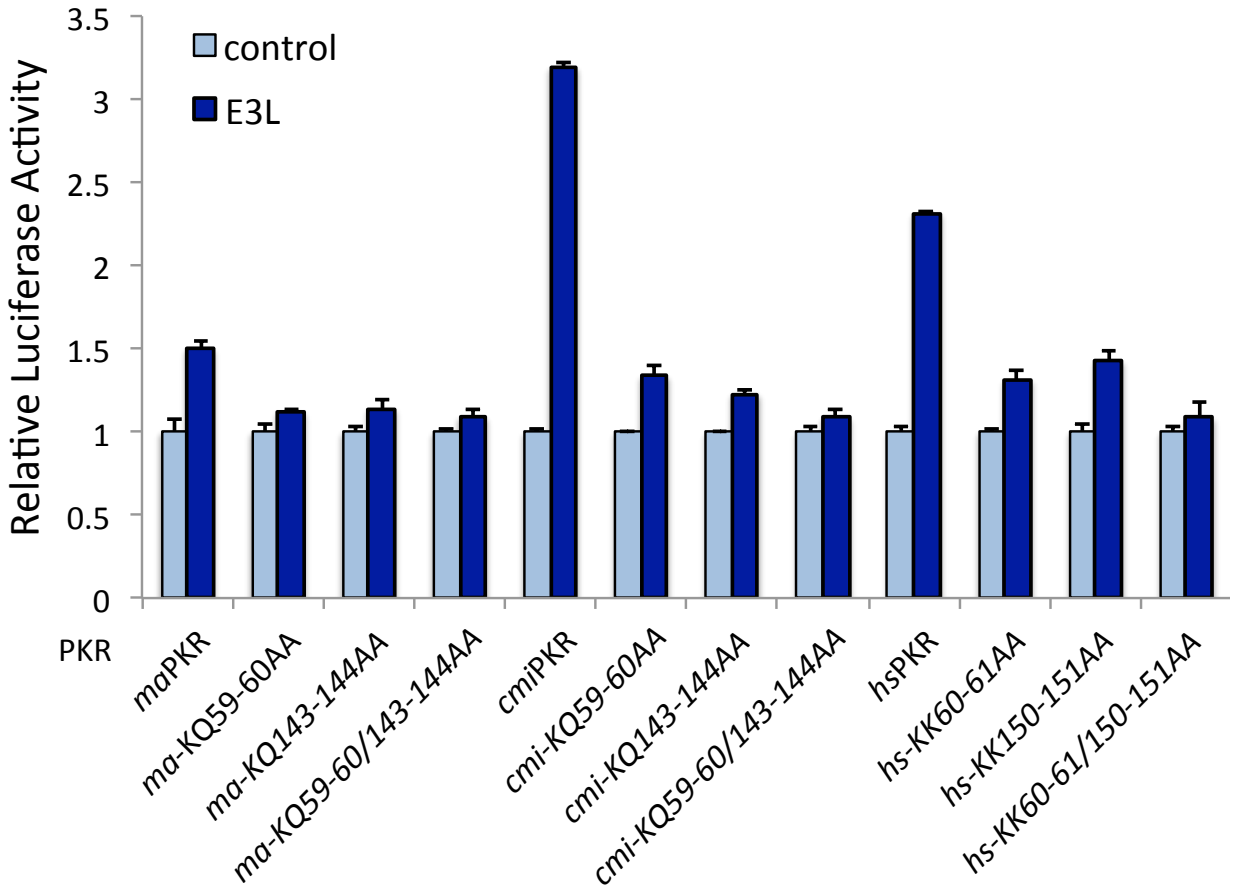

Figure 3.23 Mutations in residues important for dsRNA-binding prevent E3L inhibition.
HeLa-PKRkd cells were co-transfected with plasmids encoding firefly luciferase (0.05µg), PKR with the indicated mutations (0.2µg), and VACV E3L (0.4µg). Relative luciferase activity for each transfection was determined by normalizing measured light units to PKR-only transfected cells. Error bars indicate the standard deviations for three replicate transfections. ma= S. hamster; cmi= A. hamster; hs= human.

Because S. hamster PKR also requires dsRNA binding for its activity, we hypothesized that S. hamster PKR may exhibit a higher affinity for dsRNA than other species' PKR, which can outcompete E3L for binding to dsRNA during an infection. To test this hypothesis, we designed an experiment to see if the RBDs of S. hamster PKR could act as an auto-inhibitor of its own activity, which would suggest its ability to bind activating dsRNA is greater than that of E3L and explain its resistance assuming the sequestration model for E3L inhibition (Fig 3.24). The RBDs of S. hamster PKR, however, were not able to inhibit full-length S. hamster PKR similar to VACV E3L even at higher concentrations. Meanwhile, the S. hamster RBDs inhibited A. hamster PKR at higher concentrations, although not as well as E3L, which indicates that while the ability to bind dsRNA is important for inhibition of PKR, this ability alone is not sufficient to completely explain the PKR inhibitory function of E3L and the resistance of S. hamster PKR.

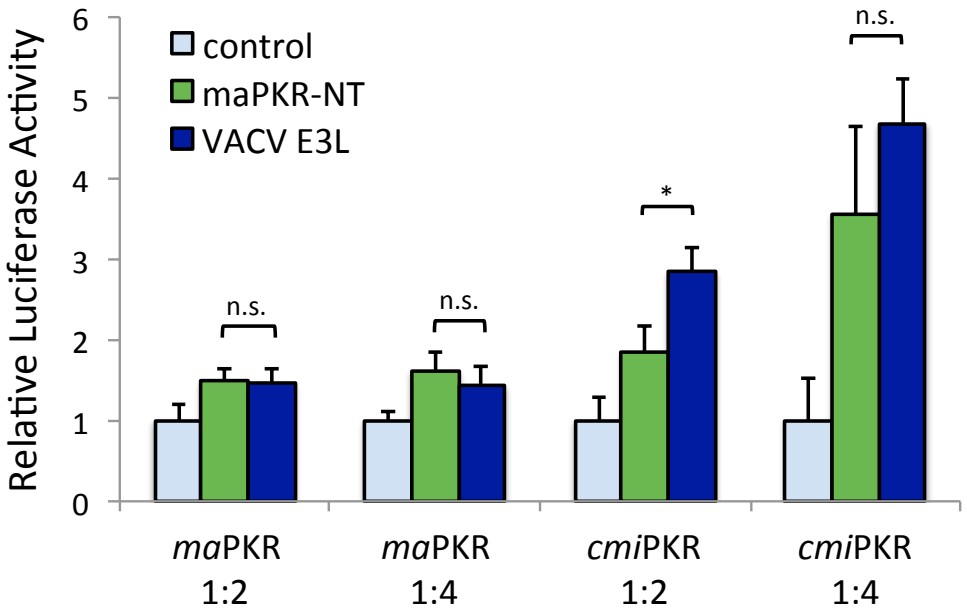

Figure 3.24 Syrian hamster dsRNA-binding domains can inhibit Armenian hamster PKR like E3L. *HeLa-PKRkd cells were co-transfected with plasmids encoding firefly luciferase (0.05µg), PKR from the indicated species (0.3µg or 0.2µg) and VACV E3L (0.6µg or 0.8µg). Relative luciferase activity for each transfection was determined by normalizing measured light units to PKR-only transfected cells. Error bars indicate the standard deviations for three replicate transfections. P-values calculated with Student's t-test. n.s.= p>0.05, *p<0.05; ma= S. hamster; cmi= A. hamster.*

The sensing and binding to cytoplasmic dsRNA by latent monomeric PKR induces a conformational change to an open configuration that allows for two PKR molecules to dimerize. This homo-dimerization is necessary for human PKR activity; however, it is not clear whether one or both PKRs in the dimer are responsible for carrying out subsequent phosphorylation reactions (3). In theory, each PKR molecule still retains the ability to perform phosphorylation reactions individually. In this way, we reasoned that a PKR molecule could theoretically be active as a monomer in different host species or different cellular environments. To test the hypothesis that S. hamster PKR might be able to avoid E3L inhibition by maintaining kinase activity as a monomer, we mutated a conserved residue in the N-lobe of PKR shown to be important for human PKR dimerization and activity (Fig 3.25) (50).

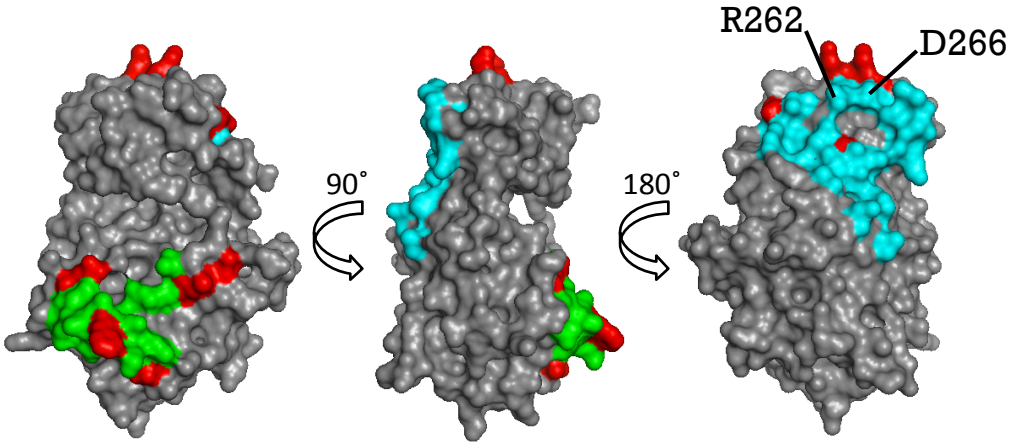

Figure 3.25 Residues under positive selection are clustered on the dimerization region of the PKR kinase domain.

The residues found to be under positive selection were projected onto the kinase domain of human PKR (PDB 2A19) and are highlighted in red. Residues contacting eIF2α are also highlighted in green and residues contacting another PKR dimer are highlighted in cyan. Several positively selected residues also clustered near the region of dimerization. Two residues in this region that form a salt-bridge important for dimerization in human PKR are indicated.

Affect of mutation	PKR Mutant Construct	% Luc. inhibition	Rel. PKR activity	E3L Sensitivity
Wild type	hsPKR	80.51±5.86	1.00±0.30	++++
Dimerization	hsPKR-D266R	-27.17±18.74	6.63±2.02	++
Dimer. Rev.	hsPKR- D266R/R262D	24.31±20.34	3.68±0.73	+/-
RNA-binding RBD1&2	hsPKR-KK60-61AA/ KK150-151AA	69.28±11.10	1.66±0.28	-
RBD1	hsPKR-KK60-61AA	7.73±13.11	5.76±1.68	+/-
RBD2	hsPKR-KK150-151AA	69.92±13.27	1.72±0.17	+/-
Wild type	maPKR	92.48±3.80	1.00±0.51	-
Dimerization	maPKR-D251R	30.61±4.88	9.80±6.19	++
Dimer. Rev.	maPKR-D251R/R247D	81.74±1.35	2.60±1.78	+++
RNA-binding RBD1&2	maPKR-KQ59-60AA/ KQ143-144AA	67.10±17.37	4.24±2.35	-
RBD1	maPKR-KQ59-60AA	64.81±24.05	5.09±2.92	-
RBD2	maPKR-KQ143-144AA	82.72±7.52	2.18±0.99	-
Wild type	cmiPKR	89.87±4.24	1.00±0.42	++++
Dimerization	cmiPKR-D253R	4.97±5.11	10.17±2.06	++++
Dimer. Rev.	cmiPKR-D253R/R249D	54.13±14.23	4.46±1.63	++++
RNA-binding RBD1&2	cmiPKR-KQ59-60AA/ KQ143-144AA	67.59±23.20	2.93±1.67	-
RBD1	cmiPKR-KQ59-60AA	68.05±15.43	3.53±0.83	+/-
RBD2	cmiPKR-KQ143-144AA	74.98±12.17	2.78±0.77	-

Table 3.4. Dimerization and dsRNA-binding mutant PKRs tested in the luciferase assay.

Listed for each construct is a number and a name, which indicates the mutations performed. The percent translational suppression by each PKR relative to vector controls (% PKR activity) are shown for each construct and the fold change in activity for each PKR construct was determined relative to the activity of the parental wild type PKR (human, S. hamster, or A. hamster PKR) within each experiment (Rel. PKR activity). Values for each PKR construct were averaged from at least two independent experiments and the standard deviations are shown. The sensitivity of each construct to inhibition by VACV E3L is shown with a "+" indicating sensitivity or "-" indicating resistance. ma= S. hamster; cmi= A. hamster; hs= human; RBD= dsRNA-binding domain; Dimer. Rev.= Dimerization reversion.

The activity levels of wild type S. hamster PKR were very similar to those observed for A. hamster PKR and several other PKR from different mammalian species. Both PKRs consistently suppressed ~90-93% of luciferase translation compared to vector control transfections (Table 3.4, and data not shown). In contrast, when we mutated residue 251 in S. hamster PKR from an aspartate to an arginine, the mutant PKR only suppressed ~30% of

luciferase translation exhibiting a nearly 11-fold decrease in PKR activity (Fig 3.26). We observed an even greater decrease in A. hamster and human PKR activity with the corresponding mutations, which both lost all or nearly all translational suppression activity. This indicates that S. hamster PKR, like both A. hamster and human PKR, requires the formation of the same salt-bridge during dimerization for the majority of its activity. Nevertheless, the mutated S. hamster PKR still retained a greater ability to suppress luciferase translation than the other species' PKRs suggesting that a small portion of its activity may in fact be due to active PKR monomers. Alternatively, these results may indicate that the formation of the salt-bridge is not as critical to the dimerization of S. hamster PKR or that S. hamster PKR dimers are further stabilized by other biochemical interactions.

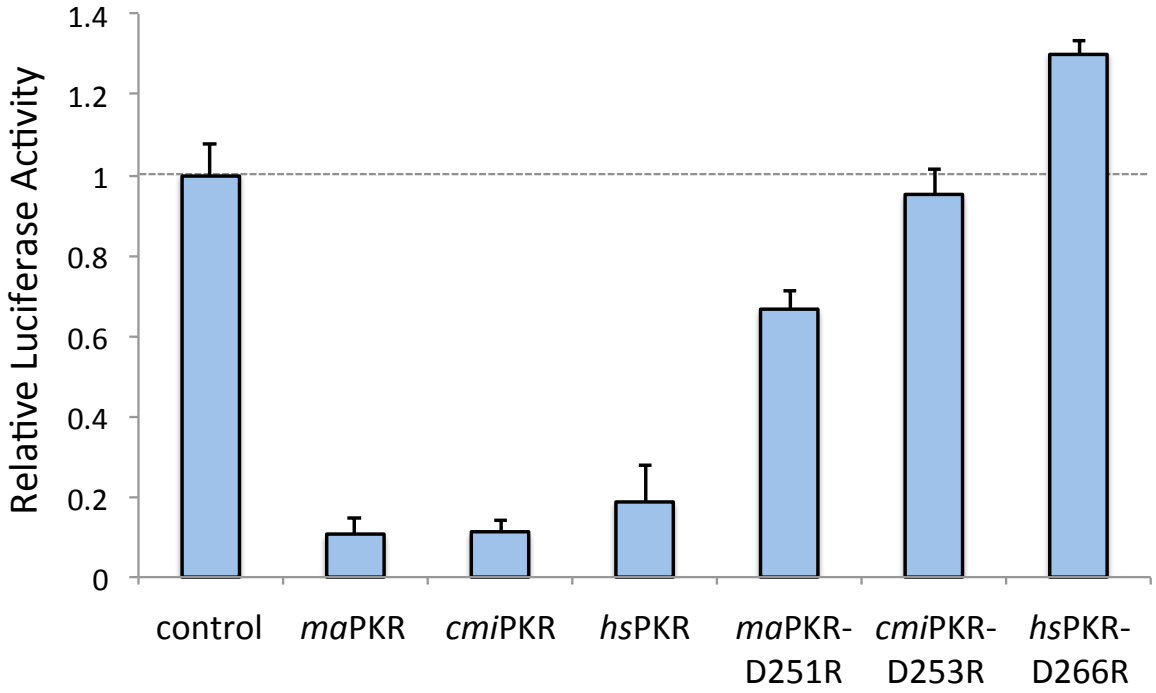

Figure 3.26 Hamster PKRs require residues forming salt-bridge during dimerization for PKR activity.

HeLa-PKRkd cells were co-transfected with plasmids encoding firefly luciferase (0.05µg) and PKR with the indicated mutations (0.2µg). Relative luciferase activity for each transfection was determined by normalizing measured light units to vector-only transfected cells. Error bars indicate the standard deviations for three replicate transfections. The dashed line indicates the control background level of luciferase translation without PKR. ma= S. hamster; cmi= A. hamster; hs= human.

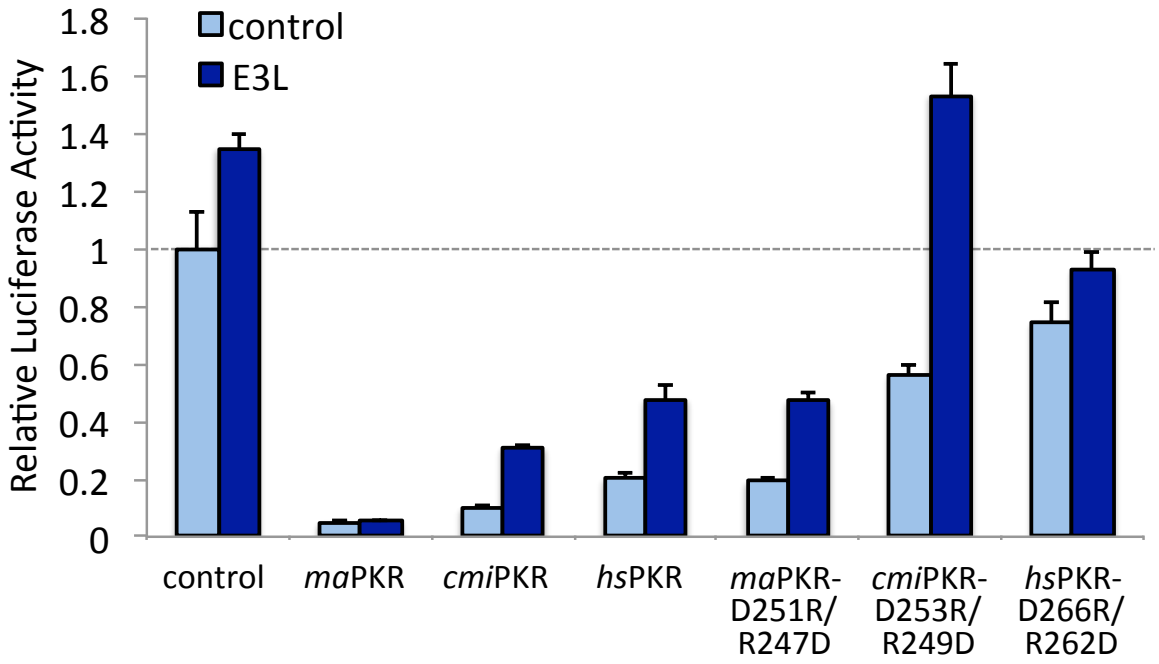

Figure 3.27 Reversion of salt-bridge residues in dimerization region of PKR does not completely restore PKR activity and makes Syrian hamster PKR sensitive to E3L.

HeLa-PKRkd cells were co-transfected with plasmids encoding firefly luciferase (0.05µg), PKR with the indicated mutations (0.2µg) and VACV E3L (0.4µg). Relative luciferase activity for each transfection was determined by normalizing measured light units to vector-only transfected cells. Error bars indicate the standard deviations for three replicate transfections. The dashed line indicates the control background level of luciferase translation without PKR. ma= S. hamster; cmi= A. hamster; hs= human.

Making an additional mutation of the second residue involved in the salt-bridge (R262D in human PKR) is expected to rescue PKR activity by restoring the ability to form the salt-bridge that strengthens the PKR homodimers. When we mutated this second residue in S. hamster PKR to rescue dimerization, PKR activity was greatly increased, however, the double mutant PKR was still ~2.6X less active than the wild type (Fig 3.27, Table 3.4). More dramatically, the same reversion mutation in human PKR likewise did not fully restore its PKR activity as predicted from results with the same mutations in a yeast assay (50). Instead the double mutant only suppressed ~24% of luciferase translation, which was also ~3.7X less active than the wild type protein on average, and the double mutant of A. hamster PKR was ~4.5X less active than its wild type version. From these results we surmised that the importance of the relative positions of surrounding residues in the dimer interaction interface are also important to the formation or

stability of the salt-bridge and that the simple translocation of the two critical residues does not fully restore the stability of this interaction in HeLa cells, and possibly resulted in weak dimer formation between the mutant PKRs.

While the inhibition of inactive mutant PKRs (PKRs that did not suppress luciferase translation relative to the vector control) cannot be inferred, inhibition by VACV E3L of the double mutants, for which some activity was restored, could be analyzed. In fact, these mutants provided a unique opportunity to observe the effect of inferred weak dimer formation on their inhibition by E3L. We therefore tested E3L inhibition of the double dimerization mutant PKRs with their wild type counterparts (Fig 3.27). Interestingly, from our results, we observed a relative increase in the inhibition of S. hamster PKR for the double mutant that corresponded to a ~2.5-fold increase in luciferase translation similar to that observed for wild type human PKR or A. hamster PKR. The sensitivity of this mutant S. hamster PKR to E3L inhibition was striking considering the extent to which PKR activity was restored for this mutant. The moderate PKR activity of the A. hamster double mutant PKR was still efficiently inhibited by E3L, but the low activity of the human PKR mutant prevented making an accurate assessment of E3L inhibition. The ability of E3L to inhibit the double mutant S. hamster PKR, however, indicates that E3L likely inhibits PKR by disrupting dimerization, which supports the hetero-dimerization model of E3L inhibition.

Discussion

The broad host range of VACV can be attributed to the activities of several host range genes that serve to inhibit the immune response within host cells. Two important host range genes in VACV are E3L and K3L, which inhibit the cellular protein kinase R (PKR). In the previous chapter, we showed that PKR from closely related hamster species exhibited strikingly different sensitivities to inhibition by VACV E3L and K3L, which correlated with the replication of VACV mutants and eIF2α phosphorylation in cell lines from the corresponding hamster species. In this analysis, we built off our previous results and used the observation that S. hamster and A. hamster PKR were oppositely resistant to inhibition by E3L and K3L, respectively, to investigate the mechanisms by which these proteins are able to accomplish this feat. Many studies looking at PKR sensitivity to inhibition have been done in yeast, but we used a cell culture-based assay that is more sensitive to differences in sensitivity and allowed for a

more medium-throughput analysis of several hybrid hamster PKRs mutants. Using a combined approach of domain swapping experiments and point mutational analyses at sites of positive selection, we mapped the resistance of S. hamster PKR to VACV E3L to the second RBD and the linker region and identified two amino acids in the kinase domain of A. hamster PKR that confer its resistance to VACV K3L. A summary of each PKR mutant's relative PKR activity and sensitivity to inhibition by VACV E3L or VACV K3L is described in Table 3.5.

PKR Mutant Construct	Rel. PKR activity	E3L Sensitivity	K3L Sensitivity
1. maPKR	1.00±0.49	-	++++
2. cmiPKR	1.18±0.31	++++	-
3. hsPKR	2.06±1.13	++++	+
4. mmPKR	0.92±0.14	++++	++++
5. ma/cmiPKR	0.91±0.22	++	-
6. 1+2RBDma/cmiPKR	0.88±0.20	+++	-
7. 1RBDma/cmiPKR	0.85±0.17	++++	-
8. 2RBDma/cmiPKR	1.22±0.22	++	+/-
9. ma-LR/cmiPKR	0.94±0.07	+++	-
10. 2RBD+LRma/cmiPKR	0.90±0.09	++	-
11. cmi/maPKR	1.25±0.34	+++++	++++++
12. 1+2RBDcmi/maPKR	1.13±0.24	++	++++
13. 1RBDcmi/maPKR	1.17±0.25	+	+++
14. 2RBDcmi/maPKR	0.92±0.25	+	+++++
15. cmi-LR/maPKR	1.11±0.14	++	+++++
16. 2RBD+LRcmi/maPKR	0.92±0.09	++++	++++++
17. maPKR/cmi-C-lobe	0.68±0.07	+	-
18. 1RBDcmi/maPKR/cmi-C-lobe	0.73±0.12	++	-
19. maPKR/cmi-N-lobe	1.11±0.11	-	+++++
20. 1RBDcmi/maPKR/cmi-N-lobe	1.52±0.23	++	+++++
21. ma/mmPKR	1.04±0.32	+/-	++++
22. 1+2RBDma/mmPKR	1.23±0.23	++	+++++
23. mm/maPKR	1.28±0.49	++	+++
24. 1+2RBDmm/maPKR	1.40±0.43	+	++
25. 1RBDhs/maPKR	1.10±0.14	+	++++
26. 2RBDhs/maPKR	2.05±0.13	-	++++
27. 1+2RBDhs/maPKR	1.56±0.14	+	++++
28. maPKR-sv (Δ164-217)	1.18±0.29	-	++
29. maPKRΔ164-227	0.82±0.14	+/-	+++
30. maPKRΔ164-233	0.85±0.16	+++	+++
31. maPKRΔ164-239	0.82±0.07	++	+++
32. maPKRΔLR (Δ164-241)	1.26±0.42	++	++
33. cmiPKRΔ164-219	0.90±0.02	+++	n.d.

34. ma/mmPKRΔLR (Δ164-241)	1.00±0.24	+	n.d.
35. maPKR/cmi-aG (4mut)	0.99±0.21	-	-
36. maPKR-II463-464DF	0.96±0.20	-	-
37. maPKR-T471S	1.00±0.15	-	++++
38. maPKR-S467I	1.14±0.15	+	++++
39. maPKR-I464F	1.01±0.04	+/-	++
40. maPKR-I463D	1.65±0.15	-	++
41. cmiPKR/ma-aG (4mut)	2.17±0.94	+++	+++
42. cmiPKR-DF465-466II	2.10±0.92	+++	+++
43. cmiPKR-S471T	1.34±0.01	+++	-
44. cmiPKR-I467S	1.48±0.005	+++	-
45. cmiPKR-F464I	2.21±0.52	+++	+
46. cmiPKR-D463I	1.22±0.20	+++	+
47. maPKR-FT90-91LS	1.00±0.19	-	n.d.
48. cmiPKR-LS90-91FT	1.20±0.29	+++	n.d.
49. maPKR-F310S	1.05±0.14	-	+++
50. maPKR-R21K/T23K	1.01±0.14	+	++++
51. maPKR-R21K/T23K/F310S	0.92±0.11	+	++++
52. maPKR-H28Q/F30H	1.17±0.15	-	n.d.
53. maPKR-L232P	1.00±0.08	-	n.d.
54. cmiPKR-P234L*	1.32±0.28	++++	n.d.
55. maPKR-PR228-229SG*	1.12±0.06	+/-	n.d.
56. maPKR-P228S/R229G/L232P*	1.31±0.07	+	n.d.
57. cmiPKR-SG230-231PR*	1.48±0.19	++++	n.d.
58. cmiPKR-S230P/G231R/P234L*	1.30±0.21	++++	n.d.
59. maPKR-M218T*	1.35±0.40	-	n.d.

Table 3.5. Hamster PKR mutant constructs tested in the luciferase assay.

*Listed for each construct is a number and a name, which indicates the mutations or domain swaps performed. The activity of each PKR construct was determined relative to the activity of S. hamster PKR within each experiment. Relative light units from S. hamster PKR only transfections were averaged and normalized to 1. Activity levels less than 1 correspond to higher levels of PKR activity (increased suppression of translation). Values for each PKR construct were averaged from at least two independent experiments and the standard deviations are shown. Activity levels of wild type A. hamster, human and mouse PKR were also compared to S. hamster PKR. The sensitivity of each construct to inhibition by VACV E3L or K3L is shown with a "+" indicating sensitivity or "-" indicating resistance. *= FLAG-tagged versions of the construct were tested; n.d.= not determined; ma= S. hamster; cmi= A. hamster; hs= human; mm= mouse; RBD= dsRNA-binding domain; sv= splice variant; LR= linker region.*

The co-crystal structure of dimeric PKR kinase domain with its substrate eIF2α has been very useful for analyzing the structural relevance of different residues in PKR since it was

determined (16). Within the kinase domain of PKR, K3L likely interacts with the same region in the C-terminal lobe that interacts with eIF2α, and this has driven positive selection at residues in solvent exposed portions of the PKR enzyme (Fig 3.16). The rapid evolution of the kinase domain of PKR has been demonstrated in vertebrates and primates, and previous studies suggested that positively selected residues in PKR contribute to differential sensitivity of PKR from different species to VACV K3L (17, 18). Our results that positively selected residues in the helix αG of A. hamster PKR kinase domain explain its resistance to K3L support these previous studies, which also identified residues within this helix structure to be important for PKR interactions with VACV K3L. It is remarkable that this region in PKR, which must maintain its ability to interact with the highly conserved eIF2α, can vary so much between even closely related species and that only a few amino acid changes can completely change the sensitivity of a species' PKR to inhibition by pseudosubstrate inhibitors, such as K3L.

Whereas we would expect species-specific differences in K3L's inhibition of PKR due to the high sequence diversity of PKR and K3L's mode of inhibition, which requires direct protein-protein interactions, the resistance of S. hamster PKR to VACV E3L inhibition is surprising. The extension of this resistance to other viral dsRNA-binding proteins also indicates a more general mechanism for this resistance, which may have been beneficial for the survival of this species at some point in its evolutionary history. The species-specific resistance to E3L inhibition we observed for S. hamster PKR challenges the long held model for E3L inhibition of PKR by sequestering activating dsRNA and instead suggests a mechanism involving a direct protein-protein interaction, which is more likely to drive positive selection in the interacting proteins. We, however, were not able to detect any single positively residue or combination of residues in our analysis that could alter the resistance of S. hamster PKR to inhibition by E3L. Although our mutational analysis was not exhaustive, it remains possible that our positive selection analysis was not broad enough to observe suitable signatures of this selection, or that the rare nature of the interaction between S. hamster PKR and E3L does not lend itself to detection in analyses for positive selection, as we have not observed this resistance in any of the 16 other species' PKRs we have in the lab. Nevertheless, from our domain swapping experiments, we determined that multiple domains in S. hamster PKR contribute to the resistance to E3L but that the second RBD and the linker region of S. hamster PKR are most important for conferring this resistance. We also determined that the kinase domain likely also plays a role and residues important for PKR

dimerization in the N-terminal lobe of the kinase domain contribute to the ability of E3L to inhibit PKR.

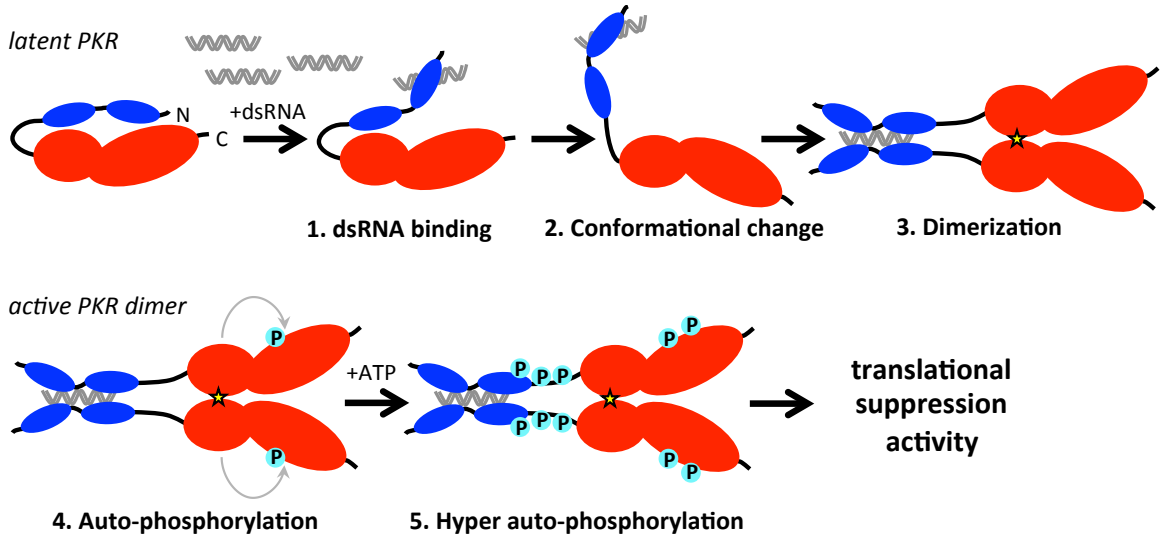

Figure 3.28 Diagram of the stages of PKR activation.

PKR becomes activated by binding dsRNA and is fully active following dimerization and auto-phosphorylation reactions. Hyper-autophosphorylation occurs at multiple locations within activated PKR. The salt-bridge formed during PKR dimerization is indicated with a star.

The dimerization of two PKR molecules is part of a sequence of events for the activation of PKR that occurs following the detection of cytoplasmic dsRNA (Fig. 3.28). Our results looking at the role of PKR's ability to bind dsRNA or form stable dimers by mutating residues important for both functions validated this conventional model of PKR activation. PKR activation requires the binding of dsRNA by the first RBD, which is independent of and precedes dimerization with another PKR molecule (49). Similarly, our data indicate that dsRNA-binding by the first RBD in hamster and human PKR is most critical to their ability to suppress translation. Latent PKR, which nuclear magnetic resonance data suggests is held in an autoinhibitory, closed conformation, undergoes a conformational change to a more open configuration after binding dsRNA and forms a dimer with a second PKR molecule (51). Dimers formed by activated PKRs are strengthened by hydrogen bonds and by the formation of a salt-bridge across residues in the N-lobe of the kinase domain, without which the activity of PKR is greatly diminished (Fig. 3.26) (50). While our mutant PKRs with mutations predicted to prevent

the formation of the necessary salt-bridge for dimerization exhibited a significant reduction in PKR activity, mutations predicted to restore the salt-bridge, did not fully recover this lost activity. It was surprising, however, that only the S. hamster double mutant PKR regained activity levels comparable to other wild type PKRs, while the activity of the A. hamster or human PKR double mutants on average suppressed less than 55% or 25% of luciferase translation, respectively. It is possible then, that wild type S. hamster PKR already forms dimers that are stronger and more stable, and therefore mutation of these residues only weakly disrupts the stability of this interaction, whereas it is more disruptive for the other species' PKRs. In support of the potential importance of dimerization in the evasion of viral inhibitors by PKR, our positive selection analysis revealed a second clustering of positively selected residues around the dimer contact region in the kinase domain (Fig. 3.25). However, because exchange of the N-lobe alone did not alter the sensitivity of S. hamster PKR to inhibition by E3L, the importance of these residues for S. hamster PKRs' resistance is unclear.

For complete activation, PKR is autophosphorylated at several serine and threonine residues in a region known as the activation loop (5, 52). This autophosphorylation, particularly at T446 in human PKR, is necessary for PKR catalytic activity, although it is thought that hyperphosphorylation at other sites may also serve to stabilize PKR dimers (3). While it remains to be tested, it is possible that S. hamster PKR dimers are further stabilized by such hyperphosphorylation reactions within the protein. In protein lysates collected from transfected cells, we consistently observed a second shifted band for S. hamster PKR that we did not observe for any of the other PKRs that may represent a hyper-autophosphorylated molecule (Ch. 2). A previous study with a human PKR mutant lacking part of the linker region to mimic the splice variant S. hamster PKR exhibited enhanced autophosphorylation, which suggests that linker region length and PKR autophosphorylation are correlated (53).

In this study, we found that the deletion of residues 224-229 in the linker region of S. hamster PKR influenced its resistance to E3L, and further deletion of the remaining linker region resulted in S. hamster PKRs that were also sensitive to E3L inhibition. Work from others suggests that species-specific contributions of the linker region to the activation of PKR are possible as this region of PKR is highly variable in length. While the role of the linker region in PKR activation and activity is poorly understood, there is evidence that the linker plays a role in mediating interactions between the RBDs and the kinase domain during PKR dimerization and

activation, although the RNA-binding activity of the RBDs also affects dimerization (39, 53). PKRs with shorter linker regions found in rodent PKRs such as rat PKR (60 amino acids) were autophosphorylated and could phosphorylate eIF2α in the absence of RNA activators at much lower protein concentrations than human PKR, which has a relatively long linker region (82 amino acids) (40). Additionally, the splice variant form of S. hamster PKR missing 53 amino acids in the linker region was found to be constitutively active in *in vitro* assays for PKR activation and did not respond to RNA activators (Schwartz and Conn, unpublished). This could suggest that some of S. hamster PKR activity (at least the splice variant isoform) may be RNA-independent, which we would not expect to be affected by viral inhibitors that bind excess dsRNA like VACV E3L, HSV-1 Us11 or reovirus σ3. Furthermore, a splice-variant form of human PKR in this study was activated more than the full length human PKR by longer dsRNA molecules (40bp) indicating that the properties of the linker region may impart a way to distinguish and respond to different forms of dsRNA *in vivo*. PKR is able to recognize viral RNA from a broad range of virus families, so it is likely that RNA molecules beyond the canonical dsRNA can activate PKR. PKR from different species, such as S. hamster PKR may therefore be more able to distinguish or detect longer or structured RNA molecules that others cannot.

PKR is a key component of the cell's innate antiviral response that must be overcome by viruses in order to replicate. In VACV, E3L and K3L are responsible for inhibiting the activity of PKR in susceptible host cells. The mechanism of pseudosubstrate inhibition employed by K3L has been well studied, and our analysis confirmed this mechanism in interactions with hamster PKRs (11, 12, 17, 18). The high sequence diversity of PKR, particularly in the kinase domain, and the direct protein-protein interactions involved with K3L convey a great degree of species-specificity for the activity of this viral protein. However, the mechanism of VACV E3L's inhibition of PKR is less clear, especially as it contributes to VACV host range.

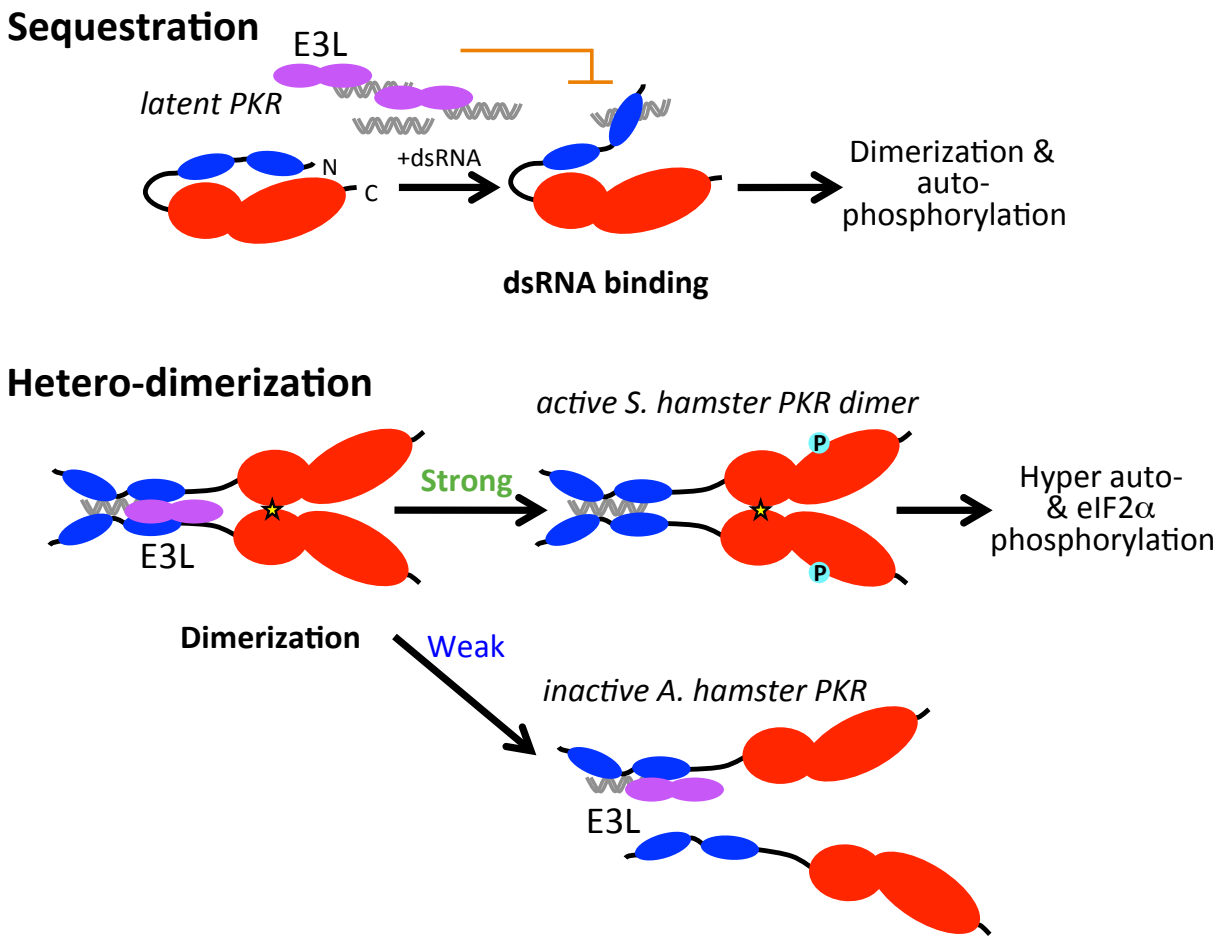

Figure 3.29 Diagram of models of E3L inhibition of PKR.

The dsRNA sequestration model and hetero-dimerization model for E3L inhibition of PKR are shown. In the sequestration model, E3L inhibits PKR by sequestering activating dsRNA prior to PKR dimerization and autophosphorylation. In the hetero-dimerization model, E3L disrupts weak PKR dimers via direct interactions mediated by dsRNA-binding. Stronger or more stable PKR dimers can resist inhibition and remain active.

The study of E3L's interactions with PKR continues to be an area of intense research. There are two models for the inhibitory function of E3L, which are not mutually exclusive (Fig. 3.29). Early work showing the importance of E3L's dsRNA-binding function for inhibition of PKR suggested that E3L binds and sequesters dsRNA to avoid activation of PKR (8, 10, 14, 54). This model, however, requires a stoichiometric abundance of E3L proteins to completely prevent detection by PKR, which has been suggested but would be likely difficult to accomplish in an infected cell (55). Moreover, work from others has separated the dsRNA-binding functions of

E3L with its inhibition of PKR and host range function (15, 42). Our results instead indicate that mutations affecting dimerization also affect inhibition by E3L, and therefore E3L's interactions with PKR are not limited to the stages prior to its activation as is suggested by the sequestration model. Binding dsRNA by PKR is still critical to these interactions since we observed mutations that affect dsRNA binding in PKR also completely restricted E3L from inhibiting otherwise sensitive PKRs (Fig. 3.23). Together our data suggest a model for inhibition whereby E3L forms heterodimers with PKR via a dsRNA bridge, or following its dsRNA-induced conformational change, which prevents or disrupts PKR dimerization. Human PKR, for example, forms relatively weak dimers (K_d ~500μM), and it may be that PKR from most other species also only weakly dimerize (56). Disrupting weak dimers in this way would be a broadly effective form of inhibition and would help to explain the near absolute requirement of E3L for VACV infection of host cells from different species (Ch. 2). In the case of S. hamster PKR, stronger PKR dimers, stabilized by hyper-autophosphorylation, additional biochemical interactions between adjacent amino acids, or by a higher affinity to activating dsRNA, would not be inhibited in this way. From the results presented in this chapter, we do not exclude any of these mechanisms from contributing to the resistance to E3L inhibition by S. hamster PKR and all are potentially acting synergistically to lead to the development of this general resistance to viral dsRNA-binding inhibitors.

Author contributions

This study was initiated and the experiments were designed by S.L.H. and S.R. Experiments were performed by S.L.H. and C.P. Technical assistance was provided by S.V. Positive selection analyses were performed by S.L.H., L.T., and S.R. The paper was written by S.L.H and S.R.

References

1. Dalet A, Gatti E, Pierre P (2015) Integration of PKR-dependent translation inhibition with innate immunity is required for a coordinated anti-viral response. *FEBS Letters* 589(14):1539–1545.

2. Pindel A, Sadler A (2011) The Role of Protein Kinase R in the Interferon Response. *J Interferon Cytokine Res* 31(1):59–70.

3. Dey M, Cao C, Dar AC, Tamura T, Ozato K, Sicheri F, Dever TE (2005) Mechanistic link between PKR dimerization, autophosphorylation, and eIF2alpha substrate recognition. *Cell* 122(6):901–913.

4. Nanduri S, Rahman F, Williams BR, Qin J (2000) A dynamically tuned double-stranded RNA binding mechanism for the activation of antiviral kinase PKR. *EMBO J* 19(20):5567–5574.

5. Zhang F, Romano PR, Nagamura-Inoue T, Tian B, Dever TE, Mathews MB, Ozato K, Hinnebusch AG (2001) Binding of double-stranded RNA to protein kinase PKR is required for dimerization and promotes critical autophosphorylation events in the activation loop. *J Biol Chem* 276(27):24946–24958.

6. Dauber B, Wolff T (2009) Activation of the Antiviral Kinase PKR and Viral Countermeasures. *Viruses* 1(3):523–544.

7. Beattie E, Tartaglia J, Paoletti E (1991) Vaccinia Virus-Encoded eIF2alpha Homolog Abrogates the Antiviral Effect of Interferon. *Virology* 183:419–422.

8. Chang H-W, Watson JC, Jacobs BL (1992) The E3L gene of vaccinia virus encodes an inhibitor of the interferon-induced, double-stranded RNA-dependent protein kinase. *Proc Natl Acad Sci USA* 89:4825–4829.

9. Beattie E, Paoletti E, Tartaglia J (1995) Distinct Patterns of IFN Sensitivity Observed in Cells Infected with Vaccinia K3L- and E3L- Mutant Viruses. *Virology* 210(2):254–263.

10. Langland JO, Jacobs BL (2002) The Role of the PKR-Inhibitory Genes, E3L and K3L, in Determining Vaccinia Virus Host Range. *Virology* 299(1):133–141.

11. Kawagishi-Kobayashi M, Silverman JB, Ung TL, Dever TE (1997) Regulation of the Protein Kinase PKR by the Vaccinia Virus Pseudosubstrate Inhibitor K3L Is Dependent on Residues Conserved between the K3L Protein and the PKR Substrate eIF2alpha. *Mol Cell Biol* 17:4146–4158.

12. Dar AC, Sicheri F (2002) X-Ray Crystal Structure and Functional Analysis of Vaccinia Virus K3L Reveals Molecular Determinants for PKR Subversion and Substrate Recognition. *Mol Cell* 10:295–305.

13. White SD, Jacobs BL (2012) The Amino Terminus of the Vaccinia Virus E3 Protein Is Necessary To Inhibit the Interferon Response. *J Virol* 86(10):5895–5904.

14. Langland JO, Kash JC, Carter V, Thomas JM, Katze MG, Jacobs BL (2006) Suppression of Proinflammatory Signal Transduction and Gene Expression by the Dual Nucleic Acid Binding Domains of the Vaccinia Virus E3L Proteins. *J Virol* 80(20):10083–10095.

15. Dueck KJ, Hu YS, Chen P, Deschambault Y, Lee J, Varga J, Cao J (2015) Mutational analysis of vaccinia virus E3 protein: the biological functions do not correlate with its biochemical capacity to bind double-stranded RNA. *J Virol* 89(10):5382–5394.

16. Dar AC, Dever TE, Sicheri F (2005) Higher-Order Substrate Recognition of eIF2α by the RNA-Dependent Protein Kinase PKR. *Cell* 122(6):887–900.

17. Rothenburg S, Seo EJ, Gibbs JS, Dever TE, Dittmar K (2009) Rapid evolution of protein kinase PKR alters sensitivity to viral inhibitors. *Nat Struct Mol Biol* 16(1):63–70.

18. Elde NC, Child SJ, Geballe AP, Malik HS (2009) Protein kinase R reveals an evolutionary model for defeating viral mimicry. *Nature* 457(7228):485–489.

19. Seet BT, Johnston JB, Brunetti CR, Barrett JW, Everett H, Cameron C, Sypula J, Nazarian SH, Lucas A, McFadden G (2003) Poxviruses and Immune Evasion. *Annu Rev Immunol* 21(1):377–423.

20. Peng C, Haller SL, Rahman MM, McFadden G, Rothenburg S (2016) Myxoma virus M156 is a specific inhibitor of rabbit PKR but contains a loss-of-function mutation in Australian virus isolates. *Proc Natl Acad Sci USA* 113(14):3855-3860. doi:10.1073/pnas.1515613113.

21. Edgar RC (2004) MUSCLE: multiple sequence alignment with high accuracy and high throughput. *Nucleic Acids Res* 32(5):1792–1797.

22. Castresana J (2002) *GBLOCKS: Selection of Conserved Blocks from Multiple Alignments for their Use in Phylogenetic Analysis. Version 0.91 b.* (European Molecular Biology Laboratory (EMBL)) Available at: http://molevol. cmima. csic. es/castresana/Gblocks. html.

23. Guindon S, Dufayard JF, Lefort V, Anisimova M, Hordijk W, Gascuel O (2010) New Algorithms and Methods to Estimate Maximum-Likelihood Phylogenies: Assessing the Performance of PhyML 3.0. *Syst Biol* 59(3):307–321.

24. Posada D, Crandall KA (1998) MODELTEST: testing the model of DNA substitution. *Bioinformatics* 14(9):817–818.

25. Yang Z (2007) PAML 4: phylogenetic analysis by maximum likelihood. *Mol Biol*

Evol 24(8):1586–1591.

26. DeLano WL (2004) *The Pymol Molecular Graphics System version 1.0* (DeLano Scientific LLC, Palo Alto, CA).

27. Shors T, Kibler KV, Perkins KB, Seidler-Wulff R, Banaszak MP, Jacobs BL (1997) Complementation of Vaccinia Virus Deleted of the E3L Gene by Mutants of E3L. *Virology* 239:269–276.

28. Rahman MM, Liu J, Chan WM, Rothenburg S, McFadden G (2013) Myxoma virus protein M029 is a dual function immunomodulator that inhibits PKR and also conscripts RHA/DHX9 to promote expanded host tropism and viral replication. *PLoS Pathog* 9(7):e1003465.

29. Myskiw C, Arsenio J, Hammett C, van Bruggen R, Deschambault Y, Beausoleil N, Babiuk S, Cao J (2011) Comparative Analysis of Poxvirus Orthologues of the Vaccinia Virus E3 Protein: Modulation of Protein Kinase R Activity, Cytokine Responses, and Virus Pathogenicity. *J Virol* 85(23):12280–12291.

30. Guerra S, Abaitua F, Martinez-Sobrido L, Esteban M, Garcia-Sastre A, Rodriguez D (2011) Host-Range Restriction of Vaccinia Virus E3L Deletion Mutant Can Be Overcome In Vitro, but Not In Vivo, by Expression of the Influenza Virus NS1 Protein. *PLoS ONE* 6(12):e28677.

31. Shors T, Jacobs BL (1997) Complementation of Deletion of the Vaccinia Virus E3L Gene by the Escherichia coli RNase III Gene. *Virology* 227:77–87.

32. Beattie E, Denzler KL, Tartaglia J, Perkus ME, Paoletti E, Jacobs B (1995) Reversal of the Interferon-Sensitive Phenotype of a Vaccinia Virus Lacking E3L by Expression of the Reovirus S4 Gene. *J Virol* 69:499–505.

33. Cassady KA, Gross M (2002) The Herpes Simplex Virus Type 1 US11 Protein Interacts with Protein Kinase R in Infected Cells and Requires a 30-Amino-Acid Sequence Adjacent to a Kinase Substrate Domain. *J Virol* 76(5):2029–2035.

34. Poppers J, Mulvey M, Khoo D, Mohr I (2000) Inhibition of PKR Activation by the Proline-Rich RNA Binding Domain of the Herpes Simplex Virus Type 1 Us11 Protein. *J Virol* 74(23):11215-11221.

35. Huismans H, Joklik WK (1976) Reovirus-coded polypeptides in infected cells: isolation of two native monomeric polypeptides with affinity for single-stranded and double-stranded RNA, respectively. *Virology* 70(2):411–424.

36. Imani F, Jacobs BL (1988) Inhibitory activity for the interferon-induced protein kinase is associated with the reovirus serotype 1 Sigma 3 protein. *Proc Natl Acad Sci USA* 85:7887–7891.

37. Beattie E, Kauffman EB, Martinez H, Perkus ME, Jacobs BL, Paoletti E, Tartaglia J

(1996) Host-range restriction of vaccinia virus E3L-specific deletion mutants. *Virus Genes* 12(1):89–94.

38. Lemaire PA, Tessmer I, Craig R, Erie DA, Cole JL (2006) Unactivated PKR exists in an open conformation capable of binding nucleotides. *Biochemistry* 45(30):9074–9084.

39. McKenna SA, Lindhout DA, Kim I, Liu CW, Gelev VM, Wagner G, Puglisi JD (2007) Molecular framework for the activation of RNA-dependent protein kinase. *J Biol Chem* 282(15):11474–11486.

40. Sunita S, Schwartz SL, Conn GL (2015) The Regulatory and Kinase Domains but Not the Interdomain Linker Determine Human Double-stranded RNA-activated Kinase (PKR) Sensitivity to Inhibition by Viral Non-coding RNAs. *J Biol Chem* 290(47):28156–28165.

41. Elde NC, Malik HS (2009) The evolutionary conundrum of pathogen mimicry. *Nat Rev Micro* 7(11):787–797.

42. Romano PR, Zhang F, Tan SL, Garcia-Barrio MT, Katze MG, Dever TE, Hinnebusch AG (1998) Inhibition of double-stranded RNA-dependent protein kinase PKR by vaccinia virus E3: role of complex formation and the E3 N-terminal domain. *Mol Cell Biol* 18(12):7304–7316.

43. Sharp TV, Moonan F, Romashko A, Joshi B, Barber GN, Jagus R (1998) The vaccinia virus E3L gene product interacts with both the regulatory and the substrate binding regions of PKR: implications for PKR autoregulation. *Virology* 250(2):302–315.

44. McCormack SJ, Thomis DC, Samuel CE (1992) Mechanism of interferon action: identification of a RNA binding domain within the N-terminal region of the human RNA-dependent P1/eIF-2 alpha protein kinase. *Virology* 188(1):47–56.

45. Feng GS, Chong K, Kumar A, Williams BR (1992) Identification of double-stranded RNA-binding domains in the interferon-induced double-stranded RNA-activated p68 kinase. *Proc Natl Acad Sci USA* 89(12):5447–5451.

46. Tian B, Bevilacqua PC, Diegelman-Parente A, Mathews MB (2004) The double-stranded-RNA-binding motif: interference and much more. *Nat Rev Mol Cell Biol* 5(12):1013–1023.

47. Chang H-W, Watson JC, Jacobs BL (1992) The E3L gene of vaccinia virus encodes an inhibitor of the interferon-induced, double-stranded RNA-dependent protein kinase. *Proc Natl Acad Sci USA* 89:4825–4829.

48. Wu S, Kaufman RJ (1996) A Model for the Double-stranded RNA (dsRNA)-dependent Dimerization and Activation of the dsRNA-activated Protein Kinase PKR. *J Biol Chem* 272(January 10):1291–1296.

49. Wu S, Kaufman RJ (1996) Double-stranded (ds) RNA binding and not dimerization correlates with the activation of the dsRNA-dependent protein kinase (PKR). *J Biol Chem* 271(3):1756–1763.

50. Dey M, Cao C, Sicheri F, Dever TE (2007) Conserved intermolecular salt bridge required for activation of protein kinases PKR, GCN2, and PERK. *J Biol Chem* 282(9):6653–6660.

51. Gelev V, Aktas H, Marintchev A, Ito T, Frueh D, Hemond M, Rovnyak D, Debus M, Hyberts S, Usheva A, Halperin J, Wagner G (2006) Mapping of the auto-inhibitory interactions of protein kinase R by nuclear magnetic resonance. *J Mol Biol* 364(3):352–363.

52. Dey M, Mann BR, Anshu A, Mannan MA-U (2014) Activation of protein kinase PKR requires dimerization-induced cis-phosphorylation within the activation loop. *J Biol Chem* 289(9):5747–5757.

53. Husain B, Mayo C, Cole JL (2016) Role of the Interdomain Linker in RNA-Activated Protein Kinase Activation. *Biochemistry* 55(2):253–261.

54. Chang HW, HH UL, Jacobs BL (1995) Rescue of vaccinia virus lacking the E3L gene by mutants of E3L. *J Virol* 69(10):6605-6608.

55. Whitaker-Dowling P, Youngner JS (1984) Characterization of a specific kinase inhibitory factor produced by vaccinia virus which inhibits the interferon-induced protein kinase. *Virology* 137(1):171–181.

56. Lemaire PA, Lary J, Cole JL (2005) Mechanism of PKR activation: dimerization and kinase activation in the absence of double-stranded RNA. *J Mol Biol* 345(1):81–90.

Chapter 4 - The genome of the leporipoxvirus squirrel fibroma virus reveals recombination between distantly related poxviruses

Haller, S.L.[1]; Cone, K.R.[2]; Kronenberg, Z.[2]; Schieferecke, A.J[1]; Remillard, C.[1]; Grunwald, S[2]; Emerson, G.[3]; Gallardo-Romero, N.[3]; Damon, I.K.[3]; Tazi, L.[1]; Elde, N.C.[2]; and Rothenburg, S[1].

1. *Division of Biology, Kansas State University, Manhattan, Kansas 66506, USA*
2. *Department of Human Genetics, University of Utah School of Medicine, Salt Lake City, UT 84112, USA*
3. *Centers for Disease Control, DHCPP/Poxvirus and Rabies Branch, Atlanta, GA 30333, USA*

Keywords: poxvirus genome, leporipoxviruses, virus recombination, host range, PKR

Abstract

Poxviruses are large dsDNA viruses that infect a wide range of vertebrate and invertebrate species, and are currently subdivided into two subfamilies and ten genera. Members of the genus *Leporipoxviridae* infect rabbit and squirrel species and include the well-characterized myxoma virus and rabbit fibroma virus. In 1952, a novel leporipoxvirus was isolated from infected Eastern gray squirrels in Maryland. The newly named squirrel fibroma virus (SQFV) causes a disease in different North American squirrel species that is characterized by cutaneous fibromas known as squirrel fibromatosis. SQFV has been reported in many US states along the east coast since its discovery and typically causes a self-limiting disease but has been shown to cause death in young squirrels. To better understand the relationship of the SQFV to the other poxvirus species, we sequenced the complete genome of the SQFV Kilham 1952 strain and initiated a comparative study with other fully sequenced poxviruses. We analyzed the phylogenetic relationship of SQFV to other poxviruses as well as characterized its replication in cell culture using a fluorescent recombinant virus. From the genomic analysis, we uncovered several unique features that may account for the virus' host range restriction to squirrels and moderate virulence, including species-specific activity of potential host range factors and a number of gene truncations and deletions. Of most interest, we discovered that within the SQFV inverted terminal repeat sequence, which is one of the longest (19.5 kb) of any completely sequenced chordopoxvirus, there is evidence for a recombination event that occurred between an ancestral leporipoxvirus and an old-world orthopoxvirus. Additionally, we confirmed the presence of the same recombination in a SQFV isolate from an infected squirrel in Ohio isolated more than 56 years after the discovery of the original virus. This finding highlights the potential for even distantly related poxviruses to recombine in the field, which might result in altered host range and virulence.

Significance

The reporting of the complete genomic sequence for any organism is always a critical step in understanding its biology and often opens the door to many more studies. This work presents the complete genome of the previously poorly characterized squirrel fibroma virus (SQFV) and provides a comparative analysis of this virus with other related leporipoxviruses. The importance of this group of poxviruses to the medical field and to studies of viral host range and host-virus co-evolution has been well demonstrated, and therefore it is anticipated that the potential impact of future analyses with SQFV aided by the information provided here will be high in these areas. The identification of a recombination event between a SQFV ancestor and an orthopoxvirus in the field provides the first example of recombination occurring between such distantly related poxviruses, which has implications for our evolutionary understanding of these poxviruses and highlights the potential for the emergence of novel recombinant poxviruses in nature that may have altered host range and virulence.

Introduction

Leporipoxviruses are a genus within the sub-family *Chordopoxvirinae,* which are restricted to lagomorph (rabbits and hares) and squirrel host species. The prototypic and best-characterized member of this poxvirus genus is myxoma virus (MYXV), which causes a lethal disease in European (E.) rabbits called myxomatosis. Members of the *Leporipoxvirus* genus were some of the first poxvirus genomes to be completely sequenced (1, 2), which allowed a detailed characterization of the molecular biology of these viruses and the mechanisms behind their narrow host range.

There are currently four leporipoxvirus species recognized; MYXV (including genetically distinct South/Central American strain and Californian strains), rabbit fibroma virus (RFV, Shope fibroma virus), hare fibroma virus (FIBV), and squirrel fibroma virus (SQFV). Only SQFV naturally infects squirrels whereas all the others infect only leporid species for which the genus is named. SQFV has gone largely unnoticed in the scientific community, with very few studies having been conducted on SQFV since its discovery (3-6). SQFV was first identified in 1936 and isolated by Kilham et al. in 1952 from six infected gray squirrels in Maryland, USA (4). It was originally characterized as a member of the *Leporipoxvirus* genus due to similarities in disease symptoms and the pathology caused by it, the morphology and ultrastructure of the virion by electron microscopy, and its immunological cross-reactivity with other known leporipoxviruses.

Squirrel fibromatosis, caused by SQFV, is a disease of squirrel species that is characterized by the presence of multiple dermal nodules and fibromas in infected individuals. Histologically the sites of infection are typified by epidermal hyperplasia, ballooning degeneration and intracytoplasmic inclusion bodies (7). The incubation time of squirrel fibromatosis is reported to be between 7 and 14 days before tumors and fibromas become visible (8). Infected squirrels generally recover in less than two months, although the disease can be fatal in very young squirrels (5). This disease has been reported primarily in states along the eastern coast and in the southeast of the US (9). In 1998 an epizootic of squirrel fibromatosis occurred in the southern US state of Florida affecting more than 200 gray squirrels, but the reason for the high mortality caused by this outbreak is still unknown (10).

SQFV was originally believed to be restricted to gray squirrels (*Sciurus carolinensis*), as this viral disease most commonly affects this species and they were the species from which the

original virus was isolated. However, several reports from people working for the National Park Services as well as wildlife veterinarians and managers have diagnosed other squirrel species with this disease over the years since its discovery. These include both the western gray squirrel (*S. griseus*) and fox squirrel (*S. nigers*) of the same genus, as well as the American red squirrel (*Tamisciurus hudsonicus*) representing a second squirrel genus
(7, 11-14).

SQFV is readily transmittted passively between juveniles via mosquitos and it is thought that other biting insects such as the squirrel flea (*Orchopeus howardi*) may also mechanically transmit the SQFV (5). However, the sporadic nature of the disease caused by SQFV and the low frequency of outbreaks make it difficult to accurately study the epidemiology of the virus. MYXV, meanwhile, has a seasonal cycle that correlates with the presence of appropriate arthropod vectors and this relationship has been monitored closely since its release into Australia and Europe over the past ~65 years. SQFV is possibly also transmitted directly between infected squirrels since squirrel fibromatosis outbreaks usually do not spread far from the disease epicenter. It is not clear whether squirrels represent a dead-end host for the SQFV or whether the virus has recently jumped into these host species, since it is difficult to produce virus titers in adult squirrels that are sufficiently high for vector transmission (5, 15).

The expansion of improved sequencing technologies is rapidly increasing the number of poxvirus genomes that are being completely sequenced and new poxvirus species have been discovered and characterized in recent years (16-23). We present here a comprehensive comparative analysis of the complete SQFV genome with the other fully sequenced leporipoxviruses, focusing on the genetic differences between them that might explain the different host tropism of the SQFV. From our analysis we identified evidence of ongoing gene loss and fragmentation in the SQFV in putative immunomodulatory genes, evidence of horizontal gene transfer, as well as the longest inverted terminal repeat (ITR) sequence (19.5 kb) of any completely sequenced chordopoxvirus. Within this unique ITR we found evidence for a recombination event that likely occurred between the ancestral leporipoxvirus and an old-world orthopoxvirus. While recombination has been previously observed between closely related poxviruses and between leporipoxvirus members (24), the evidence for recombination in the SQFV genome is to our knowledge the first reported example of recombination occurring between such distantly related poxviruses.

Additionally, we have characterized SQFV replication in multiple mammalian cell lines as well as analyzed the potential host range function of selected SQFV proteins to begin building a framework for future molecular analyses of SQFV, which will be useful for studies on the evolution of viral host range.

Methods

Cell lines, plasmids, and viruses

RK13 (ATCC CCL-37), BHK-21 (ATCC CCL-10), BSC-1 (ATCC CCL-26), 293T (ATCC CRL-3216), HeLa (ATCC CCL-2), HeLa-PKRkd (25), Vero (ATCC CCL-81), CHO (ATCC CCL-61), and NRK (ATCC CRL-6509) were maintained in Dulbecco's Modified Essential Medium (DMEM, Life Technologies) supplemented with 5% fetal bovine serum (FBS, Fischer) and 25μg/ml gentamycin (Quality Biologicals). RK13+E3L+K3L cells (26) were grown in media additionally supplemented with 500μg/ml G418 and 300μg/ml zeocin (Life Technologies) and stably express VACV E3L and K3L. CHO cells were grown in Roswell Park Medical Institute (RPMI) media supplemented with 10% FBS and 25μg/ml gentamycin. All cells were incubated at 37˚C, 5% CO_2. The HeLa-PKRkd cells, kindly provided by Charles Samuel, stably express shRNA to knock down endogenous human PKR expression.

PKR from the indicated species and viral genes were cloned into the pSG5 mammalian expression vector (Stratagene) for transient expression driven by the SV40 promoter. The cloning of knock-down resistant human PKR, mouse PKR, Syrian hamster PKR, European rabbit PKR, and guinea pig PKR into the pSG5 plasmid was described previously (27-29). Brush rabbit PKR was cloned from total RNA collected from the paw of a brush rabbit provided by the Riparin Brush Rabbit Recovery project (Peng and Rothenburg, unpublished). Cottontail rabbit PKR was cloned from total RNA of SF-1 Eastern cotton tail cells (ATCC CCL-68, Peng and Rothenburg, unpublished). M156R and M029L were cloned from MXYV Lausanne (Lu) strain, and E3L was cloned from VACV Western Reserve (WR) strain. The E3L and K3L orthologs from the SQFV (S033 and S152) were PCR amplified from DNA prepared from a single-passage SQFV-Kilham in RK13 cells, and were cloned into the pSG5 expression vector using SacI and XhoI restriction sites. The primers used to clone S152 were KS07-SacI-1F GAT CGA GCT CGC CAC CAT GGA TCC TTT ACC AGG GAG and KS08-XhoI-1R GAT CCT CGA GTC ATT AAC CCG TAA AAA AAC GAC GTA GAT C. The primers used to clone S033 were

KS09-SacI-1F CTA GGA GCT CGC CAC CAT GAT GGA TTC CAT TAA TAC CTT ATT GAG and KS10-XhoI-1R CGA TCT CGA GCT ATC AAA ATT TTA TAA CAA CAT GCT TCA ATA TAA TGT CC. Alignments of the K3 and E3 orthologs and percent identity scores were generated by the ClustalW method in the sequence analysis software MegAlign (DNAStar, Inc.; Madison, WI USA).

Viruses used in this work include SQFV-Kilham (ATCC VR-236), SQFV-mCherry, which expresses mCherry from a synthetic early/late promoter inserted between ORFs S135 and S136 (described here), rabbit fibroma virus (RFV; Shope fibroma virus, (30)), MYXV-GFP, which expresses GFP from a synthetic early/late promoter inserted between ORFs M135R and M136R (31), and vaccinia virus (VACV-WR)-GFP, in which GFP is inserted downstream of a 3xFLAG tagged A7L gene and is controlled by the viral late p11 promoter (32).

Virus Infections

For all virus infections, sonicated virus samples were first diluted in DMEM (or RPMI) supplemented with 2.5% FBS to perform infections at the indicated multiplicities of infection (MOI). In 6-well plates, $2.5x10^5$ or $5x10^5$ cells were plated in each well 24-48 hours prior to infection to allow the monolayer to become confluent. Before adding the virus inoculum to each well, the growth media was first removed and the virus inoculum was incubated with the cells for 1-2 hours at 37˚C. After this incubation, the inoculum was removed and the cell monolayers were washed once with PBS before adding fresh growth media. Virus infections were then collected immediately into the media (0hpi) or incubated for the indicated lengths of time before being imaged or collected for titration. For virus purification, confluent 100mm plates of RK13 cells were infected with SQFV-Kilham or SQFV-mCherry at an approximate MOI=0.001 due to the low titers of the original virus used, and the infections were allowed to incubate for 6-7 days to allow the infection to spread throughout the plates before harvesting the infected cells for virus purification.

The purchased stock of SQFV-Kilham strain (ATCC VR-236) was subsequently expanded in RK13 cells. This single-passage virus was then further expanded in RK13 cells and purified by sucrose gradient ultracentrifugation. DNA was isolated from 20% of the total volume of the purified virus by two rounds of phenol:chloroform extraction and submitted for full genome sequencing using the Illumina MiSeq platform (San Diego, CA, USA).

For infections with the wild isolate of SQFV obtained from the CDC (SQFV-CDC, homogenate 2008-040), confluent monolayers of RK13 or BSC-1 cells in T-75s or 100mm plates were infected directly with a dilution of the squirrel lesion homogenate after sonicating it in a cup sonicator (2x1min). After a 1-2 hour incubation, the SQFV-CDC inoculum was left on the cells to allow any un-adsorbed virus to remain in the flask and fresh growth media was added. Virus samples were collected from infections directly into the media 2-6 days post infection or DNA was isolated from infected cells 5-7 days post infection. Collected virus was used either directly (undiluted) or in serial dilution to infect new RK13, BHK-21, or BSC-1 cells to passage the virus for propagation. While some cytopathic effect could be observed at 48hpi on RK13 cells with the original inoculum and from undiluted samples of the first passage virus (P1, data not shown), further passages with virus samples collected from the second passage (P2) did not induce a cytopathic effect in infected wells, nor could enough SQFV DNA be isolated for PCR detection. Attempts to propagate and purify the SQFV-CDC were therefore unsuccessful. DNA isolated from P1 infections were used for PCR amplification and sequencing of the amplicons as well as for full genome sequencing on the Illumina-MiSeq platform (San Diego, CA, USA).

Virus titers for all viruses used were determined by standard plaque assay (or focus forming assay) on RK13+E3L+K3L cells. All viruses used in this study form distinct foci or plaques on these cells and are readily quantified with a light or fluorescent microscope. For the parental SQFV-Kilham not expressing mCherry, foci were counted 4-6 days post infection. VACV-GFP and MXYV-GFP titers were counted 2-3 days post infection, while RFV and SQFV-mCherry titers were counted 3-4 or 4-6 days post infection, respectively to allow distinct focus formation.

DNA sequencing and genome assembly and annotation

Next generation sequencing was performed using the Illumina MiSeq platform to obtain the complete genome sequence of the SQFV-Kilham. Raw sequence data was processed and aligned to form three contiguous sequence files. Two of the contigs (one large and one small) corresponded to the inverted terminal repeats (ITR) on either end of the genome (small) and the other to the larger part of the genome (large). The third contig contained sequences matching host mitochondrial DNA and was therefore excluded from our analysis. The large and small contigs were then joined to create one sequence file for the entire genome. Primers flanking the

junction of the large and small contigs were designed to confirm the sequence by Sanger sequencing the PCR product (Table 4.1).

Segments of the genome were analyzed using BLAST and BLASTx (Basic Local Alignment Sequencing Tool, NCBI, (33)) to identify ORFs corresponding to known poxvirus sequences. The position of the beginning and end of each ORF was assigned based on the longest continuous in-frame ORF corresponding to each identified gene using the ORF finder tool in Seqbuilder (DNAStar, Inc.). Long intergenic spaces where no poxvirus ORF was identified were compared to all sequences in the database using BLAST and BLASTx to identify potential novel ORFs or horizontally transferred genes. Putative functions were assigned according to known functions of orthologous proteins.

For determining the relative protein sequence identities in the ITR, the protein sequences for each ORF were obtained from the indicated representative poxvirus species (Table 4.4). Each protein sequence was aligned individually with its orthologs using ClustalW in the program MegAlign (DNAStar, Inc.), and sequence identities were calculated.

The first nucleotide position of the genome was designated as the first nucleotide of the small contig corresponding to the left-hand ITR. Open reading frames were numbered starting with S001 in the left-hand ITR and ending with S165 in the right-hand ITR and given the letter designation "S" for Squirrel fibroma virus. The previous annotation of the rabbit fibroma virus (RFV or Shope's fibroma virus) also used "S" designations for ORFs, so we have used "RFV" instead to refer to RFV ORFs to differentiate the two annotations (1). Duplicated ORFs in either ITR were annotated separately to identify the ITR they belong to (i.e. S001 and S165 are identical, inverted ORFs).

Sequences of long intergenic spaces, sequence repeats, and gene truncations were PCR-amplified and confirmed by Sanger sequencing amplified PCR products (Table 4.1). Sequences that were not well resolved in the original contigs were also Sanger sequenced to obtain the complete genome.

Primer pairs used in this study	Size (bp)	Genomic Region
SQFV-149R-1F CCTGCTTTAAGAAAAAACAACGTAGG SQFV-151R-1R GGACGATTGAAGAAATTTTTTGAAAAACTCC	562	From end of S148R to beginning of S149R covering the intergenic space
SQFV-150R-1F CCAACAAAGATTTGTTTTTTAATGAAAATAAAG SQFV-151R-2R CCTGTTTTATATCATCCGGGTAC	568	From small gene fragment homologous to M150R to middle of S149R covering frameshift site in S149R
SQFV-151R-1F CTACCATATGAGTATGGATACTCC SQFV-151R-3R GCTTATAATGTTACTTATATGAAAAACATCTC	502	From middle of S149R to end of gene sequence covering frameshift site in S149R
SQFV-151R-2F CGTTACTATTCATGGGTAGGG SQFV-154L-1R CTAGATACTATATAAATCAACAAAAGTG	857	From end of S149R sequence to end of S151L covering large intergenic space and putative HGT ORF
SQFV-124R-1F GCTATTCATAGTGTACGGAGTC SQFV-126R-1R CATAATTTTATAACTTGTTTTTTTATATCCAAAGG ATTAAAAAAAG	694	From end of S127R to beginning of S129R covering S128R
SQFV-130R-1F CAAAGGGGGAAAGCGAC SQFV-132L-1R GAGCTAATTTACTTATATATTTTAGCAAAGTTATT TAG	617	From end of S133R to end of S134L covering the gene fragment homologous to M131R and large intergenic space
SQFV-137R-1F CATAGTTGTTACGTTTACGGAATTG SQFV-139-1R CGATCGATATGTCAAACTTTACATAGTTAC	969	From end of S137R to beginning of S139R covering truncated S138L and long ATA repeat
SQFV-138L-1F (w/139-1R) GTATAAGTCGTTAGACTTAAACGGAAC	550	From S138L fragment to beginning of S139R
SQFV-156R-1F GATTACACGTGGATCTACGTCG SQFV-006-9-1R CAAGAAACTCAAAAGGGTACGTG	603	From end of S152R to beginning of S153R covering large intergenic space
DpV84007-1F CTTTATATGTTTTAACCTTTATAATATTGTCTATTA AG SQFV-003.2-1F GCGGTATGTTCGATTTCATGAAG	1118	From beginning of S010L/S156R to middle of S011L/S155R covering large intergenic space

SQFV 006L-1F GTCATTTGTTAATTTCTTAACCGTGTTTAC SQFV-010L-1R GCGGAACATAATCATGTCCTTAC	469	From end of S013L in 5' ITR to end of S014L outside the 5' ITR
SQFV-155R-1R CTTAACCGTGTTTACAAACGTGG SQFV-155R-1F CCATCAATACATCCTCTGTTGTAC	505	From end of S153R in 3' ITR to middle of S153R outside the 3' ITR
SQFV-B22R-1F CCTTTTCTGGTGAGAGGTG SQFV-B22R-1R GAGGCTATCAAGTCCACAATAAATC	459	In middle of S001L/S165R covering string of unidentifiable nucleotides (N's)
SQFV-B8-203/MT4-1F CGATAGGAAGAATATAACCAGGAAC SQFV-DPV-ANK-1R GGATCATCAAAGCATCCGATTATATG	493	From start of S006L/S160R to middle of DPV ANK covering the putative recombination site
SQFV-large contig-1F GTTATTCGATCGCCGTGGATATATC SQFV-small contig-1R GATGCAACTAGATCCAGATCAC	406	From beginning of S008L/S158R to just after S009L/S157R covering breakpoint for large and small sequence contigs
SQFV-072L-1F CTTGGATTCCATTTAATGTAAGAAACAAC SQFV-074R-1R GTATAATTTTCCATCCTTGTATGTAAAAGCTCTC	755	From beginning of S075L to beginning of S077R covering S076R and the 60aa insertion
SQFV-DPV-007-1R CTATGTGGAGACCTATGTCGG SQFV-DPV-010-1F GTACATTAACACATGCATCTTCTTTATC	280	From beginning of S009L/S157R to end of S010L/S156R
BA135 SQFVintgn-1F CTACACAAGTATGTGATGTTATCTAAGTTG BA140 SQFV136-2R CACATCACATAACAGTATGTCTAAATTACC	455	SQFV 3' recombination arm corresponding to the intergenic space before S136 to the beginning of S136
BA136 686-ELprm+133-OH-1F CGAGTTTTATTTTTAAGAGATGATTTACTAAAAAT TGAAATTTTATTTTTTTTTTTTGG BA139 686+SQFV-OH-1R CAACTTAGATAACATCACATACTTGTGTAGCTATT ACTTGTACAGCTCGTCCATGC	810	Covering mCherry gene with 27-30bp overhangs corresponding to the intergenic space between S135 and S136 with a poxvirus early/late promoter
BA138 SQFV133intgn-1R TAAATCATCTCTTAAAAATAAAACTCGTACACTTT G BA149 SQFV133-2F GGAAAACGGTTACAAAGTGTTCAGG	412	SQFV 5' recombination arm corresponding to the end of S135 into the intergenic space before S136

Table 4.1 Primer pairs used in this study.

Primer pair sequences used to amplify and sequence regions of the SQFV-Kilham and SQFV-CDC genome are listed along with the expected size of the PCR product and a general description of the genomic region amplified.

Promoter motif analysis

Upstream sequences -100bp to +10bp for putatively early and intermediate genes and -50 to +10bp for late genes in the SQFV genome were grouped according to the promoter classification of the corresponding orthologs in RFV and MYXV (Table 4.2). Upstream sequences corresponding to 42 putative early genes were used as the input in the online MEME Suite version 4.11.1 (Multiple EM for Motif Elicitation, (34)) to identify the early promoter motif, and similarly for intermediate (8 genes) and late (52 genes) gene sequences with specified motif lengths of between 6 and 30bp (for early and late motifs) or 6 and 50bp (for intermediate motifs). Motifs generated from each analysis were then compared with the same promoter motif identified in RFV for verification (1). Identified early and late motifs were then used as input in the program FIMO (Find Individual Motif Occurrences, MEME Suite) to identify similar promoter motifs in the upstream sequences from the remaining ORFs ($p<0.0001$). ORFs where both an early motif and late motif were identified were classified as early/late genes, while those where no motif was identified were left unassigned unless the orthologs from both MYXV and RFV had the same promoter class designation and the promoter motif in SQFV was assumed (indicated with a question mark following the promoter designation).

Early		Late		Intermediate
M006L	M121R	M004.1L	M088L	M040L
M011L	M126R	M010L	M091L	M042L
M012L	M129R	M019L	M092L	M045L
M013L	M132L	M020L	M093L	M053R
M014L	M138L	M022L	M094R	M089L
M015L	M141R	M023R	M096L	M090L
M017L	M142R	M026R	M099L	M095L
M018L	M146R	M028L	M100R	M108R
M021L	M147R	M032R	M101L	
M024L	M148R	M038L	M102L	
M025L	M149R	M039L	M103L	
M029L	M151R	M042L	M104L	
M030L	M154L	M043L	M105L	
M031R		M045L	M106L	
M033R		M048L	M107L	
M034L		M052L	M109L	
M036L		M054R	M115L	
M040L		M055R	M116L	
M047R		M057L	M118L	
M056R		M058R	M119L	
M062R		M059R	M122R	
M063R		M060R	M133R	
M064R		M069L	M137R	
M079R		M070R	M143R	
M084R		M071L		
M097R		M072L		
M111R		M074R		
M113R		M081R		
M117L		M086L		

Table 4.2 Genes used in promoter analysis

Upstream sequences for the SQFV orthologs to each MYXV ORF listed in the table were used to determine the promoter motifs in SQFV. Gene names are given according to their MYXV designation and are grouped according to their promoter classification in MYXV or RFV and as they were grouped to generate the consensus early and late promoter motifs shown in Fig. 4.3.

Generation of recombinant squirrel fibroma virus

Primers were designed to insert the mCherry gene into a location of the genome with a large intergenic space to avoid interrupting termination or promoter sequences (Table 4.1). The region between ORFs S135 and S136 was chosen based on the initial sequence information available. A fusion PCR of the genomic regions flanking the insertion site (~400bp on either arm) and the mCherry gene was generated using ~30bp overhangs on the mCherry PCR product corresponding to the SQFV genomic sequence at the insertion site. A VACV synthetic early/late

promoter was designed into the primers to drive expression of the mCherry gene in the fusion PCR product. The fusion PCR was then cloned into the pCR2.1 TOPO-TA vector (Invitrogen) for amplification. The insert used for virus recombination was excised from the plasmid using EcoRI and gel purified according to the manufacturer's instructions (Qiagen). The purified recombination sequence was then transfected using Lipofectamine 2000 (Invitrogen) into SQFV-Kilham infected cells immediately following the addition of fresh growth media. Virus was collected from the recombination after 24 hours and recombinant viruses were selected by mCherry expression. Virus clones expressing mCherry were submitted to multiple rounds of plaque purification before performing a single amplification step on RK13 cells in a T-75 followed by a second amplification in 100mm plates of RK13 cells for virus purification. DNA was isolated from the purified recombinant virus for PCR analysis and sequence confirmation of the correct insertion of the mCherry gene in the genome.

Phylogenetic analyses

To generate the phylogenetic tree of fully sequenced poxviruses, protein sequences of 23 single-copy genes present in all of the analyzed species were collected from the NCBI GenBank for 38 poxvirus species (Tables 4.3 and 4.4) and aligned individually using MAFFT (Multiple Alignment using Fast Fourier Transform, version 7, (35)) or Kalign (36) multiple sequence alignment programs. The aligned protein sequences were then concatenated manually and the concatenated alignment was trimmed using Gblocks (version 0.91b, (37)) using a low stringency model to exclude large sequence gaps. The trimmed alignment was submitted to ProtTest (version 3; (38)) to select the best-fit model of protein evolution (Model used: LG+I+G+F) and analyzed in PhyML (version 3.0; (39)) to generate a maximum-likelihood tree with bootstrapping (100 replicates), which was viewed in FigTree (40). The entomopoxviruses were used as the outgroup for these analyses and branch lengths represent sequence divergence in amino acid substitutions per site. For single gene analyses, protein sequences were collected from poxvirus species encoding orthologous proteins, and the sequences were aligned using MUSCLE (Multiple Sequence Comparison by Log-Expectation, (41)). The alignment was then submitted to PhyML to generate a midpoint-rooted maximum-likelihood tree.

VACV-Cop Genes	Putative function
A2L	Transcription factor VLTF-3
A3L	Major core protein P4b precursor
A7L	Early transcription factor large subunit
A10L	Major core protein P4a precursor
A16L	Fusion complex myristylprotein
A18R	ATP-dependent DNA helicase
A22R	Holliday junction resolvase
A24R	RNA polymerase subunit
A32L	ATPase
D5R	NTPase, AAA-ATPase
D6R	Early transcription factor
D12L	mRNA capping enzyme small subunit
E1L	Poly (A) plymerase catalytic subunit
E9L	DNA polymerase
E10R	Thiol-oxidoreductase
F10L	Serine/threonine/tyrosine kinase
G9R	Fusion complex myristylprotein
H2R	IMV fusion complex protein
H6R	DNA topoisomerase I
I7L	Core cysteine protease
I8R	DNA/RNA helicase
J5L	IMV fusion complex protein
J6R	RNA polymerase subunit

Table 4.3 VACV-Cop genes used in the phylogenetic analysis

A list of the gene orthologs with their VACV-Cop designations and their putative functions that were used in the concatenated alignment for the phylogenetic analysis.

Genomes used in this analysis	Abbr.	RefSeq ID	Accession number
Amsacta moorei entomopoxvirus 'L'	AMEV	NC_002520	AF250284.1
Bovine papular stomatitis virus strain BV-AR02	BPSV	NC_005337	AY386265.1
Camelpox virus M-96, Kazakhstan	CMLV	NC_003391	AF438165.1
Canarypox virus strain ATCC VR-111	CNPV	NC_005309	AY318871.1
Cotia virus SPAn232	COTV	NC_016924	HQ647181.2
Cowpox virus strain Brighton Red	CPXV-BR	NC_003663	AF482758.2
Cowpox virus strain GRI-90	CPXV-GRI	---	X94355.2
Nile crocodilepox virus	CRV	NC_008030	DQ356948.1
Deerpox virus W-848-83	DPV-848	NC_006966	AY689436.1
Deerpox virus W-1170-84	DPV-1170	NC_006967	AY689437.1
Ectromelia virus strain Moscow	ECTV	NC_004105	AF012825.2
Fowlpox virus	FWPV	NC_002188	AF198100.1
Goatpox virus Pellor	GTPV	NC_004003	AY077835.1
Horsepox virus isolate MNR-76	HSPV	---	DQ792504.1
Lumpy skin disease virus NI-2490	LSDV	NC_003027	AF325528.1
Molluscum contagiosum virus subtype 1	MOCV	NC_001731	U60315.1
Monkeypox virus isolate Sierra Leone	MPXV-SIE	---	AY741551
Monkeypox virus strain Zaire-96-I-16	MPXV-Z96	NC_003310	AF380138.1
Melanoplus sanguinipes entomopox virus	MSEV	NC_001993	AF063866.1
Myxoma virus strain California/San Francisco 1950	MYXV-MSW	---	KF148065.1
Myxoma virus strain Lausanne	MYXV-Lu	NC_001132	AF170726.2
Orf virus strain OV-SA00	ORFV	NC_005336	AY386264.1
Pseudocowpox virus strain VR634	PCPV	NC_013804	GQ329670.1
Raccoonpox virus	RCPV	NC_027213	KP143769.1
Rabbit fibroma virus	RFV	NC_001266	AF170722.1
Rabbitpox virus	RPXV	---	AY484669.1
Salmon gill poxvirus	SGPV	NC_027707	KT159937.1
Sheeppox virus 10700-99 strain TU-V02127	SPPV	NC_004002	AY077832.1
Squirrelpox virus strain Red squirrel UK	SQPV	NC_022563	HE601899.1
Squirrel fibroma virus strain Kilham 1952	SQFV	---	this work
Swinepox virus isolate 17077-99	SWPV	NC_003389	AF410153.1
Taterapox virus strain Dahomey 1968	TATV	NC_008291	DQ437594.1
Tanapox virus isolate TPV-RoC	TPV-RoC	---	EF420157.1
Vaccinia virus Copenhagen	VACV-Cop	---	M35027.1
Variola virus strain Bangladesh 1975 v75-550 Banu	VARV-Banu	---	DQ437581.1
Yoka virus strain DakArB 4268	YKV	NC_015960	HQ849551.1
Yaba-like disease virus	YLDV	NC_002642	AJ293568.1
Yaba monkey tumor virus	YMTV	NC_005179	AY386371.1

Table 4.4 Poxvirus genomes used in the phylogenetic analysis

All of the poxvirus genomes used in the phylogenetic analysis in this study are listed with their abbreviated names and accession and/or RefSeq numbers.

PKR inhibition luciferase assay

The luciferase assay for inhibition of PKR activity was described previously (28, 29). Briefly, $5x10^4$ HeLa-PKRkd cells were seeded 24 hours before transfection in 24-well plates. For each transfection, 0.05µg of firefly luciferase encoding plasmid (pGL3promoter, Promega), 0.2µg PKR encoding plasmids (pSG5), and 0.4µg MYXV M156, SQFV S151, MYXV M029, SQFV S033, or VACV E3L were transfected using GenJet-Hela (Signagen) in triplicate. Cell lysates were harvested 48 hours after transfection using mammalian lysis buffer (Goldbio), and the luciferase activity was determined by measuring light in a luminometer (Berthold) after adding luciferin substrate (Promega). Luciferase activity from vector control transfections were compared to transfections with only PKR encoding plasmids to assess the PKR activity for each species, which was then used to normalize co-transfections of the corresponding PKR with each viral inhibitor.

Results

Genome of the squirrel fibroma virus

General features of the genome

The SQFV genome (SQFV-Kilham strain) is 168,586 nucleotides in length and has an A/T content of 65.5%. The length of the genome is similar to the two other fully sequenced *Leporipoxvirus* members, MXYV and RFV, but is longer than either by nearly 10kb. Based on homologies to known poxvirus genes and using a 40 amino acid cut-off for identifying novel open reading frames (ORFs), we determined that the SQFV genome encodes 153 predicted ORFs with 12 complete ORFs duplicated in the inverted terminal repeats (ITRs) (Fig 4.1, Table 4.5). The ITRs of the SQFV are 19.5kb in length, and therefore the SQFV has the largest ITRs of all sequenced chordopoxviruses, with the exception of a few laboratory-passaged strains of cowpox virus (CPXV) strains (42, 43).

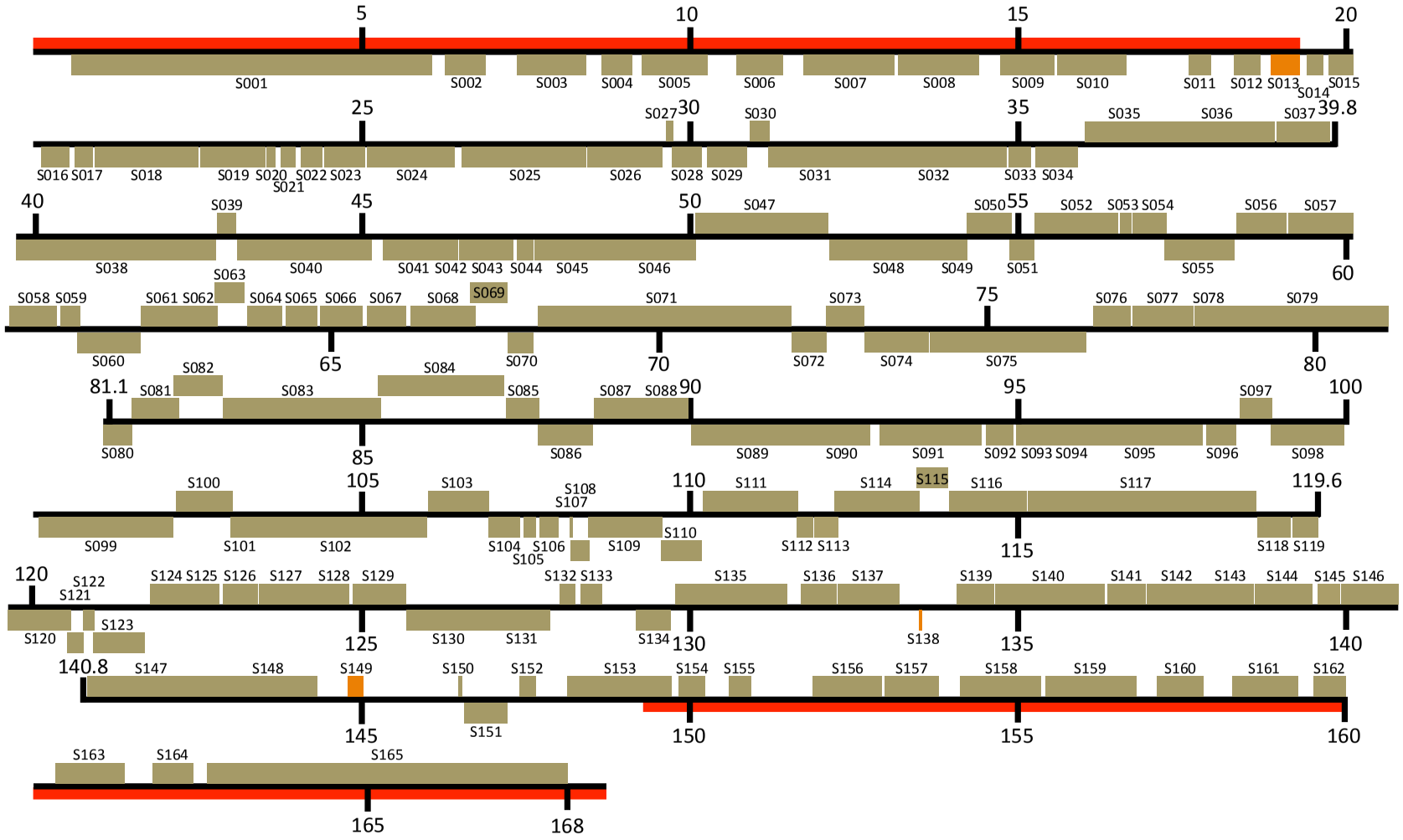
5
10
15
20
S001
S002
S003
S004
S005
S006
S007
S008
S009
S010
S011
S012
S013
S014
S015
25
30
35
39.8
S027
S030
S035
S036
S037
S016
S017
S018
S019
S020
S021
S022
S023
S024
S025
S026
S028
S029
S031
S032
S033
S034
40
45
50
55
60
S039
S047
S050
S052
S053
S054
S056
S057
S038
S040
S041
S042
S043
S044
S045
S046
S048
S049
S051
S055
S063
S058
S059
S061
S062
S064
S065
S066
S067
S068
S069
S071
S073
75
S076
S077
S078
S079
S060
65
S070
70
S072
S074
S075
80
S082
81.1
S081
S083
S084
S085
S087
S088
90
95
100
S097
S080
85
S086
S089
S090
S091
S092
S093
S094
S095
S096
S098
S100
105
S103
S108
S107
110
S111
S114
S115
S116
S117
119.6
S099
S101
S102
S104
S106
S105
S109
S110
S112
S113
115
S118
S119
120
S122
S121
S124
S125
S126
S127
S128
S129
S132
S133
S135
S136
S137
S139
S140
S141
S142
S143
S144
S145
S146
S123
S120
125
S130
S131
S134
130
S138
135
140
140.8
S147
S148
S149
S150
S152
S153
S154
S155
S156
S157
S158
S159
S160
S161
S162
S151
145
150
155
160
S163
S164
S165
165
168

Figure 4.1 Genome map of SQFV-Kilham

The genome of the SQFV-Kilham is 168.586kb long encoding 153 unique open reading frames with 12 complete ORFs repeated at either end of the genome in the inverted-terminal repeats (ITR, highlighted in red). Each ORF is represented to scale by a filled box and their transcriptional direction is indicated with genes that are read to the right shown above the black line, and genes read to the left end of the genome shown below the black line. Major gene truncations are represented by orange boxes demarcating the remaining ORF.

The boundaries between the ITR and the unique region of the genome are at the beginning of S013 on the left end and in the middle of S153 on the right end. The right ITR boundary actually cuts into the ORF of S153, which is partially duplicated as S013 on the left end. This partially duplicated ORF, however, may not be expressed as no promoter element could be identified and a large portion of the N-terminus is missing compared to its counterpart at the other end of the genome.

We numbered the ORFs starting from S001 in the ITR to S165 corresponding to the complementary ORF in the right ITR. The ORFs of the SQFV genome are arranged and transcribed in a similar manner to other leporipoxviruses, and most of the genes found in RFV and MYXV are also present in SQFV. As is common for genes near the genomic termini in chordopoxviruses, all of the genes in the SQFV ITRs are transcribed away from the center of the genome, which presumably reduces the formation of double-stranded (ds) RNA during virus replication and the stimulation of an interferon response (44).

ORF	Start (bp)	Stop (bp)	Size (aa)	Prom.	Predicted Function/Features	Ortholog	Amino Acid Identity	BLASTX e-values
S001/ S165	6078/ 162,510	576/ 168,012	1833	L	glycoprotein, unknown(45)	CPXV219	0.78	0.00E+00
S002/ S164	6902/ 161,686	6284/ 162,304	618	E	unknown	CPXV218	0.69	3.00E-92
S003/ S163	8405/ 160,183	7331/ 161,257	358	L	soluble α/β IFN receptor(46)	MPXV B16R	0.69	3.00E-162
S004/ S162	9141/ 159,447	8694/ 159,894	149	E/L	NF-κB signaling inhibitor(47-49)	CPXV208	0.85	5.00E-93
S005/ S161	10,267/ 158,321	9253/ 159,335	338	?	IL-1 convertase(50, 51)	CPXV CrmA	0.85	0.00E+00
S006/ S160	11,419/ 157,169	10,717/ 157,871	234	E/L	ER protein, apoptosis regulation(52, 53)	CPXV B8R	0.68	2.00E-102
S007/ S159	13,143/ 155,445	11,727/ 156,861	472	E	ankyrin repeat(54)	DPV165	0.33	4.00E-52
S008/ S158	14,393/ 154,195	13,172/ 155,416	407	L	phospholipase D-like(55, 56)	LSDV146	0.58	8.00E-145
S009/ S157	15,556/ 153,032	14,743/ 153,845	271	E	soluble IFN-γ receptor(57)	DPV010	0.37	2.00E-41
S010/ S156	16,647/ 151,941	15,597/ 152,991	350	E/L	IL-1 receptor(57)	DPV007	0.49	2.00E-103
S011/ S155	17,936/ 150,652	17,603/ 150,984	111	?	unknown	RFV003.2L	0.81	2.00E-62
S012/ S154	18,696/ 149,892	18,457/ 150,132	80	L	kelch repeat(58)	RFV004.1R	0.85	4.00E-30
S013	19,246	18,853	131	?	putative E3 Ub ligase; truncated, partial duplication of S152(58)	M006L	0.73	2.00E-65
S014	19,650	19,401	83	E/L	EGF-like growth factor(59)	RFV010L	0.64	1.00E-27
S015	20,123	19,634	163	E?	membrane virulence factor, apoptosis regulator(60)	RFV011L	0.66	3.00E-62
S016	20,557	20,131	142	E	dUTPase(61, 62)	M012L	0.85	5.00E-85
S017	20,913	20,640	91	E/L	pyrin domain/inflammasome(63, 64)	M013L	0.68	5.00E-32

S018	22,504	20,950	518	E?	kelch repeat, putative E3 Ub ligase(58, 65)	RFV014L	0.76	0.00E+00
S019	23,525	22,558	322	E/L	RNA reductase (small subunit)(66)	RFV015L	0.91	0.00E+00
S020	23,697	23,553	48	?	unknown	M016L	0.79	5.00E-21
S021	24,012	23,780	77	E	unknown	M017L	0.79	2.00E-33
S022	24,403	24,196	69	E/L	unknown	M018L	0.84	4.00E-23
S023	25,106	24,461	215	L	fusion/entry(67)	M019L	0.92	2.00E-133
S024	26,424	25,086	446	L	S/T/Y protein kinase 2(68)	RFV020L	0.94	0.00E+00
S025	28,422	26,541	627	E	EEV maturation(69, 70)	M021L	0.83	0.00E+00
S026	29,568	28,455	371	L	envelope antigen(71, 72)	M022L	0.94	0.00E+00
S027	29,668	29,764	32	L?	unknown	M023R	0.66	7.70E-01
S028	30,183	29,739	148	E/L	unknown	RFV024L	0.93	2.00E-99
S029	30,875	30,247	209	E	unknown(73)	M025L	0.88	9.00E-128
S030	30,915	31,218	101	E/L	DNA-binding phosphoprotein(74)	M026L	0.97	3.00E-65
S031	32,630	31,220	470	L	poly(A) polymerase catalytic subunit(75)	M027L	0.96	0.00E+00
S032	34,825	32,629	732	L	unknown, EV formation(76)	M028L	0.86	0.00E+00
S033	35,197	34,867	110	E	IFN resistance; PKR inhibitor(26, 77)	M029L	0.80	2.00E-49
S034	35,922	35,258	221	E	RNA polymerase subunit(78)	RFV030L	0.89	7.00E-136
S035	36,029	37,220	397	E?	virosome protein(79)	RFV031R	0.80	0.00E+00
S036	37,227	38,922	565	E/L	unknown, morphogenesis(80)	M032R	0.94	0.00E+00
S037	38,934	39,749	271	E	core protein(81, 82)	M33R	0.98	0.00E+00
S038	42,770	39,752	1006	E/L	DNA polymerase(83)	M034L	0.93	0.00E+00

S039	42,805	43,093	96	L	thiol-oxidoreductase(84, 85)	M035R	0.94	3.00E-60
S040	45,162	43,119	681	E	Erk1/2 signaling(86)	M036L	0.83	0.00E+00
S041	46,248	45,309	313	L?	DNA-binding, late morphogenesis, core protein(87)	M038L	0.95	0.00E+00
S042	46,476	46,251	75	E/L	membrane protein, entry/fusion(88)	M039L	0.85	1.00E-36
S043	47,304	46,479	275	L	DNA-binding phosphoprotein(89)	M040L	0.93	2.00E-162
S044	47,621	47,387	78	?	structural protein(90)	M041L	0.94	8.00E-43
S045	48,802	47,644	386	L	core protein, telomere binding(91, 92)	RFV042L	0.87	0.00E+00
S046	50,084	48,797	429	L	morphogenesis, cysteine protease, core protein(93, 94)	M043L	0.97	0.00E+00
S047	50,089	52,123	678	?	DNA/RNA helicase(95, 96)	RFV044R	0.89	0.00E+00
S048	53,899	52,129	590	L	metallo-endoproteinase, morphogenesis(97-99)	M045L	0.89	0.00E+00
S049	54,231	53,898	111	L	fusion/entry(100)	M046L	0.95	5.00E-53
S050	54,224	54,902	226	E	IBT-dependent protein, late elongation factor(101)	M047R	0.90	3.00E-127
S051	55,249	54,862	129	L	glutaredoxin 2, membrane protein(102, 103)	RFV048L	0.94	4.00E-74
S052	55,251	56,544	431	?	core protein(104)	RFV049R	0.87	0.00E+00
S053	56,552	56,741	63	E	RNA polymerase subunit(105)	M050R	0.98	5.00E-36
S054	56,743	57,265	174	?	unknown(106)	M051R	0.91	1.00E-113
S055	58,289	57,239	350	L	structural protein, IV formation(107)	M052L	0.94	0.00E+00
S056	58,317	59,097	260	E/L	late transcription factor(108, 109)	RFV053R	0.98	0.00E+00
S057	59,121	60,117	332	L	myristylprotein, fusion complex(110)	M054R	0.92	0.00E+00
S058	60,120	60,846	242	L	myristylprotein, IMV virion protein(111, 112)	M055R	0.97	5.00E-159
S059	60,897	61,194	99	E	morphogenesis, IV formation(113)	RFV056R	0.82	6.00E-50

S060	62,109	61,149	320	L	core protein, early transcription(114)	RFV057L	0.93	0.00E+00
S061	62,133	62,886	251	L?	DNA binding structural protein precursor, major core protein(115, 116)	RFV058R	0.93	1.00E-166
S062	62,908	63,295	129	L	fusion/entry(117)	M059R	0.94	6.00E-66
S063	63,251	63,698	149	L	dimeric virion protein(118)	RFV060R	0.87	6.00E-89
S064	63,734	64,268	178	E	thymidine kinase(119)	M061R	0.87	7.00E-113
S065	64,330	64,804	158	E/L	host range(120, 121)	M062R	0.80	5.00E-84
S066	64,862	65,483	207	E	host range(122)	M063R	0.70	1.00E-85
S067	65,547	66,153	202	E/L	host range(123)	M064R	0.80	5.00E-80
S068	66,215	67,214	333	?	poly(A) polymerase regulatory subunit(124, 125)	M065R	0.97	0.00E+00
S069	67,131	67,686	185	E	RNA polymerase subunit	M066R	0.95	3.00E-125
S070	68,093	67,694	133	E	fusion complex(126)	M067L	0.96	2.00E-87
S071	68,167	72,025	1286	E/L	RNA polymerase subunit(127)	M068R	0.98	0.00E+00
S072	72,548	72,031	172	L	S/Y phosphatase(128)	M069L	0.98	8.00E-122
S073	72,563	73,133	190	L	fusion complex(129)	M070R	0.94	2.00E-131
S074	74,115	73,140	325	L	IMV envelope protein(130)	M071L	0.88	0.00E+00
S075	76,506	74,118	796	L	RNA pol. assoc. transcription factor(32, 131)	M072L	0.95	0.00E+00
S076	76,633	77,179	182	E/L	late transcription factor(132)	M073R	0.96	2.00E-37
S077	77,213	78,155	314	E/L	topoisomerase I, telomere resolvase(133, 134)	RFV074R	0.96	0.00E+00
S078	78,157	78,601	148	?	unknown, membrane biogenesis(135)	M075R	0.91	2.00E-90
S079	78,605	81,110	835	E?	mRNA capping enzyme, large subunit(136, 137)	RFV076R	0.92	0.00E+00
S080	81,506	81,077	143	L	virion component(138)	M077L	0.86	2.00E-84

S081	81,511	82,230	240	?	structural protein(138)	M078R	0.84	6.00E-148
S082	82,231	82,884	218	E	uracil DNA glycosylase(139)	M079R	0.96	3.00E-156
S083	82,920	85,278	786	E/L	rep./recomb. NTPase, AAA-ATPase, genome uncoating factor(140)	M080R	0.96	0.00E+00
S084	85,277	87,182	635	?	early transcription factor(32, 141)	M081R	0.98	0.00E+00
S085	87,216	87,705	163	E	RNA polymerase subunit(142)	M082R	0.96	1.00E-110
S086	88,536	87,681	285	?	carbonic anhydrase-like structural protein(143, 144)	M083L	0.84	2.00E-163
S087	88,547	89,201	218	E?	mut-T like protein, decapping enzyme(145)	RFV084L	0.91	3.00E-140
S088	89,200	89,977	259	L	mut-T like protein neg. gene regulator, decapping enzyme(146, 147)	M085R	0.92	4.00E-173
S089	91,879	89,983	632	L	NTPase I, DNA helicase(148, 149)	RFV086L	0.91	0.00E+00
S090	92,760	91,899	287	E/L	mRNA capping enzyme sm. subunit, transcript. initiation factor(150)	M087L	0.97	0.00E+00
S091	94,445	92,786	553	L	rifampicin resistance, IMV protein(151, 152)	M088L	0.95	0.00E+00
S092	94,930	94,479	150	L	trans-activator, late transcription factor 2(153)	RFV089L	0.91	7.00E-95
S093	95,634	94,962	224	E	trans-activator, late transcription factor 3(154)	M090L	0.99	3.00E-147
S094	95,858	95,633	75	L	thiol-oxidoreductase(155, 156)	M091L	0.96	3.00E-44
S095	97,831	95,869	654	L	major core protein P4b precursor(157)	M092L	0.94	0.00E+00
S096	98,334	97,871	154	L	core protein(158)	RFV093L	0.73	2.00E-51
S097	98,373	98,862	163	L	RNA polymerase subunit(159)	M094R	0.92	4.00E-78
S098	99,983	98,864	373	I?	core protein(160)	RFV095L	0.94	0.00E+00
S099	102,149	100,013	712	L	early transcription factor large subunit(141, 161)	M096L	0.96	0.00E+00
S100	102,202	103,060	286	E	intermediate transcription factor(162)	M097R	0.94	0.00E+00

S101	103,292	103,040	84	E	membrane protein(163)	M098L	0.90	2.00E-31
S102	105,998	103,295	901	L	major core protein P4a precursor(164)	RFV099L	0.89	0.00E+00
S103	106,012	106,954	314	L	scaffolding protein(165, 166)	RFV100R	0.96	0.00E+00
S104	107,454	106,956	166	L	structural protein(167)	M101L	0.87	2.00E-86
S105	107,682	107,481	67	L	structural protein, IMV membrane protein p8; 25aa insertion(168)	M102L	0.91	2.00E-18
S106	108,027	107,739	96	L	IMV membrane protein, assembly factor(169)	M103L	0.92	4.00E-47
S107	108,205	108,046	53	L	potential immuno-modulatory protein(170)	M104L	0.92	2.00E-25
S108	108,479	108,197	94	L?	core protein	M105L	0.91	8.00E-57
S109	109,593	108,465	376	L	35K myristylprotein, fusion complex(171)	M106L	0.92	0.00E+00
S110	110,209	109,609	200	L	IMV membrane protein, morphogenesis(172)	M107L	0.85	3.00E-101
S111	110,222	111,656	478	L	transcript release factor, ATP-dep. DNA helicase(125, 173)	M108R	0.92	0.00E+00
S112	111,888	111,642	82	L	late stage morhpogenesis(174, 175)	M109L	0.78	4.00E-28
S113	112,231	111,892	113	?	core protein(176)	M110L	0.88	5.00E-67
S114	112,228	113,521	431	E?	DNA polymerase processivity factor(177)	M111R	0.85	0.00E+00
S115	113,486	113,966	160	?	Holliday junction resolvase(178, 179)	M112R	0.84	3.00E-94
S116	114,002	115,160	386	E/L	intermediate transcription factor(162)	M113R	0.92	0.00E+00
S117	115,188	118,653	1155	E	RNA polymerase subunit(180)	M114R	0.97	0.00E+00
S118	119,187	118,659	176	L	fusion protein, EV formation, IMV surface protein(181)	M115L	0.62	5.00E-65
S119	119,610	119,190	140	L	IMV membrane protein(182, 183)	M116L	0.95	5.00E-83
S120	120,524	119,618	302	E	RNA polymerase subunit(180)	M117L	0.91	0.00E+00

S121	120,723	120,495	76	L	core protein(107, 184)	M118L	0.96	5.00E-43
S122	120,861	120,741	40	L	unknown	RFV119L	0.77	2.00E-13
S123	121,662	120,897	255	L	ATPase(185)	RFV120L	0.96	6.00E-180
S124	121,755	122,277	174	E	EEV glycoprotein, NK receptor homolog(186)	M121R	0.75	5.00E-67
S125	122,289	122,802	171	L	lectin-like EEV glycoprotein, NK receptor homolog(187)	M122R	0.90	2.00E-111
S126	122,837	123,374	179	E	unknown(188)	M123R	0.88	6.00E-113
S127	123,417	124,278	287	E	unknown	RFV124R	0.85	3.00E-164
S128	124,293	124,782	163	?	unknown	M125R	0.63	8.00E-52
S129	124,834	125,647	271	E	structural protein?	M126R	0.86	4.00E-171
S130	126,974	125,645	443	?	Type II CPD photolyase(189)	M127L	0.81	0.00E+00
S131	127,852	126,976	292	?	CD47-like transmembrane integrin associated(190)	M128L	0.80	2.00E-137
S132	127,994	128,231	79	E	myristylprotein(191)	M129R	0.63	4.00E-30
S133	128,312	128,630	106	E/L	unknown	M130R	0.62	1.00E-34
S134	129,689	129,161	176	E/L	unknown	M132L	0.85	8.00E-90
S135	129,770	131,444	558	E/L	ATP-dependent DNA ligase(192)	M133R	0.88	0.00E+00
S136	131,691	132,237	182	?	Bcl-2-like fold, IL-1/TLR antagonism(193, 194)	M136R	0.83	4.00E-106
S137	132,240	133,167	309	L?	unknown(195)	M137R	0.80	0.00E+00
S138	133,651	133,543	36	?	α-2,3-sialyltransferase; truncated, likely not functional(196)	RFV138L	0.86	2.00E-47
S139	134,069	134,630	187	?	Bcl-2-like fold(193)	M139R	0.90	8.00E-123
S140	134,638	136,321	561	?	kelch repeat, Putative E3 Ub ligase(58)	M140R	0.84	0.00E+00
S141	136,349	136,940	197	E	surface antigen, OX-2 homolog(197)	M141R	0.63	2.00E-54

S142	136,948	137,857	303	E	S/T protein kinase(198)	M142R	0.89	0.00E+00
S143	137,877	138,573	232	L?	RING finger protein(199)	M143R	0.91	4.00E-141
S144	138,619	139,468	283	?	VCP precursor, complement control protein(200, 201)	M144R	0.71	2.00E-125
S145	139,555	139,879	108	E?	secreted virulence factor, Bcl-2-like fold(194, 202)	M146R	0.83	2.00E-59
S146	139,913	140,774	287	E/L	S/T protein kinase	RFV147R	0.85	0.00E+00
S147	140,850	142,863	671	E	host range, ankyrin-like(203, 204)	RFV148R	0.74	0.00E+00
S148	142,867	144,337	490	E	host range, ankyrin-like(204, 205)	M149R	0.84	0.00E+00
S149	144,798	145,044	78	E	serpin (SERP-2); truncated, frameshift(206, 207)	M151R	NA	NA
S150	146,364	146,502	46	L	unknown	28S rRNA gene frag., *O. cuniculus*	0.87	5.00E-08
S151	147,255	146,582	224	E	ERK-2/NF-kB inhibition(208)	M154L	0.76	9.00E-117
S152	147,425	147,656	77	E	IFN resistance, eIF2α homologue, PKR inhibitor(29, 209, 210)	RFV008.2L	0.80	7.00E-34
S153	148,199	149,735	512	E	putative E3 Ub ligase, kelch repeat(58)	M006L	0.68	0.00E+00

Table 4.5 SQFV genome annotation table

The annotated ORFs in SQFV are represented with the nucleotide position of the start and stop codons. Predicted lengths of translated proteins for each ORF are given in amino acids. A putative function was assigned based on the function of orthologous proteins. Amino acid sequence identities were calculated with BLASTx for the translated nucleotide sequences compared to the listed ortholog (best match). Putative early (E), intermediate (I), late/post-replicative (L) or early/late (E/L) promoter designations are listed.

Phylogeny of squirrel fibroma virus

With the complete genome sequenced, we wanted to determine the phylogenetic relationship of the SQFV to the other poxviruses, and particularly to the other leporipoxviruses. Previous studies inferred the phylogeny of the SQFV based on sequence comparisons of the DNA polymerase encoded by S038 (corresponding to VACV E9L) and a conserved membrane fusion protein encoded by S062 (corresponding to VACV G9R). From these analyses, the SQFV was placed on the same branch with MYXV and RFV within the cluster of Clade II poxviruses (7, 211). Using a concatenated alignment of 23 single-copy protein sequences, which are present in 38 fully sequenced poxvirus genomes (Tables 4.3 and 4.4), we generated a maximum-likelihood tree that depicts the evolutionary relationship of the SQFV to other poxviruses (Fig 4.2).

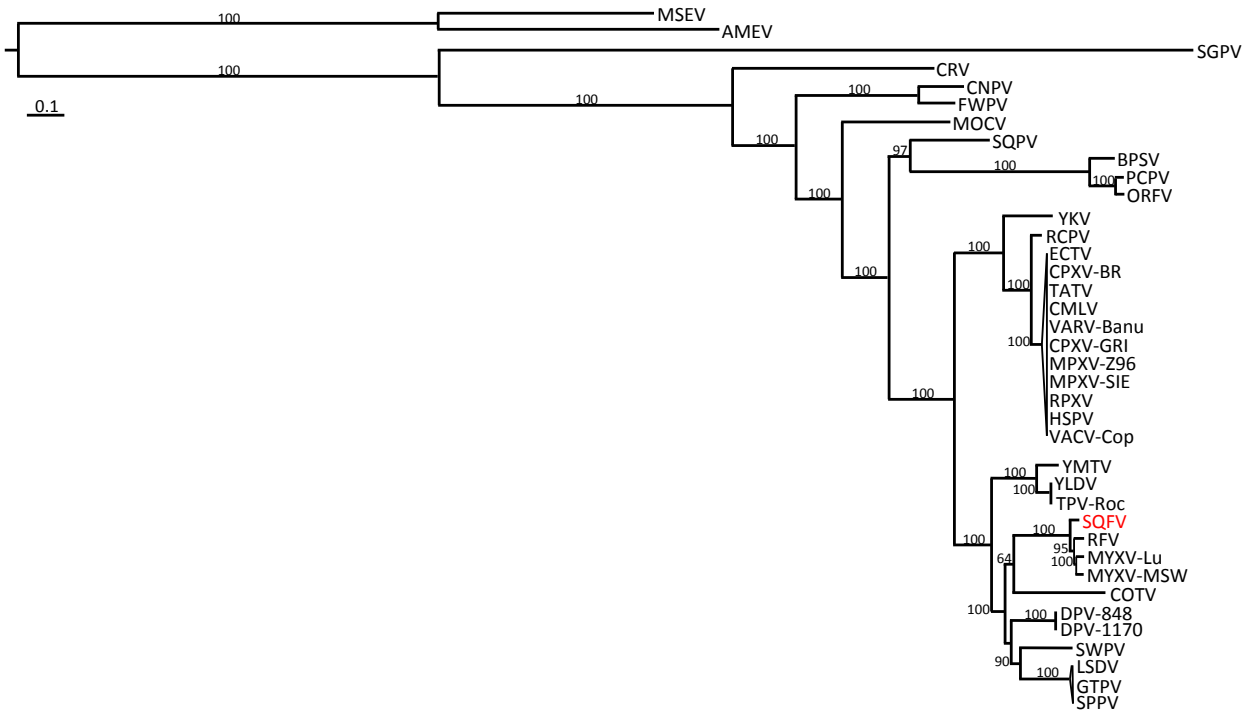

Figure 4.2 SQFV is the most divergent leporipoxvirus.

A maximum-likelihood tree of 38 fully sequenced poxviruses including SQFV was generated from an alignment of 23 concatenated single-copy gene protein sequences conserved in all the poxviruses analyzed. Bootstrap values (100 replicates) above 50 are indicated at each junction and branch separations with bootstrap values less than 50 were collapsed into a single branch tip. Branch lengths are measured in base-pair substitutions per site. Abbreviations for poxvirus species are described in Table 4.4.

The tree was rooted to melanoplus sanguinipes entomopoxvirus (MSEV) and amsacta moorei entomopoxvirus (AMEV), which represent a separate sub-family within *Poxviridae*. All major branches were supported by high bootstrap values. In agreement with a previous report, salmon gill poxvirus (SGPV), crocodilepox virus (CRV), and canarypox (CNPV) and fowlpox (FWPV) viruses branched off at the base of the *Chordopoxvirus* clade (16). As predicted, SQFV was found in a monophyletic clade with RFV and the two MYXV strains (Lu and MSW), confirming the close evolutionary relatedness of SQFV with the other leporipoxviruses. The tree also showed that the two genetically distinct European laboratory (Lu, Lausanne) and Californian (MSW) MYXV strains and RFV are more closely related to one another than to SQFV.

Transcriptional regulation

The upstream sequences of 42 putative early, 52 late, or 8 intermediate ORFs, as classified by the designation of their MYXV and RFV orthologs, were analyzed for common sequence motifs within each promoter class (Table 4.2). From this analysis distinct early promoter and late promoter motifs were identified (Fig 4.3), which are similar to the classical poxvirus promoter sequence motifs, however, we were not able to differentiate intermediate and late-stage post-replicative motifs (1, 212-214). Intermediate promoters motifs are less well conserved than the characteristic early and late promoter motifs and for several intermediate promoters identified in VACV, late promoter elements and late promoter activity could also be observed (212). We then used the identified motifs to search for similar promoter motifs in the upstream sequences of all the annotated ORFs in the SQFV genome and assigned each with a putative transcriptional class (Table 4.5).

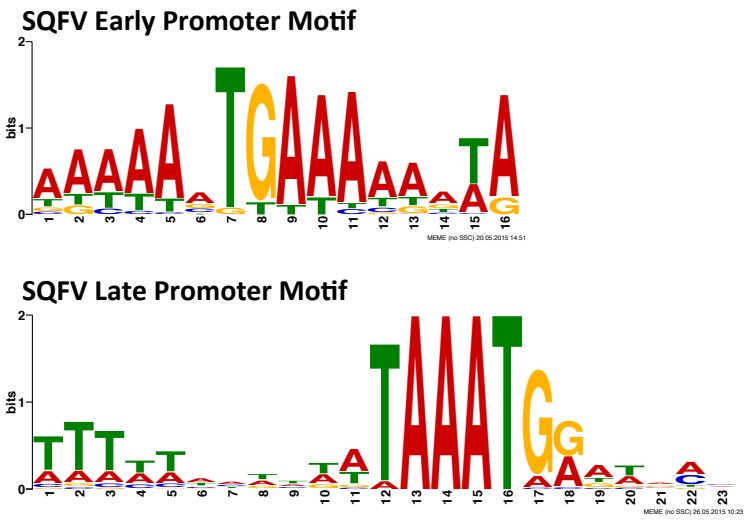

Figure 4.3 SQFV early and late promoter motifs.

SQFV promoter motifs were identified from sequences upstream of each gene using the motif identification program implemented in MEME. The frequency of occurrence of a nucleotide in each position in the early and late promoter motifs for the initial analysis is indicated to show the consensus motif sequence. SQFV early and late promoter motifs are similar to those identified in RFV (1)*, but no clear intermediate promoter motif was identified in this analysis.*

Genetic differences between squirrel fibroma virus and other leporipoxviruses

Identification of regions of dynamic gene loss/fragmentation in leporipoxviruses

Gene deletion and fragmentation is commonly observed in poxviruses due to insertion and deletions (indels) as well as disruptions of ORFs caused by premature stop codons, which have the potential to greatly impact viral gene expression, host tropism and virulence and therefore can have a great influence on the evolution of these viruses.

The genomic region corresponding to ORFs M131R to M139R in MYXV has experienced a high frequency of gene loss and fragmentation in the *Leporipoxvirus* lineage. In RFV, ORFs 135R, 136R, and 139R corresponding to M135R, M136R, and M139R in MYXV, are all fragmented with the remaining sequences not predicted to produce functional proteins (Fig. 4.5) (1). Similarly, SQFV contains a small, truncated fragment of M138L and only fragmentary remains of an ortholog of M131R, while ORFs corresponding to M134R and M135R are completely absent from the genome (Table 4.6). Genes M131R and M138L are homologs of host derived superoxide dismutase (SOD) and α-2, 3-sialyltransferase in MYXV,

respectively, and orthologs of both are present in RFV (Fig. 4.4, Table 4.6) (1). Interestingly, the M131R ORF is also disrupted in MYXV-MSW, which was isolated in California, but otherwise all sequenced chordopoxviruses encode genes for a homolog of SOD suggesting its importance for poxvirus virulence or immune regulation (Fig. 4.5) (1, 215-217). Additionally, MYXV strains lacking M138L have been experimentally shown to be attenuated *in vivo* (196). While the incomplete loss of these ORFs from the SQFV genome may indicate a relatively recent loss of these genes in SQFV, whether their loss is a result of a change in the host range of SQFV or contributes to the different host tropism of this virus compared to the other leporipoxviruses remains to be tested.

Gene	MYXV-Lu	MYXV-MSW	RFV	SQFV
M131R	✔	X	✔	X
M132L	✔	✔	✔	✔
M133R	✔	✔	✔	✔
M134R	✔	✔	✔	X
M135R	✔	✔	X	X
M136R	✔	✔	X	✔
M137R	✔	✔	✔	✔
M138L	✔	✔	✔	X
M139R	✔	✔	X	✔

Figure 4.4 Genomic region of dynamic gene loss and fragmentation in leporipoxviruses.
There are multiple occurrences of gene fragmentation or gene loss in MYXV-MSW, RFV and SQFV in the genomic region corresponding to ORFs M131R to M139R in MYXV. The gene loss and fragmentation appears to have occurred independently in each with only one missing gene common between RFV and SQFV and between MYXV-MSW and SQFV.

MYXV	RFV	SQFV	Predicted function
M000.5L/R	Absent	Absent	unknown
M001L/R	RFV001L/R	Absent	secreted chemokine binding protein
M002L/R	RFV002L/R	Absent	TNF-R homolog
M003.1L/R	RFV003.1L/R	Absent	NF-κB signaling inhibitor
M004L/R	RFV004L/R	Absent	apoptosis regulator
M005L/R	RFV005L/R	Absent	E3 Ub ligase
M006L	RFV006L	Absent	kelch repeat
M007L/R	RFV007L/R	Absent	IFN-γ receptor homolog
M008L/R	RFV008L/R	Absent	kelch repeat
M008.1L/R	fragmented	Absent	SERP-1
M009L (509aa)	RFV009L (partially duplicated, 510aa)	S013L (truncated, partial duplication of S153R, 131aa)	kelch repeat
M023R (61aa)	RFV023R (35aa)	S027R (32aa)	late protein
M129R (136aa)	RFV129R (78aa)	S132R (79aa)	myristylated protein
M131R	RFV131R	fragmented	Cu/Zn SOD homolog
M134R	RFV134R	Absent	glycoprotein, unknown
M135R	fragmented	Absent	IL-1/6 receptor homolog
M136R	fragmented	S136R	A52R-like, bcl-2 fold
M138L (290aa)	RFV138L (290aa)	S138R (truncated, 36aa)	α-2,3-sialyltransferase
M139R	fragmented	S139R	A52R-like, bcl-2 fold
M150R	fragmented	fragmented	NF-κB inhibition
M151R (333aa)	RFV151R (333aa)	S149R (frameshift truncation, 78aa)	SERP-2
M152R	fragmented	Absent	SERP-3
M153R	RFV153R	Absent	RGD motif

Table 4.6 A comparison of leporipoxvirus gene differences.

A comparison was made for all differences in the gene content of the three leporipoxvirus species with respect to the MYXV orthologs. Genes listed as absent are entirely missing from the genome, while genes listed as fragmented still have some remaining gene fragments. Truncated genes are indicated with the deduced protein length listed.

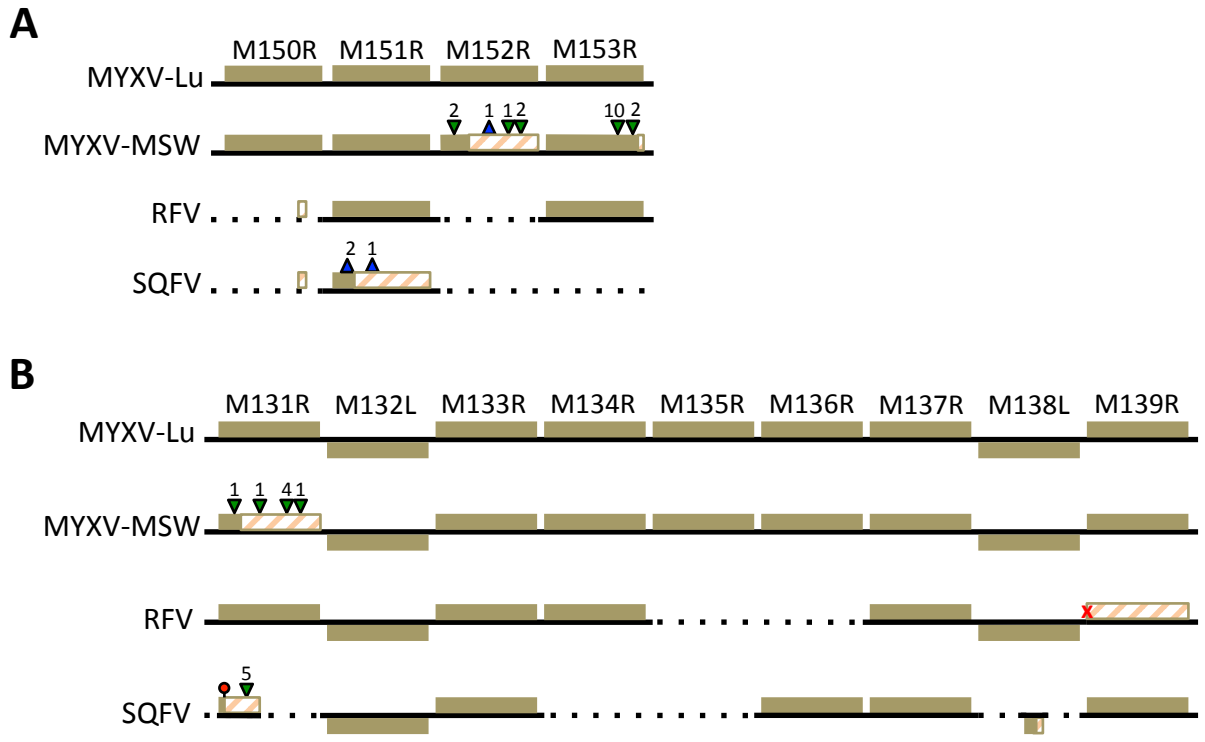

Figure 4.5. Gene inactivation and gene loss in leporipoxvirus genomes.

Horizontal lines represent the genomic sequence corresponding to the region between M150R and M153R (A) or M131R and M139R (B) in MYXV-Lu and the orthologous sequences in MYXV-MSW, RFV and SQFV. ORFs are represented by brown boxes or striped orange boxes for orthologous sequences that are present but are not predicted to be expressed (not drawn to scale). Base pair insertions (blue triangles) or deletions (inverted green triangles) present in ORFs, which lead to frameshifts are indicated with the number of nucleotides inserted or deleted listed above. Inactivation of the start codon in RFV 139R is shown with a red "x", but many other inactivating indels are present within this ORF. The insertion of an early stop codon in the SQFV 131R ortholog is indicated with a red circle. The dashed line indicates the orthologous sequence is missing.

Loss of other potential immunomodulatory genes in the squirrel fibroma virus

Because of the distinct phenotype and high pathogenicity of MYXV in E. rabbits, several genes in MYXV have been characterized as having a role in modulating the host immune response through their experimental deletion from the virus (218). Many of these genes are also conserved in RFV and likely perform similar functions in this virus. There are some important differences, however, that may contribute to the low pathogenicity of RFV in E. rabbits and therefore could also play a role in the virulence of SQFV in its host species (1).

Serine protease inhibitors (serpins) are a large family of proteins that inhibit proteolytic cleavage by other proteases (219). In poxviruses serpins are important for inhibiting the apoptotic and inflammatory response. SQFV does not encode any functional copies of orthologs to the MYXV serpin family genes M008.1R/L, M151R, or M152R (also known as SERP-1, SERP-2, and SERP-3, respectively). Of the three serpin genes found in the MYXV (Lu) genome, M151R and M152R are fragmented or interrupted by multiple indels in both the RFV and MYXV-MSW genomes, and both are completely absent from the SQFV genome (Table 4.6 and Fig. 4.5). SERP-1 (M008.1L/R) regulates the inflammatory response during MYXV infection (220, 221) and has been used as an anti-inflammatory agent in humans (222). SERP-3 (M152R) is a virulence factor for MYXV (223) and SERP-2 (M151R) is an inhibitor of the interleukin-1β-converting enzyme blocking inflammation (206). In SQFV, the S149 ORF encodes a nearly complete ortholog of M151R, which is the only intact serpin gene found in RFV or MYXV-MSW. However, a two-base pair insertion 182 nucleotides into the ORF causes a frameshift that is predicted to result in a truncated protein containing only 78 amino acids (Tables 4.5 and 4.6). Another single base pair insertion occurs 401 nucleotides downstream of the first insertion that would further disrupt the ORF, suggesting that this gene is likely not functional in SQFV (Fig. 4.5).

Additionally, the right end of the genome corresponding to ORFs M150R to M156R in MYXV is highly variable between the different leporipoxviruses. In MYXV, the protein product of M150R blocks inflammation induced by NF-κB (224). A very small fragment of this ORF is still identifiable in the SQFV genome between ORF S148 and S149 but is likely not expressed. This gene is also fragmented in RFV as well as in the left ITR of MXYV-MSW, although the right ITR of MYXV-MSW contains an intact full-length copy of M150R that may compensate for the fragmentation of the other copy (Fig. 4.5). M153R in MYXV has a predicted RGD motif, which is found in integrin family proteins and is important for mediating cell attachment. This protein has been shown to down-regulate expression of MHC-I and surface molecules that are important for attracting immune cells (225, 226). A complete copy of this gene is present in the RFV genome but is missing entirely from the SQFV genome. The absence of any fragment of orthologs for both M152R and M153R indicates that these genes were probably lost together in a single genomic excision event. A single copy of orthologs to MYXV M154L and M156R are both present in SQFV, but in RFV, the ortholog of M156R is duplicated and ORFs

corresponding from M150R to M156R in MYXV-MSW are also duplicated in both ITRs. The proximity of these ORFs to the ITR boundary has likely contributed to the variation in gene copy number in RFV and the MYXVs since their divergence (1, 215, 227).

Genes orthologous to MYXV M001L/R, M002L/R, M003.1L/R, M004L/R, M005L/R, M006L/R, M007L/R, M008L/R, and M008.1L/R are all absent from the SQFV genome but are present in RFV (Table 4.6). The ortholog of M009L in SQFV is also truncated and is likely not functional. The loss of all of these genes, which include homologs of tumor necrosis factor (TNF) and interferon (IFN)-γ receptors, inhibitors of NF-κB signaling and apoptosis, a secreted chemokine and a serpin probably impacts the modulation of the host immune response by SQFV.

Potential horizontal gene transfer

It is established that many poxvirus genes probably originated from their hosts as several still have a high sequence identity with their host gene homologs. The superoxide dismutase (SOD) from RFV, for example, still bears a remarkable resemblance to mammalian SODs (1), and the homolog of vascular endothelial growth factor found in many poxviruses is thought to be a modified version of similar host proteins (228). Considering that the entire replication cycle of poxviruses takes place in the cytoplasm, the mechanism for how they are able to incorporate host genes into their genome is unknown. Nevertheless, the horizontal transfer of genes from host to virus has played an important role in the evolution of this family of viruses. Between the ORFs S149 and S151, corresponding to M151R and M154R in MYXV, there is a short 46 amino acid long ORF for which part of the coding sequence is most similar to a fragment of the 28S rRNA gene from the E. rabbit (Fig. 4.6; Table 4.5). We also identified the same unique ORF in a SQFV isolate collected from an infected squirrel (SQFV-CDC). We tentatively annotated this ORF as S150 but its classification as a true ORF that is expressed during SQFV infection still needs to be evaluated. The identification of a putative late/post-replicative promoter motif 41bp upstream of the annotated start codon provides evidence to support the potential expression of this ORF and its classification as a novel gene in SQFV acquired horizontally from a mammalian host.

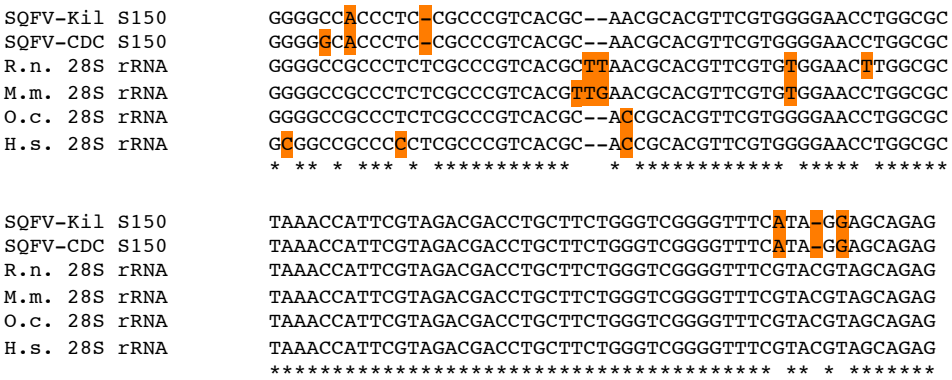

Figure 4.6 Multiple sequence alignment of S150 and similar sequences in GenBank.
Nucleotide sequences identified in BLAST searches with the S150 ORF were aligned in MUSCLE and trimmed manually to highlight the region of S150 that is homologous. Most homologous sequences identified were from the 28S ribosomal RNA gene. Nucleotides differing from the consensus are highlighted in orange and 100% identity is indicated with an asterisk. R.n.= Rattus norvegicus (NR_046246.1); M.m.= Mus musculus (NR_003279.1); O.c.= Orytolagus cuniculus (AF460236.1); H.s.= Homo sapiens (M27830.1).

Evidence for recombination with an orthopoxvirus

In annotating the SQFV genome, we noted the high sequence identity of several genes within the SQFV ITR with orthopoxvirus genes. Despite the SQFV ITR being nearly twice as long as that of either RFV or MYXV, many of the genes found in the ITR region of RFV and MXYV are missing in SQFV (Table 4.6). We therefore decided to analyze the relative sequence identity levels of each ORF in the SQFV ITR with orthologs from poxvirus species representing different genera to determine the most closely related sequences and infer the origin of the genes (Fig 4.7). We used cowpox virus GRI (CPXV) and raccoonpox virus (RCPV) to represent old-world and new-world *Orthopoxviridae* (OPV) member species, respectively, as well as sheeppox virus (SPPV), deerpox virus (DPV), RFV and MYXV to represent other Clade II viruses.

The first six ORFs in the SQFV ITR showed the highest protein sequence identity to the orthologs from the OPV representatives, with an average identity of 69.6% to RCPV proteins and 77.1% to CPXV proteins for all six ORFs. None of the orthologs of these ORFs from the Clade II poxviruses exhibited more than 35% amino acid sequence identity to the SQFV proteins, and a few were not encoded by some or all Clade II poxviruses. Three out of the first ten ORFs in the SQFV ITR represent novel proteins in the *Leporipoxvirus* genus having no

comparable orthologs in either MYXV or RFV (S002, S003, and S010), while the remaining seven deduced proteins exhibited only a minimal identity with corresponding leporipoxvirus proteins (18.8-33% amino acid sequence identity).

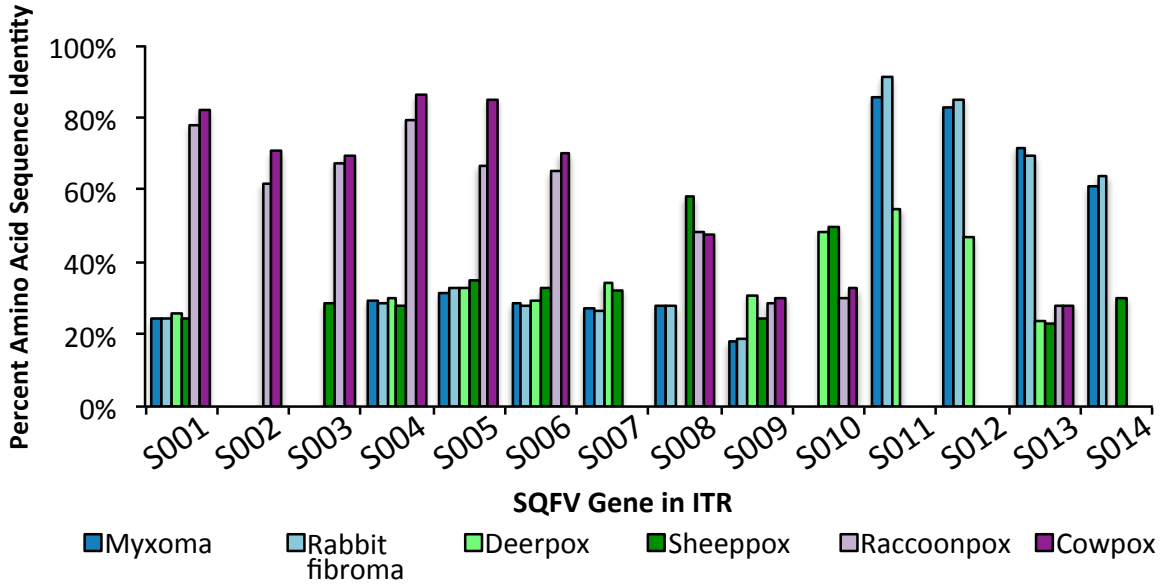

Figure 4.7 Protein sequence identities of SQFV ITR genes to poxvirus orthologs.
Protein sequences of the first 14 genes in the ITR of SQFV were aligned with orthologous proteins from representatives of the Orthopoxvirus clade (cowpox-GRI and raccoonpox viruses), Clade II poxviruses (sheeppox and deerpox viruses) and Leporipoxvirus genus (myxoma and rabbit fibroma viruses). Percent identity from individual protein multiple sequence alignments were calculated with MegAlign and are plotted for each ORF. Where no orthologous protein was present, there is no bar shown.

Deduced proteins encoded by ORFs S007 through S010 exhibited only moderate identity levels to any of the orthologs from the poxviruses tested (highest identity was 58.0% for S008 to ORF 139 from SPPV). Both S008 and S010 exhibited relatively high sequence identity to orthologs from SPPV and DPV suggesting these genes might have originated from a related Clade II poxvirus. This may also be the case for S007 and S009, which had the highest sequence identity with the ortholog from DPV, although the overall protein sequence identity for these ORFs was much lower (32.4% and 24.1% identity, respectively). Only proteins corresponding to ORFs S011 through S014 (S014 being the first ORF outside of the ITR) showed the highest identity to leporipoxvirus orthologs. Two of these four proteins in fact have no ortholog in either OPV analyzed (S011 and S012).

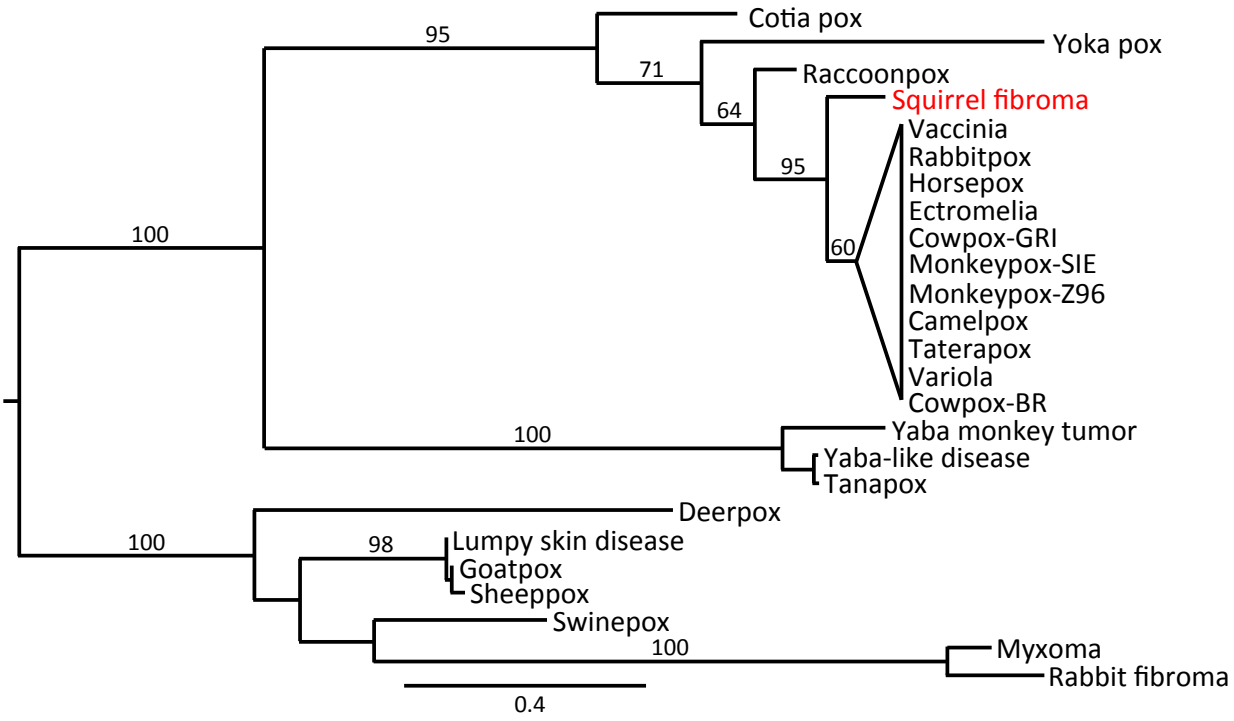

Figure 4.8 Phylogenetic analysis of SQFV ORF S004/S162 indicates recombination with an old-world OPV.

A midpoint-rooted maximum-likelihood tree was generated from the alignment of the OPV-like protein sequence of S004/S162 in the SQFV ITR with orthologs from 25 other poxviruses. Bootstrap values above 50 (100 replicates) for branch separations are indicated. The placement of the SQFV protein suggests that it is more closely related to orthologous proteins from old-world OPVs than to the ortholog in raccoonpox virus, a North American OPV.

To better understand the origin of the OPV-like ORFs, we generated a maximum-likelihood tree generated from the alignment of the protein sequence encoded by the fourth ORF (S004) in SQFV, for which there are orthologs from 25 other poxviruses (present in a single genomic copy). This ORF encodes a gene orthologous to VACV-WR B14R (CPXV B13R), which is a virulence factor for VACV that interferes with NFκB signaling by inhibiting the IκB kinase (IKK) (47, 48). The SQFV protein encoded by S004 was clearly separated from the Clade II poxviruses and the leporipoxviruses and instead nested with orthologous proteins from orthopoxviruses (Fig. 4.8). Interestingly, this analysis predicted S004 to be more closely related to orthologs from the group of so-called “old-world” poxviruses rather than to the North

American poxvirus protein from RCPV, which is in agreement with the slightly higher sequence identity of SQFV ORFs S001-S006 with CPXV than with RCPV protein orthologs.

Analysis of a distinct squirrel fibroma virus isolate

In 2008, the Centers for Disease Control and Prevention (CDC) Poxvirus and Rabies branch identified a squirrel in Ohio, USA that had several nodular lesions on its body during a baiting experiment for a vaccinia-vectored rabies vaccine (Fig 4.9). DNA collected from the lesions did not yield positive results for vaccinia virus in OPV-specific assays. Diagnostic PCR was done at that time using pan-pox primers amplifying a highly conserved RNA polymerase subunit, which identified the causative agent to be SQFV. We obtained two squirrel lesion samples from the CDC and used the homogenized lesion material to attempt amplification of the virus in cell culture. Our several attempts to grow the virus were largely unsuccessful, as were attempts made at the CDC. However, we were able to isolate viral DNA from our infected cell cultures and amplify SQFV-specific genomic regions by PCR (Fig 4.10).

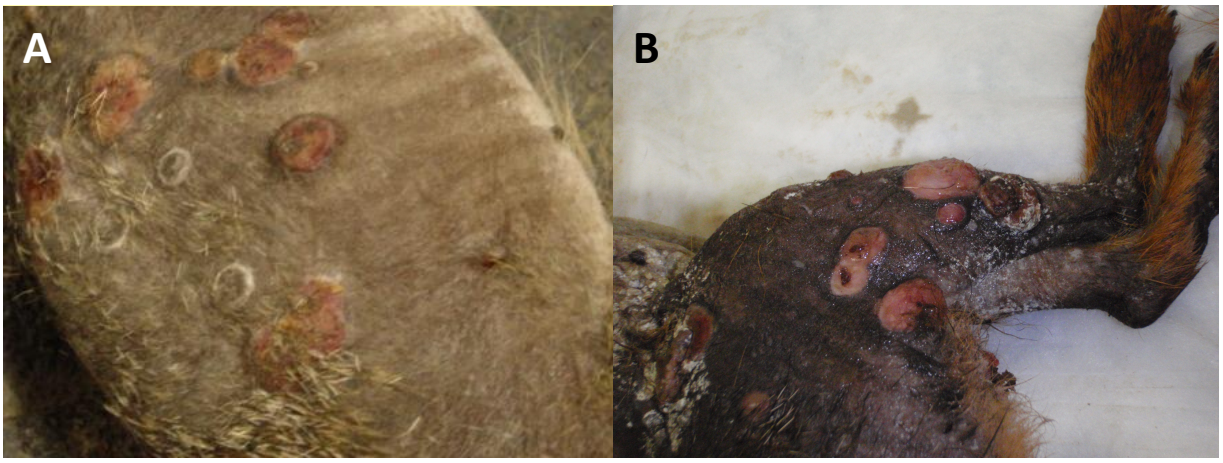

Figure 4.9 Fox squirrel lesions from presumable SQFV infection.
In 2008, during a CDC directed vaccinia-vectored rabies vaccine baiting experiment in Ohio, a female, juvenile fox squirrel with multiple nodular lesions was identified. Lesions were present over the entire body including the back (dorsal area pictured in A) and limbs (right hind limb pictured in B). Photo credit: Gallardo-Romero, N. Centers for Disease Control and Prevention, Poxvirus and Rabies Branch.

The SQFV-Kilham strain was originally isolated in 1952 from six gray squirrels in Maryland, and the virus was subsequently passaged twice in gray squirrels, four times in

woodchucks and twice in domestic cottontail rabbits (4). To dispel concerns that the passaging of the virus might have introduced mutations not present in the original wild variants, we used PCR to amplify and sequence several genomic regions of the SQFV isolate from Ohio (SQFV-CDC). Twelve amplified regions were sequenced and compared to the SQFV-Kilham reference genome covering a total of 5.5kb, and altogether six differences between the two strains were identified (99.7% nucleotide sequence identity) with two differences resulting in predicted amino acid differences in coding regions (Fig 4.11). The remaining sequence variations were present in intergenic regions and near repetitive nucleotide sequences.

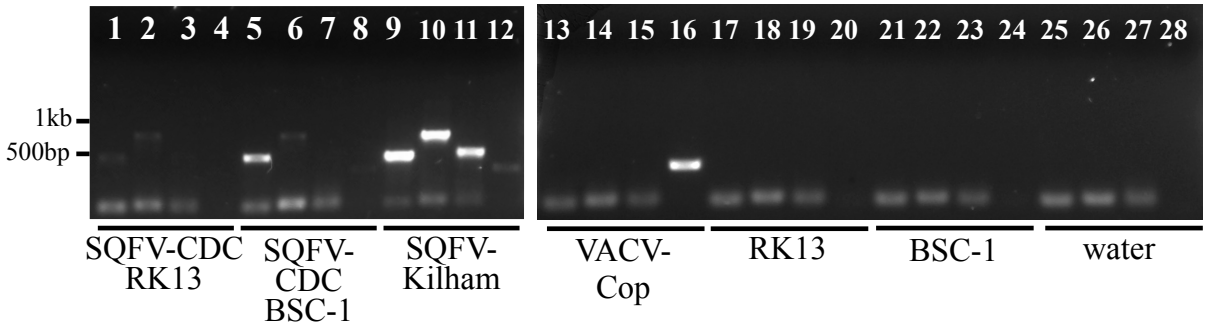

Amplified Product
1) recombination site in ITR
2) S076R, internal gene
3) S149R, internal gene
4) S046L, universal poxvirus primers

Figure 4.10 SQFV-CDC isolate DNA PCR.

DNA isolated from infected RK13 or BSC-1 cells was used as template for PCR analysis with primers specific for the recombination site in the ITR, two SQFV-specific gene regions outside of the ITR and one conserved gene using universal poxvirus primers.

Of the regions sequenced from the SQFV-CDC, two regions of particular interest were the recombination site in the ITR and the putative host acquired ORF S150. The presence of the recombination site that lies between ORFs S006 and S007 separating the OPV-like genes from the rest of the ITR was verified in the wild SQFV isolate DNA and was identical in sequence to the SQFV-Kilham strain sequence. Additionally, a positive PCR product was generated using primers targeted within the S001 B22R ortholog suggesting that at least one of the OPV-like ORFs is present in the wild SQFV strain. The presence of the putative ORF S150 was also confirmed in the wild strain with only one single nucleotide polymorphism identified that, if

expressed, would result in a proline to alanine amino acid change in the translated protein (Figs. 4.6 and 4.11).

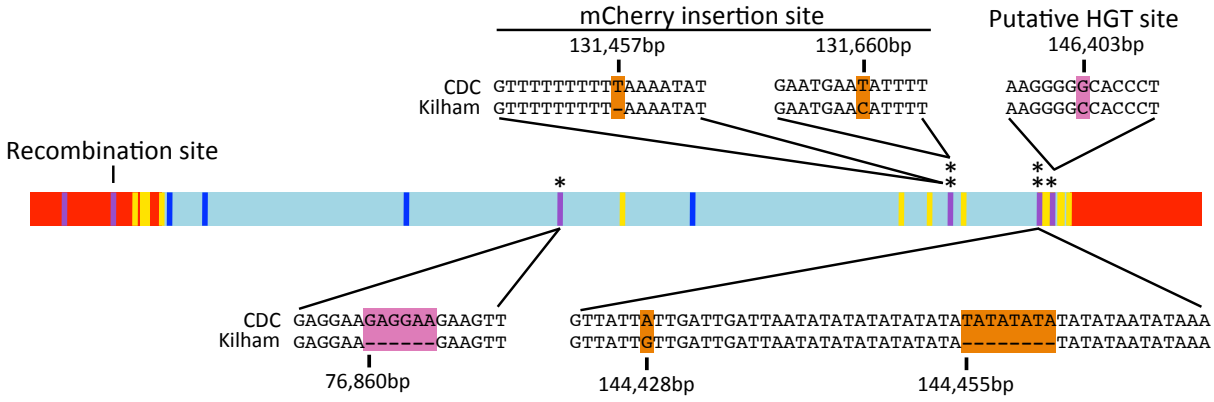

Figure 4.11 Map of SQFV regions amplified by PCR and confirmed by Sanger sequencing.
In the genome map, the ITR of the SQFV is shown in red and the remaining genomic region is shown in light blue. Regions amplified by PCR to confirm the correctness of the sequence in the SQFV-Kilham strain are represented by yellow or purple bars (bar width is an approximation of region covered; actual PCR lengths are detailed in Table 4.1). Regions amplified and sequenced from the SQFV-CDC isolate strain are represented by dark blue or purple bars. Purple bars are regions of the genome that were confirmed by Sanger sequencing in both the SQFV-Kilham and SQFV-CDC strains. Differences between the SQFV-CDC isolate strain sequence and the SQFV-Kilham strain are indicated with an asterisk above the amplified region. The nucleotide position for each genetic difference shown corresponds to the site in SQFV-Kilham. Differences that occur within a coding region are highlighted in pink, including the SNP in the putative horizontally transferred gene S150, which results in a Pro to Ala change if expressed. All other observed differences occur in intergenic sequences and are not predicted to result in differences in protein coding or expression.

Squirrel fibroma virus replication in cell culture

The SQFV has not been extensively characterized experimentally apart from early reports of animal infections after the initial isolation (4) and epidemiological reports from its sporadic emergence in squirrels (10, 14). To understand and characterize the replication of the SQFV in cell culture, we infected RK13 cells with the SQFV-Kilham and monitored its replication over 96 hours (Fig. 4.12). SQFV infection of RK13 cells did not cause plaque formation but only resulted in the formation of very small foci, which were difficult to clearly differentiate from the

normal accumulation of cell debris in confluent cell monolayers. Only infection foci large enough to be clearly identified were counted to reduce false positives from counting uninfected cell clusters. Thus the determined titers were likely lower than the actual titers. In order to obtain a virus for which replication could be more easily and reliably monitored, we engineered a SQFV that expresses the red fluorescent protein mCherry driven by a synthetic poxvirus early/late promoter (229). The mCherry gene was integrated into the intergenic region between S135 and S136 genes, which corresponds to the region that was previously used to generate a GFP-expressing MYXV (31). Additionally, we tested SQFV replication in BHK-21 since several viruses replicate well in these cells to see if higher virus titers could be obtained. The infection kinetics of the SQFV-mCherry virus was tested in RK13 (Fig 4.13) and BHK-21 (Fig 4.14) cells over a four-day period. SQFV-mCherry exhibited similar growth kinetics as the parental SQFV-Kilham virus in RK13 cells, although the parental virus appeared to reach titers ~8X lower than the SQFV-mCherry after 96 hours of infection, which was likely due to an underestimation of the foci generated by SQFV-Kilham.

The SQFV displayed a delayed replication phenotype compared to the other leporipoxviruses tested as well as vaccinia virus (Fig 4.13 and 4.14). A noticeable drop in titer from 0 hours post infection (hpi) was consistently observed after 12 hours of infection, likely representing the viral eclipse phase. Virus titers then quickly recovered to levels above input by 24hpi. Replication of both the SQFV-Kilham and SQFV-mCherry viruses increased logarithmically over the 96-hour period and eventually reached titers similar to both of the other leporipoxviruses, whose titers reached a plateau by 72hpi. From monitoring mCherry expression, the SQFV-mCherry continued to replicate beyond 120hpi (5 days) in both BHK-21 and RK13 cells (Fig 4.16 and data not shown). By comparison, RK13 cells infected with MYXV-GFP were visibly saturated with GFP by 72hpi (Fig 4.15), and cells infected with VACV-GFP were saturated by 48hpi, while SQFV-mCherry infected cells never completely disseminated through the monolayer nor reached visible saturation of the fluorescent signal. The VACV-GFP infected RK13 and BHK-21 cells were completely detached by 96hpi and were therefore disposed after this time. Thus no image was collected for the 5dpi time point for this virus (Figs 4.15 and 4.16). The replication kinetics of SQFV-mCherry in BHK-21 cells was very similar to its replication in RK13 cells and was even slightly better than RFV replication in these cells surpassing titers reached by RFV at 72hpi and steadily increasing after that (Fig 4.14).

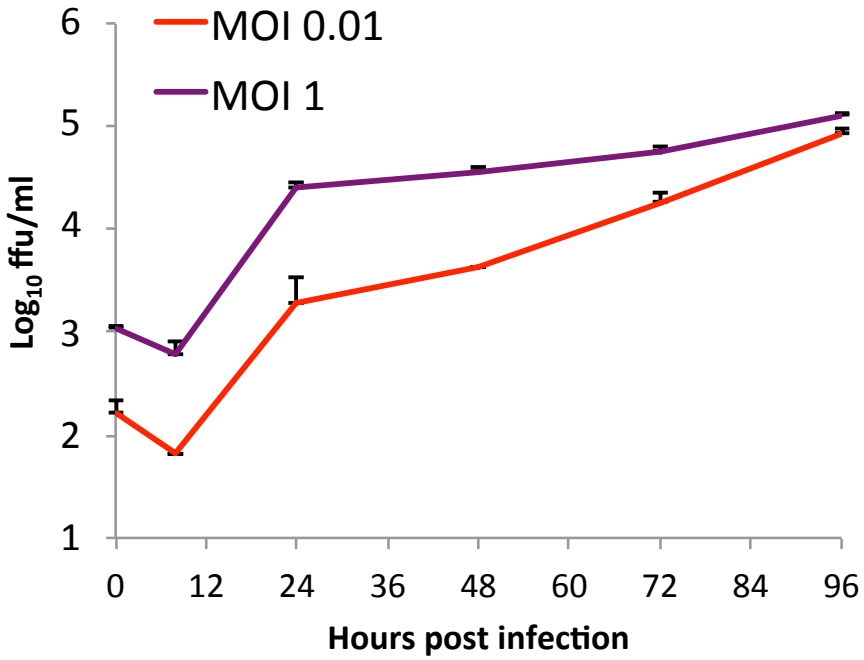

Figure 4.12 Replication of SQFV-Kilham in RK13 cells.

Confluent monolayers of RK13 cells in 6-well plates were infected with SQFV-Kilham at estimated MOI=1 and MOI=0.01. Titers were measured by counting focus forming units (ffu) on RK13 cells. Error bars represent the standard deviation of two independent replicate infections.

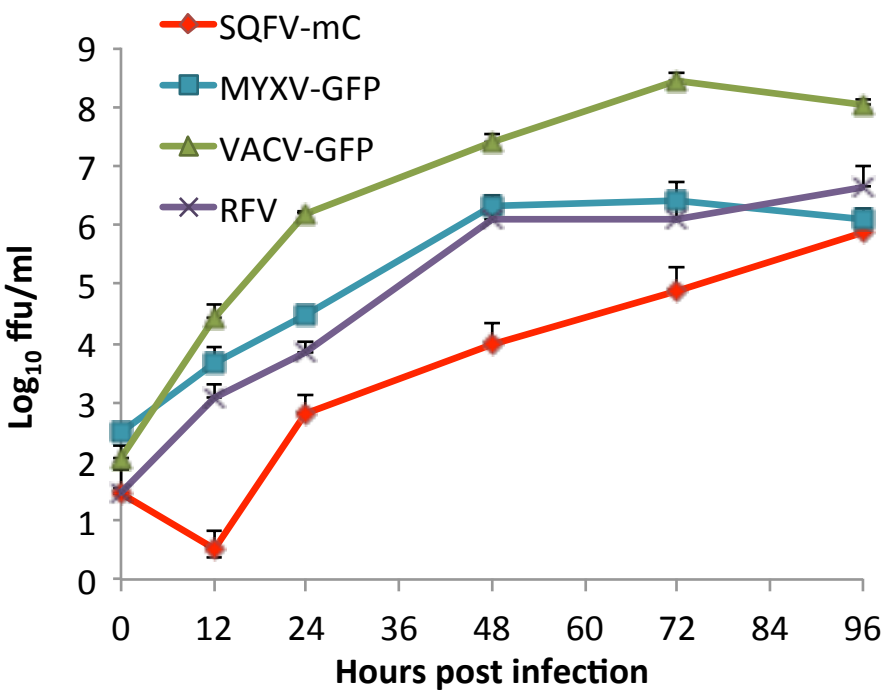

Figure 4.13 Replication kinetics of SQFV-mCherry and other poxviruses in RK13 cells.

Confluent monolayers of RK13 cells in 6-well plates were infected with SQFV-Kilham-mCherry (SQFV-mC), MYXV-Lu-GFP (MYXV-GFP), VACV-WR-GFP (VACV-GFP), or RFV at MOI=0.01. Titers were measured by counting focus forming units (ffu) or plaque forming units (pfu, for VACV) on RK13 cells. Error bars represent the standard deviation of three independent replicate experiments.

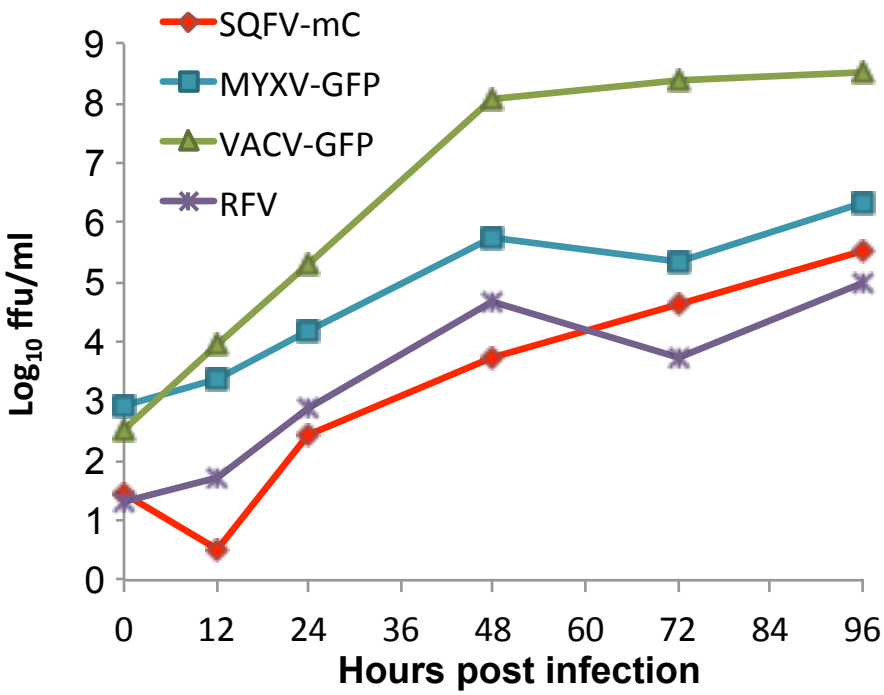

Figure 4.14 Replication kinetics of SQFV-mCherry and other poxviruses in BHK-21 cells. *Confluent monolayers of BHK-21 cells in 6-well plates were infected with SQFV-Kilham-mCherry (SQFV-mC), MYXV-GFP, VACV-GFP, or RFV at MOI=0.01. Titers were measured for the indicated time points by counting focus forming units (ffu) or plaque forming units (pfu, VACV-GFP) on RK13+E3L+K3L cells and are displayed on a logarithmic scale.*

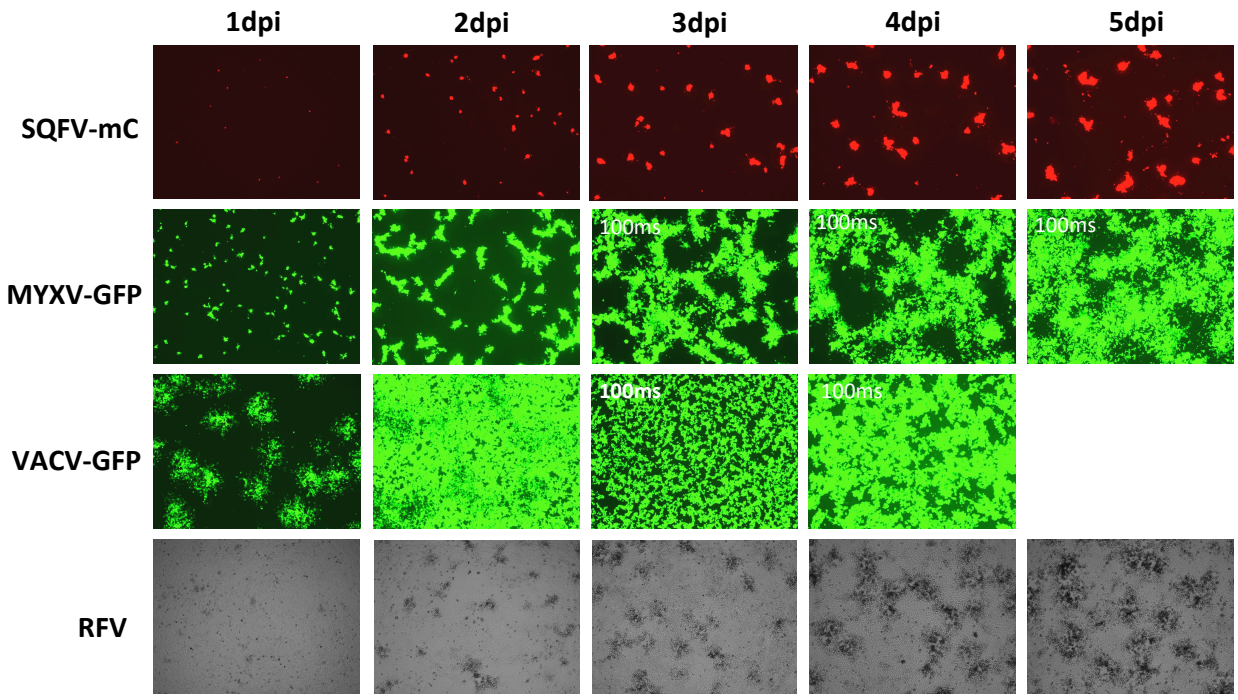

Figure 4.15 SQFV-mCherry forms tight foci of infection on RK13 cells.

Using the mCherry expressing SQFV (mC), replication of the SQFV could be easily monitored and compared to other fluorescent viruses from MXYV (Lu) and VACV (WR). Confluent monolayers of RK13 cells in 6-well plates were infected with each virus at MOI=0.01 and pictures were taken of the infected wells daily (100X magnification). All images of mCherry fluorescence were taken using a 600ms exposure time, while GFP fluorescent images were exposed for 300ms for days 1 and 2 post infection and 100ms for days 3-5 post infection due to the high intensity of the fluorescence at these times.

A cytopathic effect could be observed and compared for all four viruses in the RK13 cells, but none of the leporipoxviruses caused a visible cytopathic effect in the BHK-21 cells. At 24hpi only very small foci of SQFV-mCherry replication could be observed in RK13 cells compared to the large plaques formed by VACV-GFP and the large foci formed by MYXV-GFP (Fig 4.15). The size and brightness of the mCherry expressed from infection foci continued to increase over the study period, but the spread of the virus from the initial sites of infection was limited compared to that observed for MYXV-GFP. Some secondary infection foci were observed by 96hpi (4 days) in the SQFV-mCherry infected RK13 cells, but the majority of virus produced appeared to be restricted to the original cluster of infected cells. This may suggest inefficient viral spread, which may have an impact on the pathogenicity of this virus in its host. Attempts to express mCherry in RFV from the same genomic location as SQFV were

unsuccessful, but foci formed by RFV in the RK13 cells were easily identifiable by light microscopy. We observed a steady increase in infection focus size for RFV over the study period as well in the RK13 cells. By size comparison, RFV foci were larger and covered a larger proportion of the well than SQFV-mCherry at the same time points but were slightly smaller in size than those formed by MYXV-GFP. It is noteworthy, however, that in some experiments, RFV actually reached higher titers than MXYV-GFP at earlier time points in RK13 cells (Fig 4.17). These qualitative observations of the infection progression directly correspond to the observed titers for the SQFV-mCherry compared to both leporipoxviruses and VACV-GFP (Fig 4.13).

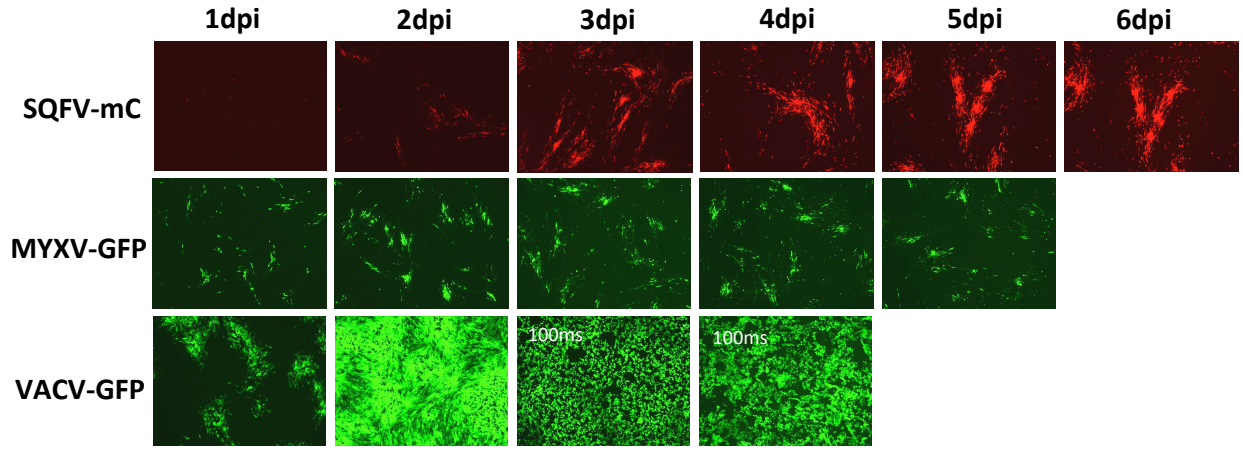

Figure 4.16 Replication of SQFV-mCherry, MYXV-GFP, and VACV-GFP in BHK-21 cells. *Confluent monolayers of BHK-21 cells in 6-well plates were infected with each virus at MOI=0.01 and pictures were taken of the infected wells daily (100X magnification). All images of mCherry fluorescence were taken using a 600ms exposure time, and all GFP fluorescent images were exposed for 300ms unless otherwise noted.*

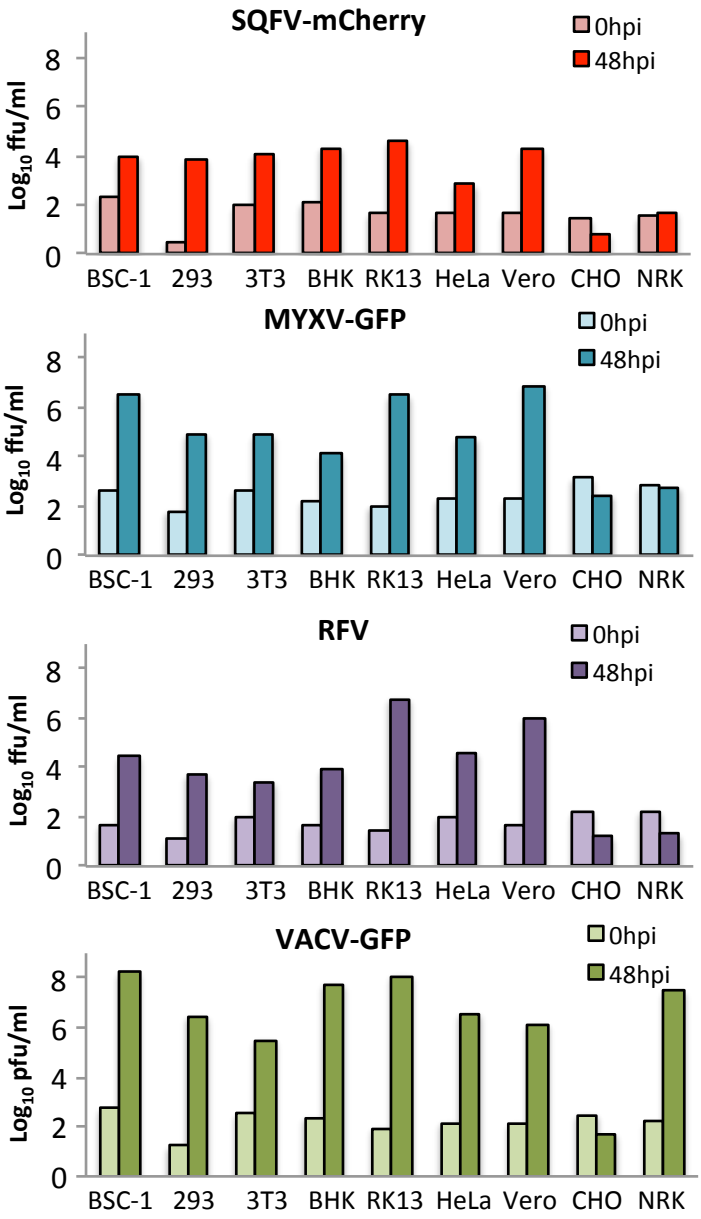

Figure 4.17 SQFV-mCherry replication in mammalian cell lines compared to other poxviruses. *Nine different mammalian cell lines were infected with SQFV-mCherry, MYXV-Lu-GFP, VACV-WR-GFP, and RFV at an MOI = 0.01. Titers were measured by counting focus forming units (ffu) or plaque forming units (pfu) on RK13+E3L+K3L cells and compared for each infection at 0 and 48 hours post infection (hpi). Titers are displayed on a logarithmic scale.*

In addition, to assess the replication of SQFV-mCherry in both RK13 and BHK-21 cells, we tested and compared its replication in 7 other mammalian cell lines to investigate the host range of SQFV (Figs 4.17-4.24). We observed a similar cell tropism for SQFV to both RFV and

MYXV-GFP. At 48hpi, both MYXV-GFP and VACV-GFP reached higher titers than SQFV-mCherry in every cell line tested except in BHK-21 cells where SQFV-mCherry actually reached titers slightly higher than MYXV-GFP, which was not observed in the replication curve, although differences in input may explain this difference (Fig 4.14 and 4.17). Lower levels of GFP expression can also be observed from MYXV-GFP infected BHK-21 cells (Fig 4.16) suggesting MYXV does not replicate well in these cells. SQFV-mCherry actually reached higher titers than RFV in three of the tested cell lines (293T, NIH/3T3, and BHK-21), but RFV reached the highest titer of all three leporipoxviruses in the rabbit derived RK13 cells. VACV-GFP replicated to higher titers than the three other viruses in almost all cell lines tested, but MYXV-GFP actually reached the highest titers by 48hpi in the African green monkey Vero cells. Vero cells lack a functional IFN response and were included in this analysis in an attempt to find a cell line that would yield high titers of the SQFV for amplification (230). However, SQFV-mCherry replicated to similar titers (~10^4 ffu/ml) in 6 of the 9 cell lines tested, including Vero cells. Only minimal replication was observed for SQFV-mCherry in human HeLa cells (~500 ffu/ml) with just a few small fluorescent foci observed (Fig 4.21). Chinese hamster CHO cells have previously been shown to be non-permissive to VACV infection without the expression of a CPXV gene, CP77 (231) and were included to test leporipoxvirus replication (Figs 4.17 and 4.19). None of the four viruses were able to replicate in these cells including VACV-GFP, confirming previous results. Furthermore, none of the leporipoxviruses were able to replicate in rat (*Rattus norvegicus*) NRK cells, while VACV-GFP reached high titers in these cells by 48hpi (Figs. 4.17 and 4.18).

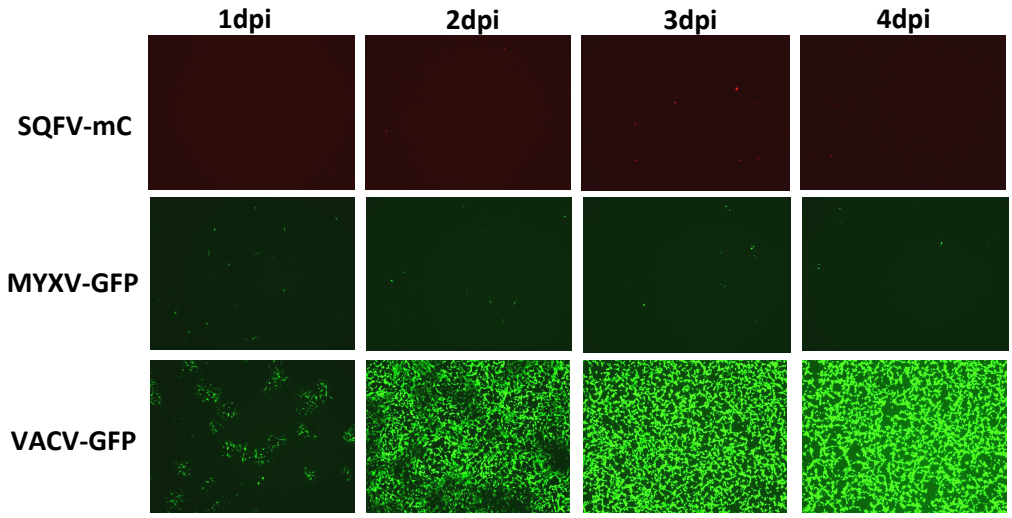

Figure 4.18 SQFV-mCherry (mC) replication in NRK cells.

Confluent monolayers of NRK cells in 6-well plates were infected with each virus at MOI=0.01 and pictures were taken of the infected wells daily (100X magnification). All images of mCherry fluorescence were taken using a 600ms exposure time, and all GFP fluorescent images were exposed for 300ms. None of the leporipoxviruses replicated in the rat NRK cells, but there was high GFP expression from VACV-GFP infections.

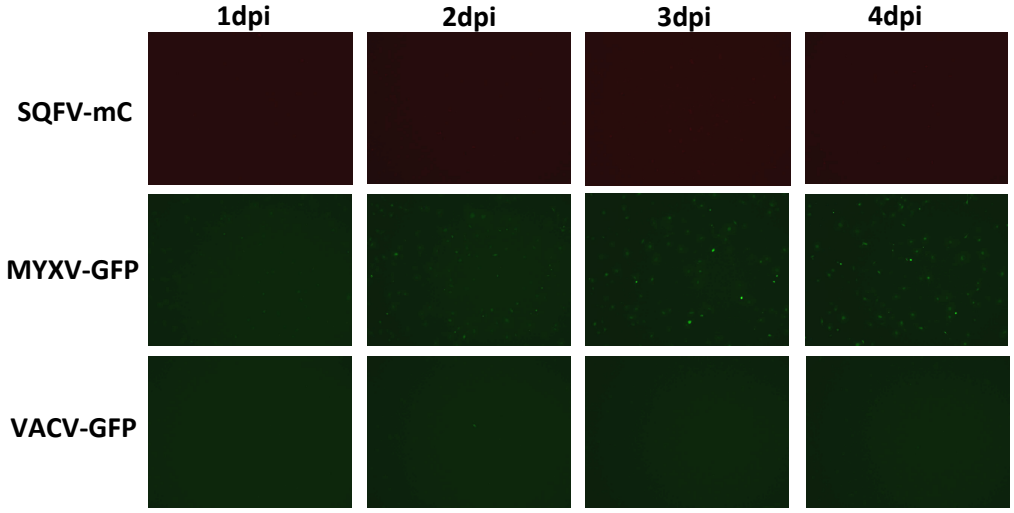

Figure 4.19 SQFV-mCherry (mC) replication in CHO cells.

Confluent monolayers of CHO cells in 6-well plates were infected with each virus at MOI=0.01 and pictures were taken of the infected wells daily (100X magnification). All images of mCherry fluorescence were taken using a 600ms exposure time, and all GFP fluorescent images were exposed for 300ms. No replication was observed for any of the viruses in these cells.

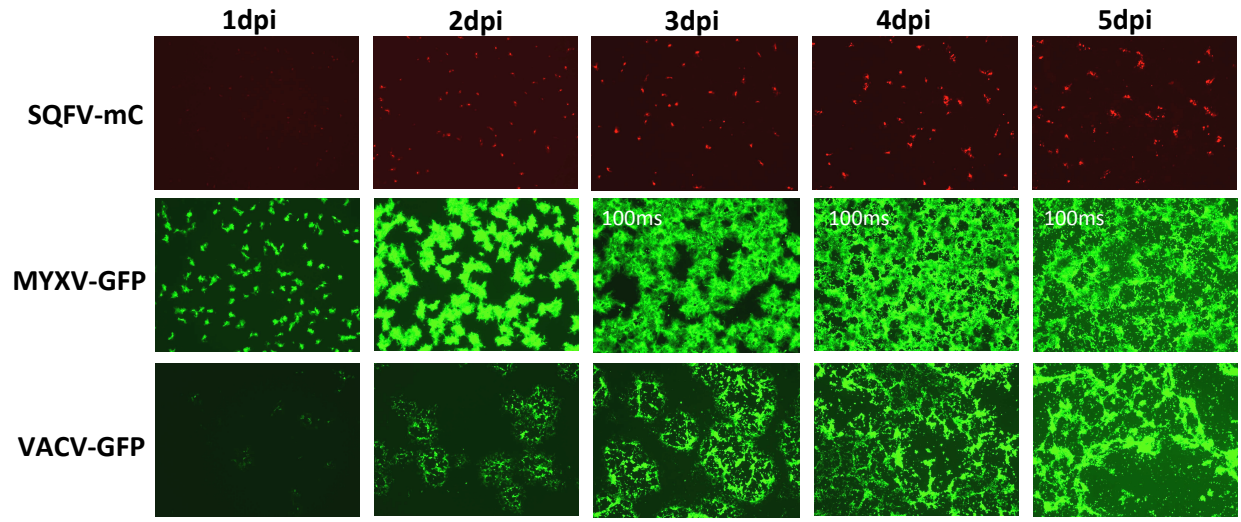

Figure 4.20 SQFV-mCherry (mC) replication in Vero cells.

Confluent monolayers of Vero cells in 6-well plates were infected with each virus at MOI=0.01 and pictures were taken of the infected wells daily (100X magnification). All images of mCherry fluorescence were taken using a 600ms exposure time, and all GFP fluorescent images were exposed for 300ms unless otherwise indicated. Fluorescent foci formed in SQFV-mCherry infected wells were very small but continued to increase in size over time. GFP expression from MYXV-GFP and VACV-GFP infections was higher, particularly for MYXV-GFP.

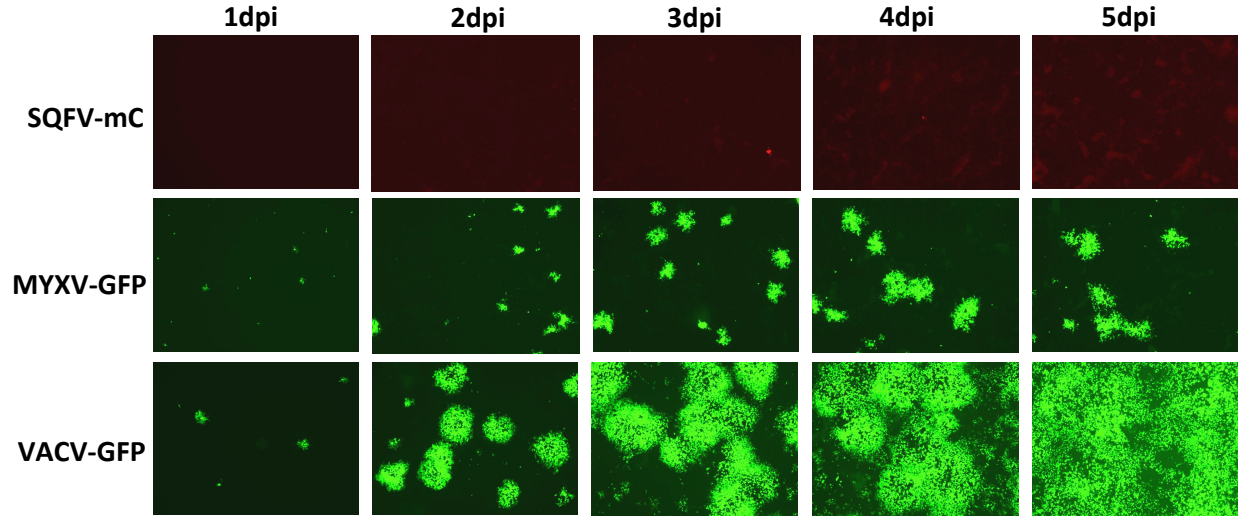

Figure 4.21 SQFV-mCherry (mC) replication in HeLa cells.

Confluent monolayers of HeLa cells in 6-well plates were infected with each virus at MOI=0.01 and pictures were taken of the infected wells daily (100X magnification). All images of mCherry fluorescence were taken using a 600ms exposure time, and all GFP fluorescent images were exposed for 300ms. Fluorescent foci from MYXV-GFP infected cells were restricted in size compared to VACV-GFP foci.

Only a few mCherry expressing foci were observed in SQFV-mCherry infected wells, but most of the cells were not infected.

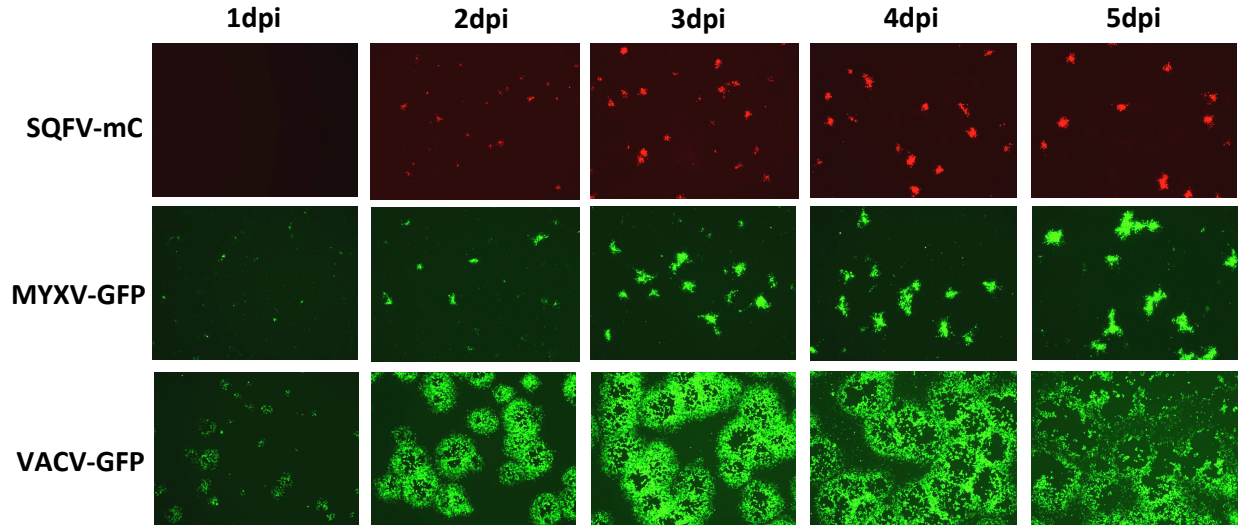

Figure 4.22 SQFV-mCherry (mC) replication in 293T cells.

Confluent monolayers of 293T cells in 6-well plates were infected with each virus at MOI=0.01 and pictures were taken of the infected wells daily (100X magnification). All images of mCherry fluorescence were taken using a 600ms exposure time, and all GFP fluorescent images were exposed for 300ms. Fluorescent foci for both MYXV-GFP and SQFV-mCherry increased in size at a similar pace, but foci formed by SQFV-mCherry did not spread as far as MYXV-GFP.

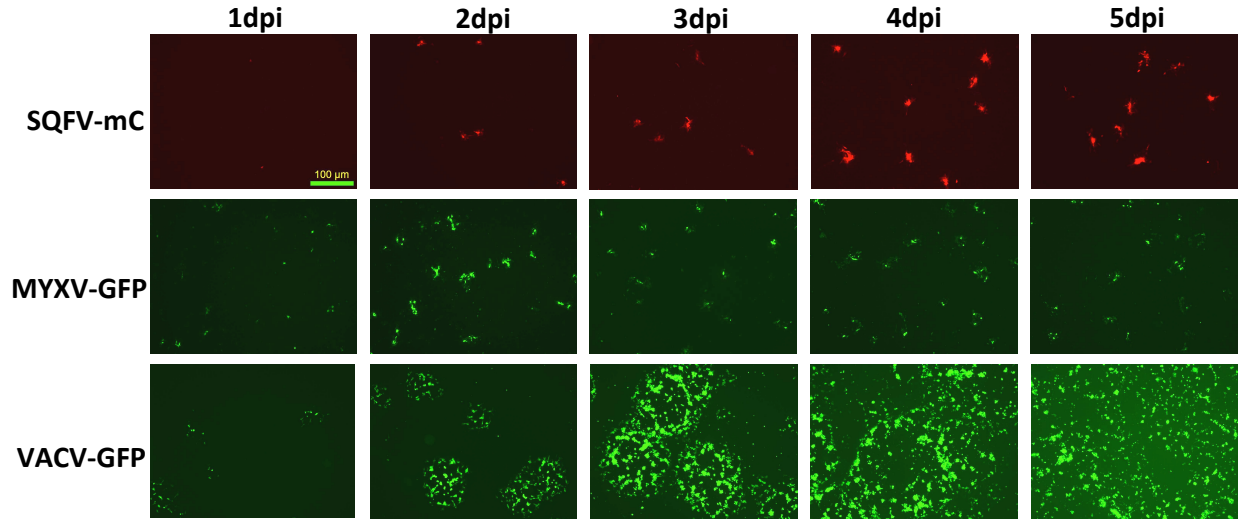

Figure 4.23 SQFV-mCherry (mC) replication in NIH/3T3 cells.

Confluent monolayers of NIH/3T3 cells in 6-well plates were infected with each virus at MOI=0.01 and pictures were taken of the infected wells daily (100X magnification). All images of mCherry fluorescence were taken using a 600ms exposure time, and all GFP fluorescent images were exposed for 300ms.

Fluorescent foci from SQFV-mCherry infected cells were less dense, but larger and brighter than foci from MYXV-GFP infected cells by 3dpi, whose replication was very restricted in these cells.

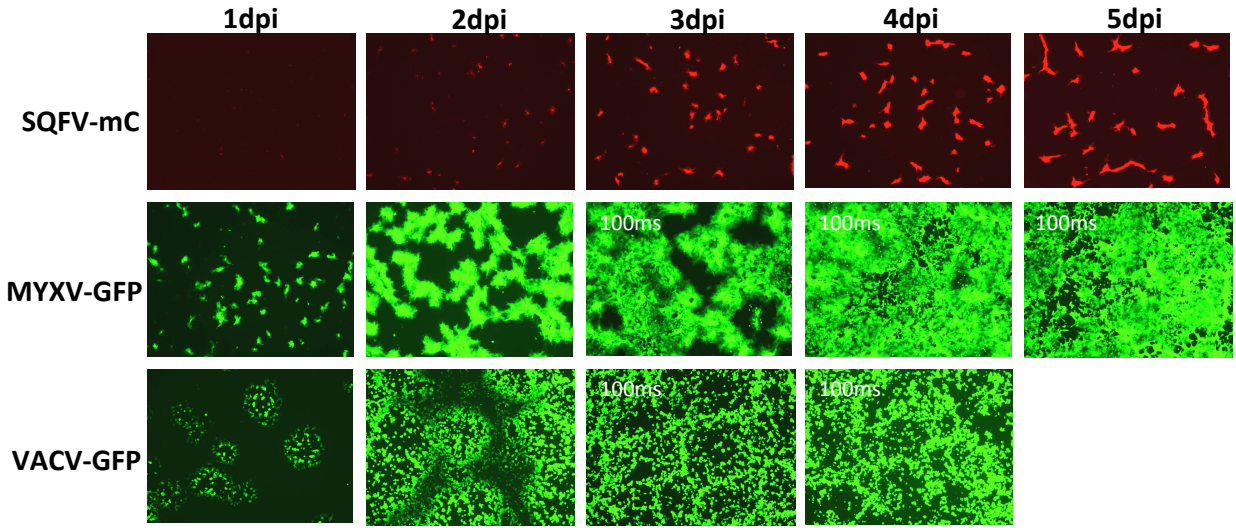

Figure 4.24 SQFV-mCherry (mC) replication in BSC-1 cells.

Confluent monolayers of BSC-1 cells in 6-well plates were infected with each virus at MOI=0.01 and pictures were taken of the infected wells daily (100X magnification). All images of mCherry fluorescence were taken using a 600ms exposure time, and all GFP fluorescent images were exposed for 300ms unless otherwise noted. VACV-GFP infected cells were discarded after 4dpi as cells were completely infected and detached.

Squirrel fibroma virus PKR inhibitors

Work from our lab and others has shown that inhibition of the antiviral response induced by the host RNA-dependent protein kinase (PKR) is a critical barrier to infection for poxviruses including VACV and MYXV (25, 29). PKR is a protein that senses cytoplasmic dsRNA generated during a virus infection, and once activated, phosphorylates the alpha subunit of the eukaryotic translation initiation factor 2 (eIF2α) to suppress general protein translation. MYXV genes M156R and M029L are orthologs of VACV K3L and E3L, respectively, which inhibit PKR at different stages of its activation and activity (26, 29, 209).

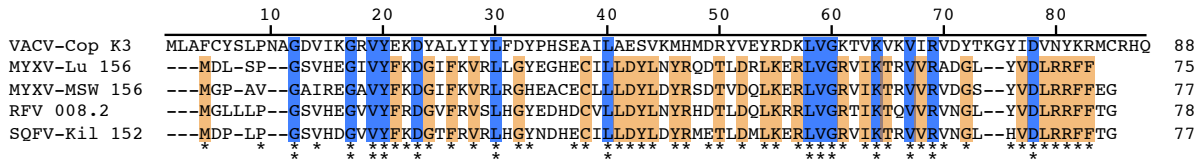

Figure 4.25 Sequence alignment of K3 orthologs.

Protein sequences from MYXV-Lu, MYXV-MSW RFV, and SQFV-Kilham were aligned in MUSCLE with VACV K3. Residues that are identical to the consensus are highlighted in blue and residues conserved in the leporipoxvirus orthologs are highlighted in orange. The SQFV K3 ortholog, S152R, is most similar to the other leporipoxvirus orthologs having 81.8% protein sequence identity with M156 from MYXV-Lu, 80.0% protein sequence identity to RFV156, 73.3% protein sequence identity to M156 from MYXV-MSW, and only 31.1% protein sequence identity to VACV K3. Asterisks indicate amino acid conservation (two asterisks for conservation in all five virus proteins and one asterisk for amino acid conservation in four out of the five).

An ortholog of MYXV M156R is present at a single location near the right end of the genome of SQFV (ORF S152). The ortholog in SQFV exhibits a higher protein sequence identity with both M156 and RFV 008.2, the K3 ortholog in RFV, than it does to VACV K3 (Fig 4.25). A recent study showed that M156R inhibits PKR from rabbit species specifically, and in subsequent work M156R was shown to inhibit PKR from its natural host, the brush rabbit (b. rabbit, *S. bachmani*), with the highest efficiency (29) (Peng and Rothenburg, unpublished). This species-specific inhibition likely contributes to the restriction of this virus to rabbit host species. In order to determine if the K3L ortholog in SQFV can inhibit PKR and if there is any species-specificity to this inhibition that may contribute to its restricted host range, we cloned the S152 gene from the SQFV into a mammalian expression vector and tested its ability to inhibit PKR from human, Syrian hamster, mouse, European rabbit, brush rabbit, cottontail rabbit and Guinea pig in a luciferase transfection assay, which has been used previously to look at PKR inhibition by viral inhibitors (28, 29). Due to the lack of sequence information available for tree squirrel species, we were not able to test PKR from a squirrel, although several attempts were made to clone PKR from a fox squirrel.

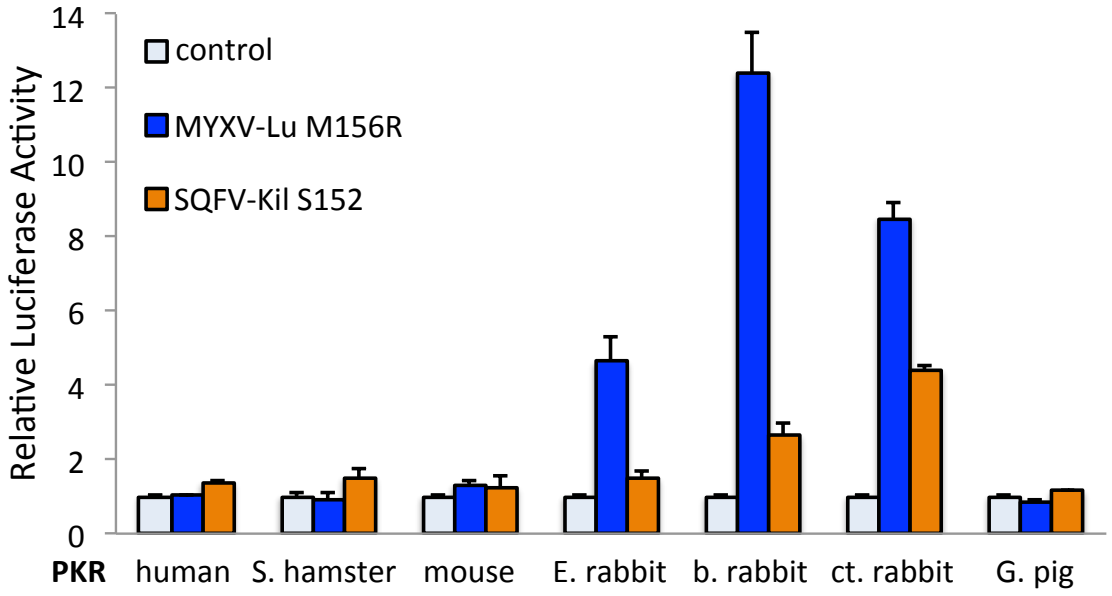

Figure 4.26 Species-specific inhibition of PKR by MYXV M156R and SQFV S152.
HeLa-PKRkd cells were co-transfected with plasmids encoding PKR from different species (0.2µg), MYXV M156R or SQFV S152 (0.4µg), and firefly luciferase (0.05µg). Luciferase activity was normalized to PKR only transfections for each species' PKR and error bars represent the standard deviation of three replicate transfections.

Confirming previous results, M156R from MYXV only inhibited PKR derived from rabbit species, and PKR from the b. rabbit, myxoma virus' natural host, was most sensitive to inhibition by MYXV M156R. Similarly SQFV S152 was unable to inhibit the PKR from most species tested (human, Syrian (S.) hamster, mouse and Guinea (G.) pig), but surprisingly unlike with M156R, PKR from the European (E.) rabbit was also resistant to inhibition by SQFV S152 (Fig 4.26). Only the b. rabbit and cottontail (ct., *S. floridanus*) rabbit PKRs were sensitive to inhibition by S151. The resistance of E. rabbit PKR to inhibition by S152 is curious because we showed that SQFV replicates in E. rabbit derived RK13 cells, albeit relatively slowly compared to either MXYV or RFV. Nevertheless, SQFV must be able to overcome PKR activity in these cells.

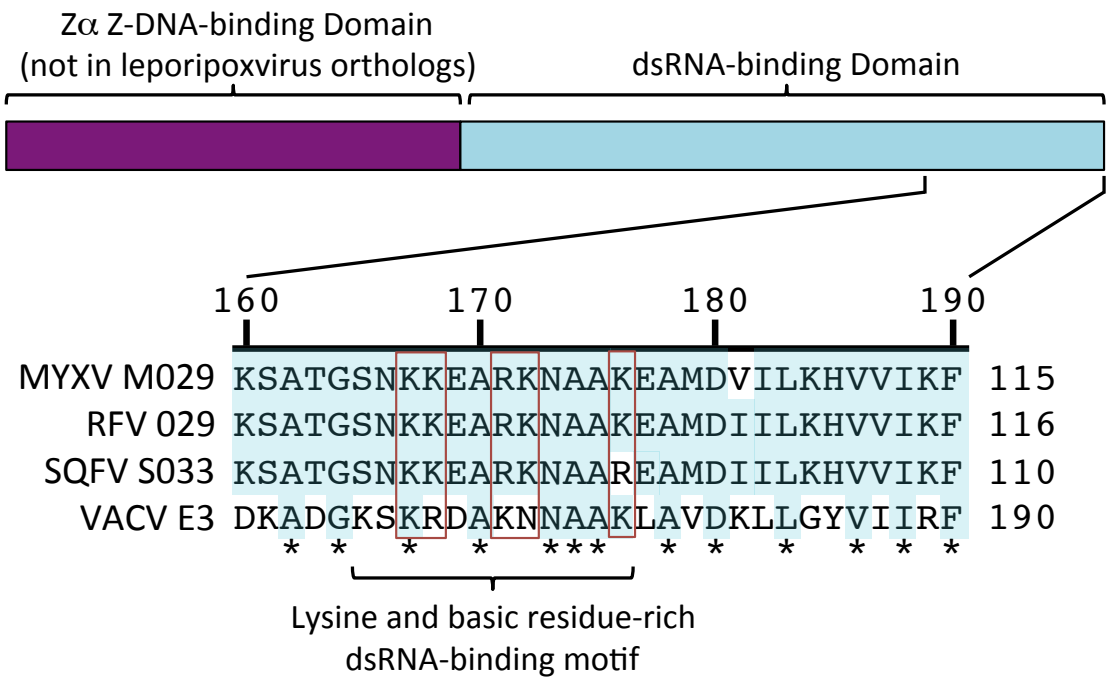

Figure 4.27 Alignment of SQFV S033 dsRNA-binding motif with other E3 orthologs.

A domain map of VACV E3L is shown indicating the Zα and dsRNA-binding domains. The E3L ortholog from SQFV resembles both M029L and RFV 029L in that it lacks the N-terminal Zα Z-DNA-binding domain found in VACV E3L and in E3L orthologs from other poxviruses. A multiple sequence alignment of MYXV M029, RFV 029, SQFV S033, and VACV E3 proteins was made using ClustalW, and the last 30 residues are expanded to show the similarity in the dsRNA-binding domains of the E3 orthologs. Amino acid residues that are identical are highlighted in light blue. Residues conserved in all four orthologs are indicated with an asterisk.

An ortholog of VACV E3L is also present in the SQFV genome (ORF S033) that exhibits a 40.0% identity to the VACV E3L protein and an 85.3% identity to M029L, the ortholog from MYXV. VACV E3L is composed of two functional domains: an N-terminal Zα Z-DNA binding domain and a C-terminal dsRNA-binding domain, while the E3L orthologs found in the leporipoxviruses and SQFV lack the portion encoding the Zα domain and only encode the dsRNA-binding domain (Fig 4.27). The C-terminal dsRNA-binding domain of VACV E3L contains a lysine-rich motif that is important for binding dsRNA and inhibiting PKR, and deletion of the last 26 amino acids of VACV E3L abolishes its ability to bind dsRNA and inhibit PKR (232). When we compared these with the protein sequence of the E3L ortholog in SQFV, a

similar lysine and basic residue-rich motif was identified in the C-terminus that bears homology with the leporipoxvirus orthologs (Fig 4.27).

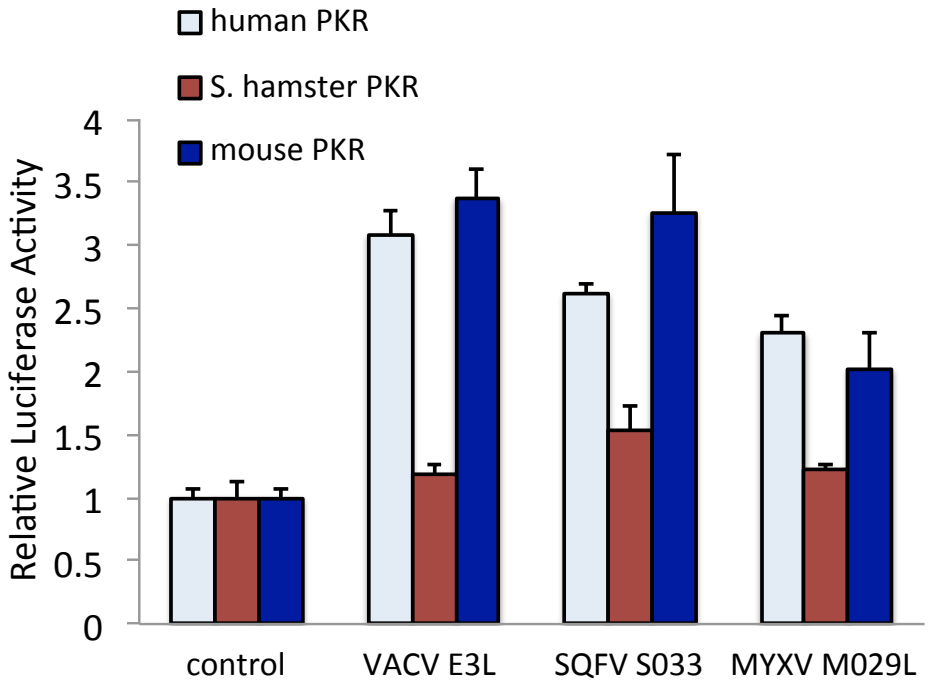

Figure 4.28 SQFV S033 is a functional inhibitor of PKR.

HeLa-PKRkd cells were co-transfected with plasmids encoding human, Syrian (S.) hamster, or mouse PKR (0.2μg), VACV E3L, SQFV S033, or MYXV M029L (0.4μg), and firefly luciferase (0.05μg). Luciferase activity for each transfection was normalized to transfections with each PKR alone with luciferase. Error bars indicate the standard deviation of three replicate transfections.

We cloned S033 from SQFV and tested its ability to inhibit PKR compared to VACV E3L and MYXV M029L. S033 inhibited PKR from human and mouse PKR similarly to VACV E3L and even slightly better than MXYV M029L (Fig 4.28). The S. hamster PKR, which our previous results show is resistant to inhibition by VACV E3L and other dsRNA-binding proteins (Ch. 2), was largely insensitive to inhibition by SQFV S033, but interestingly, we consistently see a slight increase in luciferase activity that would suggest S033 is able to partially inhibit S. hamster PKR activity. Whether this modest inhibition would be enough to prevent translational shut-down by this species' PKR during a virus infection is still unclear. However, this data clearly indicate that the E3L ortholog in SQFV is a functional inhibitor of PKR from human and

mouse species. Previous work indicates that M029L from MYXV is not a species-specific inhibitor of PKR, but like VACV E3L, M029L is critical for virus replication both in cell culture and *in vivo* (26, 29). It is therefore likely that S033 is also an important immunomodulatory protein for SQFV.

Discussion

The genome of the SQFV has offered several new clues into its evolutionary history and relationship to the members of the *Leporipoxvirus* genus. Of the four recognized leporipoxvirus species (MYXV, RFV, FIBV, and SQFV), SQFV is the only virus that is not naturally restricted to lagomorph host species (rabbits and hares). All of the leporipoxvirus species have very limited host ranges and infect only a few species (15). The impact of these dedicated host-virus relationships on leporipoxviruses such as MYXV has resulted in the accumulation of genetic differences that result in species-specific activity of the viral proteins, some of which have a host range function (29, 121).

Our phylogenetic analysis shows that SQFV forms a monophyletic clade with the two MYXV strains and RFV within the group of Clade II viruses, and thus confirms the characterization of SQFV as a member of the *Leporipoxvirus* genus (Fig. 4.2). The analysis further show that MYXV-Lu and MYXV-MSW were more closely related to each other than to either RFV or SQFV, and that the MYXV strains are more closely related to RFV than to SQFV, which indicates that SQFV is the most divergent of the sequenced leporipoxviruses. The phylogeny of the chordopoxviruses further shows that the arrangement of the basal branches mirrors the evolution of vertebrate classes, with salmon gill poxvirus, which infects salmon, forming the most basal branch, followed by crocodilepox virus (infects Nile crocodiles) and the avipoxviruses, canarypox and fowlpoxviruses (infect birds), and finally the clade of poxviruses that infect mammals including the orthopoxviruses and Clade II poxviruses. Although non-mammal-infecting poxviruses are underrepresented, this indicates that the poxviruses did not switch between major host classes and supports an early origin of the poxvirus family.

It is also interesting to note, that the South American MYXV strains encode the most genes common to this genus, while the other leporipoxviruses, including MYXV-MSW, RFV, and SQFV, evidently lost several of these orthologs found in the South American strains (Figs 4.4 and 4.5, Table 4.6). It seems, therefore, that the genome of the South American MYXV

strains, including MYXV-Lu, best represents the ancestral leporipoxvirus genome, and different evolutionary pressures to retain or lose these genes marked the divergence of SQFV, RFV and MYXV within this lineage of poxviruses.

Poxvirus genomes can be divided into broad regions of genes based on their function and overall conservation in poxviruses. Genes of the central core region of poxvirus genomes are broadly conserved across the family both in their genomic arrangement and in their sequences. These genes encode proteins necessary for replicating the viral genome, viral transcription factors, and structural genes involved in viral morphogenesis (233). The genes near the genomic termini, on the other hand, are more often associated with host immune evasion and host range functions and are more variable between poxvirus species. In general, *Leporipoxvirus* genus members all share a relatively high sequence identity to each other. MYXV and RFV exhibit on average 87% protein identity in the central core region of the genome and around 70% in the termini. The genetic conservation of SQFV in comparison with these other leporipoxvirus members is similarly high with amino acid sequence identities for proteins encoded in the central region of the genome averaging 87.5% to either RFV or MYXV and ranging between 62% and 98% for individual proteins.

The major exception to this conservation is found in the ITR of SQFV, where the first six genes remarkably show the highest protein sequence identity levels to orthopoxvirus (OPV) orthologs. Additionally, ORFs S007 through S010 exhibit low sequence identities to orthologous proteins of other sequenced poxviruses. However, due to a higher sequence identity with orthologous proteins found in capripoxviruses than to any other orthologs tested, it is possible that these genes originated from an as-of-yet unidentified Clade II poxvirus. The presence of the OPV-like genes in the ITR of SQFV provide strong evidence that the leporipoxvirus ancestral to SQFV recombined with an OPV to acquire these genes. Furthermore, although the origin of the four ITR genes following these six genes is unknown, the distinct change in sequence identity for these encoded proteins suggest a second recombination occurred with the ancestral SQFV and another possibly more related poxvirus. From the sequence of SQFV-Kilham alone, it is not apparent whether this second recombination occurred in the ancestral OPV prior to the initial recombination that resulted in the acquisition of the first six OPV-like ORFs or whether the ancestral SQFV first acquired the divergent ORFs from another poxvirus and later recombined with an OPV. The sequencing of more SQFV isolates that have altered ITR gene contents may

shed light on this question. The findings that an identical recombination site sequence as well as an ortholog of CPXV B22R is also present in the genome of the SQFV-CDC isolate from Ohio clearly indicate that the OPV-like genes identified in SQFV-Kilham are maintained in natural populations of the virus and have remained genetically stable over the 56 years since the isolation of SQFV in Maryland (4).

One explanation for the maintenance of these novel genes in the genome of SQFV may be that several of these genes have putatively homologous functions to genes that are missing from the rest of the genome relative to the other leporipoxviruses (Table 4.7). For example, S010 encodes a putative IL-1 receptor homolog with the highest sequence identity to ORF 007 in DPV. This protein could perform a similar function as M135R in MYXV, which is an IL-1/6 receptor homolog whose direct ortholog is missing in SQFV and is also fragmented in RFV. The absence of this gene in RFV, along with orthologs for both M136R and M139R, which share a predicted bcl-2-like fold domain and may play a role in inhibiting the apoptotic response during infection, might also have an effect on the virulence and host range of this virus. Because SQFV, which shares an ancestor with MYXV and RFV according to our phylogeny, encodes complete ORFs for orthologs of both M136R and M139R, their absence from the RFV genome may suggest there was a less stringent selective pressure to maintain multiple proteins that inhibit the apoptotic response for this virus (Fig 4.4, Table 4.5).

SQFV	**MYXV**	**Putative Function**
S001/S165	M134R	glycoprotein, unknown
S004/S162	M003.1L/R	intracellular virulence factor, NF-κB signaling inhibitor
S005/S161	M151R	SERP-2/IL-1 convertase inhibitor
S006/S160	M004L/R	apoptosis regulation
S009/S157	M007L/R	IFN-γ receptor homolog
S010/S156	M135R	IL-1 receptor homolog

Table 4.7 Recombined genes may compensate for missing leporipoxvirus genes.
A table of genes found in the SQFV ITR is shown that have similar predicted functions to the leporipoxvirus genes that have been lost in SQFV.

The complete absence of both orthologous sequences of M134R and M135R in the SQFV genome might have resulted from a single excision of both genes entirely, and it is possible that the loss of the M134R ortholog in SQFV occurred soon after or simultaneously with the acquisition of a B22R ortholog in the ITR during recombination with an OPV. M134R, which is homologous to CPXV B22R although sharing relatively low amino acid sequence identities, is present near the right end of the genome in MYXV and RFV. Cowpox virus B22R encodes a large glycoprotein with an unknown function but whose presence in poxvirus genomes is well conserved (45). In some poxvirus lineages, several copies of B22R orthologs are encoded despite the large size of this gene, suggesting it has a functional importance (234).

Another interesting feature is that SQFV has lost all functional orthologs of its MXYV serpin family genes. However, SQFV S005/S160 encodes an ortholog of CPXV CrmA, which is related to MXYV SERP-2 (M151R) (Table 4.7). RFV also lacks orthologs of both SERP-1 (M008.1L/R) and SERP-3 (M152R), but while fragmented remains of each are present in RFV, no evidence of either exists in the SQFV genome. RFV, however, maintains a complete SERP-2 ortholog (RFV 151R). Deletion of M151R from MYXV has been shown to attenuate virus replication *in vivo* and reduce infection-associated pathology (206). Because it has been clearly demonstrated for MYXV that the activity of poxviral serpins is important for virulence and host range, it is possible that the activity of S005/S161 protein product exerts similar functions. The two-base pair insertion in S149, the ortholog of M151R that results in the truncation of this gene is interesting in that the rest of the ORF remains intact. This could indicate that the frameshifting mutation was acquired recently and likely after the OPV-like SERP-2 was added to the genome of this leporipoxvirus.

Additionally, in the ITRs of both RFV and MYXV, M003.1L/R, M004L/R and M007L/R encode proteins that play important roles in modulating the immune response during MYXV infection (1, 2). Orthologs for all of these genes are missing in SQFV (Table 4.6). SQFV S009/S157, which exhibits the highest sequence similarity with ORF 010 in DPV, shares a predicted function with M007L/R (M-T7) as an IFN-γ receptor homolog, which is a critical virulence factor for MYXV in E. rabbits (235). SQFV ORFs S004/S162 and S006/S160 encode proteins with putatively similar functions as M003.1L/R and M004L/R, respectively, but both are most similar in sequence to the OPV orthologs. In fact, the first six OPV-like genes in the ITR of SQFV all show the highest sequence identity with OPV orthologs and are syntenic with

their counterparts in the CPXV genome (Fig 4.29). CPXV has a very broad host range and like other OPVs, its host range includes several rodent species such as rats and mice (236-238). While there is no complete genome sequence for any arboreal squirrel species for which the SQFV has been shown to infect, squirrels are classified as members of the order *Rodentia* and are therefore more closely related to other rodent species than they are to lagomorph rabbit and hare species. It is possible that the acquisition of these OPV-like genes was important in the evolution of the SQFV host range relative to the other leporipoxviruses.

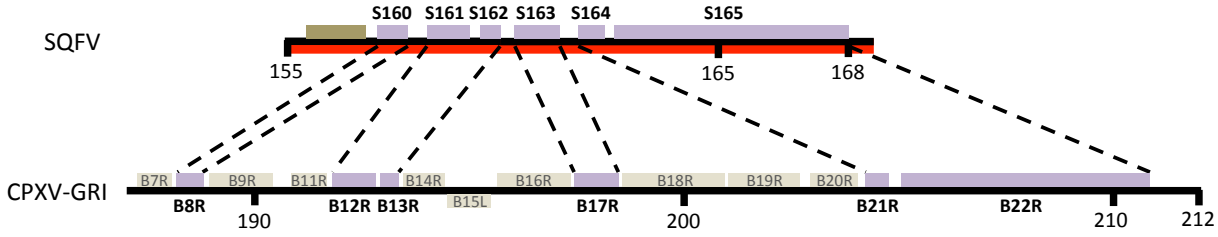

Figure 4.29 Conserved synteny of SQFV and CPXV genes.

The six outermost genes present in both ends of the SQFV ITR (right end of genome shown) bear the highest amino acid sequence identity with orthologous genes found in orthopoxviruses (OPV). A comparison of the SQFV OPV-like gene order in the ITR with their orthologs as they are ordered in the genome of the cowpox virus-GRI-90 (CPXV-GRI) is shown. Light purple boxes represent the OPV-like ORFs in SQFV and the closest orthologs in CPXV-GRI. In the CPXV genome, genes B8R through B22R are present in the far right end of the genome, but are not part of the CPXV ITR. The B22R gene in CPXV-GRI is followed by 3.7kb of open reading frames before the 8.3kb ITR begins (not shown). Several genes (light brown boxes) between these orthologous CPXV genes are also found in the CPXV genome that are not in the SQFV genome.

Cowpox viruses are also included in a group of OPVs that are referred to as “old-world” OPVs in contrast to the OPVs found in North America such as the volepox virus and raccoonpox virus (RCPV) identified in recent years (17, 211, 239). Sequence analyses suggest a clear genetic separation of these viruses from the old-world OPVs first identified in Europe, Asia, and Africa (240). The high protein sequence identity of the OPV-like ORFs in the ITR of SQFV to an old-world OPV and the close relationship of S004/S162 to orthologous sequences from old-world OPVs suggest that the recombination event that resulted in the acquisition of the six OPV-like ORFs in the ITR of SQFV occurred with an old-world OPV rather than a North American OPV.

To date, all cases of SQFV infection have been reported in North America, but for recombination to occur, they must have co-infected a host cell, and therefore they must also have been in the same geographic location. It is possible that OPVs may have been present in North America that went unrecognized but remained genetically similar to the well-known OPVs present in Europe and Asia, such as CPXV, VACV and VARV. The actual distribution of these so-called "old-world" OPVs then may have been broader than previously appreciated.

Within the SQFV genome, there are only three genes whose predicted functions are unique to the *Leporipoxvirus* genus (Table 4.8). Two of these genes, S003/S163 and S008/S158 are predicted to encode a soluble α/β IFN receptor and phospholipase D-like protein, respectively, while the third gene, S002/S164 is homologous to CPXV B21R, whose function is unknown. The soluble α/β IFN receptor is likely to have an immunomodulatory function, but the importance of the phospholipase D-like protein in viral virulence or host range is unclear. Phospholipase D family proteins can be found in other poxviruses and are surface proteins that may play a role in protein trafficking and the formation of the intracellular envelope from post-Golgi vesicles (241).

SQFV	**RFV**	**MYXV**	**Predicted function**
S002/S164	Absent	Absent	unknown
S003/S163	Absent	Absent	soluble α/β IFN receptor
S008/S158	Absent	Absent	phospholipase D-like
S150	Absent	Absent	unknown

Table 4.8 Novel genes in SQFV not found in other leporipoxviruses.

Genes found in SQFV that have no ortholog in the other leporipoxviruses are shown with their predicted functions

.

We found that both SQFV orthologs of MYXV M029L and M156R are functional inhibitors of the antiviral host protein, PKR (26, 29). We have unsuccessfully attempted to clone squirrel PKR from a fox squirrel (*Sciurus nigers*) to test for species-specific inhibition that may account for the host range restriction of SQFV, but cloning was made difficult by the lack of sequence information for this species. Nevertheless, the exclusive sensitivity of PKR from North American rabbit species to S152 suggest some species-specific selection for PKR inhibition may have occurred. In particular, the southeastern cottontail rabbit PKR was most sensitive to

inhibition by S152, which is interesting considering the two largest outbreaks of SQFV occurred in gray squirrels of eastern Florida within the same territory as the eastern cottontail. Cottontail rabbits were infected experimentally in some of the original experiments with the SQFV but they are not known to be naturally infected by the virus (4). While the importance of PKR inhibition in determining the host range of SQFV requires further studies, the results presented here offer evidence that a direct ancestor of SQFV may have once been able to infect rabbit populations in regions near where it has been found. Alternatively, this rabbit species or similar species may have been or still is a reservoir host for the virus between outbreaks in squirrels. Further evidence supporting the idea that SQFV originally infected rabbit species comes from the presence of the potential horizontally transferred ORF in the SQFV genome, S150. This short ORF bears the highest similarity to part of the 28S rRNA gene in European rabbits suggesting it may have come from a rabbit host (Fig. 4.6). This gene however, is highly conserved in mammals. Therefore it is possible that the ORF actually originated from a squirrel, but the lack of sequence information for appropriate squirrel species in the database prevents the detection of such similarities.

SQFV infections in nature are infrequently and sporadically reported, but this virus only causes a noticeable disease in young or immunocompromised individuals. With the exception of the epizootics that have occurred in populations of gray squirrels in Florida, there are few well-described cases (10). Similarly, MYXV infections of its natural hosts, the American brush rabbit and tapeti, are largely benign and are only rarely lethal. This may indicate that like MYXV in American rabbits, SQFV has reached a co-evolutionary equilibrium with its squirrel host species. It is currently unknown what caused the outbreaks of SQFV to occur in the 1990's, but it would be interesting to compare the sequence of virus isolates from these outbreaks with this reference genome to see what changes might explain the altered virulence.

Our results suggest that SQFV replicates in cell culture similarly to both MYXV and RFV, but most notably, SQFV replication was slower than either RFV or MYXV in most of the cell lines tested. Future studies looking into the putative functions of the SQFV genes involved in these differences are needed. Furthermore, MYXV, as a rabbit specific pathogen, cannot replicate in normal human cells but due to an observation that MYXV can replicate in some human cancer cells, MYXV is currently being investigated as an oncolytic virus to be used to treat cancer (242). The restricted host-range of SQFV and the attenuated replication phenotype of

this virus in human cells make the idea of using SQFV as a possible oncolytic agent promising and worth future investigation.

Author contributions

This study was initiated and the experiments were conceived and designed by S.L.H. and S.R. Illumina-MiSeq sequencing reactions and compiling of raw sequences were performed by Z.K., K.R.C., S.G., and N.E. Sequence annotation and evolutionary analyses were performed by S.L.H, A.J.S, L.T., and S.R. The wild SQFV isolate was donated by N.G-R., I.K.D. and G.E. Cell culture experiments and recombinant virus construction was performed by S.L.H, A.J.S., and C.R.

References

1. Willer DO, McFadden G, Evans DH (1999) The complete genome sequence of shope (rabbit) fibroma virus. *Virology* 264(2):319–343.

2. Cameron C, Hota-Mitchell S, Chen L, Barrett J, Cao JX, Macaulay C, Willer DO, Evans DH, McFadden G (1999) The complete DNA sequence of myxoma virus. *Virology* 264(2):298–318.

3. Kirschstein RL, Rabson AS, Kilham L (1958) Pulmonary lesions produced by fibroma viruses in squirrels and rabbits. *Cancer Res.* 18(1):1340-1344.

4. Kilham L, Herman CM, Fisher ER (1953) Naturally occurring fibromas of grey squirrels related to Shope's rabbit fibroma. *Exp Biol Med*. 82:298-301.

5. Kilham L (1955) Metastasizing viral fibromas of grey squirrels: pathogenesis and mosquito transmission *Am J Epidemiol* 61(1):55-63.

6. King JM, Woolf A, Shively JN (1972) Naturally occurring squirrel fibroma with involvement of internal organs. *J Wildl Dis* 8(4):321–324.

7. Bangari DS, Miller MA, Stevenson GW, Thacker HL, Sharma A, Mittal SK (2009) Cutaneous and systemic poxviral disease in red (Tamiasciurus hudsonicus) and gray (Sciurus carolinensis) squirrels. *Vet Pathol* 46(4):667–672.

8. Hirth RS, Wyand DS, Osborne AD, Burke CN (1969) Epidermal changes caused by squirrel poxvirus. *J Am Vet Med Assoc* 155(7):1120–1125.

9. Robinson AJ, Kerr PJ (2001) Poxvirus infections. *Infect Dis Wild Mammals*. pp179-201.

10. Terrell SP, Forrester DJ, Mederer H, Regan TW (2002) An Epizootic of Fibromatosis in Gray Squirrels (Sciurus Carolinensis) in Florida. *J Wildl Dis* 38(2):305–312.

11. Regnery RL (1975) Preliminary studies on an unusual poxvirus of the western grey squirrel (Sciurus griseus griseus) of North America. *Intervirology* 5(6):364–366.

12. Herman CM, Reilly JR (1955) Skin tumors on squirrels. *J Wildl Manage* 19(3):402-403.

13. Kellam J (2010) Documentation of a poxvirus (Squirrel Fibromatosis) infected Big Cypress fox squirrel within Big Cypress National Preserve: Final report. *National Park Service, Big Cypress National Preserve*:1–3.

14. Rivas AE, Righton AL, Bugman AM, Kihn AE, Coleman DA, Singh K, Whittington JK (2014) Pathology in practice. Cutaneous and disseminated infection with squirrel fibroma virus (SFV). *J Am Vet Med Assoc* 245(4):389–391.

15. Kerr PJ, Liu J, Cattadori I, Ghedin E, Read AF (2015) Myxoma virus and the Leporipoxviruses: an evolutionary paradigm. *Viruses*. 7:1020-1061.

16. Gjessing MC, Yutin N, Tengs T, Senkevich T, Koonin E, Ronning HP, Alarcon M, Yiving S, Lie K-I, Saure B, Tran L, Moss B, Dale OB (2015) Salmon Gill Poxvirus, the Deepest Representative of the Chordopoxvirinae. *J Virol* 89(18):9348–9367.

17. Fleischauer C, Upton C, Victoria J, Jones GJB, Roper RL (2015) Genome sequence and comparative virulence of raccoonpox virus: the first North American poxvirus sequence. *J Gen Virol* 96(9):2806–2821.

18. Emerson GL, Nordhausen R, Garner MM, Huckabee JR, Johnson S, Wohrie RD, Davidson WB, Wilkins K, Li Y, Doty JB, Gallardo-Romero NF, Metcalfe MG, Karen KL, Damon IK, Carroll DS (2013) Novel poxvirus in big brown bats, northwestern United States. *Emerging Infect Dis* 19(6):1002–1004.

19. Afonso PP, Silva PM, Schnellrath LC, Jesus DM, Hu J, Yang Y, Renne R, Attia M, Condit RC, Moussatche N, Damaso CR (2012) Biological characterization and next-generation genome sequencing of the unclassified Cotia virus SPAn232 (Poxviridae). *J Virol* 86(9):5039–5054.

20. Zhao G, Droit L, Tesh RB, Popov VL, Little NS, Upton C, Virgin HW, Wang D (2011) The Genome of Yoka Poxvirus. *J Virol* 85(19):9657–9657.

21. Zeng X, Chi X, Li W, Hao W, Li M, Huang X, Huang Y, Rock DL, Luo S, Wang S (2014) Complete genome sequence analysis of goatpox virus isolated from China shows high variation. *Vet Microbiol* 173(1-2):38–49.

22. Mitsuhashi W, Miyamoto K, Wada S (2014) The complete genome sequence of the Alphaentomopoxvirus Anomala cuprea entomopoxvirus, including its terminal hairpin loop sequences, suggests a potentially unique mode of apoptosis inhibition and mode of DNA replication. *Virology* 452-453:95–116.

23. Offerman K, Carulei O, van der Walt AP, Douglass N, Williamson A-L (2014) The complete genome sequences of poxviruses isolated from a penguin and a pigeon in South Africa and comparison to other sequenced avipoxviruses. *BMC Genomics* 15:463.

24. Upton C, Macen JL, Maranchuk RA, DeLange AM (1988) Tumorigenic poxviruses: fine analysis of the recombination junctions in malignant rabbit fibroma virus, a recombinant between Shope fibroma virus and myxoma virus. *Virology*. 166(1):229-239.

25. Zhang P, Jacobs BL, Samuel CE (2008) Loss of Protein Kinase PKR Expression in Human HeLa Cells Complements the Vaccinia Virus E3L Deletion Mutant Phenotype by Restoration of Viral Protein Synthesis. *J Virol* 82(2):840–848.

26. Rahman MM, Liu J, Chan WM, Rothenburg S, McFadden G (2013) Myxoma virus protein M029 is a dual function immunomodulator that inhibits PKR and also conscripts RHA/DHX9 to promote expanded host tropism and viral replication. *PLoS Pathog*

9(7):e1003465.

27. Seet BT, Johnston JB, Brunetti CR, Barrett JW, Everett H, Cameron C, Sypula J, Nazarian SH, Lucas A, McFadden G (2003) Poxviruses and Immune Evasion. *Annu Rev Immunol* 21(1):377–423.

28. Rothenburg S, Seo EJ, Gibbs JS, Dever TE, Dittmar K (2008) Rapid evolution of protein kinase PKR alters sensitivity to viral inhibitors. *Nat Struct Mol Biol* 16(1):63–70.

29. Peng C, Haller SL, Rahman MM, McFadden G, Rothenburg S (2016) Myxoma virus M156 is a specific inhibitor of rabbit PKR but contains a loss-of-function mutation in Australian virus isolates. *Proc Natl Acad Sci USA* 113(14):3855-3860. doi:10.1073/pnas.1515613113.

30. Kasza L (1974) Isolation and characterization of a rabbit fibroma virus from a naturally occurring tumor. *Am J Vet Res* 35(1):87–89.

31. Johnston JB, Barrett JW, Chang W, Chung C-S, Zeng W, Masters J, Mann M, Wang F, Cao J, McFadden G (2003) Role of the serine-threonine kinase PAK-1 in myxoma virus replication. *J Virol* 77(10):5877–5888.

32. Yang Z, Moss B (2009) Interaction of the vaccinia virus RNA polymerase-associated 94-kilodalton protein with the early transcription factor. *J Virol* 83(23):12018–12026.

33. Altschul SF, Gish W, Miller W, Myers EW, Lipman DJ (1990) Basic local alignment search tool. *J Mol Biol* 215(3):403–410.

34. Bailey TL, Boden M, Buske FA, Frith M, Grant CE, Clementi L, Ren J, Li WW, Noble WS (2009) MEME SUITE: tools for motif discovery and searching. *Nucleic Acids Res* 37(Web Server):W202–W208.

35. Katoh K, Standley DM (2013) MAFFT multiple sequence alignment software version 7: improvements in performance and usability. *Mol Biol Evol* 30(4):772–780.

36. Lassmann T, Sonnhammer ELL (2005) Kalign--an accurate and fast multiple sequence alignment algorithm. *BMC Bioinformatics* 6:298.

37. Castresana J (2002) *GBLOCKS: Selection of Conserved Blocks from Multiple Alignments for their Use in Phylogenetic Analysis. Version 0.91 b.* (European Molecular Biology Laboratory (EMBL)) Available at: http://molevol. cmima. csic. es/castresana/Gblocks. html.

38. Darriba D, Taboada GL, Doallo R, Posada DV (2011) ProtTest 3: fast selection of best-fit models of protein evolution. *Bioinformatics* 27(8):1164–1165.

39. Guindon S, Dufayard JF, Anisimova M, Hordijk W, Gascuel O (2010) New Algorithms and Methods to Estimate Maximum-Likelihood Phylogenies: Assessing the Performance of PhyML 3.0. *Syst Biol* 59(3):307–321.

40. Rambaut A, Drummond A (2009) *FigTree. Version 1.3. 1. Institute of Evolutionary Biology* (University of Edinburgh).

41. Edgar RC (2004) MUSCLE: multiple sequence alignment with high accuracy and high throughput. *Nucleic Acids Res* 32(5):1792–1797.

42. Haller SL, Peng C, McFadden G, Rothenburg S (2014) Poxviruses and the evolution of host range and virulence. *Infect Genet Evol* 21:15–40.

43. Pickup DJ, Ink BS, Parsons BL, Hu W, Joklik WK (1984) Spontaneous deletions and duplications of sequences in the genome of cowpox virus. *Proc Natl Acad Sci USA* 81(21):6817–6821.

44. Smith GL, Symons JA, Alcamí A (1998) Poxviruses: interfering with interferon. *Sem Virol* 8(5):409-418.

45. Reynolds SE, Moss B (2015) Characterization of a large, proteolytically processed cowpox virus membrane glycoprotein conserved in most chordopoxviruses. *Virology*. 483:209-217.

46. Alcamí A, Symons JA, Smith GL (2000) The vaccinia virus soluble alpha/beta interferon (IFN) receptor binds to the cell surface and protects cells from the antiviral effects of IFN. *J Virol* 74(23):11230–11239.

47. Chen RA-J, Jacobs N, Smith GL (2006) Vaccinia virus strain Western Reserve protein B14 is an intracellular virulence factor. *J Gen Virol* 87(Pt 6):1451–1458.

48. Chen RA-J, Ryzhakov G, Cooray S, Randow F, Smith GL (2008) Inhibition of IkappaB kinase by vaccinia virus virulence factor B14. *PLoS Pathog* 4(2):e22.

49. Fagan-Garcia K, Barry M (2011) A vaccinia virus deletion mutant reveals the presence of additional inhibitors of NF-kappaB. *J Virol* 85(2):883–894.

50. Dobbelstein M, Shenk T (1996) Protection against apoptosis by the vaccinia virus SPI-2 (B13R) gene product. *J Virol* 70(9):6479–6485.

51. Kettle S, Alcami A, Khanna A, Ehret R, Jassoy C, Smith GL (1997) Vaccinia virus serpin B13R (SPI-2) inhibits interleukin-1beta-converting enzyme and protects virus-infected cells from TNF- and Fas-mediated apoptosis, but does not prevent IL-1beta-induced fever. *J Gen Virol* 78 (Pt 3):677–685.

52. Mossman KL (1997) Studies of Immunosuppressive Poxiruses.

53. Hnatiuk S, Barry M, Zeng W, Liu L, Lucas A, Percy D, McFadden G (1999) Role of the C-terminal RDEL motif of the myxoma virus M-T4 protein in terms of apoptosis regulation and viral pathogenesis. *Virology* 263(2):290–306.

54. Afonso CL, Delhon G, Tulman ER, Lu Z, Zsak A, Becerra VM, Zsak L, Kutish GF,

Rock DL (2005) Genome of deerpox virus. *J Virol* 79(2):966–977.

55. Tulman ER, Afonso CL, Lu Z, Zsak L, Kutish GF, Rock DL (2001) Genome of lumpy skin disease virus. *J Virol* 75(15):7122–7130.

56. Sung TC, Roper RL, Zhang Y, Rudge SA, Temel R, Hammond SM, Morris AJ, Moss B, Engebrecht J, Frohman MA (1997) Mutagenesis of phospholipase D defines a superfamily including a trans-Golgi viral protein required for poxvirus pathogenicity. *EMBO J* 16(15):4519–4530.

57. Afonso CL, Delhon G, Tulman ER, Lu Z, Zsak A, Becerra VM, Zsak L, Kutish GF, Rock DL (2005) Genome of deerpox virus. *J Virol* 79(2):966-977.

58. Beard PM, Froggatt GC, Smith GL (2006) Vaccinia virus kelch protein A55 is a 64 kDa intracellular factor that affects virus-induced cytopathic effect and the outcome of infection in a murine intradermal model. *J Gen Virol* 87(Pt 6):1521–1529.

59. Martin S, Harris DT, Shisler J (2012) The C11R Gene, Which Encodes the Vaccinia Virus Growth Factor, Is Partially Responsible for MVA-Induced NF-κB and ERK2 Activation. *J Virol* 86(18):9629-9639.

60. Pisklakova A (2015) An Oncolytic Myxoma Virus Construct (M011L Knock-out) Induces Apoptosis and is a Potent Pro-Apoptotic Therapy in both Human and Immunocompetent Murine Glioblastoma Cancer Stem Cells Models (P4.247). *Neurology*. 84(14).

61. Upton C, Stuart DT, McFadden G (1993) Identification of a poxvirus gene encoding a uracil DNA glycosylase. *Proc Natl Acad Sci USA* 90(10):4518–4522.

62. Stuart DT, Upton C, Higman MA, Niles EG, McFadden G (1993) A poxvirus-encoded uracil DNA glycosylase is essential for virus viability. *J Virol* 67(5):2503–2512.

63. Rahman MM, McFadden G (2011) Myxoma Virus Lacking the Pyrin-Like Protein M013 Is Sensed in Human Myeloid Cells by both NLRP3 and Multiple Toll-Like Receptors, Which Independently Activate the Inflammasome and NF- B Innate Response Pathways. *J Virol* 85(23):12505–12517.

64. Rahman MM, Mohamed MR, Kim M, Smallwood S, McFadden G (2009) Co-regulation of NF-kappaB and inflammasome-mediated inflammatory responses by myxoma virus pyrin domain-containing protein M013. *PLoS Pathog* 5(10):e1000635.

65. Froggatt GC, Smith GL (2007) Vaccinia virus gene F3L encodes an intracellular protein that affects the innate immune response. *J Gen Virol* 88(7):1917-1921.

66. Slabaugh M, Roseman N, Davis R, Mathews C (1988) Vaccinia virus-encoded ribonucleotide reductase: sequence conservation of the gene for the small subunit and its amplification in hydroxyurea-resistant mutants. *J Virol* 62(2):519–527.

67. Brown E, Senkevich TG, Moss B (2006) Vaccinia virus F9 virion membrane protein is required for entry but not virus assembly, in contrast to the related L1 protein. *J Virol* 80(19):9455–9464.

68. Lin S, Broyles SS (1994) Vaccinia protein kinase 2: a second essential serine/threonine protein kinase encoded by vaccinia virus. *Proc Natl Acad Sci USA* 91(16):7653–7657.

69. Zhang WH, Wilcock D, Smith GL (2000) Vaccinia virus F12L protein is required for actin tail formation, normal plaque size, and virulence. *J Virol* 74(24):11654–11662.

70. van Eijl H, Hollinshead M, Rodger G, Zhang W-H, Smith GL (2002) The vaccinia virus F12L protein is associated with intracellular enveloped virus particles and is required for their egress to the cell surface. *J Gen Virol* 83(Pt 1):195–207.

71. Blasco R, Cole NB, Moss B (1991) Sequence analysis, expression, and deletion of a vaccinia virus gene encoding a homolog of profilin, a eukaryotic actin-binding protein. *J Virol* 65(9):4598–4608.

72. Vliegen I, Yang G, Hruby D, Jordan R, Neyts J (2012) Deletion of the vaccinia virus F13L gene results in a highly attenuated virus that mounts a protective immune response against subsequent vaccinia virus challenge. *Antiviral Res* 93(1):160–166.

73. Senkevich TG, Koonin EV, Moss B (2011) Vaccinia virus F16 protein, a predicted catalytically inactive member of the prokaryotic serine recombinase superfamily, is targeted to nucleoli. *Virology* 417(2):334–342.

74. Kao SY, Ressner E, Kates J, Bauer WR (1981) Purification and characterization of a superhelix binding protein from vaccinia virus. *Virology* 111(2):500–508.

75. Gershon PD, Ahn BY, Garfield M, Moss B (1991) Poly(A) polymerase and a dissociable polyadenylation stimulatory factor encoded by vaccinia virus. *Cell* 66(6):1269–1278.

76. Domi A, Weisberg AS, Moss B (2008) Vaccinia virus E2L null mutants exhibit a major reduction in extracellular virion formation and virus spread. *J Virol* 82(9):4215–4226.

77. Chang H-W, Watson JC, Jacobs BL (1992) The E3L gene of vaccinia virus encodes an inhibitor of the interferon-induced, double-stranded RNA-dependent protein kinase. *Proc Natl Acad Sci USA* 89:4825–4829.

78. Jones EV, Puckett C, Moss B (1987) DNA-dependent RNA polymerase subunits encoded within the vaccinia virus genome. *J Virol* 61(6):1765–1771.

79. Murcia-Nicolas A, Bolbach G, Blais JC, Beaud G (1999) Identification by mass spectroscopy of three major early proteins associated with virosomes in vaccinia virus-infected cells. *Virus Res* 59(1):1–12.

80. Boyd O, Turner PC, Moyer RW, Condit RC (2010) The E6 protein from vaccinia virus is required for the formation of immature virions. *Virology*. 399(2):201-211.

81. Schramm B, Locker JK (2005) Cytoplasmic organization of Poxvirus DNA replication. *Traffic*. 6:839-846.

82. Kato S, Condit RC, Moussatché N (2007) The vaccinia virus E8R gene product is required for formation of transcriptionally active virions. *Virology*. 367(2):398-412.

83. Earl PL, Jones EV, Moss B (1986) Homology between DNA polymerases of poxviruses, herpesviruses, and adenoviruses: nucleotide sequence of the vaccinia virus DNA polymerase gene. *Proc Natl Acad Sci USA* 83(11):3659–3663.

84. Senkevich TG, Weisberg AS, Moss B (2000) Vaccinia virus E10R protein is associated with the membranes of intracellular mature virions and has a role in morphogenesis. *Virology* 278(1):244–252.

85. Senkevich TG, White CL, Koonin EV, Moss B (2000) A viral member of the ERV1/ALR protein family participates in a cytoplasmic pathway of disulfide bond formation. *Proc Natl Acad Sci USA* 97(22):12068–12073.

86. Schweneker M, Lukassen S, Spaeth M, Wolferstaetter M, Babel E, Brinkmann K, Wielert U, Chaplin P, Suter M, Hausmann J (2012) The vaccinia virus O1 protein is required for sustained activation of extracellular signal-regulated kinase 1/2 and promotes viral virulence. *J Virol* 86(4):2323–2336.

87. Shchelkunov SN, Riazankina OI, Gashnikov PB, Totmenin AB, Chizhikov VE, Malygin EG (1991) [Molecular biological study of the vaccinia virus genome. IV. The late nonstructural 36K protein of vaccinia virus is vitally important]. *Mol Biol (Mosk)* 25(2):396–404.

88. Nichols RJ, Stanitsa E, Unger B, Traktman P (2008) The vaccinia virus gene I2L encodes a membrane protein with an essential role in virion entry. *J Virol* 82(20):10247-10261.

89. Greseth MD, Boyle KA, Bluma MS, Unger B, Wiebe MS, Soares-Martins JA, Wickramasekera NT, Wahlberg J, Traktman P (2012) Molecular genetic and biochemical characterization of the vaccinia virus I3 protein, the replicative single-stranded DNA binding protein. *J Virol* 86(11):6197–6209.

90. Sood CL, Ward JM, Moss B (2008) Vaccinia virus encodes I5, a small hydrophobic virion membrane protein that enhances replication and virulence in mice. *J Virol* 82(20):10071–10078.

91. DeMasi J, Du S, Lennon D, Traktman P (2001) Vaccinia virus telomeres: interaction with the viral I1, I6, and K4 proteins. *J Virol* 75(21):10090–10105.

92. Grubisha O, Traktman P (2003) Genetic analysis of the vaccinia virus I6 telomere-binding protein uncovers a key role in genome encapsidation. *J Virol* 77(20):10929–10942.

93. Byrd CM, Bolken TC, Hruby DE (2002) The vaccinia virus I7L gene product is the core protein proteinase. *J Virol* 76(17):8973–8976.

94. Ansarah-Sobrinho C, Moss B (2004) Role of the I7 protein in proteolytic processing of vaccinia virus membrane and core components. *J Virol* 78(12):6335–6343.

95. Shuman S (1992) Vaccinia virus RNA helicase: an essential enzyme related to the DE-H family of RNA-dependent NTPases. *Proc Natl Acad Sci USA* 89(22):10935–10939.

96. Gross CH, Shuman S (1995) Mutational analysis of vaccinia virus nucleoside triphosphate phosphohydrolase II, a DExH box RNA helicase. *J Virol* 69(8):4727–4736.

97. Ansarah-Sobrinho C, Moss B (2004) Vaccinia virus G1 protein, a predicted metalloprotease, is essential for morphogenesis of infectious virions but not for cleavage of major core proteins. *J Virol* 78(13):6855–6863.

98. Hedengren-Olcott M, Byrd CM, Watson J, Hruby DE (2004) The vaccinia virus G1L putative metalloproteinase is essential for viral replication in vivo. *J Virol* 78(18):9947–9953.

99. Honeychurch KM, Byrd CM, Hruby DE (2006) Mutational analysis of the potential catalytic residues of the VV G1L metalloproteinase. *Virology* 3:7.

100. Izmailyan RA, Huang C-Y, Mohammad S, Isaacs SN, Chang W (2006) The envelope G3L protein is essential for entry of vaccinia virus into host cells. *J Virol* 80(17):8402–8410.

101. Meis RJ, Condit RC (1991) Genetic and molecular biological characterization of a vaccinia virus gene which renders the virus dependent on isatin-beta-thiosemicarbazone (IBT). *Virology* 182(2):442–454.

102. White CL, Weisberg AS, Moss B (2000) A glutaredoxin, encoded by the G4L gene of vaccinia virus, is essential for virion morphogenesis. *J Virol* 74(19):9175–9183.

103. White CL, Senkevich TG, Moss B (2002) Vaccinia virus G4L glutaredoxin is an essential intermediate of a cytoplasmic disulfide bond pathway required for virion assembly. *J Virol* 76(2):467-472.

104. Da Silva M, Shen L, Tcherepanov V, Watson C, Upton C (2006) Predicted function of the vaccinia virus G5R protein. *Bioinformatics* 22(23):2846–2850.

105. Da Fonseca FG, Weisberg AS, Caeiro MF (2004) Vaccinia virus mutants with alanine substitutions in the conserved G5R gene fail to initiate morphogenesis at the nonpermissive temperature. *J Virol* 78(19):10238-10248.

106. Senkevich TG, Wyatt LS, Weisberg AS, Koonin EV, Moss B (2008) A conserved poxvirus NlpC/P60 superfamily protein contributes to vaccinia virus virulence in mice but not to replication in cell culture. *Virology* 374(2):506–514.

107. Szajner P, Jaffe H, Weisberg AS, Moss B (2003) Vaccinia virus G7L protein Interacts with the A30L protein and is required for association of viral membranes with dense viroplasm to form immature virions. *J Virol* 77(6):3418–3429.

108. Zhang Y, Keck JG, Moss B (1992) Transcription of viral late genes is dependent on expression of the viral intermediate gene G8R in cells infected with an inducible conditional-lethal mutant vaccinia virus. *J Virol* 66(11):6470–6479.

109. Da Silva M, Upton C (2009) Vaccinia virus G8R protein: a structural ortholog of proliferating cell nuclear antigen (PCNA). *PLoS ONE* 4(5):e5479.

110. Ojeda S, Domi A, Moss B (2006) Vaccinia virus G9 protein is an essential component of the poxvirus entry-fusion complex. *J Virol* 80(19):9822–9830.

111. Franke CA, Wilson EM, Hruby DE (1990) Use of a cell-free system to identify the vaccinia virus L1R gene product as the major late myristylated virion protein M25. *J Virol* 64(12):5988–5996.

112. Ravanello MP, Hruby DE (1994) Characterization of the vaccinia virus L1R myristylprotein as a component of the intracellular virion envelope. *J Gen Virol* 75(6):1479-1483.

113. Maruri-Avidal L, Weisberg AS, Moss B (2011) Vaccinia virus L2 protein associates with the endoplasmic reticulum near the growing edge of crescent precursors of immature virions and stabilizes a subset of viral membrane proteins. *J Virol* 85(23):12431–12441.

114. Resch W, Moss B (2005) The conserved poxvirus L3 virion protein is required for transcription of vaccinia virus early genes. *J Virol* 79(23):14719–14729.

115. Bayliss CD, Smith GL (1997) Vaccinia virion protein VP8, the 25 kDa product of the L4R gene, binds single-stranded DNA and RNA with similar affinity. *Nucleic Acids Res* 25(20):3984–3990.

116. Jesus DM, Moussatché N, Condit RC (2014) Vaccinia virus mutations in the L4R gene encoding a virion structural protein produce abnormal mature particles lacking a nucleocapsid. *J Virol* 88(24):14017–14029.

117. Townsley AC, Senkevich TG, Moss B (2005) The product of the vaccinia virus L5R gene is a fourth membrane protein encoded by all poxviruses that is required for cell entry and cell-cell fusion. *J Virol* 79(17):10988–10998.

118. Chiu W-L, Chang W (2002) Vaccinia virus J1R protein: a viral membrane protein that is essential for virion morphogenesis. *J Virol* 76(19):9575–9587.

119. Bajszar G, Wittek R, Weir JP, Moss B (1983) Vaccinia virus thymidine kinase and neighboring genes: mRNAs and polypeptides of wild-type virus and putative nonsense mutants. *J Virol* 45(1):62-72.

120. Meng X, Schoggins J, Rose L, Cao J, Ploss A, Rice CM, Xiang Y (2012) C7L family of poxvirus host range genes inhibits antiviral activities induced by type I interferons and interferon regulatory factor 1. *J Virol* 86(8):4538–4547.

121. Liu J, Wennier S, Zhang L, McFadden G (2011) M062 is a host range factor essential for myxoma virus pathogenesis and functions as an antagonist of host SAMD9 in human cells. *J Virol* 85(7):3270–3282.

122. Barrett JW, Chang CS, Wang G, Werden SJ, Shao Z (2007) Myxoma virus M063R is a host range gene essential for virus replication in rabbit cells. *Virology*. 361:123-132.

123. Liu J, Wennier S, Moussatche N, Reinhard M, Condit RC, McFadden G (2012) Myxoma virus M064 is a novel member of the poxvirus C7L superfamily of host range factors that controls the kinetics of myxomatosis in European rabbits. *J Virol* 86(9):5371–5375.

124. Mohamed MR, Latner DR, Condit RC, Niles EG (2001) Interaction between the J3R subunit of vaccinia virus poly(A) polymerase and the H4L subunit of the viral RNA polymerase. *Virology* 280(1):143–152.

125. Latner DR, Xiang Y, Lewis JI, Condit J, Condit RC (2000) The vaccinia virus bifunctional gene J3 (nucleoside-2'-O-)-methyltransferase and poly(A) polymerase stimulatory factor is implicated as a positive transcription elongation factor by two genetic approaches. *Virology* 269(2):345–355.

126. Zajac P, Spehner D, Drillien R (1995) The vaccinia virus J5L open reading frame encodes a polypeptide expressed late during infection and required for viral multiplication. *Virus Res* 37(2):163–173.

127. Broyles SS, Moss B (1986) Homology between RNA polymerases of poxviruses, prokaryotes, and eukaryotes: nucleotide sequence and transcriptional analysis of vaccinia virus genes encoding 147-kDa and 22-kDa subunits. *Proc Natl Acad Sci USA* 83:3141-3145.

128. Najarro P, Traktman P, Lewis JA (2001) Vaccinia virus blocks gamma interferon signal transduction: viral VH1 phosphatase reverses Stat1 activation. *J Virol* 75(7):3185–3196.

129. Senkevich TG, Moss B (2005) Vaccinia virus H2 protein is an essential component of a complex involved in virus entry and cell-cell fusion. *J Virol* 79(8):4744–4754.

130. Lin CL, Chung CS, Heine HG, Chang W (2000) Vaccinia virus envelope H3L protein binds to cell surface heparan sulfate and is important for intracellular mature virion morphogenesis and virus infection in vitro and in vivo. *J Virol* 74(7):3353–3365.

131. Ahn BY, Moss B (1992) RNA polymerase-associated transcription specificity factor encoded by vaccinia virus. *Proc Natl Acad Sci USA* 89(8):3536–3540.

132. Kovacs GR, Moss B (1996) The vaccinia virus H5R gene encodes late gene transcription factor 4: purification, cloning, and overexpression. *J Virol* 70(10):6796–6802.

133. Shuman S, Moss B (1987) Identification of a vaccinia virus gene encoding a type I DNA topoisomerase. *Proc Natl Acad Sci USA* 84(21):7478–7482.

134. Da Fonseca F, Moss B (2003) Poxvirus DNA topoisomerase knockout mutant exhibits decreased infectivity associated with reduced early transcription. *Proc Natl Acad Sci USA* 100(20):11291–11296.

135. Meng X, Wu X, Yan B, Deng J, Xiang Y (2013) Analysis of the role of vaccinia virus H7 in virion membrane biogenesis with an H7-deletion mutant. *J Virol* 87(14):8247–8253.

136. Morgan JR, Cohen LK, Roberts BE (1984) Identification of the DNA sequences encoding the large subunit of the mRNA-capping enzyme of vaccinia virus. *J Virol* 52(1):206–214.

137. Vos JC, Sasker M, Stunnenberg HG (1991) Vaccinia virus capping enzyme is a transcription initiation factor. *EMBO J* 10(9):2553–2558.

138. Dyster LM, Niles EG (1991) Genetic and biochemical characterization of vaccinia virus genes D2L and D3R which encode virion structural proteins. *Virology* 182(2):455–467.

139. De Silva FS, Moss B (2008) Effects of vaccinia virus uracil DNA glycosylase catalytic site and deoxyuridine triphosphatase deletion mutations individually and together on replication in active and quiescent cells and pathogenesis in mice. *Virology* 5(1):145-157.

140. Kilcher S, Schmidt FI, Schneider C, Kopf M, Helenius A, Mercer J (2014) siRNA screen of early poxvirus genes identifies the AAA+ ATPase D5 as the virus genome-uncoating factor. *Cell Host Microbe* 15(1):103–112.

141. Hu X, Wolffe EJ, Weisberg AS, Carroll LJ, Moss B (1998) Repression of the A8L gene, encoding the early transcription factor 82-kilodalton subunit, inhibits morphogenesis of vaccinia virions. *J Virol* 72(1):104–112.

142. Quick SD, Broyles SS (1990) Vaccinia virus gene D7R encodes a 20,000-dalton subunit of the viral DNA-dependent RNA polymerase. *Virology* 178(2):603–605.

143. Niles EG, Seto J (1988) Vaccinia virus gene D8 encodes a virion transmembrane protein. *J Virol* 62(10):3772–3778.

144. Hsiao JC, Chung CS, Chang W (1999) Vaccinia virus envelope D8L protein binds to cell surface chondroitin sulfate and mediates the adsorption of intracellular mature virions to cells. *J Virol* 73(10):8750-8761.

145. Parrish S, Moss B (2007) Characterization of a second vaccinia virus mRNA-decapping enzyme conserved in poxviruses. *J Virol* 81(23):12973–12978.

146. Parrish S, Resch W, Moss B (2007) Vaccinia virus D10 protein has mRNA decapping

activity, providing a mechanism for control of host and viral gene expression. *Proc Natl Acad Sci USA* 104(7):2139–2144.

147. Parrish S, Moss B (2006) Characterization of a vaccinia virus mutant with a deletion of the D10R gene encoding a putative negative regulator of gene expression. *J Virol* 80(2):553–561.

148. Rodriguez JF, Kahn JS, Esteban M (1986) Molecular cloning, encoding sequence, and expression of vaccinia virus nucleic acid-dependent nucleoside triphosphatase gene. *Proc Natl Acad Sci USA* 83(24):9566–9570.

149. Broyles SS, Moss B (1987) Identification of the vaccinia virus gene encoding nucleoside triphosphate phosphohydrolase I, a DNA-dependent ATPase. *J Virol* 61(5):1738–1742.

150. Niles EG, Lee-Chen GJ, Shuman S, Moss B (1989) Vaccinia virus gene D12L encodes the small subunit of the viral mRNA capping enzyme. *Virology* 172(2):513-522.

151. Baldick CJ, Moss B (1987) Resistance of vaccinia virus to rifampicin conferred by a single nucleotide substitution near the predicted NH2 terminus of a gene encoding an Mr 62,000 polypeptide. *Virology* 156(1):138–145.

152. McNulty-Kowalczyk A, Paoletti E (1993) Mutations in ORF D13L and other genetic loci alter the rifampicin phenotype of vaccinia virus. *Virology* 194(2):638–646.

153. Keck JG, Kovacs GR, Moss B (1993) Overexpression, purification, and late transcription factor activity of the 17-kilodalton protein encoded by the vaccinia virus A1L gene. *J Virol* 67(10):5740–5748.

154. Hubbs AE, Wright CF (1996) The A2L intermediate gene product is required for in vitro transcription from a vaccinia virus late promoter. *J Virol* 70(1):327–331.

155. Senkevich TG, White CL, Weisberg A, Granek JA, Wolffe EJ, Koonin EV, Moss B (2002) Expression of the vaccinia virus A2.5L redox protein is required for virion morphogenesis. *Virology* 300(2):296–303.

156. Senkevich TG, White CL, Koonin EV, Moss B (2002) Complete pathway for protein disulfide bond formation encoded by poxviruses. *Proc Natl Acad Sci USA* 99(10):6667–6672.

157. Rosel J, Moss B (1985) Transcriptional and translational mapping and nucleotide sequence analysis of a vaccinia virus gene encoding the precursor of the major core polypeptide 4b. *J Virol* 56(3):830–838.

158. Jensen ON, Houthaeve T, Shevchenko A, Cudmore S, Ashford T, Mann M, Griffiths G, Locker JK (1996) Identification of the major membrane and core proteins of vaccinia virus by two-dimensional electrophoresis. *J Virol* 70(11):7485–7497.

159. Ahn BY, Rosel J, Cole NB, Moss B (1992) Identification and expression of rpo19, a

vaccinia virus gene encoding a 19-kilodalton DNA-dependent RNA polymerase subunit. *J Virol* 66(2):971–982.

160. Meng X, Embry A, Sochia D, Xiang Y (2007) Vaccinia virus A6L encodes a virion core protein required for formation of mature virion. *J Virol* 81(3):1433–1443.

161. Hu X, Carroll LJ, Wolffe EJ, Moss B (1996) De novo synthesis of the early transcription factor 70-kilodalton subunit is required for morphogenesis of vaccinia virions. *J Virol* 70(11):7669–7677.

162. Sanz P, Moss B (1999) Identification of a transcription factor, encoded by two vaccinia virus early genes, that regulates the intermediate stage of viral gene expression. *Proc Natl Acad Sci USA* 96(6):2692–2697.

163. Yeh WW, Moss B, Wolffe EJ (2000) The vaccinia virus A9L gene encodes a membrane protein required for an early step in virion morphogenesis. *J Virol* 74(20):9701–9711.

164. Heljasvaara R, Rodriguez D, Risco C, Carrascosa JL, Esteban M, Rodriguez JR (2001) The major core protein P4a (A10L gene) of vaccinia virus is essential for correct assembly of viral DNA into the nucleoprotein complex to form immature viral particles. *J Virol* 75(13):5778–5795.

165. Resch W, Weisberg AS, Moss B (2005) Vaccinia virus nonstructural protein encoded by the A11R gene is required for formation of the virion membrane. *J Virol* 79(11):6598–6609.

166. Wu X, Meng X, Yan B, Rose L, Deng J, Xiang Y (2012) Vaccinia virus virion membrane biogenesis protein A11 associates with viral membranes in a manner that requires the expression of another membrane biogenesis protein, A6. *J Virol* 86(20):11276–11286.

167. Yang SJ (2007) Characterization of vaccinia virus A12L protein proteolysis and its participation in virus assembly. *Virology* 4:78-90.

168. Unger B, Traktman P (2004) Vaccinia virus morphogenesis: a13 phosphoprotein is required for assembly of mature virions. *J Virol* 78(16):8885–8901.

169. Rodríguez JR, Risco C, Carrascosa JL, Esteban M, Rodríguez D (1998) Vaccinia virus 15-kilodalton (A14L) protein is essential for assembly and attachment of viral crescents to virosomes. *J Virol* 72(2):1287–1296.

170. Betakova T, Wolffe EJ, Moss B (2000) The vaccinia virus A14.5L gene encodes a hydrophobic 53-amino-acid virion membrane protein that enhances virulence in mice and is conserved among vertebrate poxviruses. *J Virol* 74(9):4085–4092.

171. Ojeda S, Senkevich TG, Moss B (2006) Entry of vaccinia virus and cell-cell fusion require a highly conserved cysteine-rich membrane protein encoded by the A16L gene. *J Virol* 80(1):51–61.

172. Rodríguez D, Esteban M, Rodríguez JR (1995) Vaccinia virus A17L gene product is essential for an early step in virion morphogenesis. *J Virol* 69(8):4640–4648.

173. Lackner CA, Condit RC (2000) Vaccinia virus gene A18R DNA helicase is a transcript release factor. *J Biol Chem* 275(2):1485–1494.

174. Satheshkumar PS, Olano LR, Hammer CH, Zhao M, Moss B (2013) Interactions of the vaccinia virus A19 protein. *J Virol* 87(19):10710–10720.

175. Satheshkumar PS, Weisberg AS, Moss B (2013) Vaccinia virus A19 protein participates in the transformation of spherical immature particles to barrel-shaped infectious virions. *J Virol* 87(19):10700–10709.

176. Townsley AC, Senkevich TG, Moss B (2005) Vaccinia virus A21 virion membrane protein is required for cell entry and fusion. *J Virol* 79(15):9458–9469.

177. Ishii K, Moss B (2001) Role of vaccinia virus A20R protein in DNA replication: construction and characterization of temperature-sensitive mutants. *J Virol* 75(4):1656–1663.

178. Garcia AD, Moss B (2001) Repression of vaccinia virus Holliday junction resolvase inhibits processing of viral DNA into unit-length genomes. *J Virol* 75(14):6460–6471.

179. Culyba MJ, Harrison JE, Hwang Y, Bushman FD (2006) DNA cleavage by the A22R resolvase of vaccinia virus. *Virology* 352(2):466–476.

180. Amegadzie BY, et al. (1991) Identification, sequence, and expression of the gene encoding the second-largest subunit of the vaccinia virus DNA-dependent RNA polymerase. *Virology* 180(1):88–98.

181. Chung CS, Hsiao JC, Chang YS, Chang W (1998) A27L protein mediates vaccinia virus interaction with cell surface heparan sulfate. *J Virol* 72(2):1577–1585.

182. Senkevich TG, Ward BM, Moss B (2004) Vaccinia virus A28L gene encodes an essential protein component of the virion membrane with intramolecular disulfide bonds formed by the viral cytoplasmic redox pathway. *J Virol* 78(5):2348–2356.

183. Senkevich TG, Ward BM, Moss B (2004) Vaccinia virus entry into cells is dependent on a virion surface protein encoded by the A28L gene. *J Virol* 78(5):2357–2366.

184. Mercer J, Traktman P (2005) Genetic and cell biological characterization of the vaccinia virus A30 and G7 phosphoproteins. *J Virol* 79(11):7146–7161.

185. Koonin EV, Senkevich TG, Chernos VI (1993) Gene A32 product of vaccinia virus may be an ATPase involved in viral DNA packaging as indicated by sequence comparisons with other putative viral ATPases. *Virus Genes* 7(3):289-295.

186. Roper RL, Wolffe EJ, Weisberg A, Moss B (1998) The envelope protein encoded by the

A33R gene is required for formation of actin-containing microvilli and efficient cell-to-cell spread of vaccinia virus. *J Virol* 72(5):4192–4204.

187. McIntosh AA, Smith GL (1996) Vaccinia virus glycoprotein A34R is required for infectivity of extracellular enveloped virus. *J Virol* 70(1):272–281.

188. Roper RL (2006) Characterization of the vaccinia virus A35R protein and its role in virulence. *J Virol* 80(1):306–313.

189. Bennett CJ, Webb M, Willer DO, Evans DH (2003) Genetic and phylogenetic characterization of the type II cyclobutane pyrimidine dimer photolyases encoded by Leporipoxviruses. *Virology* 315(1):10–19.

190. Cameron CM, Barrett JW, Mann M, Lucas A, McFadden G (2005) Myxoma virus M128L is expressed as a cell surface CD47-like virulence factor that contributes to the downregulation of macrophage activation in vivo. *Virology* 337(1):55–67.

191. Martin KH, Grosenbach DW, Franke CA, Hruby DE (1997) Identification and analysis of three myristylated vaccinia virus late proteins. *J Virol* 71(7):5218–5226.

192. Colinas RJ, Goebel SJ, Davis SW, Johnson GP, Norton EK, Paoletti E (1990) A DNA ligase gene in the Copenhagen strain of vaccinia virus is nonessential for viral replication and recombination. *Virology* 179(1):267–275.

193. Bowie A, Kiss-Toth E, Symons JA, Smith GL, Dower SK, O'Neill LA (2000) A46R and A52R from vaccinia virus are antagonists of host IL-1 and toll-like receptor signaling. *Proc Natl Acad Sci USA* 97(18):10162–10167.

194. González JM, Esteban M (2010) A poxvirus Bcl-2-like gene family involved in regulation of host immune response: sequence similarity and evolutionary history. *Virology* 7:59.

195. Gammon DB, Duraffour S, Rozelle DK, Hehnly H, Sharma R, Sparks ME, West CC, Chen Y, Moresco JJ, Andrei G, Connor JH, Conte D, Gundersen-Rindal DE, Marshall, WL, Yates JR, Silverman N, Mello CC (2014) A single vertebrate DNA virus protein disarms invertebrate immunity to RNA virus infection. *Elife* 3. doi:10.7554/eLife.02910.

196. Boutard B, Vankerckhove S, Markine-Goriaynoff M, Sarlet M, Desmecht D, McFadden G, Vanderplasschen A, Gillet L (2015) The α2,3-sialyltransferase encoded by myxoma virus is a virulence factor that contributes to immunosuppression. *PLoS ONE* 10(2):e0118806.

197. Cameron CM, Barrett JW, Liu L, Lucas AR, McFadden G (2005) Myxoma virus M141R expresses a viral CD200 (vOX-2) that is responsible for down-regulation of macrophage and T-cell activation in vivo. *J Virol* 79(10):6052–6067.

198. Banham AH, Smith GL (1992) Vaccinia virus gene B1R encodes a 34-kDa serine/threonine protein kinase that localizes in cytoplasmic factories and is packaged

into virions. *Virology* 191(2):803–812.

199. Nerenberg BTH, Taylor J, Bartee E, Gouveia K, Barry M, Fruh K (2005) The poxviral RING protein p28 is a ubiquitin ligase that targets ubiquitin to viral replication factories. *J Virol* 79(1):597-601.

200. McKenzie R, Kotwal GJ, Moss B, Hammer CH, Frank MM (1992) Regulation of complement activity by vaccinia virus complement-control protein. *J Infect Dis* 166(6):1245–1250.

201. Sahu A, Isaacs SN, Soulika AM, Lambris JD (1998) Interaction of vaccinia virus complement control protein with human complement proteins: factor I-mediated degradation of C3b to iC3b1 inactivates the alternative complement pathway. *J Immunol* 160(11):5596–5604.

202. Jacobs N, Bartlett NW, Clark RH, Smith GL (2008) Vaccinia virus lacking the Bcl-2-like protein N1 induces a stronger natural killer cell response to infection. *J Gen Virol* 89(Pt 11):2877–2881.

203. Colamonici OR, Domanski P, Sweitzer SM, Larner A, Buller RM (1995) Vaccinia virus B18R gene encodes a type I interferon-binding protein that blocks interferon alpha transmembrane signaling. *J Biol Chem* 270(27):15974–15978.

204. Blanié S, Mortier J, Delverdier M, Bertagnoli S, Camus-Bouclainville C (2009) M148R and M149R are two virulence factors for myxoma virus pathogenesis in the European rabbit. *Vet Res* 40(1):11.

205. Burles K, Irwin C, Burton R-L, Schriewer J, Evans DH, Buller RM, Barry M (2014) Initial characterization of vaccinia virus B4 suggests a role in virus spread. *Virology* 456-457:108–120.

206. Messud-Petit F, Gelfi J, Delverdier M, Amardeilh MF, Py R, Sutter G, Bertagnoli S (1998) Serp2, an inhibitor of the interleukin-1beta-converting enzyme, is critical in the pathobiology of myxoma virus. *J Virol* 72(10):7830–7839.

207. Turner PC, Sancho MC, Thoennes SR, Caputo A, Bleackley RC, Moyer RW (1999) Myxoma virus Serp2 is a weak inhibitor of granzyme B and interleukin-1beta-converting enzyme in vitro and unlike CrmA cannot block apoptosis in cowpox virus-infected cells. *J Virol* 73(8):6394–6404.

208. Gedey R, Jin X-L, Hinthong O, Shisler JL (2006) Poxviral regulation of the host NF-kappaB response: the vaccinia virus M2L protein inhibits induction of NF-kappaB activation via an ERK2 pathway in virus-infected human embryonic kidney cells. *J Virol* 80(17):8676–8685.

209. Davies MV, Chang H-W, Jacobs BL, Kaufman RJ (1993) The E3L and K3L Vaccinia Virus Gene Products Stimulate Translation through Inhibition of the Double-Stranded RNA-Dependent Protein Kinase by Different Mechanisms. *J Virol* 67:1688–1692.

210. Ramelot TA, Cort JR, Yee AA, Liu F, Goshe MB, Edwards AM, Smith RD, Arrowsmith CH, Dever TE, Kennedy MA (2002) Myxoma Virus Immunomodulatory Protein M156R is a Structural Mimic of Eukaryotic Translation Initiation Factor eIF2α. *J Mol Biol* 322(5):943–954.

211. Gallardo-Romero NF, Velasco-Villa A, Weiss SL, Emerson GL, Carroll DS, Hughes CM, Li Y, Karem KL, Damon IK, Olson VA (2011) Detection of North American orthopoxviruses by real time-PCR. *Virology* 8:313.

212. Yang Z, Reynolds SE, Martens CA, Bruno DP, Porcella SF, Moss B (2011) Expression profiling of the intermediate and late stages of poxvirus replication. *J Virol* 85(19):9899–9908.

213. Yang Z, Bruno DP, Martens CA, Porcella SF, Moss B (2010) Simultaneous high-resolution analysis of vaccinia virus and host cell transcriptomes by deep RNA sequencing. *Proc Natl Acad Sci USA* 107(25):11513–11518.

214. Yang Z, Maruri-Avidal L, Sisler J, Stuart CA, Moss B (2013) Cascade regulation of vaccinia virus gene expression is modulated by multistage promoters. *Virology* 447(1-2):213–220.

215. Kerr PJ, Rogers MB, Fitch A, DePasse JV, Cattadori IM, Hudson PJ, Tscharke DC, Holmes EC, Ghedin E (2013) Comparative analysis of the complete genome sequence of the California MSW strain of myxoma virus reveals potential host adaptations. *J Virol* 87(22):12080–12089.

216. Teoh MLT, Walasek PJ, Evans DH (2003) Leporipoxvirus Cu,Zn-superoxide dismutase (SOD) homologs are catalytically inert decoy proteins that bind copper chaperone for SOD. *J Biol Chem* 278(35):33175–33184.

217. Teoh MLT, Turner PV, Evans DH (2005) Tumorigenic poxviruses up-regulate intracellular superoxide to inhibit apoptosis and promote cell proliferation. *J Virol* 79(9):5799–5811.

218. Nash P, Barrett J, Cao JX, Hota-Mitchell S, Lalani S, Everett H, Xu XM, Robichaud J, Hnatiuk S, Ainslie C, Seet BT, McFadden G (1999) Immunomodulation by viruses: the myxoma virus story. *Immunol Rev* 168:103–120.

219. Law RHP, Zhang Q, McGowan S, Buckle AM, Silverman GA, Wong W, Rosado CJ, Langendor CG, Pike RN, Bird PI, Whisstock JC (2006) An overview of the serpin superfamily. *Genome Biol* 7(5):216.

220. Upton C, Macen JL, Wishart DS, McFadden G (1990) Myxoma virus and malignant rabbit fibroma virus encode a serpin-like protein important for virus virulence. *Virology* 179(2):618–631.

221. Macen JL, Upton C, Nation N, McFadden G (1993) SERP1, a serine proteinase inhibitor encoded by myxoma virus, is a secreted glycoprotein that interferes with inflammation.

Virology 195(2):348–363.

222. Lucas A, McFadden G (2004) Secreted immunomodulatory viral proteins as novel biotherapeutics. *J Immunol* 173(8):4765-4774.

223. Guerin JL, Gelfi J, Camus C, Delverdier M, Whisstock JC, Amardeihl MF, Py R, Bertagnoli S, Messud-Petit F (2001) Characterization and functional analysis of Serp3: a novel myxoma virus-encoded serpin involved in virulence. *J Gen Virol* 82(Pt 6):1407–1417.

224. Camus-Bouclainville C, Fiette L, Bouchiha S, Pignolet B, Counor D, Filipe C, Gelfi J, Messud-Petit F (2004) A virulence factor of myxoma virus colocalizes with NF-kappaB in the nucleus and interferes with inflammation. *J Virol* 78(5):2510–2516.

225. Guerin J-L, Gelfi J, Boullier S, Delverdier M, Bellanger F-A, Bertagnoli S, Drexler I, Sutter G, Messud-Petit F (2002) Myxoma virus leukemia-associated protein is responsible for major histocompatibility complex class I and Fas-CD95 down-regulation and defines scrapins, a new group of surface cellular receptor abductor proteins. *J Virol* 76(6):2912–2923.

226. Mansouri M, Bartee E, Gouveia K, Nerenberg TH, Barrett J, Thomas L, Thomas G, McFadden G, Fruh K (2003) The PHD/LAP-domain protein M153R of myxomavirus is a ubiquitin ligase that induces the rapid internalization and lysosomal destruction of CD4. *J Virol* 77(2):1427–1440.

227. Kerr PJ, Rogers MB, Fitch A, DePasse JV, Cattadori IM, Twaddle AC, Hudson PJ, Tscharke DC, Read AF, Holmes EC, Ghedin E (2013) Genome scale evolution of myxoma virus reveals host-pathogen adaptation and rapid geographic spread. *J Virol* 87(23):12900–12915.

228. Lyttle DJ, Fraser KM, Fleming SB, Mercer AA, Robinson AJ (1994) Homologs of vascular endothelial growth factor are encoded by the poxvirus orf virus. *J Virol* 68(1):84–92.

229. Chakrabarti S, Sisler JR, Moss B (1997) Compact, synthetic, vaccinia virus early/late promoter for protein expression. *Biotechniques.* 23(6):1094-1097.

230. Emeny JM, Morgan MJ (1979) Regulation of the interferon system: evidence that Vero cells have a genetic defect in interferon production. *J Gen Virol* 43(1):247–252.

231. Spehner D, Gillard S, Drillien R, Kirn A (1988) A cowpox virus gene required for multiplication in Chinese hamster ovary cells. *J Virol* 62(4):1297–1304.

232. Chang H-W, Jacobs BL (1993) Identification of a Conserved Motif That Is Necessary for Binding of the Vaccinia Virus E3L Gene Products to Double-Stranded RNA. *Virology* 194:537–547.

233. Gubser C, Hué S, Kellam P, Smith GL (2004) Poxvirus genomes: a phylogenetic

analysis. *J Gen Virol* 85(Pt 1):105–117.

234. Afonso CL, Tulman ER, Lu Z, Zsak L, Kutish GF, Rock DL (2000) The genome of fowlpox virus. *J Virol* 74(8):3815–3831.

235. Mossman K, Upton C, McFadden G (1995) The myxoma virus-soluble interferon-gamma receptor homolog, M-T7, inhibits interferon-gamma in a species-specific manner. *J Biol Chem* 270(7):3031–3038.

236. Essbauer S, Pfeffer M, Meyer H (2010) Zoonotic poxviruses. *Vet Microbiol* 140(3-4):229–236.

237. Baxby D, Bennett M, Getty B (1994) Human cowpox 1969–93: a review based on 54 cases. *Br J Dermatol* 131(5):598-607.

238. Baxby D, Bennett M (1997) Cowpox: a re-evaluation of the risks of human cowpox based on new epidemiological information. *Viral Zoonoses and Food of Animal Origin* 1-12.

239. Gallardo-Romero NF, Drew CP, Weiss SL, Metcalfe MG, Nakazawa YJ, Smith SK, Emerson GL, Hutson CL, Salzer JL, Barlett JH, Olson VA, Clemmons CJ, Davidson WB, Zaki SR, Karen KL, Damon IK, Carroll DS (2012) The pox in the North American backyard: Volepox virus pathogenesis in California mice (Peromyscus californicus). *PLoS ONE* 7(8):e43881.

240. Emerson GL, Li Y, Frace MA, Olsen-Rasmussen MA, Khristova ML, Govil D, Sammons SA, Regnery RL, Karem KL, Damon IK, Carroll DS (2009) The phylogenetics and ecology of the orthopoxviruses endemic to North America. *PLoS ONE* 4(10):e7666.

241. Husain M, Moss B (2002) Similarities in the induction of post-Golgi vesicles by the vaccinia virus F13L protein and phospholipase D. *J Virol* 76(15):7777–7789.

242. Chan WM, Bartee EC, Moreb JS, Dower K, Connor JH, McFadden G (2013) Myxoma and vaccinia viruses bind differentially to human leukocytes. *J Virol* 87(8):4445–4460.

Chapter 5 - Concluding remarks and future directions

Variola virus, the causative agent of smallpox, was the most lethal infectious disease in human history in terms of lives lost. This virus has a very narrow host range, only infecting humans, however, other related poxviruses, such as vaccinia virus (VACV), which is used as a vaccine against smallpox, have a much broader host range and can infect several different species. The virulence and host range of poxviruses is controlled by their interactions with the host immune system, and particularly interactions of host innate immune response proteins with viral proteins and molecules. These interactions drive evolution of both the host and the virus and often their co-evolution together. Therefore understanding the mechanisms that control the host tropism and species-specific virulence of poxviruses will aid in the identification and prediction of emerging viral threats, which is critical to being able to react to and protect against their spread within a community. The research projects described in this thesis highlight differences at the host-virus interface that are responsible for differences in poxviral host range.

Using combined bioinformatic and molecular approaches to investigate host range in poxviruses, we demonstrated that overcoming the antiviral effects of host PKR is essential for poxviruses like VACV to replicate successfully within a host cell. In addition we showed that species-specific variation in PKR from different mammalian species dramatically affects host susceptibility to poxvirus infection as well as the host range of poxviruses such as VACV in a variety of mammalian cell types. In the second and third chapters of this thesis, we focused on two host range factors from VACV, namely E3L and K3L, and determined that their interactions with PKR from different species could explain their host range functions. Using a highly sensitive cell culture-based transfection assay for PKR inhibition, we were able to compare the sensitivity of PKR from several different species to both viral inhibitors from VACV. Additionally, in chapter 4, we analyzed the genome of a poorly characterized leporipoxvirus with a restricted host range to better understand the genetic underpinnings of poxvirus evolution and host range.

The results presented in chapter 2 show that there is a surprising variability in the sensitivity of PKR from even closely related species to both E3L and K3L. From these analyses we identified resistance to E3L inhibition by *Mesocricetus* hamster PKRs, which we confirmed in both a yeast growth assay as well as in virus infected cells, and we also identified resistance to

K3L inhibition by the closely related Armenian hamster PKR. Through a series of cell line infection experiments, our results suggest that inhibition of PKR by both VACV E3L and K3L contributes to the large host range and cell tropism of this virus. The rapid evolution of PKR in vertebrates has allowed for PKR from some species to develop resistance to the activity of E3L or K3L, which necessitates the presence of both in VACV to infect cells from a variety of species, including the hamster species examined in these studies. Further confirmation of the importance of PKR inhibition to the host range function of E3L and K3L by using the cells generated in the second chapter that express exogenous PKRs in an isogenic background will serve to strengthen this conclusion. The generation of the tetracycline inducible PKR expressing cells will additionally allow a controlled analysis of the effects of differential PKR expression on the replication of mutant VACVs lacking E3L or K3L. Others have proposed such cell type-specific differences in PKR expression or dsRNA production as a contributing factor for observed differences in the replication of VACV mutants lacking E3L or K3L in different cell types (1). While we cannot exclude these or other cell-type specific effects from the results of these studies, our work clearly shows that species-specific inhibition of PKR can explain the majority of the host range defects of VACV deleted for E3L and particularly for VACV deleted for K3L in different host cells. In addition, the inducible expression system we generated will allow the investigation of potential species-specific effects of other contributing innate immune response factors to the host range of VACV or other viruses.

As part of our analysis into the host range function of E3L and K3L for VACV, we uncovered the unique ability of the Syrian and Turkish hamster to resist inhibition by E3L. In chapter 3, we analyzed the mechanism of this resistance by using domain swapping and mutational analyses with Syrian hamster PKR and the Armenian hamster PKR, which had the added benefit of allowing us to investigate the resistance of this PKR to VACV K3L. This mechanistic characterization between these closely related PKRs revealed a general mechanism of resistance for the Syrian hamster PKR to inhibition by dsRNA-binding proteins, including E3L as well as reovirus σ3 and Herpes simplex virus Us11, which depended on residues involved in dsRNA-binding as well as PKR dimerization in the second dsRNA-binding domain and the interdomain linker region. Our analyses also confirmed the importance of specific residues in the helix αG of the PKR kinase domain for interactions with VACV K3L. The exchange of only two amino acid residues within this helical structure was able to completely

confer resistance to inhibition by K3L in a previously sensitive PKR. Previous work from us and others has implicated this region of PKR for interactions with pseudosubstrate inhibitors from poxviruses, and our own results with hamster PKRs provide an important validation of these studies (2, 3). (Peng and Rothenburg, unpublished).

The resistance of Syrian hamster PKR to inhibition by E3L is a significant finding as it challenges the widely held assumption that the immunomodulatory activity of E3L is primarily mediated through the sequestration of excess dsRNA generated during virus replication. We hypothesized that instead of solely relying on a broadly acting and species-independent activity such as dsRNA-binding, direct interactions of E3L with PKR proteins also play an important role in the anti-immune activity of E3L for VACV. The species-specific nature of the observed resistance to E3L was unique to the *Mesocricetus* hamster PKRs and suggested a feature of these species' PKR proteins was responsible. While we were able to map this resistance by investigating the individual and combined contributions of each domain in PKR to this interaction in the luciferase assay, we reasoned that direct protein-protein interactions between E3L and PKR proteins in different species over time would have placed a positive selective pressure on PKR at residues critical for these interactions. Therefore, our analysis for positive selection in rodent and lagomorph PKRs was aimed at uncovering otherwise unobvious residues in each domain that would contribute to its resistance to viral dsRNA-binding proteins such as E3L. However, our results instead pointed to a more complex molecular interaction involving the activation and dimerization of PKR itself. The conclusions drawn from the experiments described in chapter 3 serve as a hypothetical starting point to direct future investigations into this phenomenon. Further biochemical confirmation and evaluation of dsRNA-binding and affinity, differential phosphorylation states, or variations in dimer strength or stability for Syrian hamster PKR during VACV infection will be necessary to pinpoint the most important properties of this host protein that confer its resistance to E3L and other viral dsRNA-binding proteins.

Other evolution-guided analyses have yielded insights into critical host-virus protein-protein interactions between PKR and its viral inhibitors (2, 3). Such analyses have been useful for detecting the genetic imprints of similar evolutionary co-adaptation of other host and virus proteins such as TRIM-5α with capsid proteins from retroviruses (4-7). Our inability to detect a role for positively selected residues in the resistance to VACV E3L likely speaks to the nature of the resistance mechanism rather than to a deficiency in our analysis, since we were able to

identify positively selected residues that contributed to the resistance of Armenian hamster PKR to VACV K3L, although the mechanism of this interaction is arguably better suited to identification of critical residues by this method.

An alternative approach to investigate the unique interaction between Syrian hamster PKR and VACV E3L that was not explored in depth in this thesis work is to look from the side of the virus. Our results from chapter 2 indicate that VACV deleted for K3L (vp872) is heavily attenuated in Syrian hamster BHK-21 cells. We recently initiated a study using experimental evolution of vp872 in BHK-21 cells to see if we could artificially place selective pressure on VACV E3L to improve virus replication in these cells. We have isolated DNA from serially passaged virus progeny and cloned multiple E3L amplicons into plasmids for sequence analysis. We might see changes in the sequence of E3L in response to this selective pressure over time. In a previous study, experimental evolution of VACV lacking E3L led to the rapid expansion of the K3L gene locus and to the subsequent selection for a hyperactive mutant K3L that was a better inhibitor of PKR (8). It will be interesting to see if we can observe a similar expansion of the E3L locus following selection in BHK-21 cells or if selection for other mechanisms to overcome the otherwise poor inhibition of PKR by E3L develops.

The research described in chapters 2 and 3 show the complexity of E3L inhibition of PKR, which relies on the interaction with multiple domains in PKR and is presumably dependent on both E3L and PKR binding to dsRNA. Future research on this project could look at the specific RNAs that are bound by both E3L and PKR to determine if there is a sequence or structure-specific preference by either protein that would help to partially explain the ability of Syrian hamster PKR to resist inhibition by E3L. The implications of this work would be great as it would show that PKR can evolve to select for virus-specific sequences or features in the dsRNA generated during a virus infection; a mechanism that would allow PKR to bypass direct interactions with viral inhibitors and exit the ongoing host-virus arms race generated by these protein-protein interactions. To this end, it will be important to test other PKR proteins from more species to identify other PKRs that are resistant to E3L or other viral dsRNA-binding protein inhibitors, such as NS1 from Influenza virus to know if this mechanism of resistance is rare or if it has evolved in other animal lineages. Because several viruses encode inhibitors of PKR, the results from this work and future work will have a broad impact on studies using other host-virus systems as well.

Many poxviruses only cause mild diseases in their reservoir or natural hosts, such as MYXV in American rabbit species, which probably reflects a co-evolutionary relationship between the viruses and their hosts. From the MYXV example it is important to note that as this virus was forced to switch hosts during its deliberate release into the Australian continent and into feral European rabbit populations there, the virulence of the virus in the new host was dramatically different and more lethal. These types of host-switching events can be devastating particularly when they involve closely related species. The current knowledge for predicting such host-switching events is insufficient.

The evolution of host range and virulence in poxviruses is intricately connected to the host-virus relationship and is influenced by both the physical and immunological environments in which they exist. Over the evolution of poxviruses, their genomes have been frequently subjected to gene duplication, inactivation, and deletion events. Additionally, the acquisition of host genes is commonly observed, and these horizontally transferred genes are likely an important factor in the evolution of host range. Gene loss and inactivation are also thought to contribute to host adaptation and specialization, such as with VARV adaptation to humans.

Despite a relatively high degree of gene conservation with the other fully sequenced leporipoxviruses, we discovered several occurrences of gene loss and fragmentation as well as evidence of gene acquisition in the genome of the SQFV. The region corresponding to MYXV M131R to M139 appears to be an extremely dynamic region of gene loss and fragmentation in leporipoxviruses. Additionally, the region corresponding to MYXV M150R to M154L has also experienced a high degree of genetic optimization through gene inactivation and truncation in leporipoxvirus species. Remarkably, the MYXV Lausanne (Lu) strain appears to encode all of the genes within these regions that were presumably present in the ancestral leporipoxvirus whereas the other leporipoxviruses have subsequently lost one or more genes from these regions. This is in spite of the fact that our phylogeny indicates that SQFV shares the most distant common ancestor of the leporipoxvirus lineage with RFV and both MYXV strains.

There are very few examples of genes present in the SQFV genome for which there are no orthologs present in any of the other sequenced leporipoxviruses. In fact, one such ORF is not found in any other sequenced poxvirus and likely represents a horizontally transferred host gene. S150 is a very small ORF that shares high sequence identity with a fragment of a mammalian 28S ribosomal RNA gene. The importance of this ORF for SQFV virulence or host range is not

known nor whether this ORF is even expressed during SQFV infection, however, further analysis of this SQFV gene may be interesting as there are no other examples of poxviruses encoding ribosomal RNA genes. One distinguishing feature of viruses is their inability to exist independently of a host cell and their dependence on host translational machinery including ribosomes. It is unlikely that this small ORF provides a true ribosomal function for the SQFV, but it would be interesting to see if it did have some effect on viral protein translation in some way such as by directing host translational machinery to viral mRNAs during infection. The identification of this same ORF in the wild SQFV isolate provided important verification of its presence in the SQFV genome. As many genes in poxviruses are thought to have originated from host genes, the identification of this small ORF that may have been acquired relatively recently as it is not present in any other leporipoxviruses could still bear some of the genetic clues of the original transfer that may yield insight into the mechanism of these events that are yet unclear.

From the genomic analysis of SQFV in chapter 4, we uncovered several unique features that may account for the virus' host range restriction to squirrels. Most notably, in the ITR region of the SQFV genome, we identified evidence for a recombination event that occurred between an ancestral leporipoxvirus and a virus related to old-world orthopoxviruses as well as a second recombination event that occurred with a different non-leporipoxvirus, which we were also able to confirm in the wild SQFV isolate. The acquisition of genes in the ITR of SQFV from these recombination events may have been coincident with the loss of other genes from SQFV or otherwise preceded their loss. Several of the acquired genes, most of which likely have an immunomodulatory function, are orthologous to genes that have been lost in SQFV relative to the other leporipoxviruses. For instance, the loss of the well-conserved B22R-ortholog corresponding to M134R in MYXV is surprising, but this gene might have become dispensable after the acquisition of the ortholog of CPXV B22R in the ITR. Moreover, the loss of a M007L/R (M-T7) ortholog, which has a host range function for MYXV, is also likely supported by the acquisition of an IFN-γ receptor homolog orthologous to that found in CPXV. As is discussed in chapter 4 of this thesis, the potential host-specificity of these recombined genes is probably contributing to the distinct host range of the SQFV compared to the other leporipoxviruses.

While many important immunomodulatory gene orthologs lost in SQFV relative to MYXV have been functionally replaced by genes present in its unique ITR, one important host

range gene that remains missing from the SQFV genome is an ortholog to M002L/R (M-T2), which encodes a TNF receptor homolog and interferes with TNF mediated NFκB signaling (9, 10). M-T2 orthologs are only found in leporipoxviruses, but several orthopoxviruses encode TNF receptor related proteins of the Crm family (11). The relevance of its absence from the SQFV genome is not yet known, but may also affect the host range or virulence of this virus. Additionally, since the SQFV naturally infects North American squirrels, it will be helpful for understanding the evolution of this virus to sequence more isolates of this virus from nature. From the wild SQFV isolate collected from the infected squirrel, we have already processed DNA for full genome sequencing. The results obtained by comparing these genome sequences will allow us to identify important differences that have occurred during viral evolution over more than 50 years in nature and may have implications for the evolutionary understanding of these poxviruses.

The recombination events identified in the SQFV genome are to our knowledge the first clear examples pointing to a naturally occurring recombinant poxvirus, and both represent the first example of such recombination events occurring between distantly related poxviruses. Until now, recombination has only been observed or analyzed between closely related poxvirus species. This finding therefore highlights the potential for even distantly related poxviruses to recombine in the field, which might result in altered host range and virulence. The highly recombinogenic potential of poxviruses increases the likelihood that such hybrid poxviruses will emerge.

The eradication of VARV from nature and the cessation of mass vaccinations with VACV leave human populations vulnerable to infection by other orthopoxviruses. While most zoonotic poxviruses that infect humans have been relatively mild, the emergence of MPXV strains with high case fatality rates in Africa (~10%) serves as a reminder that these or other poxviruses may yet evolve (12). This may occur through continuous host-virus co-adaptation to become more human-specific or through more rapid host-switching events potentially driven by recombination with other poxviruses or by horizontal transfer of host genes that increase their virulence such as those described in this thesis work. The continued study of the molecular determinants of poxvirus host range is therefore warranted.

References

1. Langland JO, Jacobs BL (2002) The Role of the PKR-Inhibitory Genes, E3L and K3L, in Determining Vaccinia Virus Host Range. *Virology* 299(1):133–141.

2. Rothenburg S, Seo EJ, Gibbs JS, Dever TE, Dittmar K (2009) Rapid evolution of protein kinase PKR alters sensitivity to viral inhibitors. *Nat Struct Mol Biol* 16(1):63–70.

3. Elde NC, Child SJ, Geballe AP, Malik HS (2009) Protein kinase R reveals an evolutionary model for defeating viral mimicry. *Nature* 457(7228):485–489.

4. Sayah DM, Sokolskaja E, Berthoux L, Luban J (2004) Cyclophilin A retrotransposition into TRIM5 explains owl monkey resistance to HIV-1. *Nature* 430(6999):569–573.

5. Virgen CA, Kratovac Z, Bieniasz PD, Hatziioannou T (2008) Independent genesis of chimeric TRIM5-cyclophilin proteins in two primate species. *Proc Natl Acad Sci USA* 105(9):3563–3568.

6. Johnson WE, Sawyer SL (2009) Molecular evolution of the antiretroviral TRIM5 gene. *Immunogenetics* 61(3):163–176.

7. Stremlau M, Perron M, Welikala S, Sodroski J (2005) Species-specific variation in the B30. 2 (SPRY) domain of TRIM5α determines the potency of human immunodeficiency virus restriction. *J Virol* 79:3139–3145.

8. Elde NC, Child SJ, Eickbush MT, Kitzman JO, Rogers KS, Shendure J, Geballe AP, Malik HS (2012) Poxviruses Deploy Genomic Accordions to Adapt Rapidly against Host Antiviral Defenses. *Cell* 150(4):831–841.

9. Smith CA, Davis T, Anderson D, Solam L, Beckmann M, Jerzy R, Dower S, Cosman D, Goodwin R (1990) A receptor for tumor necrosis factor defines an unusual family of cellular and viral proteins. *Science.* 248(4958):1019-1023.

10. Smith CA, Davis T, Wignall JM, Din WS, Farrah T, Upton C, McFadden G, Goodwin RG (1991) T2 open reading frame from the Shope fibroma virus encodes a soluble form of the TNF receptor. *Biochem Biophys Res Commun* 176(1):335–342.

11. Bratke KA, McLysaght A, Rothenburg S (2013) A survey of host range genes in poxvirus genomes. *Infect Genet Evol* 14:406–425.

12. Essbauer S, Pfeffer M, Meyer H (2010) Zoonotic poxviruses. *Vet Microbiol* 140(3-4):229–236.